

**EXTRA CELLULAR MATRIX REMODELING IN
FIBRIN BASED VASCULAR TISSUE ENGINEERING:
EFFECT OF GROWTH FACTORS AND
GLYCOSAMINOGLYCANS**

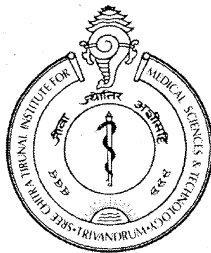
A THESIS SUBMITTED

BY

DIVYA P

**IN PARTIAL FULFILLMENT OF THE REQUIREMENTS
FOR THE DEGREE OF**

DOCTOR OF PHILOSOPHY



**SREE CHITRA TIRUNAL INSTITUTE FOR
MEDICAL SCIENCES AND TECHNOLOGY
THIRUVANANTHAPURAM – 695 012**

DECLARATION

I, Divya P, hereby declare that I had personally carried out the work depicted in the thesis entitled “**Extra cellular matrix Remodeling in Fibrin based Vascular Tissue Engineering: Effect of Growth Factors and Glycosaminoglycans**” under the direct supervision of Dr. Lissy K Krishnan, Scientist F & Leader, Thrombosis Research Unit, Biomedical Technology wing, Sree Chitra Tirunal Institute for Medical Sciences and Technology, Thiruvananthapuram, Kerala, India. External help sought are acknowledged.


Divya P

Dr. Lissy K Krishnan
Scientist F and Leader

Thrombosis Research Unit,
Biomedical Technology Wing,
Sree Chitra Tirunal Institute for Medical
Sciences and Technology,
Thiruvananthapuram – 695012.

CERTIFICATE

This is to certify that Ms. Divya P., in the division of Thrombosis Research Unit of this institute, has fulfilled the requirements of the regulations relating to the nature and prescribed period of research for the Ph.D degree of the Sree Chitra Tirunal Institute for Medical Sciences and Technology, Thiruvananthapuram. The work relating to her thesis entitled “**Extra cellular matrix Remodeling in Fibrin based Vascular Tissue Engineering: Effect of Growth Factors and Glycosaminoglycans**” was carried out under my direct supervision.



Dr. Lissy K Krishnan

The Thesis

Entitled

**EXTRA CELLULAR MATRIX REMODELING IN
FIBRIN BASED VASCULAR TISSUE ENGINEERING:
EFFECT OF GROWTH FACTORS AND
GLYCOSAMINOGLYCANS**

Submitted

By

Divya P

For

Doctor of Philosophy

of

**SREE CHITRA TIRUNAL INSTITUTE FOR
MEDICAL SCIENCES AND TECHNOLOGY
THIRUVANANTHAPURAM**

Evaluated and approved

by



Dr. Lissy K Krishnan
(Supervisor)



Dr. Sudhakaran PR
Department of Biochemistry,
University of Kerala, Thiruvananthapuram

To my parents

CONTENTS

ACKNOWLEDGEMENTS.....	viii
LIST OF FIGURES.....	x
LIST OF TABLES.....	xiii
ABBREVIATIONS.....	xiv
NOTATIONS.....	xvii
SYNOPSIS.....	xviii
CHAPTER 1 INTRODUCTION.....	1
1.1. SUMMARY.....	1
1.2. REVIEW OF LITERATURE.....	5
1.2.1. Cardiovascular disease and regenerative therapy.....	5
1.2.2. Vascular tissue engineering.....	7
1.2.2.1. Cell seeded collagen gels.....	7
1.2.2.2. Acellular and cell seeded decellularised xenografts/allografts.....	9
1.2.2.3. Perivascular implants.....	10
1.2.2.4. Cell self assembly.....	11
1.2.2.5. Cell seeded biodegradable synthetic polymer scaffolds.....	12
1.2.3. Challenges in vascular tissue engineering.....	13
1.3. DEVELOPMENT OF STUDY HYPOTHESIS.....	14
1.3.1. Role of Extra cellular matrix in tissue integration.....	14
1.3.2. Cell - Extra cellular matrix interactions.....	14
1.3.3. Influence of growth factors in vascular regeneration.....	16
1.3.4. Role of glycosaminoglycans in angiogenesis.....	16
1.3.5. Extra cellular matrix remodeling in physiology.....	18
1.3.6. Fibrin - A biological scaffold.....	21
1.3.7. Biodegradable polymers- A synthetic scaffold.....	24
1.3.8. Advantages of Poly (ϵ -caprolactone) as a scaffold.....	27
1.3.9. STUDY HYPOTHESIS.....	28
1.4. OBJECTIVES.....	28
CHAPTER 2 MATERIALS AND METHODS.....	31
2.1. ENDOTHELIAL CELL CULTURE.....	31
2.1.1. Isolation and Expansion of Human Umbilical Vein Endothelial Cells.....	31
2.1.2. Subculture of HUVEC.....	32
2.1.3. Characterization of cultured cells.....	33
2.1.3.1. Morphology Analysis.....	33
2.1.3.2. Cellular Uptake of Dil Labeled Acetylated LDL.....	33
2.1.3.3. Cellular Expression of vWF.....	34
2.2. PREPARATION OF GROWTH FACTORS.....	34
2.2.1. Preparation of crude angiogenic growth factors (AGF) from Bovine Hypothalamus.....	34
2.2.2. Preparation of Platelet Growth Factors.....	34
2.3. FIBRIN MATRIX COATING ON TISSUE CULTURE POLYSTYRENE.....	35
2.3.1. Preparation of fibrin composite coated Tissue Culture Polystyrene.....	35
2.3.2. Preparation of growth factor incorporated matrices.....	36
2.3.3. Preparation of glycosaminoglycan incorporated matrices.....	36
2.3.4. Preparation of growth factor and glycosaminoglycan incorporated matrices.....	37
2.4. STANDARDIZATION OF A FIBRIN MATRIX COMPOSITION TO ACHIEVE ECM DEPOSITION IN TISSUE CULTURE POLYSTYRENE BY CULTURING HUVEC.....	37
2.4.1. Cell adhesion.....	37
2.4.1.1. Fluorescent Staining for Actin.....	37
2.4.1.2. Vinculin Staining to detect focal adhesion.....	38
2.4.2. Cell Proliferation.....	38
2.4.2.1. Tritiated Thymidine uptake.....	38

2.4.2.2. PCNA analysis.....	39
2.4.3. Cell Apoptosis using Flow Cytometry.....	39
2.4.4. Fibrin matrix degradation - D Dimer assay.....	40
2.4.5. Solubilization and recovery of matrices.....	41
2.4.6. Post Culture Analysis of matrices.....	41
2.4.6.1. Histochemical staining.....	41
2.4.6.2. Immunostaining.....	41
2.4.6.3. Fluorimetry.....	42
2.4.7. mRNA expression studies.....	42
2.4.7.1. RNA isolation and reverse transcription.....	42
2.4.7.2. Real-Time PCR.....	43
2.4.8. Statistical analysis.....	43
2.5. FABRICATION AND PHYSICO-CHEMICAL CHARACTERIZATION OF A POROUS FIBRIN – POLY (E-CAPROLACTONE) (PCL) SCAFFOLD FOR VASCULAR TISSUE ENGINEERING APPLICATIONS.....	44
2.5.1. Scaffold preparation.....	44
2.5.2. Fibrin composite coating on the PCL scaffold.....	44
2.5.3. Characterization of scaffold.....	44
2.5.3.1. Fourier transform infrared spectroscopy (FTIR) studies.....	44
2.5.3.2. Pore size determination.....	45
2.5.3.3. In vitro degradation studies.....	45
2.5.3.3.1. Gravimetric analysis.....	45
2.5.3.3.2. Viscosity average Molecular weight determination.....	45
2.5.3.4. Mechanical Properties Evaluation.....	46
2.5.4. Characterization of endothelial cell seeded scaffold.....	46
2.5.4.1. Endothelial cell seeding.....	46
2.5.4.2. EC adhesion and spreading.....	46
2.5.4.3. Environmental scanning electron microscopy.....	46
2.5.4.4. Mechanical Properties evaluation.....	47
2.5.5. Statistical analysis.....	47
2.6. ENDOTHELIAL CELL GROWTH AND FUNCTIONAL TISSUE GENERATION.....	47
2.6.1. Cell proliferation.....	47
2.6.1.1. PCNA staining.....	47
2.6.1.2. Tritiated Thymidine Uptake.....	47
2.6.2. Apoptosis.....	48
2.6.3. Long term cell growth.....	48
2.6.4. Cell Solubilization and Matrix Staining.....	48
2.6.5. EC Phenotype.....	49
2.6.5.1. RNA isolation and reverse transcription.....	49
2.6.5.2. Real-Time PCR.....	50
2.6.6. Assessment of Nitric oxide release.....	51
2.6.7. Effect of shear stress on EC monolayer.....	51
2.6.8. Evaluation of Blood Compatibility.....	51
2.6.8.1. Qualitative analysis of platelet adhesion by scanning electron microscopy.....	52
2.6.8.2. Quantification of Platelet Adhesion by Radioscintigraphy.....	52
2.6.8.2.1. Labeling of Platelets with ¹²⁵ I.....	52
2.6.8.2.2. Exposure of materials to labeled PRP.....	53
2.6.8.2.3. Quantification of Adhered Platelets.....	53
2.6.8.3. Statistical analysis.....	53
CHAPTER 3 - STANDARDIZATION OF A FIBRIN MATRIX COMPOSITION TO ACHIEVE ECM DEPOSITION IN TISSUE CULTURE POLYSTYRENE BY CULTURING HUVEC.....	54
3.1. ABSTRACT.....	54
3.2. Endothelial cell characterization.....	55
3.3. Standardization of basic fibrin composite matrix.....	58
3.3.1. EC adhesion.....	58
3.3.2. Cell Proliferation & Apoptosis.....	61
3.3.3. Comparison of fibrin composite matrix (CCPS) to commercial fibronectin coated plates (FNPS).....	63
3.4. Effect of growth factors and glycosaminoglycans on cell adhesion and proliferation.....	68
3.4.1. GF/s incorporated matrices.....	68

3.4.2. GAG/s incorporated matrices	68
3.4.3. GFs and/ GAGs incorporated matrices	68
3.5. ECM remodeling	74
3.5.1. Fibrin matrix degradation	74
3.5.2. ECM deposition	76
3.5.2.1. Growth factor incorporated matrices	76
3.5.2.1.1. Histochemical Staining	76
3.5.2.1.2. Immuno-specific staining	77
3.5.2.1.3. Immunofluorescence staining	81
3.5.2.1.4. Quantitative analysis of ECM deposition	82
3.5.2.2. Glycosaminoglycan incorporated matrices	86
3.5.2.2.1. Immunofluorescence staining	86
3.5.2.2.2. Quantitative analysis	86
3.5.2.3. Growth factor and glycosaminoglycan incorporated matrices	86
3.5.2.3.1. Immunofluorescence staining	86
3.5.2.3.2. Quantitative analysis	86
3.5.2.4. mRNA expression for collagen I, collagen IV and elastin	93
3.5.2.4.1. Growth factor incorporated matrices	93
3.5.2.4.2. Glycosaminoglycan incorporated matrices	95
3.5.2.4.3. Growth factor and glycosaminoglycan incorporated matrices	96

CHAPTER 4 - FABRICATION AND PHYSICOCHEMICAL CHARACTERIZATION OF A POROUS FIBRIN – POLY (E- CAPROLACTONE) (PCL) SCAFFOLD FOR VASCULAR TISSUE ENGINEERING APPLICATIONS. 103

4.1. ABSTRACT	103
4.2. Polymer scaffold	104
4.2.1. Morphology	104
4.2.2. Chemical characterization	105
4.2.2.1. FTIR Studies	105
4.2.3. Physical properties	106
4.2.3.1. Mechanical properties	106
4.2.3.2. Porosity/ Pore size	108
4.2.4. Scaffold Stability/ Degradation	110
4.2.4.1. Gravimetric analysis	110
4.2.4.2. Viscosity average molecular weight measurement	111
4.2.5. Endothelial cell growth on porous PCL..	112
4.3. Hybrid scaffold characterization	113
4.3.1. Morphology	113
4.3.2. Chemical characterization	114
4.3.2.1. FTIR Studies	114
4.3.3. Physical characterization	115
4.3.3.1. Porosity and pore size	115
4.3.4. Biological properties	117
4.3.4.1. Analysis of cell growth on hybrid scaffold	117
4.3.5. Mechanical properties	120

CHAPTER 5 - ENDOTHELIAL CELL GROWTH AND FUNCTIONAL TISSUE GENERATION. 123

5.1. ABSTRACT	123
5.2. Cell adhesion and proliferation	123
5.2.1. Visualization of EC on scaffold	123
5.2.2. Quantification of Adhesion & Proliferation	124
5.2.3. Proliferation using PCNA as marker	126
5.3. Cell viability	127
5.4. Analysis of ECM remodeling	129
5.4.1. Elastin Deposition	129
5.4.2. Collagen IV Deposition	131
5.5. ECM remodeling	134
5.6. Characterization of EC phenotype	136
5.7. Nitric oxide release	139
5.8. Response to shear stress	140

5.9. Platelet Adhesion.....	142
5.9.1. Qualitative analysis.....	142
5.9.2. Quantitative analysis by Radioscintigraphy.....	142
CHAPTER 6 SUMMARY AND CONCLUSIONS	147
6.1. RESTATEMENT OF THE PROBLEM	147
6.2. DESCRIPTION OF PROCEDURES.....	149
6.3. MAJOR FINDINGS	151
6.4. CONCLUSIONS.....	154
6.5. RECOMMENDATIONS FOR FURTHER INVESTIGATION	155
BIBLIOGRAPHY	158
ANNEXURE-1	183

ACKNOWLEDGEMENTS

I would like to express my deep and sincere gratitude to my Guide Dr. Lissy K. Krishnan, Thrombosis Research Unit, SCTIMST. Her wide knowledge and her logical way of thinking have been of great value for me. Her understanding, encouragement, stimulating suggestions, constructive criticism, and excellent advice helped me in all the time of research. It was of her great support in science and "beyond science" life that I got the opportunity to initiate and complete this thesis.

I would like to thank the members of my Doctoral Advisory Committee, Dr. Anoopkumar T, Division of Molecular Medicine and Dr. Maya Nandakumar, Division of Microbiology, who monitored my work and for providing me with valuable comments during the progress of this thesis.

I am grateful to the Director, SCTIMST and the Head, Biomedical Technology Wing for providing all the necessary facilities throughout my studentship and for opportunities given to attend various training programs and to attend seminars and workshops. My sincere thanks to Dr. George AV, Registrar, SCTIMST, for the academic assistance, for constant encouragement, sound advice and for being always helpful.

I wish to express my warm and sincere thanks to Dr. Kalyanakrishnan V, Head of Dental Products lab, who introduced me to the field of polymers, for his detailed and constructive comments, for interesting discussions and for his important support throughout this work. I am also grateful to the staff of Dental Products Lab for providing me an excellent work environment during my polymer studies there; Dr. Lizymol PP for her prompt and generous feedback to my queries, and Ms. Minshiya PP and Mr. Rejin for their cheerful assistance.

I am indebted to the staff of Department of Obstetrics and Gynecology, GG Hospital, Trivandrum for providing Umbilical Cord samples and Blood Bank staff of our institute for providing blood samples for the study. I am thankful to Prof. Radhakrishnan WV, Division of Pathology, for the help received during histochemical experiments. My heartfelt thanks are due to Dr. Harikrishna Varma, Mr. Suresh Babu and Mr. Vijayan, Bioceramics lab and Mr. Sreekumar, Scanning Electron Microscopy for the help received in microscopy and porosity estimation studies. I would like to thank Mr. Muraleedharan CV, Calibration Cell for the help provided during the degradation experiments.

I am thankful to Dr. Anilkumar TV for the training in Confocal microscopy and for his valuable advice and friendly assistance received. I am obliged to Dr. Fernandez AC and his group, Division of Laboratory of Animal Sciences, for their time and effort in giving me training in animal handling and for the help received during raising antibodies in rabbit. The help received from the librarians of Biomedical Technology Wing is gratefully acknowledged.

I wish to extend my warmest thanks to all my colleagues in Thrombosis Research Unit. I am grateful to Dr. Krishna Prasad C, for being always available when I needed his advice and for teaching me various techniques that were crucial during this thesis. I thank Dr. Resmi Varma, Ms. Sreerexha PR, Dr. Anila L, Ms. Madhumathi R, Ms. Priyanka Manoj, Dr. Asha S. Mathew, Mr. Jaseer Muhammed, Ms. Anumol Jose and Ms. Raagaseema VM for their technical support and generosity. I am indebted to Mrs. Mary Vasantha Bai for her loving support and for standing by me in good and bad times.

I owe my loving thanks to Arun, Nishi and Manitha for being the best of friends, for the incredible support when the going was tough, and for encouraging me during the rough patches. Many thanks to my friends Viji, Biji, Sailaja, Shiny, Becky, Viola, Beena, Josna, Asha Rani, Siddharth and Kaladhar for the good company, and lot of joyful moments.

I gratefully acknowledge the research fellowship from University Grants Commission, New Delhi. I thank Council of Scientific and Industrial Research and Department of Science and Technology, New Delhi for providing me international travel grants to attend conferences abroad. I also wish to thank Tissue Engineering and Regenerative Medicine International Society for granting me travel assistance.

The chain of my gratitude would be definitely incomplete if I forget to thank the first cause of this chain, using Aristotle's words, The Prime Mover. My deep and sincere gratitude for giving courage and guiding this humble being. Lastly, and most importantly, I wish to express my deepest gratitude to my parents and sister for the constant support, understanding and love, which have always provided me with strength and happiness throughout the years. To them I dedicate this thesis.

Divya P

LIST OF FIGURES

Figure 3.1. Phase contrast microscopic images of representative fields from HUVEC culture at different magnifications.....	56
Figure 3.2. Fluorescent Micrographs of HUVEC.....	57
Figure 3.3. Confocal images of endothelial cells stained for Actin.....	59
Figure 3.4. Confocal images of endothelial cells stained for Vinculin.....	60
Figure 3.5. Quantification of endothelial cell growth and survival.....	62
Figure 3.6. A. Qualitative evaluation of cell proliferation. B. Quantification of endothelial cell proliferation.....	65
Figure 3.7. Quantitative evaluation of cell proliferation on the matrices by PCNA analysis.....	66
Figure 3.8. Quantification of endothelial cell survival.....	66
Figure 3.9. Quantification of EC adhesion and proliferation on GF incorporated matrices using ³ H-thymidine uptake.....	69
Figure 3.10. Quantification of EC adhesion and proliferation on GAG incorporated matrices using ³ H-thymidine uptake.....	70
Figure 3.11. Quantification of EC adhesion and proliferation on GF and GAG incorporated matrices using ³ H-thymidine uptake.....	70
Figure 3.12. Quantification of EC proliferation on GF and GAG incorporated matrices by PCNA analysis.....	71
Figure 3.13. Cell viability on the GF and GAG incorporated matrices at 72 h of EC culture.....	71
Figure 3.14. Histochemical staining- Photomicrographs of GF incorporated matrices recovered after 3 days of in vitro endothelial cell culture.....	78
Figure 3.15. Histochemical staining - Photomicrographs of GF incorporated matrices recovered after 10 days of in vitro endothelial cell culture.....	78
Figure 3.16. Histochemical staining - Photomicrographs of GF incorporated matrices recovered after 20 days of in vitro endothelial cell culture.....	79
Figure 3.17. Histochemical staining - Photomicrographs of GF incorporated matrices recovered after 30 days of in vitro endothelial cell culture.....	79
Figure 3.18. Immunostaining of collagen I- Photomicrographs of GF incorporated matrices recovered after 10 days of in vitro endothelial cell culture.....	80
Figure 3.19. Immunostaining of collagen IV - Photomicrographs of GF incorporated matrices after 10 days of in vitro endothelial cell culture.....	80

Figure 3.20. Immunostaining of elastin - Photomicrographs of GF incorporated after 10 days of in vitro endothelial cell culture.....	81
Figure 3.21. Standard graph for quantification of collagen and elastin deposition.....	82
Figure 3.22. Immunostained elastin in matrices GF incorporated matrices after EC culture – fluorescent micrographs.....	83
Figure 3.23. Immunostained Collagen IV in GF incorporated matrices recovered after EC culture – fluorescent micrographs.....	84
Figure 3.24. Fluorimetry data showing the concentration of elastin (A) and collagen IV (B) on GF incorporated matrices at 10 days and 20 days.....	85
Figure 3.25. Immunostained elastin in GAG incorporated matrices recovered after EC culture.....	87
Figure 3.26. Immunostained Collagen IV in GAG incorporated matrices recovered after EC culture.....	88
Figure 3.27. Immunostained Collagen I in GAG incorporated matrices recovered after 10 days of EC culture.....	89
Figure 3.28. Fluorimetry data showing the concentration of elastin and collagen IV on the GAG incorporated matrices at 10 days and 20 days.....	90
Figure 3.29. Immunostained Elastin, Collagen IV and Collagen I in CCPS+GAG+GF matrix after 10 and 20 days of EC culture.....	91
Figure 3.30. Fluorimetry data showing the concentration of elastin and collagen on the GAG/GF incorporated matrices at 10 days.....	92
Figure 3.31. Real Time PCR data showing regulation of m RNA expression with culture time.....	94
Figure 3.32. Real Time PCR data showing regulation of m RNA expression with added GF.....	95
Figure 3.33. Real Time PCR data showing regulation of mRNA expression with added GAG.....	96
Figure 3.34. Real Time PCR data showing regulation of mRNA expression with added GAG and GF combination.....	97
Figure 4.1. Morphology of PCL Films.....	104
Figure 4.2. FTIR spectrum of PCL.....	105
Figure 4.3. FTIR spectrum PCL scaffolds.....	106
Figure 4.4. Tensile strength of bare PCL scaffolds.....	107
Figure 4.5. Elongation at break of bare PCL scaffolds.....	107
Figure 4.6. Histogram of pore size distribution.....	108
Figure 4.7. Percentage weight loss of the scaffolds.....	110
Figure 4.8. Graph showing viscosity vs PCL concentration.....	111

Figure 4.9. Confocal micrographs of actin-stained ECs on PCL scaffold.....	112
Figure 4.10. Light micrographs of scaffolds.....	114
Figure 4.11. FTIR spectra of bare PCL and hybrid scaffolds.....	115
Figure 4.12. Histogram of pore size distribution.....	116
Figure 4.13. Confocal micrographs of actin-stained ECs.....	117
Figure 4.14. Electron micrographs of scaffolds.....	119
Figure 4.15. Mechanical properties of porous PCL scaffold and (3d leached) and fibrin coated porous PCL scaffold (3d leached).....	120
Figure 4.16. Tensile strength of bare, hybrid and EC- seeded hybrid scaffolds... ..	121
Figure 4.17. Elongation at break of tissue engineered hybrid scaffolds... ..	122
Figure 5.1. Actin-stained ECs on a hybrid scaffold.....	124
Figure 5.2. Data on ³ H-thymidine uptake assay.	125
Figure 5.3. PCNA analysis... ..	126
Figure 5.4. Data on quantification of PCNA.....	126
Figure 5.5. Elastin-stained scaffold recovered after EC culture.....	130
Figure 5.6. Collagen IV-stained scaffold recovered after EC culture.....	133
Figure 5.7. ECM Remodeling: Data shows the increase in mRNA expression levels of ECM molecules at 144 h when compared to 24 h, on the different matrices.....	135
Figure 5.8. EC phenotype: Data shows a comparison of fold change in gene expression on the defined matrices at 144h when compared to 24h.....	136
Figure 5.9. Analysis of nitric oxide by nitrite assay... ..	139
Figure 5.10. Effect of shear stress on EC seeded FC PCL.....	141
Figure 5.11. Scanning electron micrographs depicting the scaffolds after 30 min PRP exposure.....	143
Figure 5.12. Radioscintigraphy data showing platelet adhesion on various PCL surfaces.. ..	144
Figure 5.13. Quantitative estimation of platelet adhesion by Radioscintigraphy. :.....	145

LIST OF TABLES

Table 2.1. Sequences of primers used in RT-PCR	50
Table 3.1. Data representing the D-Dimer levels in the medium at different periods of endothelial cell culture in defined fibrin matrix combinations.	75
Table 5.1. Viability of ECs	127

ABBREVIATIONS

3-D	Three-Dimensional
ACD	Acid Citrate Dextrose
AcLDL	Acetylated Low Density Lipoprotein
AGF	Angiogenic Growth Factors
ANOVA	Analysis of Variance
ATR-IR	Attenuated Total Reflectance Infrared Spectroscopy
bFGF	basic Fibroblast Growth Factor
BSA	Bovine serum albumin
CCPS	Composite Coated Poly Styrene
CPM	Count per Minute
DAB	Diamino Benzidine
Dacron	Poly(ethylene terephthalate)
Dil	1,1-Dioctadecyl-3,3,3,3-tetramethyl Indocarbocyanine perchlorate
EC	Endothelial Cell
EC FC PCL	Endothelial cell grown fibrin composite coated PCL
ECM	Extra Cellular Matrix
EDTA	Ethylene Diamine Tetra Acetic acid
eNOS	endothelial Nitric Oxide Synthase
EPC	Endothelial Progenitor Cells
ePTFE	expanded poly(tetra fluoro ethylene)
ERK	Extracellular signal-Regulated Kinase
ESEM	Environmental Scanning Electron Microscopy
FAK	Focal Adhesion Kinase
FBS	Fetal Bovine Serum
FC PCL	Fibrin Composite coated PCL scaffold
FC TCPS	Fibrin Composite coated Tissue Culture Polystyrene
FDP	Fibrin Degradation Product
FGF-2	Fibroblast growth factor-2

FITC	Fluorescein Iso Thio Cyanate
FN	Fibronectin
FN TCPS	Fibronectin coated Tissue Culture Polystyrene
FTIR	Fourier Transform Infrared spectroscopy
GAG	Glycosaminoglycan
GEL	Gelatin
GF	Growth factor
HA	Hyaluronic acid
HBSS	Hank's Balanced Salt Solution
HRP	Horse Radish Peroxidase
HS	Heparan Sulphate
HUV	Human Umbilical Vein
HUVEC	Human Umbilical Vein Endothelial Cell
ICAM-1	Inter Cellular Adhesion Molecule-1
IGF	Insulin like Growth Factor
IL	Interleukin
JAK	Janus kinases
LDL	Low Density Lipoprotein
MAPK	Mitogen-Activated Protein Kinase
MFI	Mean Fluorescence Intensity
MMPs	Matrix Metallo-Proteases
NO	Nitric Oxide
PA	Plasminogen Activator
PAGE	Poly Acrylamide Gel Electrophoresis
PAI-1	Plasminogen Activator Inhibitor-1
PBS	Phosphate Buffered Saline
PCL	Poly (ϵ -caprolactone)
PCNA	Proliferating Cell Nuclear Antigen
PCR	Polymerase Chain Reaction
PDGF	Platelet Derived Growth Factor
PDGFR	Platelet Derived Growth Factor Receptor
PECAM-1	Platelet-Endothelial Cell Adhesion Molecule 1

PEG	Polyethylene Glycol
PGA	Polyglycolic Acid
PGF	Platelet Growth Factors
PGI ₂	Prostaglandin I ₂
PLGA	Poly(lactic-co-glycolic acid)
PPP	Platelet Poor Plasma
PRP	Platelet Rich Plasma
PS	Phosphatidylserine
PTAH	Phosphotungstic Acid Haematoxylin
PTFE	poly(tetra fluoro ethylene)
REDV	Arg-Glu-Asp-Val
RGD	Arg-Gly-Asp
SDS	Sodium Dodecyl Sulphate
SEM	Scanning Electron Microscope
SMC	Smooth Muscle Cell
STAT	Signal Transducers and Activators of Transcription
TCA	Tri Chloro Acetic acid
TCPS	Tissue Culture Poly Styrene
TE	Tissue Engineering
TEBV	Tissue Engineered Blood Vessel
TEVG	Tissue Engineered Vascular Graft
TF	Tissue Factor
TG	Thromboglobulin
TGF	Transforming Growth Factor
tPA	tissue type Plasminogen Activator
VEGF	Vascular Endothelial Growth Factor
VEGFR2	Vascular Endothelial Growth Factor Receptor - 2
VTE	Vascular Tissue Engineering
vWF	von Willebrand Factor
Zn-Se	Zinc Selenide

NOTATIONS

α	Alpha
β	Beta
ϵ	Epsilon
μ	Micro
\sim	Approximately
\pm	Plus or Minus
%	Percentage
$^{\circ}\text{C}$	Degree Celsius
Ct	Threshold Cycle
<i>g</i>	gravity
η_{sp}	Specific viscosity
<i>c</i>	Concentration
<i>wt</i>	Weight
MPa	Mega Pascal
IU	International Units
kDa	Kilo Daltons
M	Molar
mM	Milli Molar
nM	Nano Moles
dl	Deci litre
ml	Milli Litre
μl	Micro Litre
g	Gram
mg	Milli Gram
μg	Micro Gram
ng	Nano Gram
min	Minute
h	Hours
d	Days
cm	Centi Metre
mm	Milli Metre
μm	Micro metre

SYNOPSIS

Atherosclerotic vascular disease is a leading cause of morbidity and mortality world wide. Success of current surgical replacement of diseased vessels by autologous and synthetic grafts has been limited to large-caliber vessels. Small diameter (<6 mm) artificial vascular substitutes have been found inadequate due to acute thrombogenicity of the graft, anastomotic intimal hyperplasia, aneurysm formation, infection, and progression of atherosclerotic disease. Endothelial cell (EC) seeding onto vascular conduits can lead to the formation of EC layer with non-thrombogenic lumen, but EC delamination in the acute phase of implantation is a major problem. Currently, there is a clinical need for development of biocompatible vascular graft to substitute diseased vessels and principles of tissue engineering can be applied for the purpose.

A biocompatible vascular graft would be characterized both by its mechanical attributes and post implantation healing responses. The graft should be resistant to thrombosis, infection and inflammation, and optimally should yield a neovessel resembling a native artery in structure and function. Mechanical strength is a paramount issue; grafts placed in the arterial circulation must be capable of withstanding long-term hemodynamic stress without material failure. Despite promising results obtained so far in this area of investigation, mechanical strength of the construct is a crucial factor that remains to be solved. Generally most tissue engineering approaches strive to develop biodegradable synthetic or natural material as the scaffold that provide a temporary biomechanical structure on which cells grow and

maintain normal physiological function. The ability to generate tissues with normal function necessitates development of a suitable scaffold and methods to stimulate extra cellular matrix (ECM) deposition and remodeling by cells grown *in vitro*, to achieve long term stability and mechanical strength to the construct.

In physiology, ECM provides a support essential for maintaining the organization of vascular endothelial cells into blood vessels, primarily through adhesive interactions with integrins on the endothelial cell surface. The specific mechanisms through which ECM supports EC functions are complex and involve both external structural support and regulation of multiple signaling pathways that control apoptosis, proliferation and cell shape. Thus, the ECM affects many fundamental aspects of EC biology through both mechanical and signaling functions.

Precise control of the cell-matrix interactions that provide signals remains a major challenge in vascular tissue engineering. Such external signals are generated from growth factors, cell-ECM, and cell-cell interactions, as well as from physico-chemical stimuli. In tissue engineering, ECM proteins that are deposited by the cells to remodel the environment play a major role in determining the construct stability. The ECM proteins deposited by the cells also help to resist shear stress related cell shedding and phenotype changes. However, ECM deposition needs to be regulated because excessive matrix formation may lead to unfavorable tissue remodeling. Hence, there is a need to design an optimal scaffold composition that facilitates production of appropriate matrix proteins leading to favorable tissue remodeling, which will further support vascular tissue engineering applications.

Fibrin is the natural provisional matrix for wound healing and tissue repair and it allows cells to translate environmental cues into decisions regarding gene expression that are required for tissue remodeling. In physiology multiple growth factors that are immobilized in the fibrin matrix is crucial for wound healing and tissue regeneration. Therefore, it is apparent that use of combinations of various growth factors with fibrin and other ECM proteins would provide a biomimetic environment for *in vitro* tissue regeneration. Fibronectin (FN) immobilized within the fibrin matrix promotes cell adhesion. Fibrin has been proven to be a stable matrix for endothelial cell

growth and cell-FN interactions and cell growth can be modified by the molecular environment of the protein within the ECM.

The goal of this study was to prove that fibrin matrix composition can be modified with growth factors and glycosaminoglycans to promote ECM remodeling coupled with EC growth. The matrix thus standardized should be useful to create improved scaffolds for construction of vascular grafts with functional stability of EC and the deposited ECM should prevent delamination of cell while providing good mechanical strength to resist shear stress.

OBJECTIVES

In order to achieve the goal the study was carried out in three phases. The objectives for each phase are listed below.

PHASE I

Standardization of a fibrin matrix composition to achieve ECM deposition in tissue culture polystyrene by culturing HUVEC

1. i. To compose a fibrin composite (FC) matrix that support optimum EC adhesion, spreading and proliferation.
1. ii. To establish understand the role of essential components in the matrix on EC proliferation and survival.
1. iii. To compare the effect of growth factors (GFs); angiogenic growth factors (AGF) and platelet growth factors (PGF) on Elastin, Collagen I and Collagen IV deposition by replacing fibrin matrix.
1. iv. To compare the effect of glycosaminoglycans (GAGs); hyaluronic acid (HA) and heparan sulphate (HS), on Elastin, Collagen I and Collagen IV deposition on fibrin matrix.
1. v. To establish that combinations of GAGs and GFs in the matrix can influence deposition of essential ECM components by EC in culture.

PHASE II

Fabrication and physicochemical characterization of a porous fibrin – poly (ϵ -caprolactone) (PCL) scaffold for vascular tissue engineering applications.

2. i. To standardize fabrication of a porous biodegradable polymer scaffold.
2. ii. To standardize fabrication of polymer-ECM scaffold using matrix standardized during the phase I of this study.

2. iii. To prove the tensile strength and elasticity of fabricated scaffold is suitable for blood vessel construction.
2. iv. To establish the degradation rate of the scaffold and to prove the degradation products do not affect the endothelial cell growth.

PHASE III

Endothelial cell behavior on the hybrid scaffold.

3. i. To demonstrate EC attachment, proliferation, survival and coverage of surface of the hybrid scaffold as compared to the bare polymer scaffold
3. ii. To establish EC grown on the hybrid scaffold deposit elastin and collagen IV
3. iii. To establish non-thrombogenic EC phenotype when cells are grown on fibrin composite and fibronectin coated tissue culture polystyrene.
3. iv. To establish the EC maintain normal phenotype and express mRNA for cell-specific ECM molecules.
3. v. To compare the thrombogenicity of EC grown on the hybrid scaffold against bare porous PCL using *in vitro* blood compatibility studies.

This dissertation is divided into six chapters such as; Introduction, Materials & Methods, Results I, II & III, and Summary & Conclusions.

Chapter I: Introduction

The significance of the emerging field of tissue engineering in blood vessel replacement is highlighted. Various approaches in vascular tissue engineering and the problems associated are reviewed. The role of fibrin in wound healing response and application of fibrin as scaffolds in tissue engineering is discussed. The importance of extra cellular matrix in cell growth and survival is described. ECM remodeling during angiogenesis and wound healing is elaborated and the concept that fibrin matrix can be manipulated for endothelial cell extra cellular matrix remodeling is reviewed. The need for a matrix with improved ECM remodeling together with the maintenance of normal endothelial cell function in vascular tissue engineering is defined. Finally, the hypothesis and objectives are stated.

Chapter II: Materials and Methods

The methods of isolation and characterization of human umbilical vein endothelial cells (HUVEC) is described. Various fibrin matrix compositions and the method of coating surfaces are elaborated. For the initial selection of the basic matrix, endothelial cells grown on fibrin matrices were evaluated for cell spreading and focal adhesion organization by actin and vinculin staining by confocal microscopy, cell proliferation assay was done by tritiated thymidine uptake, apoptosis on the matrices were determined by Annexin V staining by flow cytometry.

Methods described for the analysis of cell proliferation include proliferating cell nuclear antigen estimation by flow cytometry and Thymidine uptake assay to estimate population doubling time (PDT). For estimation of cell apoptosis and survival, Annexin V and propidium iodide double staining and flow cytometry is included. To identify Collagen I, Collagen IV and Elastin both histochemical and immunochemical staining of decellularised surfaces were employed and is described. Quantification of ECM deposition on the surface was carried out by flourometry and the method of generating calibration curve and estimation is elaborated. Details of RT PCR carried out for mRNA expression of collagen I, collagen IV and elastin along with method of data analysis is described.

Preparation of porous PCL scaffold using PEG as a porogen, measurement of its physicochemical properties using FTIR spectroscopy, mercury porosimetry, universal testing machine, viscosity average molecular weight measurement etc. are described. Evaluation of cytocompatibility by growing EC and environmental scanning electron microscopy is described. Further, confocal microscopy used for assessment of invasion of the scaffold by EC and characterization of the deposited ECM on scaffold are also included.

To characterize the non-thrombogenic phenotype of the EC grown on the FC-coated and FN-coated surfaces, the methods used include mRNA expression studies of nonthrombogenic and antithrombogenic molecules, synthesis of nitric oxide at static and dynamic conditions which are elaborated.

For shear stress resistance of EC on the scaffold, light microscopic analysis of cell retention and for thromboresistance qualitative assessment of platelet adhesion by scanning electron microscopy and quantification by radioscintigraphy were done and the methods are explained with appropriate references.

Chapter III: Results & Discussion- Matrix standardization

The objective of this part of the study was to select a matrix that stimulates ECM deposition without affecting the normal physiology of EC. Various compositions and formulations were made to identify the importance of each component on cell adhesion, proliferation and apoptosis. The study has identified importance of fibronectin in fibrin matrix for cell adhesion, proliferation and apoptosis. Growth factor compositions and GAG compositions were modified to understand the effect of these molecules on ECM production and remodeling. Immunological and histological staining of the recovered matrices after EC culture showed that collagen IV deposition is modulated by the presence of GFs. Expressions of mRNA, studied by quantitative PCR, demonstrated that there is a cumulative effect of GFs, AGF and PGF with upregulation of elastin and collagen expression in EC when compared to their individual effect. Even though, GAGs (HA&HS) did not have much influence on cell proliferation and expression of mRNA for elastin and collagens individually, it was found to be effective in combination. Combination of GFs and GAGs up regulated expression of elastin and collagen IV when compared to their independent effect. On comparison with commercially available fibronectin coated plates, the cell proliferation rate on the standardized fibrin composite matrix was improved. Thus the final composite matrix with a composition of GFs (AGF+PGF) and GAGs (HA+HS) was found to be very effective in ECM production and remodeling.

Chapter IV: Results & Discussion - Fabrication and physicochemical characterization of a porous PCL scaffold.

The objective of this part of the study was to fabricate a hybrid scaffold for vascular tissue engineering applications. The physicochemical characteristics of poly ϵ -caprolactone (PCL) films were evaluated and the results indicated that this can be a suitable base polymer for fabrication of hybrid scaffold for vascular tissue engineering. The fibrin composite binding onto the scaffold was proven by the -NH- group peak in FTIR analysis. The

degradation studies revealed no significant decrease in weight loss with minor decrease in viscosity average molecular weight in 60 days when the scaffold was incubated in PBS at 37⁰C with agitation at 70 rpm. The scaffold degradation products did not affect the EC growth as proven by the EC culture on the scaffold for 30 days. The cell proliferation on the scaffold was visualized by ESEM analysis. The cell-grown scaffold showed tensile strength that matches with normal artery and good cytocompatibility suggesting its suitability for tissue engineering applications.

Chapter V: Results & Discussion- Endothelial cell behavior on the hybrid scaffold.

The objective of the study was to establish that the EC invade into the pore surfaces of the hybrid scaffold with subsequent deposition of elastin and collagen. PCNA analysis proved 84% of the cell population was PCNA positive in EC cultured on FC-PCL, where as in PCL it was only 18%. The rate of increase in cell proliferation was approximately 4-fold in FC-PCL scaffold when compared to PCL where the cells failed to proliferate even one fold. The apoptotic cells were much higher in PCL where as in FC-PCL apoptosis was minimal. Cell invasion was established using the confocal microscopy of actin stained EC grown on hybrid scaffold for 15 days. After 15 days of cell growth the decellularised scaffold showed presence of elastin and collagen IV that were specifically stained with respective antibodies. The maintenance of normal EC physiology on the scaffold was proven by the regulated mRNA expression levels of von willebrand factor (vWF), endothelial nitric oxide synthase (eNOS), tissue plasminogen activator (PA), and plasminogen activator inhibitor (PAI). Quantitative increase in ECM deposition was also evidenced. Differential expression of collagen IV and elastin but not collagen I indicated that EC does not transdifferentiate during the culture period. Synthesis of NO by EC grown on the hybrid scaffold proved the normal EC function and increased NO production under dynamic condition indicated that cells are responsive to physiological changes. Absence of EC delamination after exposure of tissue engineered surface to flow condition suggests that remodeling of ECM has stabilized cells on the surface. Finally non-thrombogenic nature of the engineered surface is indicated by the absence of platelet adhesion.

Chapter VI: Summary and Conclusions

The results from Chapter III, IV & V are summarized. The results demonstrated significance of various components for cell attachment, proliferation and survival. It was evidenced that gelatin, and fibronectin are important adhesive proteins and their presence in fibrin matrix improves cell growth. Further, a combination of GFs and GAGs was found to upregulate mRNA expressions for ECM molecules and their deposition was accelerated. The hybrid scaffold that was engineered using a biodegradable polymer combined with a matrix composition that was standardized during this study showed desired physicochemical characteristics and its ability to support cell growth has proven that this novel scaffold is suitable for vascular tissue engineering. Further it was proven that the endothelial cells that grow on the hybrid scaffold maintains normal EC phenotype and produce ECM proteins that was remodeled to produce necessary mechanical properties for cells to remain in the lumen against shear stress generated due to flow.

Future directions and prospects are outlined.

Bibliography includes all relevant citations for introduction of the research problem, methodology used and for discussion of results.

CHAPTER 1

INTRODUCTION

1.1. SUMMARY

Vascular grafts are in large demand for coronary and peripheral bypass surgeries. Autologous saphenous veins or mammary arteries are the preferred conduits due to their improved long term patency (Taylor *et al.*, 1990). However, they are limited due to their short size, small diameter, and availability, as many patients require multiple grafts. The scarcity of non-affected autologous grafts in patients with vascular diseases have led to the use of synthetic vascular prostheses, such as Dacron® fabric grafts [poly(ethylene terephthalate)] and Teflon® [expanded poly(tetrafluoroethylene)] grafts (Seifalian *et al.*, 2002; Faries *et al.*, 2000). Replacement of vessels with purely synthetic polymeric conduits often leads to the failure of such graft, especially in the grafts less than 6 mm in diameter or in the areas of low blood flow, mainly due to the early formation of thrombosis. Moreover, the commonly used materials lack growth potential, and long-term results have revealed several material-related failures, such as stenosis, thromboembolization, calcium deposition and infection. Endothelialization of vascular grafts (Herring *et al.*, 1978) have also been attempted to provide a more natural and antithrombogenic blood-contacting surface but this approach has been limited by poor retention of endothelial cells on biomaterial surfaces upon exposure to blood flow.

Tissue engineering (TE) is an interdisciplinary field that applies the principles of engineering and life sciences, towards the development of biological substitutes that restore, maintain or improve tissue function (Langer and Vacanti, 1993). To produce tissue engineered constructs organ specific cells may be seeded onto biodegradable scaffold *ex vivo* and are allowed to remodel prior to transplantation. Ideally, as the scaffold degrades with time the cells should synthesize tissue-specific extra cellular matrix (ECM) eventually to produce a new functional tissue. As viable structures, tissue-engineered blood vessels should represent a responsive and self renewing tissue with an inherent potential for healing and remodeling according to the requirements of their specific environment.

Most tissue engineering strategies to create small caliber vascular grafts is attempt to closely mimic the structure, function, and physiologic environment of native vessels. Blood vessels are made of three layers named from the luminal side outward as; the tunica intima, the tunica media and the tunica adventitia. Each structural layer consist of distinct cell and matrix types whose composition reflects their function. The intima is composed of a monolayer of endothelial cells with an underlying basement membrane consisting of loosely organized type IV collagen and laminin. The endothelial cell (EC) lining provides a continuous selective permeable, hemocompatible blood contacting surface that is critical for the maintenance of vessel patency. It controls vessel tone, platelet activation, adhesion and aggregation, leukocyte adhesion and smooth muscle cell (SMC) migration and proliferation.

The collagen fibres, elastic fibres, elastic lamellae and proteoglycans normally laid down by ECs and SMCs during blood vessel development, provide vessels with elasticity and radial compliance and they may also profoundly influence vascular cell adhesion and function. The re-creation of some or all of the vessel layers and their properties may result in the development of a patent, functional vascular graft. In all likelihood, an intima, i.e., a luminal functional endothelial monolayer will be required to achieve any degree of success. The ECM is required for cell survival and proliferation in response to growth factors, rendering cells apoptotic in the absence of matrix (Re *et al.*, 1994). The vascular

wall ECM, composed of structural proteins like collagen and elastin, adhesion proteins like fibronectin and laminin, glycosaminoglycans, proteoglycans, growth factors, cytokines, matrix degrading enzymes and their inhibitors (Ruoslahti and Engvall, 1997) together regulate major cellular programs such as growth, differentiation and apoptosis. The cells and their supporting cellular elements also directly modify (remodel) their immediate extra cellular environment. In tissue engineering, ECM proteins that are deposited by the cells play a major role in determining the construct stability as well as regulation of the cell-matrix interactions (Stock *et al.*, 2001). But precise control of the cell-matrix interactions and induction of ECM remodeling remains a main challenge.

In the case of a tissue-engineered vascular graft, the major requirement is to create a substitute with the appropriate mechanical properties, not just an adequate burst pressure, but visco-elastic properties that mimic those of native arteries. Many of the vascular tissue engineering concepts being pursued resulted in a tubular construct of sufficient strength, but, they lacked the appropriate visco-elastic properties due to insufficient amount and poor assembly of elastin (Nerem, 2004). The synthesis of collagen is also found to be very slow *in vitro* both in monolayer and 3-dimensional (3-D) cultures (Lareu *et al.*, 2007). The synthesis of ECM proteins, elastin and collagen, by the cells is crucial in vascular tissue engineering to provide adequate mechanical strength and viscoelastic properties to the construct while the scaffold is degrading. Since the tissue engineered grafts must function immediately upon implantation, remodeling of the underlying ECM should take place during the culture period before implantation to achieve post-implant EC survival and vaso-responsiveness of the construct. But the production of the precise ECM was rarely achieved during *in vitro* conditions used for EC culture and while seeding them on biomaterials for making vascular conduits.

In the first biological model for tissue-engineered vascular construct that demonstrated sufficient mechanical strength, abundant endogenous synthesis of ECM by mesenchymal cells was observed when they were cultured in presence of ascorbic acid (L'Heureux *et al.*, 1998). Their construct displayed histological organization, ECM composition, cell differentiation markers, and cellular

functions observed in normal human blood vessels. Another remarkable aspect of their model was the presence of elastin fibers, an important ECM component never reported in other tissue engineered blood vessel (TEBV) (L'Heureux *et al.*, 1993; Hirai and Matsuda, 1996). But the limitation in this approach was the requirement of long term culture period. Hence, it is important to get ECM deposition at an early period of tissue construction so that construct can be developed with short culture time. Excessive ECM synthesis may inhibit the functionality of the tissue. Also, the scaffold should support easy cell expansion *in vitro* to reduce the time of construction. Optimal combinations and concentrations of cytokines and growth factors are important to regulate EC proliferation and migration.

The response of the cells to physiologic mechanical stimuli needs to be evaluated to predict their behavior in the very active *in vivo* hemodynamic environment. Stability of EC in the vascular construct is essential to resist the shear stress of blood flow, so that cells do not displace from the lumen when the flow is restored after implantation. The subendothelial ECM provides stable EC anchorage through interactions with cell surface receptors and resists shear stress.

Functional integrity of the endothelium is crucial for the maintenance of blood flow and antithrombotic capacity, because the endothelium releases humoral factors that control relaxation and contraction, thrombogenesis and fibrinolysis, and platelet activation and inhibition. Hence as the ECM remodeling takes place the cells should receive appropriate signals to maintain the normal phenotype.

Thus, successful vascular tissue engineering requires optimization of *in vitro* culture environment that would produce functional constructs. This study aims to carefully engineer an optimum matrix composition and systematically study EC proliferation and survival, simultaneously remodeling the ECM *in vitro* with the maintenance of normal cell phenotype, which may assist in the creation of a tissue engineered vascular conduit.

1.2. REVIEW OF LITERATURE

1.2.1. Cardiovascular disease and regenerative therapy

Autologous grafts for treatment of coronary artery disease include the saphenous vein, internal mammary artery, and radial artery. In some circumstances, the use of autologous material is not possible due to concomitant diseases or previous use, and artificial grafts must be used (Arrigoni *et al.*, 2006). The success rate of bypasses using conduits of diameters greater than 6 mm has been excellent, whereas the majority of bypasses using smaller conduits fail within 5 years (Leon & Griesler, 2003). Vein grafts fail most commonly due to the development of fibrous intimal hyperplasia, which is a flow restricting lesion that may occur diffusely throughout the graft or, more commonly, at focal sites near anastomoses or in the body of the graft. They are also subject to progressive atherosclerotic degeneration after implantation. Synthetic materials, mainly poly(ethylene terephthalate) (Dacron) and poly(tetrafluoroethylene) (PTFE) are frequently used for treatment of peripheral vascular disease, but they are limited to high-flow/low-resistance conditions, because of poor elasticity, low compliance, and thrombogenicity of synthetic surfaces (Hoenig *et al.*, 2005). In addition, the materials that are commonly used lack growth potential and long-term results have revealed several material related failures, such as stenosis, thromboembolization, calcium deposition and infection (Heydarkhan-Hagvall *et al.*, 2006).

In view of this, enormous efforts have been made over the last 30 years to produce alternative small-caliber grafts with acceptable patency rates. An ideal artificial vascular graft should closely mimic the natural vessel, be resistant to thrombosis, inflammation, and neointimal proliferation.

Attempts to improve synthetic polymer grafts have included embedding them with antithrombotic drugs, seeding with ECs, or developing new biomaterials. Begovac *et al.* (2003) reported surface immobilization of heparin on GORE-TEX vascular graft, the improvement being only marginal when compared to the standard prosthesis. Polyurethane vascular prosthesis was improved by dipyridamole coating on its luminal surface (Aldenhoff *et al.*, 2001). Further

research in this approach have included covalent linking of hirudin on ionic poly(carbonate) urethane polymer (Phaneuf *et al.*, 1998), tissue factor pathway inhibitor pretreatment on Dacron grafts (Sun *et al.*, 2001), and a nonthrombogenic phospholipid polymer surface (Yoneyama *et al.*, 2000) for reducing the thrombogenicity of graft surface. The surface texture of prostheses has also been altered in an attempt to increase patency and promote endothelialization (Fujisawa *et al.*, 1999).

The lack of viable ECs on the luminal surface of artificial grafts contributes to synthetic graft thrombogenicity and promotes intimal proliferation within the graft. EC seeding of synthetic grafts has been attempted to mitigate these limitations. Herring *et al.* (1978) were the first to report the successful isolation and their subsequent transplantation of ECs onto synthetic vascular grafts. They observed improved patency rates for seeded grafts compared to unseeded grafts when the cells were seeded onto 6mm Dacron grafts. This approach has been limited in some cases by poor retention of ECs on biomaterial surfaces once exposed to blood flow. Thus, significant effort has focused on improving endothelial adhesion to biomaterial surfaces.

The majority of the work on promoting EC adherence and growth to permanent non biodegradable polymers has involved the modification of surface with a single coating of endothelial specific adhesion proteins. These substances include collagen (Itoh *et al.*, 2001), collagen-elastin matrices (Goissis *et al.*, 2000), fibronectin, gelatin (Marois *et al.*, 1999), fibrin-gelatin(Kumar & Krishnan, 2002), laminin (Schneider *et al.*, 1992), ECM (Ye *et al.*, 2000), granulocyte stimulating factor (Shi *et al.*, 2002), pre clotting with blood, plasma, fibrin glue (Bach *et al.*, 2001) and serum (Haegerstrand *et al.*, 1993). Prosthetic surfaces have been coated with growth factors such as fibroblast growth factor (Gosselin *et al.*, 1996) or endothelial cell growth factor (Greisler *et al.*, 1987) or by combination coatings (Anderson *et al.*, 1987) to enhance cell retention. Synthetic grafts have been impregnated with basic fibroblast growth factor which has shown to significantly increase the amount of endothelialization occurring in situ (Doi *et al.*, 1996). Small-caliber, long-fibril ePTFE vascular grafts with covalent bonding of fibronectin achieved almost complete neointimal healing by the time of retrieval at 12 weeks. (Shimada *et al.*, 2004). Attempts to alter grafts with Arg-

Gly-Asp (RGD) sequence peptides to enhance EC adhesion (Walluscheck *et al.*, 1996) are also reported.

1.2.2. Vascular Tissue Engineering

There has been remarkable progress in research and development in the area of cardiovascular tissue engineering, especially, TEBV over the past 20 years. Functional TEBVs should be non-thrombogenic, nonimmunogenic, compatible at high blood flow rates and have similar viscoelasticity to native vessels (Nerem and Selitkar, 2001; Vara *et al.*, 2005; Heyligers *et al.*, 2005). Moreover, the grafts should be living tissues that could eventually integrate into the body and become indistinguishable from the native vessels. Several methodologies have emerged for constructing blood vessel replacements with biological functionality. These include cell seeded collagen gels, acellular techniques, cell seeded biodegradable synthetic polymer scaffolds, cell self-assembly and peri-vascular implants.

1.2.2.1. Cell seeded collagen gels

The development of a completely TE artery began with the co-culture of ECs and SMCs in ECM components such as collagen tubes (Weinberg & Bell, 1986). A layer of fibroblasts was added around the outside of the tube, and ECs were seeded onto the luminal surface. A Dacron sleeve was added between the medial and adventitial layers to provide strength to withstand physiological pressures. Electron microscopy showed that the ECs lining the lumen and the SMCs in the wall were healthy, well differentiated, and biochemically active, producing vWF and prostacyclin. Despite their reinforcement with Dacron mesh, these constructs were unable to attain adequate burst strengths for *in vivo* applications. The vessel also lacked elastin.

Ishibashi and Matsuda (1994) used knitted Dacron for support of their construct, with an intimal layer of ECs, a medial layer of SMCs, and an adventitial layer of fibroblasts in a mixed gel of collagen I and dermatan sulfate. After 12 weeks of implantation in dogs, the collagen fibers in the intimal layer were longitudinally oriented, whereas those in deeper layers were circumferentially

oriented and elastin deposition was observed. Matsuda and Miwa (1995) created hybrid constructs on knitted Dacron grafts using EC monolayer that formed on collagenous medial tissue in which SMCs were incorporated. The construct was shown to remodel *in vivo* such that the ECs on the lumen became oriented in parallel to the direction of flow, and the SMCs in the medial layer redistributed and became circumferentially oriented. Implants were successful in the canine model for 1 year. This was further improved by wrapping with biodegradable materials, such as cross-linked type-I collagen and elastin (Berglund *et al.*, 2004).

L'Heureux *et al.* (1993) introduced a culturing technique that allowed the cells to contract the collagen gel over a central mandrel without adhering to it. Constructs developed in this manner exhibited significant increase in material modulus compared with constructs cultured without a central mandrel; however, they were still not strong enough (burst pressure < 120 mmHg) to withstand arterial pressures. Hirai *et al.* (1994) varied the initial collagen concentration to improve the burst strength of the collagen constructs. Tranquillo *et al.* (1996) introduced the concept of magnetic pre-alignment during fibrillogenesis (the spontaneous formation of collagen fibrils) in an effort to induce the favorable realignment of the collagen fibrils. This approach proved to be successful with constructs cultured without a central mandrel; however, mandrel contraction was more beneficial to construct integrity than was magnetic pre-alignment. Despite the numerous efforts, these constructs were still limited by the poor mechanical integrity of the reconstituted collagen gel. To date, the collagen-based constructs can withstand a pressure of approximately 225 mm Hg, which is not acceptable for arterial replacement surgery (Nerem & Selitkar, 2001). Girton *et al.* (2000) created blood vessel equivalents with SMCs and collagen, and demonstrated that significant stiffening and strengthening of the collagen gel constructs could be achieved through glycation of the collagenous matrix. This was done by culturing constructs in a medium containing elevated levels of glucose or ribose. Application of dynamic mechanical stimulation was also adopted to improve the strength of the collagen gel-based grafts (Isenberg and Tranquillo, 2003; Selitkar *et al.*, 2000).

1.2.2.2. Acellular and cell seeded decellularised xenografts/allografts

Researchers have also looked at other approaches using natural materials for use as vascular constructs. Small intestinal submucosa has been used extensively as a conduit material for vascular graft in dogs (Badylak *et al.*, 1989; Lantz *et al.*, 1990; Sandusky *et al.*, 1992) and has shown its feasibility. High patency rates have been reported in the canine aorta, in carotid and femoral arteries, and in the superior vena cava (Lantz *et al.*, 1993). However, in an experiment in which microvessel grafts were implanted in rats, none of the grafts remained patent beyond the first hour (Prevel *et al.*, 1994). Huynh *et al.* (1999) demonstrated that a small-diameter (4-mm) graft constructed from a collagen biomaterial derived from small intestine submucosa and type I bovine collagen has the potential to develop into a functional blood vessel. In an animal model of rabbit arterial bypass, the collagen grafts displayed patency 3 months after implantation. The grafts remodeled into cellularized vessels that responded physiologically to vasoactive agents. Inoue *et al.* (1996) reported a similar technique that employed rolled human acellular dermal matrix as a small-diameter vascular graft. The patency rates of acellular dermal grafts were superior to ePTFE grafts when implanted into the rat femoral artery for 28 days. However, they exhibited false aneurysms around the longitudinal suture line.

Xenograft and allograft tissue have been investigated for use as bio prosthetic vascular devices. Cryo-preserved allografts have been used clinically as coronary artery bypass conduits, but they have limited use because of their poor patency rates and problems with aneurysms (Schmidt and Baier, 2000). Teebken *et al.* (2000) demonstrated that when decellularized porcine aortas were seeded with ECs and myofibroblasts isolated from human saphenous vein and cultured in a reactor under pulsatile flow, the ECs proliferated to form a confluent monolayer on the lumen. Similar work was performed by seeding human umbilical vein ECs or adult human vascular SMCs onto the decellularized porcine aortas after different decellularization processes (Amiel *et al.*, 2006; McFetridge *et al.*, 2004). However, studies found that cell migration into these scaffolds was inadequate due to the very tight matrix organization specific to the aortic structure. To address this problem, Simionescu *et al.* (2006) prepared pure elastin scaffolds and pure collagen scaffolds by selectively removing the collagen

component or elastin to create more porous scaffolds for cell infiltration. Enhanced potential for repopulation by host cells *in vivo* was observed after subdermal implantation. In addition, new collagen fibres and bundles were found within the re-modeled elastin scaffolds and new elastin fibres within collagen scaffolds, respectively, indicating that they are able to support *de novo* ECM synthesis.

Kaushal *et al.* (2001) seeded *ex vivo* expanded sheep endothelial progenitor cells (EPC) from peripheral blood onto decellularized porcine iliac vessels and demonstrated that the EPC-seeded grafts remained patent for 130 days as a carotid interposition graft in sheep, whereas non-seeded grafts occluded within 15 days. The EPC-explanted grafts exhibited contractile activity and nitric-oxide-mediated vascular relaxation that were similar to native carotid arteries.

Engineered blood vessel produced by endothelialization of decellularized xenografts which is easy to access is a good option (Amiel *et al.*, 2006). However, the risk of transmission of animal pathogens to human being is still a big concern. To avoid such problem, vessels from human being are the optimal choice (Schaner *et al.*, 2004). Daniel *et al.* (2005) decellularized human umbilical vein (HUV) using an automated dissection methodology and created a promising scaffold that has excellent potential for cellular integration and maintain the mechanical properties of the native blood vessels. The HUV scaffold could be a good candidate for vascular engineering.

1.2.2.3. Perivascular implants

Campbell *et al.* (1999) reported an innovative method for producing TE vascular conduits. Silastic tubing was implanted in the peritoneal cavity of a rat or rabbit. After 2 weeks, the tube was covered with layers of myofibroblasts, collagen matrix, and a single layer of mesothelium. The Silastic tubing was then removed, and the tube of tissue was reverted, with the tissue now resembling a blood vessel in structure: the layer of mesothelial cells became the intima; layers of myofibroblasts, collagen, and elastin became the media; and an outer collagenous layer became the adventitia. This tissue tube was then grafted into

the carotid artery or abdominal aorta of the same animal where the tubes remained patent for 4 months and developed structures resembling elastic lamellae.

Nugent *et al.* demonstrated that the biological effect of cells on vascular repair is maintained when they are implanted at a site distant to their original location. ECs were cultured on 3D polymer matrices and implanted in the perivascular space of balloon-injured rat or pig carotid arteries. Perivascular ECs reduced intimal thickening in both rats and pigs. Compared with control porcine arteries, porcine arteries wrapped with ECs also had reduced occlusive thrombosis and higher patency rates at 1 and 3 months (Nathan *et al.*, 1995; Nugent *et al.*, 2001). These effects were not limited to mechanically injured arteries. Side-to-side arteriovenous fistulae were created with femoral arteries and veins in pigs (Nugent *et al.*, 2002). Intimal thickening, observed within the venous segment at 1 and 2 months was significantly reduced in the EC-treated animals compared with control animals.

1.2.2.4. Cell self assembly

A key challenge in the development of a cellular model blood vessel was to create construct with required mechanical properties. L'Heureux *et al.* (1998) improved the mechanical strength of these constructs by alterations in culture conditions. They report the successful development of an arterial substitute based on *in vitro* culture of vascular cells without the use of a scaffold. A sheet of SMCs in their own ECM was wrapped around a tube, covered with a sheet of fibroblasts in their own ECM, and then the luminal surface was seeded with ECs. This construct reportedly had burst strength of over 2,000 mm Hg. In addition, the SMCs expressed desmin, and the ECs strongly inhibited platelet adhesion *in vitro*. However, when these grafts were implanted in dogs as a canine femoral arterial interposition graft, they had a patency rate of approximately 50%. In addition, the grafts required 3 months for production. This approach has been further testified in patients with haemodialysis (L'Heureux *et al.*, 2007). The vessels constructed from autologous dermal fibroblasts and ECs were implanted as arteriovenous fistulas for dialysis access and were allowed to mature *in vivo* before use. During 5 months of implantation, no failures were observed with the

first three patients, and the grafts were functioning well. These results are extremely encouraging. However, this approach is time consuming that would limit the application of these vessels in urgent cases.

1.2.2.5. Cell seeded biodegradable synthetic polymer scaffolds

Another approach involved the use of synthetic polymeric materials as scaffolds to guide cell growth. This approach is similar to that used for permanent prosthetic scaffolds, except that the scaffold degrades once the artery is formed and remodeled. Shin'oka *et al.* (1998) created a pulmonary artery conduit by seeding tubular polyglactin/polyglycolic acid (PGA) scaffolds with SMCs followed by ECs. After an *in vitro* culture period, the conduits were implanted into the pulmonary arteries of lambs and evaluated between 11 and 24 weeks. In contrast to the acellular control, the TE scaffolds appeared histologically to be nearly identical to native arteries. The first clinical application of using an engineered vessel based on biodegradable scaffold was also reported by Shin'oka *et al.* (2001). The peripheral pulmonary artery was successfully reconstructed in a 4-year-old girl with the patient's own venous cells seeded onto a polycaprolactone–polylactic acid copolymer tube that was reinforced with woven PGA. In their following study, they took another approach of using autologous bone marrow cells (BMCs) as a cell source to avoid the time-consuming cell culture step (Matsumura *et al.*, 2003; Shin'oka *et al.*, 2005). Cells were harvested on the day of surgery, seeded directly on the polymer tube and the grafts were implanted right after 2–4 h of *in vitro* incubation. Twenty-three tissue-engineered conduits and 19 tissue-engineered patches were implanted for the repair of congenital heart defects (Shin'oka *et al.*, 2005). They reported over 95% patency at 1 year without evidence of aneurysm formation or calcification. Moreover, there were no complications such as thrombosis, stenosis and obstruction of the tissue engineered grafts. But, regarding the differentiation of BMCs, this method has potential risks. Long-term follow-up is desired to confirm the remodeling of the scaffold and the durability of this approach.

Shum-Tim *et al.* (1999) demonstrated that a polymer of PGA and polyhydroxyalkanoate seeded with cells from lamb carotid arteries and grafted into lamb aorta had 100% patency at 5 months. In a similar study, Niklason *et al.*

showed 100% patency 4 weeks after implantation of pigs with modified PGA scaffolds that had been seeded with bovine SMCs and exposed to pulsatile flow conditions for 8 weeks (Niklason *et al.*, 1999). Contractile response of these grafts was only 5% of normal rabbit aorta, but they had burst pressures in excess of 2000 mm Hg. Another scaffold material investigated for vascular grafting is esterified hyaluronic acid (HA) (Remuzzi *et al.*, 2004). Unfortunately, the grafts based on esterified HA had a low axial strength and high stiffness when compared with normal porcine arteries.

1.2.3. Challenges in vascular tissue engineering

There are certain basic properties of the native vasculature that a successful tissue engineered vascular graft (TEVG) must achieve and these can be categorized into mechanical and biological properties (Nerem and Selitkar, 2001). First, the vessel must be of sufficient mechanical strength, not to rupture when exposed to arterial blood pressure and flow. This means that any technique used to fabricate the blood vessel must result in a conduit that will function mechanically immediately upon implantation. It is also essential that the TEVG match the mechanical properties of the vessel to which it is being grafted, as compliance mismatch at the anastomosis is thought to be involved in the development of intimal hyperplasia and subsequent graft failure (Salacinski *et al.*, 2001). For this, the TEVG should have appropriate remodeling of tissue in *in vitro* culture conditions so that they can be replicated *in vivo* to approach functionality in time. Elastin is a critical structural and regulatory matrix protein and plays an important and dominant role by conferring elasticity to the vessel wall (Patel *et al.*, 2006). Poor elastin synthesis during the development is a critical factor that is leading to the failure of TEVGs. From a biological standpoint, it is essential that any TEVG be anti-thrombogenic. Finally, another major requirement - and unfortunately a severe limitation in current vascular grafts - is that the vessel must be vasoresponsive in order to function adaptively under changing blood pressure and flow. Another limitation is the requirement of long culture period to produce the construct. The culture period for the construct should be short so that the supply of the constructs would not be limited in emergency cases.

1.3. DEVELOPMENT OF STUDY HYPOTHESIS

During the *in vitro* tissue engineering the EC growth is expected to be similar to the process of *in vivo* angiogenesis. If the process is mimicked *in vitro*, a functionally normal and mechanically strong endothelium that would resist the forces of blood flow may be achieved. Therefore to start the EC culture *in vitro*, a biomimetic ECM would ideally promote good cell adhesion, spreading, proliferation, survival and differentiation, followed by deposition of new ECM by growing endothelium. In addition, to form a tubular construct, a mechanically strong and biodegradable scaffold is required. Combined with polymer scaffold and biomimetic matrix a hybrid scaffold may be engineered on which EC can grow and form a functional and quiescent endothelium. To select the appropriate matrix composition and biodegradable polymer, the literature was reviewed and the specific role of each component was identified as described here.

1.3.1. Role of Extra cellular matrix in tissue integration

Adhesive interactions between ECs and the structural and superficially bound proteins that make up the ECM are critical for maintaining the properties of the endothelium. The ECM is a vital component of the cellular environment which is composed of fibrillar proteins like collagen and elastin, adhesive proteins like fibronectin and laminin, glycosaminoglycans and proteoglycans to which cells adhere and provides structural and organizational stability to the tissue. ECM specifically binds cytokines and growth factors, affecting both their availability and biological activity. The ECM is critical for all aspects of vascular biology. It serves essential functions in supporting key signaling events involved in regulating EC migration, invasion, proliferation, and survival. The provisional ECM serves as a pliable scaffold being degraded by matrix metalloproteinases during angiogenesis.

1.3.2. Cell - Extra cellular matrix interactions

Integrins are the principle mediators of cell interactions with the ECM. They are a family of non-covalently associated heterodimeric cell surface receptors composed of α - and β -subunits that mediate cell-ECM and cell-cell

adhesions. There are 18- α and 8- β subunits not including splice variants that combine to form more than 24 different integrins. Each α - β combination has its own binding specificity and signaling properties. Most integrins recognize several ECM proteins and conversely, individual matrix proteins, such as fibronectin, laminins, collagens, and vitronectin, bind to several integrins. Integrins can signal through the cell membrane in either direction: the extra cellular binding activity of integrins is regulated from the inside of the cell (inside-out signaling), while the binding of the ECM elicits signals that are transmitted into the cell (outside-in signaling) (Giancotti and Ruoslahti, 1999). Through signaling, integrins can control gene expression, cell shape, proliferation, differentiation, and survival.

EC proliferation and survival are highly dependent on adhesion to ECM through cell-surface integrins (Giancotti and Ruoslahti, 1999). In particular, activation of the p44/p42 (Erk1/Erk2) mitogen-activated protein kinase (MAPK) signal transduction pathway (Vinals *et al.*, 1999) and the expression and activities of cyclin-dependent kinases, which are required for cell cycle progression, are dependent on EC adhesion to ECM (Fang *et al.*, 1996). ECs bind to their matrix via β_1 or α_v integrins to activate JAK/STAT pathways, increasing c-fos transcription leading to proliferation, and binding of the $\alpha_v\beta_3$ integrins are required for sustained activation of MAPK/ERK pathways for angiogenesis (Brizzi *et al.*, 1999). The $\alpha_v\beta_1$ and $\alpha_5\beta_1$ fibronectin receptors are highly expressed in quiescent ECs, whereas the $\alpha_v\beta_3$ fibronectin and vitronectin receptor is expressed only during the process of angiogenesis (Brooks *et al.*, 1994). Lumen formation during development depends upon $\alpha_2\beta_1$ interaction with collagen and $\alpha_v\beta_3$, and $\alpha_5\beta_1$ interacting with the RGD sequences of fibronectin. (Eliceiri *et al.*, 1998). A second peptide domain from fibronectin, Arg-Glu-Asp-Val (REDV), is an exclusive ligand for ECs through the $\alpha_4\beta_1$ integrin (Mann *et al.*, 1999, Massia and Hubbell, 1992). Multiple integrins act together in regulating vascular morphogenesis i.e, $\alpha_2\beta_1$ and $\alpha_1\beta_1$ in collagen matrices or $\alpha_5\beta_1$ or $\alpha_v\beta_3$ in fibrin matrices and vascular stabilization by $\alpha_6\beta_1$ or $\alpha_3\beta_1$ in combination with $\alpha_2\beta_1$ or $\alpha_1\beta_1$ to create unique combinations of signals.

1.3.3. Influence of growth factors in vascular regeneration

There also appears to be a synergism between the binding of integrins to the matrix and soluble growth factors (Schwartz and Ginsberg, 2002). Research has shown that fibronectin enhances EC differentiation induced by (vascular endothelial growth factor (VEGF) (Wijelath *et al.*, 2004), and cell adhesion enhances autophosphorylation of platelet derived growth factor (PDGF) (Bottaro *et al.*, 2002). PDGF-BB induces EC migration via $\alpha_v\beta_3$ integrins in an RGD-dependent manner on fibronectin, and VEGFR2 signals with $\alpha_v\beta_3$. However, both the PDGFR and VEGFR2 receptors associate with the β -subunit of the integrin without directly causing signaling or activation of their respective tyrosine kinases, thus indicating that the integrins may amplify, or provide secondary signals that amplify, the signal provided by growth factors binding to receptor tyrosine kinases (Rupp and Little, 2001).

The growth factors or other cellular processes can change the expression of integrins or their binding ability. It has been shown that VEGF165 stimulates $\alpha_1\beta_1$, $\alpha_2\beta_1$, and $\alpha_v\beta_3$ integrins, that FGF-2 (Fibroblast growth factor-2) increases expression of $\alpha_v\beta_3$ integrins in microvascular ECs, and that VEGF enhances migration through $\alpha_v\beta_3$ as well as activating $\alpha_v\beta_5$, $\alpha_5\beta_2$, and $\alpha_2\beta_1$ integrins (Rupp and Little, 2001). The ECM also serves as a binding site for soluble or semi soluble growth factors, such as the VEGF isoforms 165 and 181 and FGF-2. The immobilization of these growth factors within the matrix offers a dynamic concentration of free molecules (Bottaro *et al.*, 2002). This dynamic chemical environment can cause differential signaling, resulting in varying cellular function and chemotaxis.

1.3.4. Role of glycosaminoglycans in angiogenesis

Most of the growth factors and cytokines that are involved in wound healing and angiogenesis are immobilized at the cell surface and in ECM through proteoglycans (PG) / glycosaminoglycan (GAG) binding (Ruoslahti and Yamaguchi, 1991). During the inflammatory phase intact hyaluronic acid (HA) in the blood clot of wound helps in the physical stabilization of the matrix. It also

stimulates cell infiltration and migration, and controls the degradation of fibrin. The degradation products of HA–fibrin matrix act as regulator molecules of the wound healing process. Small HA fragments stimulate both angiogenesis and phagocytic activity of macrophages (Weigel *et al.*, 1986).

Several studies have reported an increased production of hyaluronan during inflammation in wound repair (Toole, 1981). Another important GAG is heparan sulphate. Basic fibroblast growth factor (bFGF) is sequestered and protected by binding with heparan sulphate which gives stability to bFGF rather than free bFGF (Vlodavsky *et al.*, 1991). This binding also gives the necessary conformation for optimal interaction with the cell-surface receptors (Roberts *et al.*, 1988). The binding of FGFs to heparin appears to protect the growth factor from degradation (Ruoslahti and Yamaguchi, 1991). The activities of some proteases and anti-proteases found in inflammatory fluids can be modified *in vitro* by heparin (Kainulainen *et al.*, 1998). One of the major events in granulation tissue formation is the deposition of a loose ECM. HA is a major component of early granulation tissue (Clark, 1996) and creates an environment for cell movement by expanding the extra cellular space. During maturation of the wound, the HA content of the connective tissue tends to decrease quite rapidly while the chondroitin sulphate and dermatan sulphate contents tend to increase. These PGs are involved in collagen fibre formation. Syndecan, a cell surface heparan sulphate proteoglycan was found to be involved during this phase of healing. Syndecan 1 ecto is a strong inhibitor of heparin-mediated FGF-2 division of cells. However, on removal of syndecan 1 from the system by degradation, cells start proliferating again. Syndecan 1 also binds to the collagens and fibronectin deposited during repair, due to which the tissue reverts to a quiescent state (Kato *et al.*, 1998).

In general, GAGs are over-expressed during the early stage of wound healing and angiogenesis and come to their normal level in the remodeling phase. The cross linking between collagen and GAG provides adequate strength to the tissue and it becomes resistant to collagenase digestion. HA which allows the migration of cells to the sites of connective tissue development, is the predominant GAG during the early phase of healing (Toole, 1981).

1.3.5. Extra cellular matrix remodeling in physiology

The ECM is an intricate and complex network of proteinaceous fibers and other macromolecules that profoundly influences cellular function and tissue architecture. Among the molecules that are relevant to cell–ECM interactions are integral membrane proteins, including integrins, which provide a link between the ECM and the cytoskeleton, and extra cellular proteases and their inhibitors, which mediate focal degradation of the ECM during cellular invasion. ECM proteins interact directly with cell surface receptors to initiate signal transduction pathways and to modulate those triggered by differentiation and growth factors. The ECM also controls the activity and presentation of a wide range of growth factors. Thus modulation of the ECM, by remodeling its structure and activity, has profound effects on its function and the consequent behavior of cells residing on or within it (Streuli, 1999). The wide spectrum of ECM receptors and cognate ligands provides a source of great diversity for cell-matrix interaction and the cells monitor their local environment and respond appropriately by altering intracellular signaling pathways downstream of growth factor receptors. Different ECM components can selectively affect many types of signal transduction pathways including those leading to suppression of apoptosis and to differentiation.

Remodeling of extra cellular matrices occurs during development, wound healing, angiogenesis and in a variety of pathological processes including atherosclerosis, ischemic injury. Perturbing matrix remodeling events by preventing the turnover of ECM molecules or by increasing the levels of matrix degrading proteases or inhibitors has been shown to result in fibrosis, reduced angiogenesis and developmental abnormalities. Thus processes which control the rate and extend of matrix deposition and degradation play key roles during tissue remodeling events. Mesenchymal stem cells derived from primary epithelia require remodeling events within the matrix in order to traverse the stroma and reform specific cell types of the epithelia indicating that during development, the generation and maintenance of cellular diversity is dependent on ECM remodeling (Hay, 1990).

Angiogenesis is critically dependent on extra cellular signals that are spatially restricted by their association with components of the ECM. It involves the differentiation and organization of ECs into capillary tubes and the interplay between growth factors and cytokines. Cell adhesion molecules generally mediate innumerable cell-cell and cell-matrix interactions. These, in conjunction with the recruitment of supporting pre-ECs that encase the endothelial tubes, provide maintenance and modulatory functions to the vessel. Supporting cells usually include pericytes in small capillaries and SMCs in larger vessels. (Folkman and D'Amore, 1996; Hanahan, 1997).

Accumulation of extravascular fibrin in the extra cellular milieu is one of the hallmarks of angiogenesis (Dvorak *et al.*, 1995). In contrast to matrices composed of collagen or other macromolecules, fibrin constitutes a provisional matrix that is progressively removed and replaced by other matrix components, including collagen. Although the mechanisms by which fibrin induces mature matrix formation are poorly understood, fibrin itself is chemotactic for inflammatory cells and has been shown to regulate EC and fibroblast migration.

In all types of angiogenesis, either under physiologic or pathologic conditions, EC activation is the first process to take place. It is suggested that VEGF is a major player in angiogenesis initiation based on its ability to induce vasodilation via endothelial nitric oxide (NO) production and its EC permeability increasing effect (Ziche *et al.*, 1997). This allows plasma proteins to enter the tissue to form a fibrin-rich provisional network (Dvorak, 1986). Besides affecting vasodilation and vascular permeability, VEGF can induce the expression of proteases and receptors important in cellular invasion and tissue remodeling and is able to prevent EC apoptosis (Gupta *et al.*, 1999). After proper activation of ECs, endothelial penetration into new areas of the body is achieved by degradation of the basement membrane by matrix metallo-proteinases (MMPs). These extra cellular endopeptidases are secreted as zymogens that become activated in the ECM compartment and subsequently selectively degrade components of the ECM (Stetler Stevenson, 1999). They are produced by a variety of cells, including epithelial cells, fibroblasts, inflammatory cells, and ECs. MMP activity and, hence, angiogenesis is counteracted by the family of tissue

inhibitors of metalloproteinases (Gomez *et al.*, 1997). By preserving matrix integrity and thereby ensuring normal tissue architecture, protease inhibitors play an important permissive role during angiogenesis.

Plasmin is believed to be the most important protease for the mobilization of FGF-2 from the ECM pool. Plasmin degrades fibronectin, laminin, and the protein core of proteoglycans. Plasminogen activators (PA), urokinase-PA and tissue-PA convert the ubiquitous plasma protein plasminogen to plasmin. In addition, plasmin activates certain metalloproteinases. FGF members are directly acting proangiogenic molecules. FGF-2 consists of, in two modifications, an 18- kDa low-molecular weight form and a 22- to 24-kDa high-molecular weight form. During angiogenesis, low-molecular weight FGF-2 binding to endothelium induces FGF receptor (FGF-R) down-regulation, increased motility, proliferation and proteinase activity, and modulates integrin levels. High-molecular weight FGF-2 may act on EC proliferation after nuclear translocation in the ECs (Klein *et al.*, 1997). Recently, it was shown that a secreted FGF-2-binding protein could bind FGF-2 that is normally inactive due to strong adherence to heparan sulfate proteoglycans in the ECM. The displaced FGF-2 molecules were thus released to mediate biological function. Besides its effect on angiogenesis initiation, VEGF also affects EC proliferation. This effect can be (partly) attributed to NO and cyclic guanosine monophosphate -mediated activation of the MAPK family.

After EC proliferation, maturation and the formation of endothelial tube structures ECs accomplish the arrangement of surrounding vessel layers composed of mural cells (pericytes in small vessels and SMCs in large vessels), via the synthesis and secretion of PDGF, a mitogen and chemoattractant for a variety of mesenchymal cells. The recruitment of pericytes by PDGF-BB is critical to the stabilization and maturation of nascent vascular structures (Darland and D'Amore, 1999). Subsequent differentiation of the mural precursor cells into pericytes and SMCs is believed to be a cell-cell contact dependent process. On EC-mural cell contact, a latent form of Transforming growth factor (TGF)- β , produced by both endothelium and mural cells, is activated in a plasmin-mediated process. Activated TGF- β can induce changes in myofibroblasts and pericytes, which may contribute to the formation of a quiescent vessel, ECM

production, and maintenance of growth control. The coinciding investment of growing capillaries by pericytes with the deposition of basement membrane and cessation of vessel growth during wound healing also indicates vessel growth regulation by pericytes (Hirschi and D'Amore, 1997). FGF-1 is also implicated in EC differentiation leading to vascular tube formation. Besides inducing plasminogen activator and EC proliferation and migration, FGF-1 receptor signaling resulted in endothelial tube formation in collagen (Kanda *et al.*, 1996).

Besides the proangiogenic factors VEGF, FGF-1, and FGF-2 ; TGF- α and TGF- β , granulocyte macrophage-colony-stimulating factor, epidermal growth factor, interleukin-1 (IL-1), scatter factor, platelet-activating factor, IL-8, and substance P (Bouck *et al.*, 1996; Yoshida *et al.*, 1997) have been identified in various settings of physiologic and pathologic angiogenesis. Their effects can be either directly or indirectly on the endothelium via activation of surrounding cells to produce other factors with proangiogenic activity or modulation of receptor/s activities (Yoshida *et al.*, 1997; Giraudo *et al.*, 1998).

1.3.6. Fibrin – A biological scaffold

Development of biomimetic scaffolds which contain well defined ECM like physicochemical features to promote selective cell interactions is fundamental in the field of tissue engineering and biomaterials science. Tissue engineering scaffolds must meet a number of basic criteria; they must be resorbable, they must not elicit a foreign body response, they must possess adequate mechanical strength to perform its function upon implantation, and they must encourage and promote cell invasion and remodeling of the scaffold. The tissue engineering scaffold then serves as a bridge guiding cell mediated remodeling to reproduce the structure and organization of the intended tissue. As such, the scaffold should provide contact guidance cues directing the development of alignment and should provide chemical cues directing compositional and organizational changes in the construct. Given these requirements, fibrin has been identified as a strong candidate for use in tissue engineering applications due to its role in promoting tissue remodeling during wound healing (Neidert *et al.*, 2002).

Fibrin is the natural provisional matrix for wound healing and tissue repair. The fibrin clot provides a structural scaffold for the adhesion, proliferation and migration of cells important in wound healing. Also, fibrin and the associated proteins making up a physiologic clot have intrinsic biological activities that support and control the cellular differentiation important in wound healing. Finally, fibrin clots are readily remodeled and resorbed through normal fibrinolytic processes as cells deposit the tissue-specific ECM components during the regeneration of functional tissues. An interesting feature of fibrin is the degradation and remodeling by cell associated enzymatic activity during cell migration and wound healing (Lee and Mooney, 2001). Moreover, fibrinogen- the precursor of polymeric fibrin can be purified from blood, offering the opportunity of using an autologous source for the scaffold and eliminating immunological concerns of human or cross species donor incompatibility (Meinhart *et al.*, 1999).

Fibrinogen, the monomeric form of fibrin, undergoes fibrillogenesis after the enzyme thrombin cleaves specific fibrinopeptides, allowing molecules to assemble laterally and form linear fibrils. The fibrils are eventually broken down through a process called fibrinolysis, which involves a series of enzymes leading to the activation of plasminogen which becomes the proteolytic enzyme plasmin. *In vitro*, fibrin forms a fibrillar network that can be compacted by entrapped tissue cells (Tuan *et al.*, 1996).

Sahni and Francis (2000) demonstrated that VEGF binds specifically and saturably to both fibrinogen and fibrin. Binding of VEGF to polymerized fibrin is different from binding to fibrinogen or fibrin monomer, as only a single binding site was identified, and the maximum molar-binding ratio of VEGF: fibrin was 0.1:1, indicating that VEGF bound to only 1 in 10 monomeric units. Their results also demonstrated that the binding of VEGF to fibrinogen is not inhibited by FGF-2, thereby indicating that the binding sites on fibrinogen for these 2 angiogenic peptides are independent and separate. FGF-2, another angiogenic peptide, also binds with high affinity to fibrin and fibrinogen (Sahni *et al.*, 1998) and this binding increases the capacity of FGF-2 to stimulate EC proliferation (Sahni *et al.*, 1999). Insulin-like growth factor-1, another peptide important in wound healing, also binds to fibrinogen and fibrin through insulin-like growth factor-1 binding protein-

3 with K_d values of 0.67 and 0.7 nmol/L, respectively (Campbell *et al.*, 1999). These high-affinity interactions support a role for fibrinogen and fibrin as a reservoir of growth factors at the site of injury.

Pretreatment of graft surfaces with fibrin from various sources, e.g., venous blood and re suspended plasma cryoprecipitate, has been shown to facilitate EC adhesion and the formation of stable endothelium. Gels prepared from fibrin glue have been successfully used clinically for pre-clotting of PTFE grafts prior to endothelialization *in vitro*. (Zilla *et al.*, 1989, Greisler, 1992, Deutsch *et al.*, 1997, Merzkirch *et al.*, 2001). Fibrin has been used as a sealant and an adhesive in surgery as it plays an important role in natural wound healing (Shireman *et al.*, 1998). Sequences that enhance smooth muscle cell attachment through specific adhesion receptors can be cross-linked to the fibrin matrix (Naito *et al.*, 1992). Growth factors such as VEGF incorporated to fibrin form a stable matrix for endothelial proliferation and maturation (Kumar & Krishnan, 2001). The immobilized fibrin conjugated VEGF protein remained an active and efficient mitogen for ECs (Zisch *et al.*, 2000). Incorporation of specific biochemical factors like FGF-1 and heparin into fibrin matrices has also been demonstrated (Greisler *et al.*, 1996). It has also been suggested that mature, cross-linked fibrin is relatively non-thrombogenic and non reactive to platelets compared to other surfaces, further decreasing the risk of thrombus formation (Skarja *et al.*, 1998)

Studies of fibroblasts entrapped in fibrin gel have suggested an increased amount of collagen synthesis in comparison with fibroblasts entrapped within collagen gel (Grassl *et al.*, 2002). There is evidence of collagen synthesis by fibroblasts upon incorporation of growth factor TGF- β into fibrin gels (Tuan *et al.*, 1996). Furthermore, formation of organized elastin fibres and collagen from SMC was enhanced by TGF- β and insulin incorporation when cultures were grown in fibrin gels compared to cells entrapped in collagen gel (Long *et al.*, 2003). It is also hypothesised that the balance of the stresses between the traction forces exerted by the EC and the resistance of the insoluble fibrin matrix triggers an angiogenic signal within the cell (Vailhe *et al.*, 1997).

Fibrin can therefore be harnessed to produce improved matrices, and there are a variety of other ECM proteins (eg. Fibronectin, hyaluronan and laminin) that upon incorporation to fibrin may further enhance the properties and function of engineered tissues. Further characterization of such tissues will direct insight into cell-matrix interactions and to the development of robust engineered blood vessel substitutes for use as bypass grafts and as improved models to study vascular biology (Cummings *et al.*, 2004). Polymeric fibrin is therefore a promising candidate to provide improved properties to engineered EC layer. However its potential as a stand alone tissue engineering scaffold is limited due to poor mechanical support. So there is a need for a mechanically strong support to develop its use as a scaffold for vascular tissue engineering.

1.3.7. Biodegradable polymers- A synthetic scaffold

The 3-dimensional structure of polymer scaffold provides a template for supporting cell growth, as well as for directing new tissue formation in the tissue regeneration process. Ideally, the scaffolds should be slowly resorbed in culture or after implantation, leaving only the tissue generated by the cells. The ideal polymer for a particular application should be configured so that it possesses the appropriate mechanical strength to mimic *in vivo* conditions, rate of matrix regeneration in parallel to biodegradation rate of the polymer scaffold, does not invoke an inflammatory or toxic response, should be metabolised in the body after fulfilling its purpose, leaving no trace (bioabsorbable), must be easily processable into the final product form, either porous or compatible with a range of extremely hydrophilic additives (starch, salt) to create porosity and finally, demonstrates acceptable shelf life and is easily sterilized (Zhang *et al.*, 2007).

Several biodegradable synthetic polymer scaffolds have been investigated for their suitability in vascular engineering. Polyglycolic acid (PGA) is one of the most commonly used. By using PGA scaffolds and a biomimetic perfusion system, Niklason *et al.* (1999) produced the first autologous vascular graft and implanted into the arterial system. The grafts were patent *in vivo* up to 1 month of observation. Although PGA fiber has good biocompatibility, its breakdown products are acidic, which could induce inflammatory response.

Higgins *et al.* (2003) found that independent of acidity or osmolality, plausible products of PGA degradation appear to induce dedifferentiation of porcine SMCs *in vitro*. Because of dedifferentiation and decreased mitosis, commercially available PGA may not represent an optimal scaffold for vascular tissue engineering. Moreover, PGA degraded too fast and results in low mechanical property of engineered graft (Niklason *et al.*, 1999).

Ye *et al.* (2000) demonstrated that pre coating of PGA scaffold with autologous human ECM is a very effective method of improving cell attachment in cardiovascular tissue engineering without the potential risk of immunologic reactions. Shum Tim *et al.* (1999) evaluated a TE vascular graft in the systemic circulation which is based on a new copolymer of PGA and polyhydroxyalkanoate (PHA) and obtained promising results. All TE grafts remained patent, and no aneurysms developed by the time of sacrifice. Miller *et al.* (2004) demonstrated that endothelial and smooth muscle cell densities increased on nano-structured cast poly(lactic-co-glycolic acid) (PLGA) and can be used in the synthesis of the next-generation of more successful TEVGs. However, the cellular toxicity of the breakdown products of those materials should be investigated in long-term study. Turner and co-workers (2004) have demonstrated that Hyaff-11, a hyaluronan-based biodegradable polymer, when compressed facilitated the formation of an endothelial monolayer. Furthermore, the ECs deposited an organized subendothelial matrix containing laminin, fibronectin, type IV and type VIII collagen making it an attractive material to investigate more extensively in the future.

Roh *et al.* (2008) confirmed that scaffolds constructed from either PGA or poly-L-lactic acid non woven felts demonstrated sufficient porosity, biomechanical profile, and biocompatibility to function as vascular grafts. The scaffolds implanted as either inferior vena cava or aortic interposition grafts in mice demonstrated excellent patency without evidence of thromboembolic complications or aneurysm formation. Biodegradable polymer scaffolds made of poly (lactide-co-epsilon-caprolactone) copolymer reinforced with PGA fibers when seeded with autologous bone marrow derived vascular cells were patent

even after 8 weeks implantation into the abdominal aorta of dogs and the grafts showed significant endothelial nitric oxide synthase (eNOS) activity (Lim *et al.*, 2007). Kim *et al.* (2006) proved that gel-spun fibrous poly (L-lactide-co-caprolactone) scaffold tensile strength, elastic modulus appropriate for vascular tissue-engineering applications

Gao *et al.* (2007) demonstrated that primary baboon EPCs and baboon SMCs when cultured on Poly (glycerol sebacate) (PGS) films and scaffolds showed good proliferation, and maintained phenotypic properties upon co culture. Carampin *et al.* (2007) developed tubular matrices from biocompatible poly [(ethyl phenylalanato) (ethyl glycinato)phosphazene] by electrospinning and observed that ECs formed a monolayer after 16 days of culture. Nieponice *et al.* (2008) characterized the incorporation of muscle-derived stem cells within tubular poly (ester urethane) urea scaffolds *in vitro* using a rotational vacuum seeding device and the cells showed high proliferation rates without losing stem cell phenotype for up to 7 days of *in-vitro* culture. Uchida *et al.* (2008) fabricated patient-specific vascular scaffolds from a poly (l-lactide-co-varepsilon-caprolactone) with mechanical strength covering the range of human blood vessels (1-3 MPa) and the biocompatibility of the scaffolds were confirmed by HUVEC growth. Challenges in seeding polymeric scaffolds are still associated with achieving the necessary cell proliferation and *in vitro* matrix synthesis (Swartz *et al.*, 2005). Additionally, the polymer degradation products formed tend to alter the local cellular environment and thereby the cell function (Nerem and Ensley, 2004).

Hybrid materials with combination of natural proteins and synthetic polymers have been evaluated for vessel engineering. Li *et al.* (2006) fabricated the vascular graft scaffolds using co-electro spun of PLGA, gelatin and elastin, while Stitzel *et al.* (2006) modified the approach by co-electro spun of PLGA, type I collagen and elastin. No local or systemic toxic effects were observed when implanted the scaffolds *in vivo*. The scaffolds possessed tissue composition and mechanical properties similar to native vessels. The electro spun vessel matrix with both natural and synthetic materials could serve as a good scaffold for functional vessel engineering.

1.3.8. Advantages of Poly (ϵ -caprolactone) as a scaffold

Poly (ϵ -caprolactone) (PCL) is aliphatic polyester that has been intensively investigated as a biomaterial. It is synthetic, slow biodegradable polymer with a low glass transition temperature (-60°C) and low melting point (60°C). The advantages of this semicrystalline polymer are its slow degradation rate, ease of fabrication, pliability and adequate mechanical strength. Extensive *in vitro* and *in vivo* biocompatibility and efficacy studies have been performed, leading to the approval of PCL by the US FDA as a nontoxic and tissue-compatible material (Pitt and Schindler, 1983). It can be fabricated to conduits with the required dimensions, optimum porosity and viscoelasticity. Being aliphatic polyester, PCL degrades by hydrolysis and the body resorbs the hydrolyzed products with minimal reaction to the tissues. PCL has one of the slowest degradation rates of all biodegradable polymers (Ferrin and English, 2004) and is a good candidate for fabricating scaffolds to be used in engineering tissues that require a long scaffold degradation time-frame, and its degradation products are less detrimental to growing tissues. However, being a synthetic polymer, its ability to give signals for EC proliferation, survival and differentiation is debatable.

Serrano *et al.* (2006) demonstrated good adhesion, growth, viability, morphology and mitochondrial activity of adhered ECs on PCL scaffolds, indicating potential for vascular tissue engineering. Recently, Serrano *et al.* (2008) cultured EPCs on poly (ϵ -caprolactone) (PCL) films treated with NaOH and showed that the cells showed appropriate growth and functionality. Williamson *et al.* (2006) demonstrated attachment of ECs onto PCL which formed the luminal surface of a composite PCL-polyurethane scaffold with release of vWF, nitric oxide and intercellular adhesion molecule 1 (ICAM-1) under physiological stimuli. PCL has been modified or coated with biomimetic molecules to create a functional endothelium over the polymer surface. The PCL surface was grafted with RGD peptide to enhance the growth rate of human ECs on the surface by Chung *et al.* (2005). Gelatin grafting enhanced EC spreading and proliferation on electrospun PCL nanofibers and maintained the expression of platelet-endothelial cell adhesion molecule-1 (PECAM-1), ICAM-1, and

vascular cell adhesion molecule-1 (Ma *et al.*, 2005). Collagen coated electro spun poly (L-lactic acid)-co-poly (caprolactone) nanofibre meshes preserved expression of fibronectin, PECAM-1 and Collagen type IV and function of ECs when cultured *in vitro* (He *et al.*, 2006).

1.3.9. STUDY HYPOTHESIS

The focus of this study was to evolve an ECM composition that promotes *in vitro* EC proliferation and survival, that can retain and release signaling molecules such as growth factors and can phenotypically modulate the ECs to maintain normal physiology, and most importantly a biodegradable matrix that can support the cells to remodel the matrix and synthesize their own ECM components in appropriate quantities for long term stability of cells. This matrix upon coating on a biodegradable scaffold structure could lead to the creation of tissue engineered constructs with sufficient mechanical strength and ECM deposition.

1.4. OBJECTIVES

The goal of this study was to immobilize growth factors or glycosaminoglycans within the fibrin matrix which acts as the skeleton of the biological scaffold. Evaluations were intended to identify an optimum matrix composition that facilitate EC proliferation, long term EC survival and ECM synthesis for vascular tissue engineering. Before arriving at the suitable composite the components of the matrix need to be tested individually and in combination to understand their effects on cell growth and differentiation and to identify if its incorporation influences the ECM remodeling. The effect of each matrix composition on the behavior of ECs need to be evaluated in terms of adhesion, proliferation, survival, fibrin matrix degradation and ECM synthesis so that an optimum matrix can be selected for engineering a hybrid scaffold using a biodegradable polymer and the matrix composite. The cells need to be seeded on to the hybrid scaffolds and evaluated for adhesion, proliferation, survival, long term culture, shear stress resistance, nitric oxide release and thrombogenicity so that the suitability of the scaffold for vascular tissue engineering could be confirmed.

To achieve the goal, the study objective was segregated in three phases

PHASE I. To evaluate the role of incorporation or depletion of specific component/s of the fibrin composite matrix and to select a matrix with optimum EC adhesion, proliferation and survival, by analysis of

- The role of gelatin, growth factors and fibronectin in the basic fibrin composite matrix.
- The effectiveness of fibrin composite matrix compared to fibronectin coated tissue culture polystyrene.
- The effect of growth factors [(angiogenic growth factors (AGF) and platelet growth factors (PGF)] and glycosaminoglycans [(hyaluronic acid (HA) and heparan sulphate (HS)], individually and in combination.

PHASE II. To evaluate the matrix remodeling on different modified matrix compositions after different intervals of EC culture, to select an optimum matrix composition favorable for vascular tissue engineering, by analyzing

- Fibrin matrix degradation during EC culture on different matrix compositions.
- Deposition of elastin, collagen IV and collagen I.
- mRNA expression specific for elastin, collagen IV and collagen I.

PHASE III. To establish the selected matrix from Phase II is suitable for growing EC on a biodegradable polymer for vascular tissue engineering, by

- Preparation & characterization of biodegradable porous PCL scaffolds.
- Fabrication of a hybrid scaffold by coating the selected matrix composition on the porous PCL scaffolds.
- Comparison of bare PCL against hybrid scaffold for cell growth and survival.
- Characterization of EC phenotype on tissue engineered scaffold.
- Analysis of matrix remodeling on hybrid scaffold.

- Analysis of physiological function and mechanical properties of tissue engineered scaffold.
- Analysis of the blood compatibility of the bare, hybrid and cell seeded hybrid scaffolds.

Methods adopted for achieving the objectives are described in chapter II, and the results are illustrated and discussed in chapters III, IV and V. The results are summarized with conclusions in Chapter VI.

MATERIALS AND METHODS

2.1. ENDOTHELIAL CELL CULTURE

2.1.1. Isolation and Expansion of Human Umbilical Vein Endothelial Cells (HUVEC)

Endothelial cells were isolated from human umbilical cord veins according to the method described by Jaffe *et al.* (1973) and Gimbrone *et al.* (1974) with minor modifications. Human umbilical cord was collected in ice cold Ca^{2+} - and Mg^{2+} -free Hank's balanced salt solution (HBSS) containing antibiotics (1000 U/ml of Benzyl penicillin and 1000 $\mu\text{g}/\text{ml}$ of Streptomycin) and D-glucose (1mg/ml). The veins for the study were collected from the Obstetrics Department of G.G Hospital, Trivandrum, with required consent. The distal and proximal ends were tied with sterile silk just before removing the cord from the placenta to ensure sterility within the lumen.

The umbilical cord collected was brought to the tissue culture laboratory within 3h of harvesting the cord and all the subsequent procedures were performed under laminar flow hood. The cord was washed with fresh ice cold HBSS supplemented with 100 U/ml Benzyl penicillin and 100mg/ml streptomycin sulphate, and the damaged areas were discarded. A small piece was cut off at one end of the cord so that a fresh non retracted vein end was obtained, and the

vein was connected to custom made stainless steel cannula and secured with a 3-way stopcock. The lumen of the vein was washed thoroughly with ample quantity of ice cold HBSS using a syringe via the 3-way stopcock, to remove the remnants of blood. A small piece was cut off from the opposite end and another cannula was inserted and secured with a 3-way stopcock.

After washing, the cord vein was filled with 0.2% type I collagenase (Sigma Chemicals, USA) in Medium 199 solution and 3-way stopcock was closed. The cord was then placed on HBSS soaked sterile gauze in a Petri plate and was incubated at 37°C for 15 min. After enzyme digestion, the collagenase solution containing detached ECs was collected in a 50ml sterile centrifuge tube (NUNC, Roskilde, Denmark), using a syringe. The vein was flushed with an additional 30ml of M199 to collect loosely attached cells and is pooled with the initial suspension. The collected effluent was then centrifuged for 5min at 200 x g at 4°C using a tabletop refrigerated centrifuge (Biofuge Stratos, Haeraeus), and pellets (containing ECs) were washed twice with medium 199.

The final cell pellet was re-suspended in complete MCDB 131 medium (Gibco-BRL, USA) containing 20% fetal bovine serum (FBS) (Gibco-BRL, USA), 200 µg/ml angiogenic growth factors, Streptomycin sulfate (100µg/ml) and Benzyl Penicillin (100 U/ml). The cell suspension was then seeded on 10 cm² culture flask (NUNC), pre-coated with gelatin. The culture flask was incubated under 4.5% CO₂ at 37°C in an incubator (Thermo Forma 3110, USA). The culture was fed with fresh medium every alternate day until confluence. Before use the FBS (Gibco-BRL, USA) is heat inactivated by incubating at 56°C in a water bath for 30 min and is sterile filtered through a 0.22 µm membrane filter (Millex GP, Millipore) at room temperature. The serum is then aliquoted into 50ml tubes and is stored at -70°C until use.

2.1.2. Subculture of HUVEC

The endothelial cells were subcultured upon reaching confluence. The medium from the culture flask was removed and the confluent monolayer was rinsed with fresh warm serum free M199 for 2 times. The cells were then incubated with 0.25% Trypsin-EDTA solution (Gibco-BRL, USA) for 5min at 37°C. On observation under the microscope the cells were rounded up and detached from the surface. Serum containing medium ~3ml was added immediately to

inhibit further trypsin activity. The cell suspension was subsequently drawn in to a sterile pipette 2-3 times to break up the cell clumps, transferred to a 10ml centrifuge tube and was centrifuged at 300 g for 6 min at 4°C. The cells were re-suspended in 10% serum containing MCDB 131 and then seeded on to fresh pre-coated culture plates at split ratio 1:3. The MCDB 131 medium used for subculturing HUVEC contained 20% FBS, VEGF, penicillin (100 U per milliliter), and streptomycin (100µg/ml). The medium was replaced with fresh medium on alternate days.

2.1.3. Characterization of Cultured Cells

The endothelial nature of the cultured cells was confirmed by: 1) Morphology Analysis 2) Cellular Uptake of Dil labeled acetylated-LDL, 3) Cellular expression of von Willebrand factor

2.1.3.1. Morphology Analysis

Routine evaluation of the quality and growth pattern of the cultured cells was done using an inverted phase contrast microscope (Leica DM IRB, Germany) at 10X, 20X and 40X magnifications. Endothelial cells were characterized by the typical cobble stone morphology exhibited by confluent monolayers.

2.1.3.2. Cellular Uptake of Dil Labeled Acetylated LDL

Endothelial cells in primary cell culture can be identified by their ability to take up fluorescent AcLDL. Acetylated LDL is taken up by macrophage and endothelial cells that possess scavenger receptors specific for the modified LDL.

To evaluate the cell identity, the near confluent cells, grown in composite-coated 2cm² wells as per the method described by Voyata *et al* (1984) with some modifications. The medium was changed with fresh MCDB 131 containing 10% FBS and 10 µg/ml of 1,1-dioctadecyl-3,3,3,3-tetramethyl Indocarbocyanine perchlorate (Dil) labeled Acetylated Low Density Lipoprotein (Dil AcLDL) (Molecular Probes, USA) and was incubated for 4h at 37°C in CO₂ incubator. After 4h, the culture plate was washed three times with warm serum free M199 and was viewed under inverted fluorescent microscope (Leica DM

IRB, Germany), using Rhodamine filter. The cells from second or third passages were used for identification.

2.1.3.3. Cellular Expression of vWF

Von Willebrand factor (vWF) is a glycoprotein produced uniquely by endothelial cells and megakaryocytes. The endothelial cell monolayer cultured over fibrin composite coated cover slip bottom chamber slides (BD Biosciences) was fixed with 3.7% formaldehyde in PBS for 30 min. The fixed monolayer was then rinsed with PBS three times and quenched by incubating with 0.27% NH_4Cl /0.38% glycine in PBS for 20 min. The cells were then washed with PBS and permeabilized with 0.5% Triton X-100 (Sigma Chemicals, USA) in PBS and washed with PBS, the monolayer was then incubated with monoclonal anti-human von Willebrand Factor (vWF) antibodies (primary antibody) raised in mouse (Dako, Denmark; 1:200 dilution) in blocking buffer for 30 min. The slides were then rinsed thoroughly with PBS and then incubated with 100 μl of FITC conjugated polyclonal anti-mouse IgG raised in rabbit (secondary antibody) in blocking buffer at a dilution of 1:1000 for 20 min. Finally, the monolayer was washed thoroughly with PBS, and the cells were viewed using a fluorescence microscope (Leica DM IRB, Wetzlar, Germany) using FITC filter.

2.2. PREPARATION OF GROWTH FACTORS

2.2.1 Preparation of crude angiogenic growth factors (AGF) from Bovine Hypothalamus

In-house preparation of AGF was done according to the procedure described by Maciag et al. (1979). Bovine brain was obtained aseptically from a slaughter house in ice cold normal saline. The hypothalamus was dissected carefully; the blood containing regions were removed and were cut into pieces of 1cm^2 . The pieces were then homogenized for 3 min in 0.1M NaCl in an ice cold blender (using ~500 ml of NaCl solution), maintaining the pH of the homogenate at 7. The homogenate was stirred at 4°C for 2h with subsequent centrifugation for 40 min at 13,800 g at 4°C using Hitachi, SCR20BA centrifuge. The supernatant obtained was mixed with streptomycin sulfate to get 0.5% w/v final concentration, and incubated overnight at 4°C (pH 6.8 to 7) to extract the lipid content. The mixture was centrifuged at 4°C for 40 min at 13,800 g and the supernatant was

dialyzed against 0.1M NaCl overnight at 4°C. The dialyzed solution was centrifuged for 40 min at 13,800 g at 4°C, and the supernatant obtained was lyophilized in a freeze dryer (Modulyo 4K Freeze Dryer, Edwards, UK) and stored at -70°C for further use.

2.2.2. Preparation of Platelet Growth Factors (PGF)

Platelet rich plasma (PRP) was obtained by centrifugation of anti coagulated blood at 1200g for 5 min at 22°C using a tabletop centrifuge (Haerus, Labofuge, Germany). For preparation of washed platelets, the PRP was re suspended in Tyrodes's buffer containing Acid Citrate Dextrose (ACD) in the ratio 10:1 and washed three times by centrifugation (SCR20BA, Hitachi, Japan) at a speed of 500 g for 10 min at 22°C. The final platelet button was re suspended in Tyrode's buffer without ACD.

The isolated platelets were equilibrated with 5mM CaCl₂, for 10 min at 37°C. For induction of granule release, platelets were challenged with 1 IU of human thrombin (Sigma Chemicals, USA)/10¹⁰ of 1 ml of platelet suspension and the release was allowed to continue for 10 min by incubation in a 37°C water bath.

Released proteins were isolated by centrifugation of activated platelets at 17600 g for 1h at 4°C in refrigerated centrifuge (SCR20BA, Hitachi, Japan). The supernatant was dialyzed against HBSS overnight. After dialysis the platelet releasate was filtered through 0.22µm filter (Millex) under sterile conditions. The total protein was estimated by Lowry's method(Lowry *et al.*, 1951).

2.3. FIBRIN MATRIX COATING ON TISSUE CULTURE POLYSTYRENE

2.3.1. Preparation of fibrin composite coated Tissue Culture Polystyrene

Fibrin composite coated polystyrene (CCPS) was prepared according to the established procedure (Chennazhy and Krishnan, 2005). Bovine thrombin (Merck) was reconstituted in 35mM CaCl₂ at a concentration of 5 IU/ml. Culture plates were incubated with bovine thrombin (~ 2.5 IU cm⁻²) for 30-60 min at 37°C. Lyophilized cryoprecipitate prepared from screened pooled human plasma that contained fibrinogen and fibronectin was reconstituted in distilled water to get

2mg/ml final concentration (Total protein ~2.7 mg/ml). After incubation, excess thrombin solution was removed and 40 μ l of fibrinogen solution containing 0.2% w/v gelatin and 10 μ g AGF (5 μ g/cm² area) was added to the surface. Fibrin was allowed to polymerize at 37°C for 30min and were then frozen at -70°C for at least 2h and lyophilized. The freeze dried dishes were either used immediately for cell seeding or stored in the refrigerator for later use. For preparation of composite coated polystyrene (CCPS) without gelatin (CCPS-Gel), the solution used for coating contained only cryoprecipitate (2mg/ml) and AGF ((5 μ g/cm² area). For preparation of composite coated polystyrene without growth factors (CCPS-GF), solution used for coating contained cryoprecipitate (2mg/ml) and gelatin (0.2%) without added AGF. For composite coated but fibronectin (FN) depleted (CCPS-FN) matrices, CCPS was treated with purified antibodies (20 μ g ml⁻¹) developed in rabbits against human fibronectin (Gibco, USA). The purification of fibronectin antibodies was done using Protein A column using Akta prime protein purification system (GE Biosciences, USA) and purity was verified on SDS-PAGE. The reactivity of the antibodies with FN was verified by Western Blot of pure antigen and the FN present in cryoprecipitate.

2.3.2. Preparation of growth factor incorporated matrices

To study the effect of growth factors on extra cellular matrix deposition, fibrin matrix were prepared in 2cm² four well- polystyrene plates (NUNC) with different composition in each well: **A.** Fibrin-gelatin matrix without additional growth factors (CCPS); **B.** CCPS + AGF (Angiogenic growth factor); **C.** CCPS + PGF (Platelet growth factors); **D.** CCPS + AGF + PGF. The concentration of AGF and PGF incorporated to the matrices were 5 μ g/cm² and 0.02 μ g/cm² respectively.

2.3.3. Preparation of glycosaminoglycan incorporated matrices

To study the effect of glycosaminoglycans on extra cellular matrix deposition, fibrin matrices were prepared in four well- polystyrene plates (NUNC) with different composition in each well: **A.** Composite coated polystyrene (CCPS); **B.** CCPS + HA (Hyaluronic acid); **C.** CCPS + HS (Heparan Sulphate); **D.** CCPS + HA + HS. The concentration of hyaluronic acid and heparan sulphate incorporated to the matrices were 1.25 μ g/cm² and 2.5 IU/cm² respectively.

2.3.4. Preparation of growth factor and glycosaminoglycan incorporated matrices

To study the effect of growth factors and glycosaminoglycans on extra cellular matrix deposition, fibrin matrices were prepared in four well- polystyrene plates (NUNC) with different composition in each well (2cm² area): **A.** Composite coated polystyrene (CCPS); **B.** CCPS + GF (Growth factors + Angiogenic growth factors + Platelet growth factors); **C.** CCPS + GAG (Glycosaminoglycans + Hyaluronic acid + Heparan Sulphate); **D.** CCPS + GF + GAG (Growth factors and glycosaminoglycans). The concentration of AGF and PGF incorporated to the matrices were 5µg/cm² and 0.02µg/cm² respectively and that of hyaluronic acid and heparan sulphate were 1.25µg/cm² and 2.5 IU/cm² respectively.

2.4. STANDARDIZATION OF A FIBRIN MATRIX COMPOSITION TO ACHIEVE ECM DEPOSITION IN TISSUE CULTURE POLYSTYRENE BY CULTURING HUVEC

2.4.1. Cell adhesion

2.4.1.1. Fluorescent Staining for Actin

EC was stained for F-Actin with Texas Red Phalloidin (Molecular Probes) and the actin filament assembly was analyzed using confocal microscopy. Texas Red-X phalloidin is a high-affinity probe for F-actin that is made from a mushroom toxin conjugated with photostable Texas Red dye. If used at nanomolar concentrations, phalloitoxins are convenient probes for labeling, identifying and quantitating F-actin in cell cultures.

Third passage cells (2×10^4 cells cm⁻² area) were used for seeding on separate fibrin coated cover slip bottom slides. For analysis of cell adhesion, 24 h after seeding each well was washed with phosphate buffered saline (PBS) and was fixed using 3.7% para-formaldehyde. The fixed cells were permeabilized using 0.1% Triton X-100 (Sigma Chemicals, USA) in PBS. After washing three times with PBS, cells were stained for actin with Texas red Phalloidin for 20 min in the dark at 37°C as described by Lewis and Bridgman (1992). The cells were then washed thoroughly with PBS and were viewed using confocal microscope (Meta 510 Laser Scanning Confocal Microscope, Zeiss, Germany). The fluorescence intensity at specific area was quantified by analyzing the stained

cells using confocal microscope software options. For long-term storage, the cells were air dried and then mounted in a permanent mountant ProLong® Gold, and stored in the dark at (2–6)°C.

2.4.1.2. Vinculin Staining to detect focal adhesion

Vinculin is a membrane-cytoskeletal protein in focal adhesion plaques that is involved in linkage of integrin adhesion molecules to the actin cytoskeleton in mammalian cells. For immunostaining, third passage ECs (2×10^4 cells cm^{-2} area), were seeded onto various matrices, and after 24h in culture, cells were fixed with 3.7% Para formaldehyde in PBS, washed with PBS, and permeabilized with Triton X-100 (0.5%) in PBS for 1 min. Vinculin was stained by incubation with mouse anti-human vinculin antibody (Sigma, USA) for 30 min followed by incubation with FITC labeled secondary antibody (Sigma, USA) for 30 min and were viewed under confocal microscope with software options (Meta 510 Laser Scanning Confocal Microscope, Ziess, Germany).

2.4.2. Cell Proliferation

2.4.2.1. Tritiated Thymidine uptake

To quantify initial cell attachment, EC in log phase were labeled with tritiated thymidine (^3H -thymidine) (American Radiochemicals, USA) by placing 20 μCi ^3H -thymidine/25 cm^2 flask for 72h at 37°C [Badylak *et al.* 1999]. These cells were harvested and 3×10^4 cells cm^{-2} were used for seeding each matrix in 4-well plates. After 2h of seeding, the unattached cells were removed, and DNA was extracted for ^3H counting as per the method standardized by Shivakumar *et al* (1992). Briefly, the cells were solubilized with 0.5ml of 0.1M NaOH containing 0.1% SDS and precipitated with 0.5ml of 10% Trichloroacetic acid (TCA) (Sigma, USA) for 1h at 4°C. Then it was centrifuged at 10,000 g for 15 min at 4°C in Biofuge Stratos (Haeraeus, Germany). To the pellet, 1 ml absolute alcohol was added and kept in ice bath for 30 min. Centrifuged again at 10,000 g for 15 min at 4°C. The resulting pellet was air dried and dissolved in 0.5ml of 0.1N NaOH. An aliquot containing 3×10^4 cells was also processed for ^3H counting. ^3H count was detected using a liquid scintillation counter (Triathler Multi-label tester, Hidex, Finland). The number of cells attached was calculated from the

radioactive counts of unattached cells and the radioactive count of known number of ^3H -thymidine-loaded cells.

To quantify DNA synthesis as an indicator of cell proliferation, after removing the unattached cells at 2h, attached cells were fed with complete MCDB 131 medium containing $2\mu\text{Ci ml}^{-1}$ [^3H] thymidine. After 48h, medium was changed with fresh medium containing [^3H] thymidine and after 72h; cells were harvested from different matrices and assayed for ^3H using a liquid scintillation counter.

2.4.2.2. PCNA analysis

The proliferating cell nuclear antigen (PCNA) is a 36 kDa molecular weight protein also known as cyclin. The PCNA is expressed by proliferating cells and reaches its maximum synthesis during the S-phase of the cell cycle. Flow cytometric analysis for PCNA was done for cells cultured on the specified matrices. HUVEC was seeded on to the matrices at a plating density of 2×10^4 cells cm^{-2} . After 72h of culture, the cells were harvested, washed in PBS, fixed with 3.7% formaldehyde for 20 min, washed in PBS and were permeated with 0.1% Triton X-100 for 2 min. The cells were subsequently washed in PBS and were stained for proliferating cell nuclear antigen (PCNA Molecular Probes, USA) for 30 min in dark. The cells were washed in PBS and further diluted with FACS sheath fluid and analyzed using a flow cytometer (BD FACS ARIA, USA) to estimate the percentage of PCNA positive cells.

2.4.3. Cell Apoptosis using Flow Cytometry

The apoptosis of EC on various matrices was quantified using Vybrant Apoptosis Assay Kit (Molecular probes, USA). The kit provides a rapid and convenient assay for apoptosis. The kit contains recombinant Annexin V conjugated to fluorescein Iso Thio Cyanate (FITC annexin V), as well as a ready-to-use solution of the red-fluorescent Propidium Iodide (PI) nucleic acid binding dye. The human anticoagulant, Annexin V, is a 35–36 kDa Ca^{2+} -dependent phospholipid binding protein that has a high affinity for phosphatidylserine (PS). In normal live cells, PS is located on the cytoplasmic surface of the cell membrane. However, in apoptotic cells, PS is translocated from the inner to the outer leaflet of the plasma membrane, thus exposing PS to the external cellular

environment. Annexin V labeled with a fluorophore can identify apoptotic cells by binding to PS exposed on the outer leaflet. PI is non-permeating into live cells and apoptotic cells, but stains dead cells with red fluorescence, binding tightly to the nucleic acids in the cell. After staining a cell population with FITC Annexin V and PI in the provided binding buffer, apoptotic cells show green fluorescence, dead cells show red and green fluorescence, and live cells show little or no fluorescence.

The cells from each type of matrix were harvested at 72h after seeding at a plating density of 2×10^4 cells cm^{-2} and were stained according to manufacturer's protocol. The trypsinised cells were washed with ice cold PBS and the resulting cell pellet was re-suspended in 100 μl of annexin- binding buffer (cell density $\sim 1 \times 10^6$ cells/ml). To the cell suspension 5 μl annexin V conjugate and 1 μl of the 100 $\mu\text{g}/\text{ml}$ PI working solution were added and incubated for 15 min at RT. After staining, the cells were washed and re-suspended in FACS sheath fluid and were analyzed using a flow cytometer (FACS Aria, BD Biosciences, USA) to estimate the percentage of live/apoptotic/dead cells.

2.4.4. Fibrin matrix degradation - D Dimer assay

D-dimers or fibrin degradation products (FDPs) are formed when fibrin is broken down by enzymes (e.g. plasmin). D-dimers are unique in that they are the breakdown products of a fibrin mesh that has been stabilized by Factor XIII. To estimate degradation of initially coated fibrin, D-Dimer assay (Diagnostica Stago, France) was done at time periods 24h, 72h, 120h, 168h & 210h after seeding each well with a plating density of 3×10^4 cells cm^{-2} .

To each culture well (1.5cm^2), 300 μl of the medium was added and was aspirated from separate wells at each time interval. Twenty μl medium was subjected to Latex immunoturbidity assay according to manufacturer's protocol. Briefly, 20 μl of undiluted sample is placed next to 20 μl of Reagent 1 on the sample card. The two drops are combined using rods. The test card is then manually rocked for 2 to 3 minutes. The agglutination pattern is then compared with positive and negative controls provided with the kit. Positive samples were serially double diluted and tested till no agglutination was present in the diluted sample.

2.4.5. Solubilization and recovery of matrices

The ECM deposited by cells was recovered for immunostaining by removal of cells by detergent and base treatment, a modified procedure of Meyer *et al* (2006). Endothelial cells were cultured on matrices for defined periods after seeding each well with an initial plating density of 3×10^4 cells cm^{-2} . For the recovery of 3 day matrices, the monolayer was incubated with 1% Triton X-100 (Sigma, USA) for 30 minutes followed by subsequent washing with PBS. Detergent treatment along with a base was required to denude the cell layer for the recovery of 10 day, 20 day and 30 day matrices. Briefly, the confluent monolayer was washed with distilled water and was incubated for 3h in water at 4°C. The 4 well plates were then washed with water and were incubated with an isotonic solution containing 0.9% sodium chloride and 0.02% sodium azide for 1h at 37°C. The 4 well plates were subsequently incubated with chemical solution containing 1% Triton X-100, 0.1% ammonium hydroxide (Sigma, USA) and 0.9% sodium chloride (Sigma, USA) for 30 min with shaking at 75 rpm. The matrix was then observed under the microscope. The matrix was again washed with water if there were any artifacts and was further fixed in 3.7% para formaldehyde for 1h. The matrix was then washed with de-ionized water and dried before immunostaining.

2.4.6. Post Culture Analysis of matrices

2.4.6.1. Histochemical staining

Recovered matrices were developed using Masson's trichrome stain (Sigma, USA) which stains collagen as blue and muscle fiber (elastin) as pink (JD Bancroft & Stevens, 1990). The matrices recovered after 30 days were also stained with Phosphotungstic Acid Haematoxylin (PTAH) to identify the presence of collagen which turns pink.

2.4.6.2. Immunostaining

The matrices recovered after 3 days, 10 days and 20 days of endothelial cell growth were immunostained for elastin, collagen Type I and collagen Type IV. Primary antibodies were monoclonal anti human collagen I (Sigma, USA), monoclonal anti human collagen IV (Novocastra Laboratories) and monoclonal anti human elastin (Novocastra Laboratories). The fixed matrices were blocked

with 1% bovine serum albumin (BSA) for 20 min and then incubated with primary antibody for 1h. The wells were subsequently washed 3 times with PBS and incubated with HRP conjugated antimouse IgG [secondary antibody (Sigma, USA) for 30 min. The wells were further washed 3 times with PBS and then incubated with diaminobenzidine substrate for 15 min. After washing in PBS the stained matrices were viewed using a light microscope (Leica DMIRB, Germany).

2.4.6.3. Fluorimetry

For quantification of matrix deposited by EC, the cells were cultured over glass bottom 24-well plates (Greiner Bioone, Germany) for 10 days and 20 days on defined compositions and the matrix recovered were immunostained for elastin and collagen Type IV. Staining protocol was as described in #2.4.6.2. The secondary antibody was FITC conjugated anti-mouse IgG (Sigma, USA). Briefly, the fixed matrices were blocked with 1% BSA and then incubated with primary antibody for 1h. The wells were then washed with PBS and then incubated with FITC conjugated secondary antibody for 30 min. After washing in PBS, the immuno stained matrices were analyzed under fluorescent microscope (Leica DM IRB, Germany). Photomicrographs were taken and compared the visual appearance of the matrix. A standard graph was plotted using the Lowry protein concentrations of IgG-FITC against their fluorescent intensities. The integrated FITC fluorescence in each well was detected using band pass filter [excitation wavelength 485(20) nm, emission wavelength 535(20) nm] in micro plate reader (TECAN, Austria). From the mean fluorescent intensity from each well and from the calibration curve the amount of Elastin and Collagen IV deposition in each well is quantified.

2.4.7. mRNA expression studies

2.4.7.1. RNA isolation and reverse transcription

Endothelial cells were grown on fibrin and fibrin-growth factor composite matrices for 24h, 72h and 144h respectively. The EC seeding density was 3×10^4 cells cm^{-2} . The RNA was isolated by TRIzol Reagent (Invitrogen, USA) as per manufacturer's directions. Yield of RNA was quantified by UV measurement (Diode array spectrophotometer, Hewlett Packard, USA) and 20ng of total RNA was taken for each reverse transcription using Thermal Cycler (Master Cycler,

Eppendorf, USA) at annealing temperatures 53°C, 57°C, and 63°C respectively for collagen I, Collagen IV, and Elastin, in 25 µl total volume, 1µl dNTP (500 ng/µl), de-ionized RNAase-free water, 1µl MgCl₂ (50 mM), 2.5µl 10X RT Core buffer, 1µl each forward and reverse primer and 0.25µl M Muvl reverse transcriptase (Stratagene, USA). The primer sets were derived as **Collagen I**: Forward 5'- CCA AGG GTA ACA GCG GTG A-3', Reverse 5' - GCT TTC CTT CCT CTC CAG CA-3'; **Elastin**: Forward 5'- CGG CGC CTT CCC CGC AGT TAC CTT T-3', Reverse 5' - ACA CAA CCC CTG GAA CCG CAG CAC C-3'; **Collagen IV α 1 chain**: Forward 5'- CCT GGC TTG AAA GGT GAT AAG-3', Reverse 5' - CCC GCT ATC CCT TGA TCT C-3'; **β Actin**: Forward 5'-CTA TCC AGG CTG GTG CTA TCC-3', Reverse 5'- ATG CCA GGG TAC ATG GTG -3' from previously published reports (Seliktar *et al.*, 2003; Bell *et al.*, 2001).

2.4.7.2. Real-Time Polymerase Chain Reaction

To compare the mRNA expression levels at 24h, 72h and 144h, and between different matrices, the real-time PCR was performed using a Chromo4 system (MJ Research, USA). All reactions were carried out in a total volume of 20µl containing 10µl quantitative PCR Master mix (Finnzymes, USA), 200nM forward primer, 200nM reverse primer, 8µl template cDNA, at an annealing temperature of (53–63)°C (depending upon the primers). For each gene, quality and specificity was assessed by examining PCR melt-curves following Real Time PCR. The cDNA copy numbers of the target gene were analyzed after normalizing to the copy number of β-Actin. All experiments were done three times with duplicate samples. Significant difference in mRNA expression at 72h and 144h when compared to 24h, and between the basic fibrin matrix and growth factor and glycosaminoglycans incorporated matrices at different time periods were evaluated using Student's T-test. The differences were considered statistically significant when $p < 0.01$.

2.4.8. Statistical analysis

For each test six replicate samples were analyzed and statistical significance was determined by students T-test and Analysis of Variance (ANOVA). When $p < 0.01$ the differences were considered statistically significant.

2.5. FABRICATION AND PHYSICOCHEMICAL CHARACTERIZATION OF A POROUS FIBRIN – POLY (ϵ - CAPROLACTONE) (PCL) SCAFFOLD FOR VASCULAR TISSUE ENGINEERING APPLICATIONS.

2.5.1 Scaffold preparation

Solvent casting method was used to prepare porous PCL films. PCL granules (M_n : 42,500, Aldrich Chemicals, USA) were initially dissolved along with the porogen-polyethylene glycol (PEG) pellets (1:1 wt%, M_w : 35,000, Merck, Germany) in dichloromethane (AR grade, S.D fine Chemicals, Mumbai) to prepare a solution of nearly 4.5 wt/wt% concentration. Films of nearly 80 microns thickness were prepared casting the solution in glass moulds. After evaporation of the solvent, the films were immersed in distilled water for 3 days to 15 days to leach out PEG. The distilled water was changed after every 24h. Samples were then taken out, air dried and specimens of size 10cm x 1cm were prepared. These specimens were washed 3 times in sterile water and immersed in 70% ethanol overnight for elimination of bio burden. The scaffolds were examined using a phase contrast microscope (Leica, Model DMIRB, Germany) at a magnification of 10X to observe the porous morphology.

2.5.2. Fibrin composite coating on the PCL scaffold

The porous PCL scaffold was then coated with fibrin composite (FC PCL) as per reported procedure (Chennazhy & Krishnan, 2005) using the composition as specified in # 2.3.4. of this chapter.

Briefly, the scaffold surfaces were saturated with bovine thrombin and fibrin composite solution 2.3.4(D) was layered on the polymer films and allowed to clot for 30min at 37°C. Coated films were lyophilized in a freeze drier (Edwards, Modulyo 4K, UK). The weight of coated fibrin was gravimetrically analyzed in an analytical balance with 10 μ g sensitivity. The films were then stored at 4-6°C in a refrigerator and were used for experiments within 1-2 days.

2.5.3. Characterization of scaffold

2.5.3.1. Fourier transform infrared spectroscopy (FTIR) studies

Attenuated Total Reflectance Infrared Spectroscopy (ATR-IR) was used to study the surface chemistry of bare and fibrin coated polymer scaffold. Films

were kept on a Zn-Se crystal and spectra were recorded between 4000 and 400 cm^{-1} in a FT-IR spectrophotometer (JASCO, Model 6300, Japan, 0.07 cm^{-1} resolution) having a DLA TGS detector. The polymer scaffold leached for a period of 15 days was also compared to PEG to confirm the complete removal of the porogen.

2.5.3.2. Pore size determination

The porosity of the bare polymer scaffold and hybrid scaffold was determined using mercury intrusion porosimeter (Poremaster P33, Quantachrome Instruments, USA). The porosity of bare polymer scaffold with a leaching period of 3 days/15 days and the same after fibrin coating was also determined. A pressure of 0.799 psi to 32887 psi was applied at a temperature of 20°C and porosity distribution graph was recorded.

2.5.3.3. In vitro degradation studies

To evaluate the degradation rate of the porous PCL scaffold, PCL films of 10mm width x 100 mm breadth x 0.08mm thickness were prepared and evaluated as follows

2.5.3.3.1. Gravimetric analysis

Lyophilized PCL films without residual moisture were weighed (W_0) using an analytical balance (Genius Sartorius, Sensitivity 0.01mg) and were incubated at $37^\circ \pm 1^\circ\text{C}$ in 10 ml phosphate buffered saline (PBS, pH=7.4) taken in 15 ml polystyrene tubes (Labcon, USA), with agitation at 70 ± 5 rpm using a digital shaker incubator (Labnet International, USA). A minimum of 8 replicates were used in each case. The respective samples were removed from PBS at 30, 45 and 60 days, rinsed thoroughly in distilled water, dried at room temperature and lyophilized to remove the moisture and weighed (W_1). The percentage degradation was calculated using the equation $\text{Degradation (\%)} = 100 \times (W_0 - W_1) / W_0$, where W_0 is the initial and W_1 is the final weight of each polymer film.

2.5.3.3.2. Viscosity average Molecular weight determination.

Porous PCL scaffolds from #2.5.3.3.1 were used for viscosity measurements at the end of 60 days storage and controls were without PBS

storage. Known concentrations of polymer solutions were prepared by dissolving accurately weighed PCL samples in chloroform with a maximum concentration of 1g/dl. The specific viscosities $[\eta_{sp}]$ of the polymer solutions were determined using an automatic Visco system (Schott AVS 350, Germany). The measurements were carried out at a constant temperature of $30 \pm 0.01^\circ\text{C}$ in a water bath with a thermostat (Schott Gerat CT 1650, Germany). Reduced viscosities $[\eta_{sp/C}]$ were plotted against concentration C and from the intercept obtained molecular weights were calculated using Mark-Howink equation;

$$[\eta_{sp/C}]_{c \rightarrow 0} = KM^a$$

with a K value 1.96×10^{-4} and 'a' value 0.76 for the system.

2.5.3.4. Mechanical Properties Evaluation

The tensile strength and elongation at break of bare PCL scaffolds after leaching in PBS at periods of 0, 15, 30, 45 and 60 days were analyzed using a Universal Testing Machine (Instron 1011, UK) at a crosshead speed of 100 mm/min as per ASTM D 882-97 procedure.

2.5.4. Characterization of endothelial cell seeded scaffold

2.5.4.1. Endothelial cell seeding

EC harvested from second to fifth passages were used for seeding on the scaffold at a density of 2×10^4 cells cm^{-2} . Cells were cultured on scaffolds for 15 days and 30 days in complete medium which was changed on every alternate day.

2.5.4.2. EC adhesion and spreading

HUVEC seeded onto PCL and hybrid scaffold at a plating density 2×10^4 cells cm^{-2} area and were analyzed for actin filament assembly at 2h and 24h by staining for actin as described in #2.4.1.1. with Texas Red Phalloidin (Molecular Probes, USA) using confocal microscope (LSM Meta 510, Zeiss, Germany).

2.5.4.3. Environmental scanning electron microscopy (ESEM)

ESEM (FEI Quanta 200, Netherlands) was employed to visualize the morphology of the bare scaffold, fibrin coated scaffold and cell seeded scaffolds

after 15 days and 30 days of culture. Samples were taken directly from culture medium and were analyzed in wet condition. An electron beam voltage of 10-15kV was applied in each case. Different magnifications were used in order to view fields that cover maximum area with best clarity.

2.5.4.4. Mechanical Properties evaluation

EC were cultured on the hybrid fibrin composite scaffolds for a period of 15 days and 30 days and the tensile strength was measured as described in # 2.5.3.4. Scaffolds after porogen leaching for 3 days and 15 days were also included in the study after seeding and growing cells.

2.5.5. Statistical analysis

All experiments were carried out with at least 8 samples in each group. Significant differences between two groups were evaluated using ANOVA (single factor) with 95% confidence level. When $p < 0.05$, the differences were considered statistically significant.

2.6. ENDOTHELIAL CELL GROWTH AND FUNCTIONAL TISSUE GENERATION

2.6.1. Cell proliferation

2.6.1.1. PCNA staining

To assess the percentage of proliferating cells on PCL and hybrid scaffold, HUVEC was seeded on to the scaffolds at a plating density of 2×10^4 cells cm^{-2} . After 72h of culture, the cells were harvested estimated the percentage of PCNA positive cells as described in 2.4.2.2.

2.6.1.2. Tritiated Thymidine Uptake

Attachment and proliferation of EC was quantified using ^3H -thymidine uptake assays. To quantify cell attachment, EC in log phase were labeled with ^3H -thymidine (American Radio chemicals, USA) by placing $20\mu\text{Ci}$ ^3H -thymidine per 25cm^2 flask of EC culture for 72h at 37°C . These cells were harvested and 3×10^4 cells per cm^2 were seeded on study scaffolds. Unattached cells were aspirated after 2h and attached cells were fed with complete MCDB 131 medium

containing $2\mu\text{Ci ml}^{-1}$ [^3H] thymidine and after 72 h, EC were harvested from each study matrix. An aliquot containing 3×10^4 cells was used for ^3H counting to detect radioactivity per cell. Extraction of ^3H from unseeded, unattached, and proliferated cells were done as per the method standardized by Shivakumar *et al.* (1992) and radio active count per minute (CPM) was detected using a liquid scintillation counter (TRIATHLER Multi-label tester, HIDEX, Finland). The number of cells attached was calculated from CPM of unattached cells and that of known number of cell aliquot taken before seeding and assayed for ^3H using a liquid scintillation counter.

2.6.2. Apoptosis

The apoptosis of EC on the scaffolds were quantified using Vybrant Apoptosis Assay Kit (Molecular probes, USA). The cells were seeded onto the scaffolds at a plating density of 2×10^4 cells cm^{-2} . After 24h of seeding, the cells were harvested by trypsinization and were stained according to manufacturer's protocol. After staining, the cells were washed and re-suspended in FACS sheath fluid and were analyzed using a flow cytometer (FACS Aria, BD Biosciences, USA) to estimate the percentage of live/apoptotic/necrotic cells.

2.6.3. Long term cell growth

The cells (seeding density - 2×10^4 cells cm^{-2} area) were cultured over the hybrid scaffold for 15d and were stained for F-actin according to the 2.5.4.2. The scaffold was analyzed using confocal microscope (LSM Meta 510, Ziess, Germany). In order to detect the cells throughout the depth of the bybrid scaffold scaffold, z sectioning of the field was done.

2.6.4. Cell Solubilization and Matrix Staining

To obtain ECM for analysis, after 15days and 30days EC culture on hybrid scaffold, cells were digested by a hypotonic- alkaline- detergent- treatment cycle as described in #2.4.5. ECM thus recovered was individually stained with Collagen IV- or Elastin- specific antibodies as described in #2.4.6.3. and were analyzed using Confocal Microscope. (LSM Meta 510, Ziess, Germany) In order to detect the proteins deposited in the porous scaffold, z sectioning of the field was carried out.

2.6.5. Characterization of EC Phenotype

2.6.5.1. RNA isolation and reverse transcription

Endothelial cells were cultured on fibronectin coated tissue culture polystyrene (FN TCPS) (BD Biosciences, USA), fibrin composite coated tissue culture polystyrene (FC TCPS) and fibrin composite coated porous PCL scaffold (FC PCL) at an initial EC seeding density of 3×10^4 cells cm^{-2} to evaluate their ability to support EC growth and ECM protein expressions.

To prove normal phenotype of EC m-RNA expression of two prothrombotic factors, von Willebrand factor (vWF), plasminogen activator inhibitor-1 (PAI-1); two anti thrombotic factors, tissue plasminogen activator (tPA) and endothelial nitric oxide synthase (eNOS) were analyzed. In order to prove that EC contribute towards ECM remodeling, mRNA expression of elastin, Collagen I and Collagen IV were analyzed. EC were grown on FN TCPS, FC TCPS and FC PCL for 24h, 144h respectively. The RNA was isolated by TRI Reagent (Invitrogen, USA) as per manufacturer's directions. Yield of RNA was quantified by spectrophotometric measurement (Diode array spectrophotometer, Hewlett Packard, USA) and 20ng of total RNA was taken for reverse transcription using Thermal Cycler (Master Cycler, Eppendorf, USA) at annealing temperatures 53°C - 65°C respectively for vWF, PAI, eNOS, tPA, Collagen I, collagen IV and elastin, in a 25 μl total volume containing 10 μl total RNA, 1 μl dNTP (500 ng/ μl), DEPC water, 1 μl MgCl_2 (50 mM), 2.5 μl 10X RT Core buffer, 1 μl each forward and reverse primer and 0.25 μl M Mulv reverse transcriptase (Stratagene, USA). The primer sets were derived from previously published reports (Seliktar et al., 2003; Bell et al., 2001).

Transcripts	Primer Sequence (5' to 3')	Annealing Temperature (°C)
vWF	F: CACCATTCAGCTAAGAGGAGG R: GCCCTGGCAGTAGTGGATA	55
tPA	F: ATGGGAAGACATGAATGCAC R: GAAAGGGGAAGGAGACTTGA	53
PAI-1	F: TTGGTGAAGGGTCTGCTGTG R: GGCTCCTTTCCCAAGCAAGT	57
eNOS	F: AGCTGTGCTGGCATAACAGGA R: ATGGTAACATCGCCGCAGAC	58
Collagen I	F: CCAAGGGTAACAGCGGTGA R: GCTTTCCTTCTCTCCAGCA	57
Elastin	F: CGGCGCCTTCCCCGCAGTTACCTTT R: ACACAACCCCTGGAACCGCAGCACC	63
Collagen IV	F: CCTGGCTTGAAAGGTGATAAG R: CCCGCTATCCCTTGATCTC	53
GAPDH	F: ATTGGCTTTGGTCCGAGTCC R: GGGGGTTCTTTGGCTTTTAC	55

Table – 1.1. Sequences of primers used in RT-PCR

2.6.5.2. Real-Time PCR

To compare the mRNA expression levels at 24h and 144h, the real-time PCR was performed using a Chromo4 system (MJ Research, USA) as described in 2.4.7.2 at annealing temperature of 53–63°C as specified in the above table (Table 1) for each gene. PCR melt-curves confirmed that all reactions were specific. The cDNA copy numbers of the target gene were analyzed after being normalized to the copy number of GAPDH.

2.6.6. Assessment of Nitric oxide (NO) release

Nitric oxide release by endothelial cells grown on the hybrid scaffold was evaluated at static and dynamic conditions. Nitrite, which is the stable metabolite of NO, was estimated by modified Griess reagent (SIGMA, USA). For this assay, ECs in the third passage were seeded on the hybrid scaffold (2.5cm x 1cm x 0.08mm) at a density of 2×10^4 cells cm^{-2} and cultured for 72h to attain confluence. To eliminate the protein interference, complete medium from the culture wells were removed 1h before estimation and fresh serum-free, phenol red-free M199 medium (SIGMA, USA) was added. After incubation, medium was collected, centrifuged to remove particulates if any. An equal volume of Griess reagent was added, incubated for 15 min at room temperature and color developed was read at 540 nm using a diode array spectrophotometer (Hewlett Packard 8053, USA). To detect NO release under shear stress, the cell-grown scaffolds were perfused with Phenol red-free M199 medium at a flow rate of 50 ml/min using a peristaltic pump (MIDI-Digital, Cole Parmer, USA) for 1 h at room temperature (Shear stress ~ 20 dynes cm^{-2}). The medium was collected after 1h for NO assay. The amount of nitrite formed was calculated from a calibration curve obtained using serially diluted sodium nitrite as standard. Six samples were used for the study and the results are represented as mean \pm standard deviation.

2.6.7. Effect of shear stress on EC monolayer

To analyze cell retention after dynamic exposure of cell-grown scaffold (step 2.6.6.), the cells on the scaffold were washed with PBS three times, fixed with 0.2% glutaraldehyde (Sigma) for 1h and stained using Maygrunwald– Geimsa (Sigma, USA). The scaffold was affixed on a slide and viewed under light microscope (Lieca DM IRB, Germany) to assess if cell detaches with shear stress.

2.6.8. Evaluation of Blood Compatibility

All tests were done according to the standard ISO 10993 - Part 4:2002 (E), selection of tests for interaction of materials with blood. Blood was collected into the anticoagulant, CPDA from human volunteers. Platelet Rich Plasma (PRP) was separated from blood by centrifugation at a speed of 2500 rpm for 5 minutes. The test materials were PCL (bare), FCPCL (Fibrin composite coated

PCL/hybrid scaffold), and EC FC PCL (Endothelial cell grown fibrin composite coated PCL). Scaffold EC FC PCL were seeded with endothelial cells (2×10^4 cells / cm^2 area) and cultured for 144h to form a monolayer. Six replicates were tested for each material.

2.6.8.1. Qualitative analysis of platelet adhesion by scanning electron microscopy

The scaffolds were exposed to PRP (2×10^8 platelets/ml) for 30min under agitation in an environ shaker at a speed of 70 ± 5 rpm at $37 \pm 2^\circ\text{C}$. After the exposure period the grafts were washed with PBS, fixed with 2% gluteraldehyde overnight at 4°C , dehydrated with graded concentrations of alcohol (30%, 50%, 70%, 90% and finally 100%), and then with amyl alcohol, and critical point dried, gold sputter coated. All samples were viewed under a scanning electron microscope (Hitachi S2400, Japan).

2.6.8.2. Quantification of Platelet Adhesion by Radioscintigraphy

2.6.8.2.1. Labeling of Platelets with ^{125}I

The labeling was done according to the method of Resmi *et al.* (2004). Briefly, the PRP was centrifuged at 1000g for 15 min and the platelet pellet was re-suspended and centrifuged (three repetitions) with a modified Tyrode's Buffer containing 10% Acid citrate dextrose (ACD). The final pellet was re-suspended in Tyrode's buffer without ACD. Labeling of platelets with ^{125}I (American Radio Chemicals, USA) was done using lactoperoxidase (Sigma, USA) in presence of H_2O_2 (Sigma) ^{125}I and the enzyme was added to the platelet suspension to the required concentrations ($0.2 \text{ mCi } ^{125}\text{I} / 10^9$ platelets; 5 nM final concentration lactoperoxidase). Iodination reaction was done by addition of 5 μl aliquots of 1mM H_2O_2 at 1 min intervals for 5 min. After the reaction, unreacted ^{125}I was removed from labeled platelets using a column of Sepharose 2B (Sigma) according to the method of Tangen *et al* (1971). Platelets are eluted in the void volume and platelet count was taken using Hematology Analyzer (Cobas Minos Vet, Roche Diagnostics, France).

Aliquots of known number of ^{125}I -platelets were spot dried on a stainless steel template and exposed to phosphor screen. The radioactivity on labeled

platelets and in isotope solution used for labeling was detected using Molecular Phosphor Imaging System (GS505, Biorad, USA). Labeling efficiency (LE %) of each experiment was calculated.

2.6.8.2.2. Exposure of materials to labeled PRP

The ^{125}I -platelets were suspended in autologous plasma to get ^{125}I -PRP with a platelet count of $(2 - 2.5) \times 10^8$ /ml. Exposure of test surfaces with ^{125}I -PRP were carried out as described in #2.6.8.1. After exposure, the materials were washed thoroughly with PBS to remove nonspecifically bound platelets. The adhered platelets were fixed with 2% gluteraldehyde, overnight at 4°C. After fixation, materials were rinsed with PBS, dried and scanned using Molecular Phosphor Imaging System (GS505, Biorad, USA) along with platelet standards prepared as described in #2.6.8.2.3.

2.6.8.2.3. Quantification of Adhered Platelets

Aliquots of labeled platelets with known counts were spot dried on a stainless steel template. The materials that are fixed and dried after exposed to labeled PRP were fixed on stainless steel template, and were exposed to the phosphor screen together with the dried platelet aliquots and imaged using the Phosphor Imaging System. The mean CPM was obtained and the calibration curve of radioactivity against platelet number was generated using the software Multi Analyst (Biorad, USA) from the CPM of serially diluted known number of platelet aliquots. The same software detected the number of platelets adhered on the materials, using the calibration curve, based on the image intensity.

2.6.8.2.4. Statistical analysis

Six replicate samples were analysed for each test and statistical significance was determined by students T-test and single factor ANOVA. When $p < 0.01$ the differences were considered statistically significant.

STANDARDIZATION OF A FIBRIN MATRIX COMPOSITION TO ACHIEVE ECM DEPOSITION IN TISSUE CULTURE POLYSTYRENE BY CULTURING HUVEC

3.1. ABSTRACT

Studies in vascular tissue engineering have highlighted the importance of the *in vitro* culture conditions to produce the functional constructs. In tissue engineering, extra-cellular matrix (ECM) proteins that are deposited by the cells play a major role in determining the construct stability as well as regulation of the cell–matrix interactions. Hence, an ideal matrix/scaffold provide appropriate signals to cells that facilitate production of matrix proteins leading to tissue remodeling.

Deposition of elastin and collagen by endothelial cells grown in the lumen of the construct is desirable to improve post implant retention, mechanical stability and vasoresponsiveness. Therefore, it is necessary to standardize methods to determine the optimal conditions for new cardiovascular tissue formation with appropriate matrix formation, turnover and remodeling *in vitro*. In this study, a biomimetic approach was employed by providing growth factors (GF) and or glycosaminoglycans individually and in combinations in the fibronectin (FN) and gelatin containing fibrin matrix to induce production of elastin

and collagen by the endothelial cells *in vitro* for application in vascular tissue engineering.

The specific objectives of the first phase of the study were 1) To standardize a basic fibrin composite matrix and to evaluate the role of various components of the fibrin composite matrix for cell adhesion, proliferation and survival 2) To study the effect of glycosaminoglycans and growth factors on cell adhesion and proliferation 3) To study the effect of growth factor and glycosaminoglycan combinations on cell adhesion, proliferation and apoptosis. 4) To evaluate fibrin matrix degradation during EC culture 5) To study the effect of Growth Factors and GAGs individually and in combination on deposition of elastin, collagen I and collagen IV 6) Finally, to identify the most suitable matrix composition for vascular tissue engineering. The methods are described in chapter II and the results are illustrated and discussed here.

3.2. Endothelial cell characterization

The endothelial nature of the isolated cells has been conclusively established on the basis of morphologic, metabolic, and immunospecificity criteria. The isolated cells from human umbilical vein were characterized by their cobble stone morphology, positive staining for vWF and uptake of acetylated LDL which could be visualized in the phase contrast images as well as fluorescent micrographs. Figs. 3.1. A&B show the isolated cells at the time of seeding; the cells appear as a chain. The cell attachment at 2h on gelatin could be visualized as shown in Figs. 3.1.C&D. The typical cobble stone morphology of endothelial cells could be observed in the confluent monolayer during primary culture Figs. 3.1.E&F. The characteristic positive staining for vWF could be visualized as shown in Figure 3.2A which is localized in the Weibel Palade bodies of the cells and are distributed throughout the cytoplasm. The isolated cells after adhesion took up acetylated LDL which was also characteristic of endothelial cells Fig. 3.2.B.

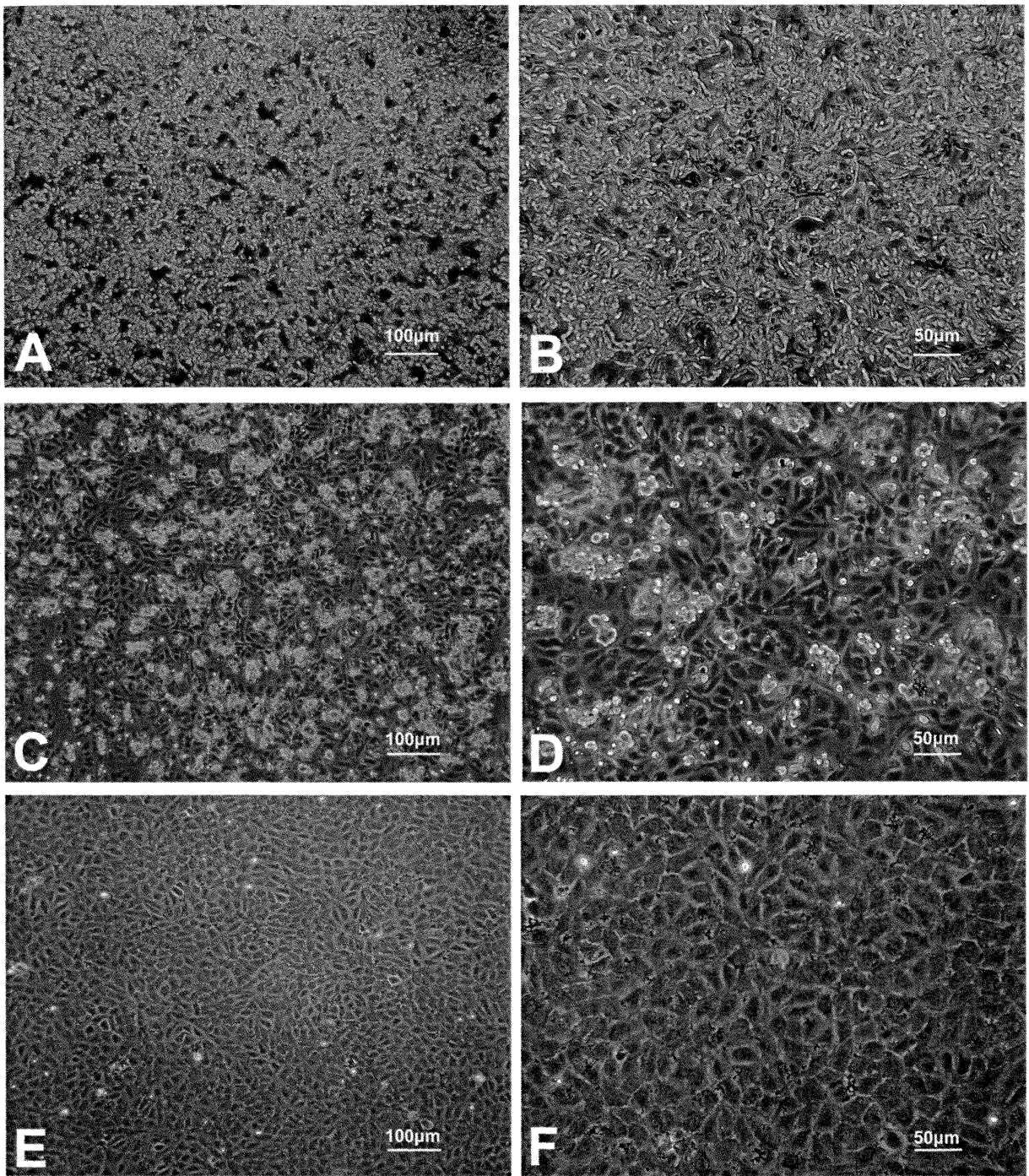


Figure 3.1. Phase contrast microscopic images of representative fields from HUVEC culture at different magnifications. A&B. Cells at the time of isolation C&D Cells after 2h of seeding. E&F. Cells after 24h of seeding

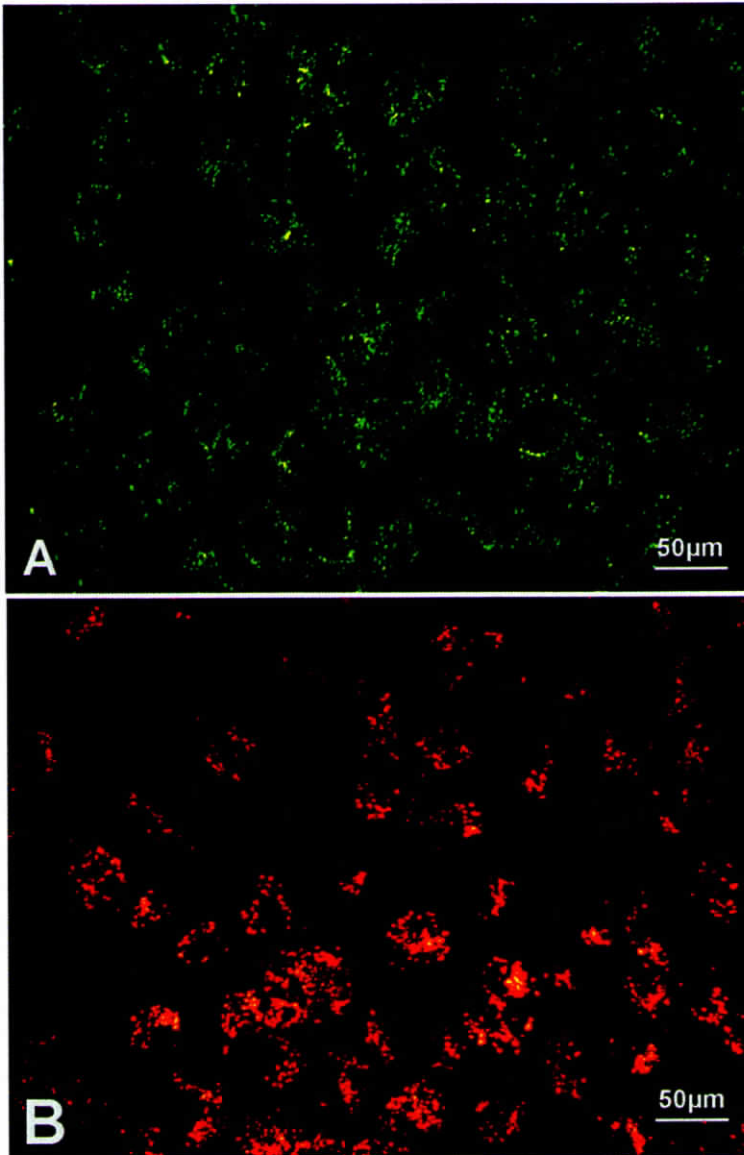


Figure 3.2. Fluorescent Micrographs of HUVEC showing A. Positive staining for vWF identified using FITC-tagged antibodies B. Uptake of DiIAcLDL.

3.3. Standardization of basic fibrin composite matrix

3.3.1. EC adhesion

Cell adhesion spreading and actin organization is found to be uniform in the case of CCPS (Fig. 3.3.A), and actin filaments are clearly visualized. On gelatin-depleted and growth factor-depleted matrices, number of cells adhered in each field was similar to that on CCPS, however, spreading is less and organized actin filaments are not seen uniformly (Figs. 3.3.B&C). Depletion of FN from composite coated matrix by treating with anti-fibronectin antibody has effectively reduced EC adhesion. On FN-depleted matrix, cell number is less, spreading is poor and the adhered cells seemed to have actin filaments but are not well organized (Fig. 3.3.D) as compared to the cells on CCPS. The mean fluorescence intensity (MFI) of actin stained cells in one region of interest (ROI) on all four matrix types are shown in Fig. 3.3.B. It is evident that the cells on CCPS gave higher fluorescence intensity at all planes across the z-axis, whereas it is reduced on CCPS-GF > CCPS-GEL > CCPS-FN. This data suggests that for good cell adhesion, spreading and actin organization, presence of fibronectin is crucial, presence of gelatin and growth factors also play a role for good actin organization. The purity of antibodies that were developed in-house was verified by SDS-PAGE and its reactivity with fibronectin in the cryoprecipitate was verified by Western blot analysis.

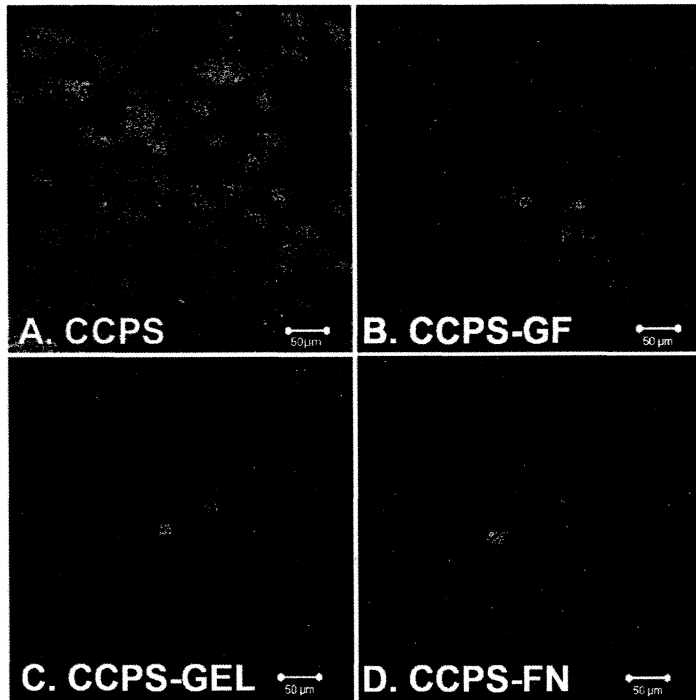
Vinculin expression on EC after 24h of seeding on different matrix types is shown in figs. 3.4.A-D. While vinculin is seen associated with more cells on CCPS (Fig. 3.4.A), it was found to be less frequent on CCPS-GF (Fig. 3.4.B), on CCPS-GEL (Fig. 3.4.C) and on CCPS-FN it is scarcely seen (Fig. 3.4.D). Presence of vinculin is maximal on CCPS as seen in Fig. 3.4.B where MFI of vinculin stained cells in one selected field, each of four matrix types are plotted against the z section depths.

3.3. Standardization of basic fibrin composite matrix

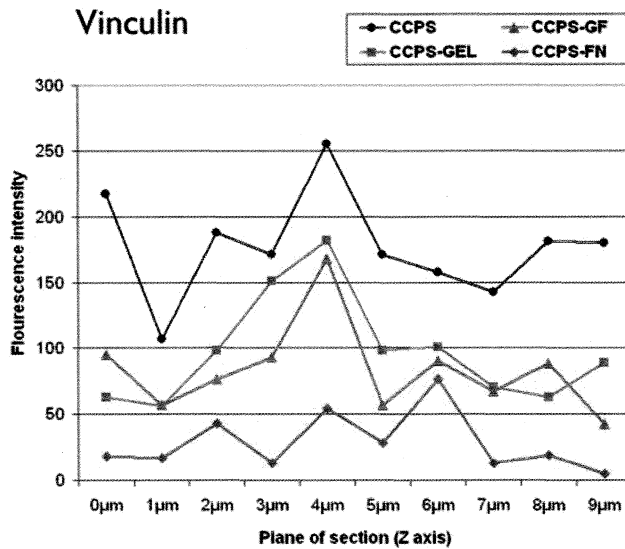
3.3.1. EC adhesion

Cell adhesion spreading and actin organization is found to be uniform in the case of CCPS (Fig. 3.3A), and actin filaments are clearly visualized. On gelatin-depleted and growth factor-depleted matrices, number of cells adhered in each field was similar to that on CCPS, however, spreading is less and organized actin filaments are not seen uniformly (Figs. 3.3B&C). Depletion of FN from composite coated matrix by treating with anti-fibronectin antibody has effectively reduced EC adhesion. On FN-depleted matrix, cell number is less, spreading is poor and the adhered cells seemed to have actin filaments but are not well organized (Fig. 3.3D) as compared to the cells on CCPS. The mean fluorescence intensity (MFI) of actin stained cells in one region of interest (ROI) on all four matrix types are shown in Fig. 3.3.B. It is evident that the cells on CCPS gave higher fluorescence intensity at all planes across the z-axis, whereas it is reduced on CCPS-GF > CCPS-GEL > CCPS-FN. This data suggests that for good cell adhesion, spreading and actin organization, presence of fibronectin is crucial, presence of gelatin and growth factors also play a role for good actin organization. The purity of antibodies that were developed in-house was verified by SDS-PAGE and its reactivity with fibronectin in the cryoprecipitate was verified by Western blot analysis.

Vinculin expression on EC after 24h of seeding on different matrix types is shown in figs. 3.4.A. While vinculin is seen associated with more cells on CCPS (Fig. 3.4A), it was found to be less frequent on CCPS-GF (Fig. 3.4B), on CCPS-GEL (Fig. 3.4C) and on CCPS-FN it is scarcely seen (Fig. 3.4D). Presence of vinculin is maximal on CCPS as seen in Fig. 3.4.B where MFI of vinculin stained cells in one selected field of four matrix types are plotted against the z-section depths.

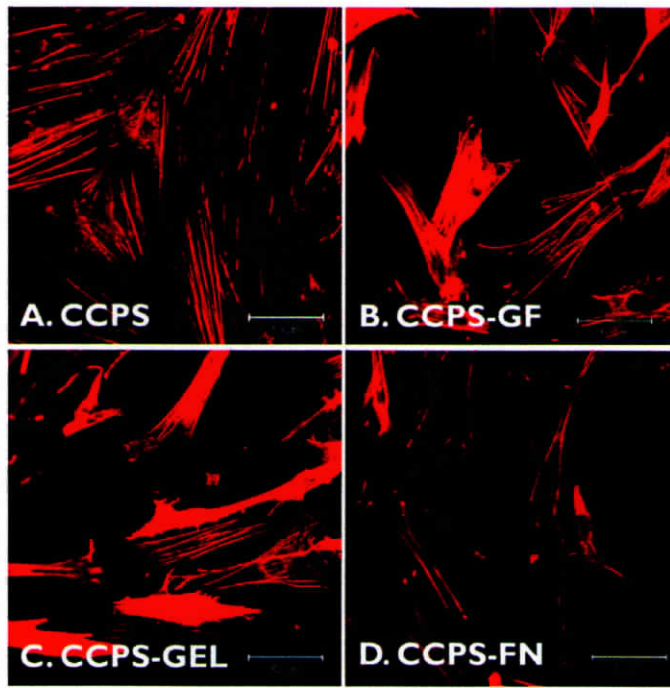


A

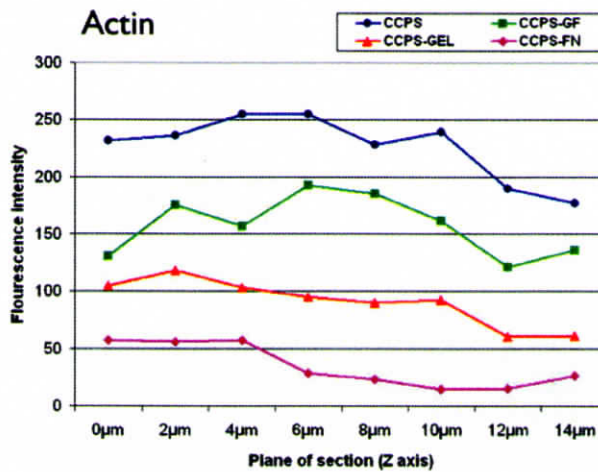


B

Figure 3.4. A-D. Confocal images of endothelial cells stained for Vinculin. Figure A. A-D are cells after 24 hours of growth on the defined matrices. A, CCPS; B, CCPS-GF; C, CCPS-GEL; D, CCPS-FN. In each case, micrographs were constructed using 10 z-sections of 1 μ m thickness. FITC was excited using Argon Laser at 488nm and the emission wavelength was collected using BP 505-530 filter. **Figure B.** Graphical representation of fluorescent intensity of a selected field of vinculin stained cells grown on the defined matrices, CCPS, CCPS-GF, CCPS-GEL, CCPS-FN are superimposed. Cumulative fluorescence intensity shown on Y-axis of the graph presents intensity against each z-cross section of the fields at 8 different z-sections of 1 μ m thickness.

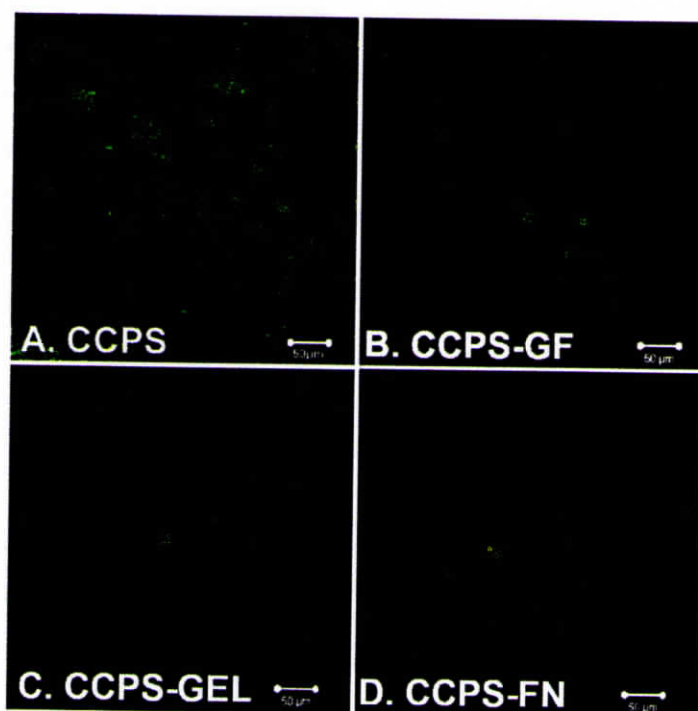


A

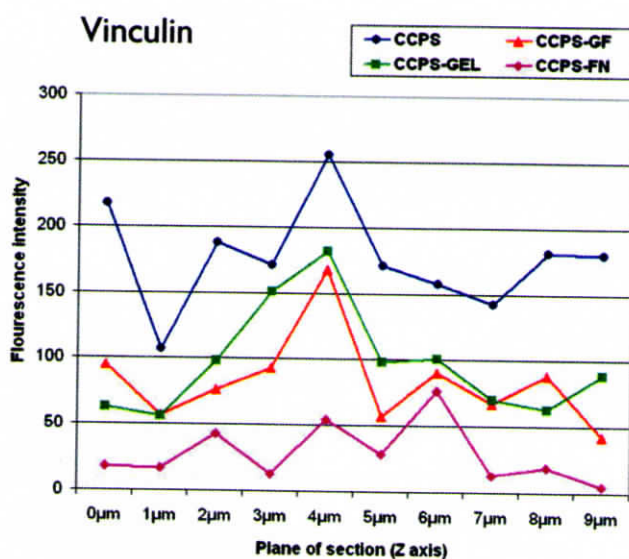


B

Figure 3.3. Confocal images of endothelial cells stained for Actin. Figure A. A-D are cells after 24h of growth on the defined matrices. A, CCPS; B, CCPS-GF; C, CCPS-GEL; D, CCPS-FN. Each image was acquired from one z-plane of the respective sample. Texas Red-Phalloidin was detected by excitation using He/Ne Laser at 594 nm that was captured at an emission wavelength 610 nm using a long pass filter. Figure B. Graphical representation of fluorescent intensity of a selected field of vinculin stained cells grown on the defined matrices, CCPS, CCPS-GF, CCPS-GEL, CCPS-FN are superimposed. Cumulative fluorescence intensity shown on Y-axis of the graph presents intensity against each z-cross section of the fields at 8 different z-sections of 2μm thickness.



A



B

Figure 3.4. A-D. Confocal images of endothelial cells stained for Vinculin. Figure A. A-D are cells after 24 hours of growth on the defined matrices. A, CCPS; B, CCPS-GF; C, CCPS-GEL; D, CCPS-FN. In each case, micrographs were constructed using 10 z-sections of 1 μm thickness. FITC was excited using Argon Laser at 488nm and the emission wavelength was collected using BP 505-530 filter. **Figure B.** Graphical representation of fluorescent intensity of a selected field of vinculin stained cells grown on the defined matrices, CCPS, CCPS-GF, CCPS-GEL, CCPS-FN are superimposed. Cumulative fluorescence intensity shown on Y-axis of the graph presents intensity against each z-cross section of the fields at 8 different z-sections of 1 μm thickness.

3.3.2. Cell Proliferation & Apoptosis

Attachment of cells at 2h after EC seeding on all types of matrix is comparable and proliferation with approximately 2 population doubling is seen on CCPS (Fig. 3.5.A) by 72h. Cell number has increased on both CCPS-GF and CCPS-GEL, but on CCPS-FN there is no increase in cell number, it has rather reduced, indicating that the initially attached cells have detached with time from the surface. Flow cytometric analysis of apoptosis of EC harvested from each matrix shows significant difference between the matrices (Fig. 3.5.B). While there is no cell death on CCPS, approximately 30% cell death is seen on both CCPS-GF and CCPS-GEL after 72h. Cell apoptosis is high (>75%) on CCPS-FN. The cell proliferation and apoptosis data suggests that presence of fibronectin within the fibrin matrix is crucial for cell proliferation and survival, whereas growth factors and gelatin also are important. Even though there is significant cell death on CCPS-GEL, CCPS-GF at the initial period (24h to 72h), the cells proliferated with healthy monolayer formation by 96h to 120h, on both matrix types. The cell number reduced further with time on FN-depleted fibrin matrix.

In physiology, ECM proteins possess multiple binding sites for cell adhesion molecules, and many motifs serve as ligands for cell surface receptors. Binding of cell surface receptors to ECM proteins initiates intracellular signaling pathways that influence cellular behavior. ECM components guide cellular differentiation and inhibit or promote cell proliferation and migration.

Here it could be seen that the CCPS promoted cell proliferation and survival when compared to the other matrices that were deprived of GF or GEL. The use of anti-fibronectin antibody has blocked fibronectin activity and we found that the cellular events were affected as evidenced from actin and vinculin staining and apoptosis and proliferation assays. In fibrinogen molecule, the COOH-terminal regions of the A α -chains, also called the α C-domains, are involved in cell adhesion via either bound fibronectin or their A α 572–574 Arg-Gly-Asp (RGD) recognition motif (Corbett et al, 1998).

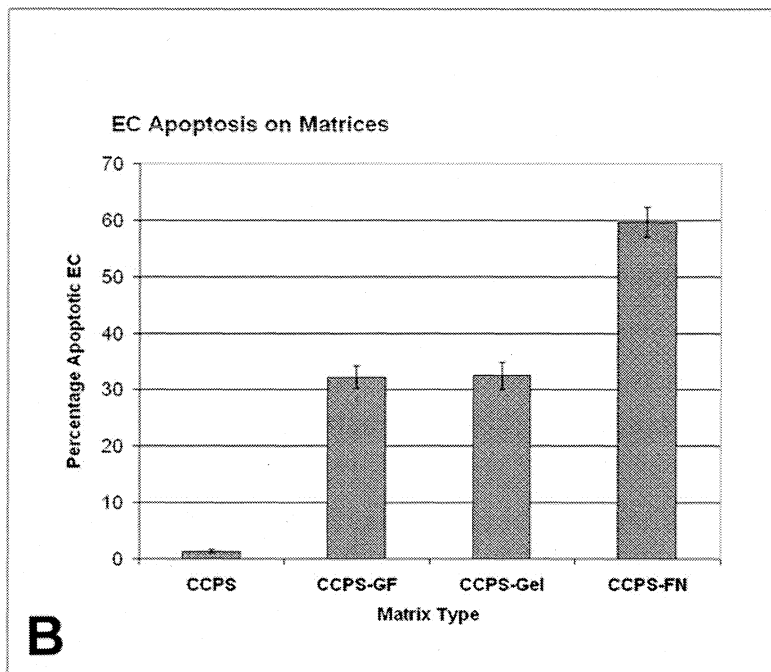
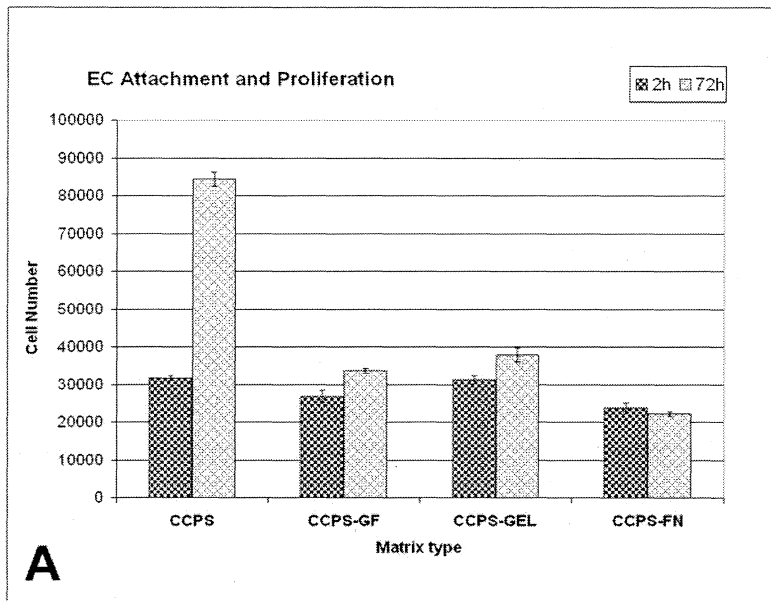


Figure 3.5. Quantification of endothelial cell growth and survival. **A**, attachment at 2 h and proliferation at 72 h Cell number on the defined matrices; CCPS, CCPS-GF, CCPS-GEL and CCPS-FN were estimated using tritiated thymidine content in the cell. **B**, Quantification of cell apoptosis on the defined matrices; CCPS, CCPS-GF, CCPS-GEL and CCPS-FN at 72 h after cell seeding were estimated using flow cytometry. Annexin V and Propidium iodide were excited using the blue laser and the emission wavelengths were captured using BP 530(20) and BP 610(20) filters respectively.

This study demonstrate that when fibrin coated surfaces are used for EC culture, the fibronectin present in the cryoprecipitate is a major component that contribute to cell adhesion, spreading, proliferation and survival. The gelatin present in the CCPS has binding sites on fibronectin that enhances gelatin retention and its uniform distribution in the composite matrix (Katagiri, 2003).

Fibroblast growth factor-2 (FGF-2) and vascular endothelial growth factor (VEGF) bind to fibrinogen and are able to potentiate EC proliferation when bound (Sahni *et al.*, 1999; 2000). Wijelath *et al.* (2002) demonstrated that association between VEGF and FN is required for full effects of VEGF-induced EC migration and proliferation. A synergistic effect in EC migration was observed when VEGF and FN were combined as compared to FN and other ECM proteins.

Therefore the effect of EC growth, survival and differentiation that is seen on the composite coated surface is contributed by fibrin and VEGF bound to it, fibronectin cross linked to fibrin, gelatin covalently attached to fibronectin and in addition the mitogenic fibrinopeptides released during fibrinogen to fibrin conversion. In tissue engineering approaches, several researchers are attempting the use of fibrin as a cell adhesion matrix.

3.3.3. Comparison of fibrin composite matrix (CCPS) to commercial fibronectin coated plates (FNPS).

In this study, fibronectin was found to be a crucial component of the fibrin composite matrix (CCPS) because deprivation of FN caused EC apoptosis. Therefore, endothelial cell behavior on CCPS was compared against commercially available fibronectin coated dishes (FNPS).

Quantification of cell adhesion and proliferation by Tritiated Thymidine uptake assay showed that the number of cells adhered on CCPS and FNPS were similar but the cell proliferation was higher on CCPS (Fig. 3.6). The phase contrast images depicting the morphology of EC when cultured over CCPS and FNPS is shown in the figure 3.6.A. By 72h the ECs were confluent with the typical cobble stone morphology over the CCPS whereas in FNPS uncovered

could be seen. The PCNA analysis also showed an increased percentage of PCNA positive cells on CCPS (86%) whereas on FNPS it was 73% when analyzed after 72h post seeding (Fig. 3.7). The result confirms that even though fibronectin is crucial for cell adhesion and proliferation the presence of multiple components like growth factors and gelatin in the matrix enhances the cell proliferation rate. The cell survival rates on the two matrices were comparable (Fig. 3.8).

The cells proliferated well on FNPS and CCPS but the percentage of PCNA positive cells were higher on fibrin composite coated dishes compared to fibronectin coated plates. This observation was also confirmed by the Tritiated Thymidine uptake data. It has been reported that although, fibrin is the predominant protein of provisional clot matrix, other adhesive glycoproteins such as FN are its constituents (Clark et al., 1982). During wound healing, the cross linking of FN to the fibrin clot enhances the stability of the clot, and both fibrin and FN act in concert to promote cell migration into the clot and modulate gene expression of cells within the clot (Knox et al., 1986). Altering the composition of a fibrin clot with FN promotes matrix composition-specific modulation of cellular responses (Corbett et al, 1996). Sechler et al (1998) reported that cells react differently with FN in matrix fibrils (within the ECM) or in cross-linked fibrillar structures (in the provisional matrix) than with dimeric FN coated on a surface. Although cells can attach, spread, migrate, and proliferate on FN-coated surfaces, these processes are altered in response to matrix FN. The presence of other ECM proteins can also modulate FN function by facilitating more rapid changes in cell-matrix interactions (Chung et al, 1995). In this study the fibrin composite contained fibronectin, gelatin, and growth factors that mimicked the wound healing milieu. Therefore the increase in cell proliferation may be due to the improved microenvironment provided to the cells with enhanced amounts of cell adhesion and signaling molecules compared to the fibronectin coated dishes.

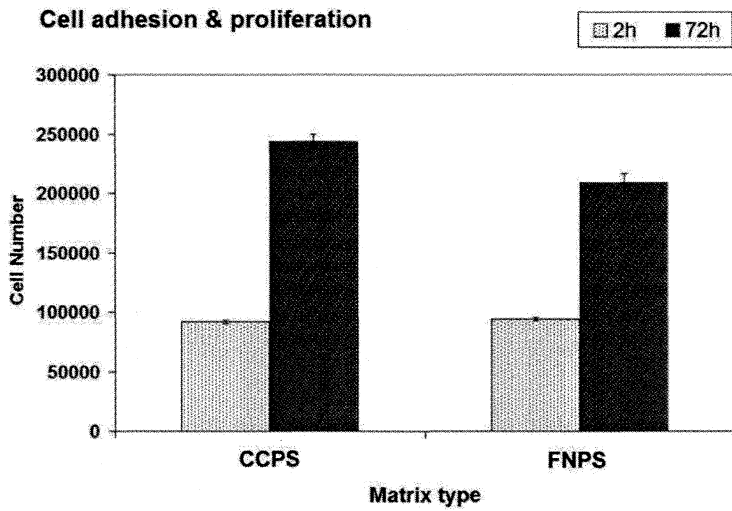
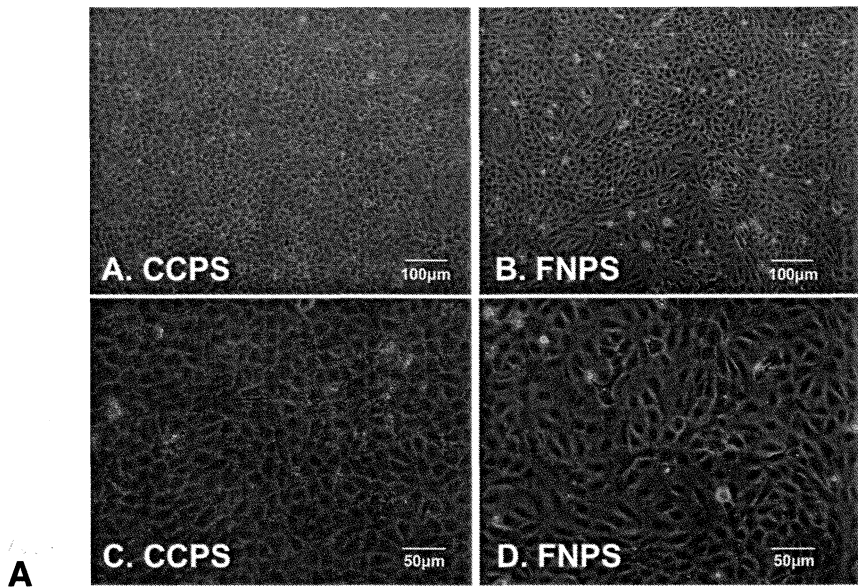


Figure 3.6. A. Qualitative evaluation of cell proliferation: Phase contrast micrographs showing the EC after 72h of culture on the matrices. A&C, CCPS; B&D, FNPS. **B. Quantification of endothelial cell proliferation** on the matrices by Tritiated Thymidine uptake assay

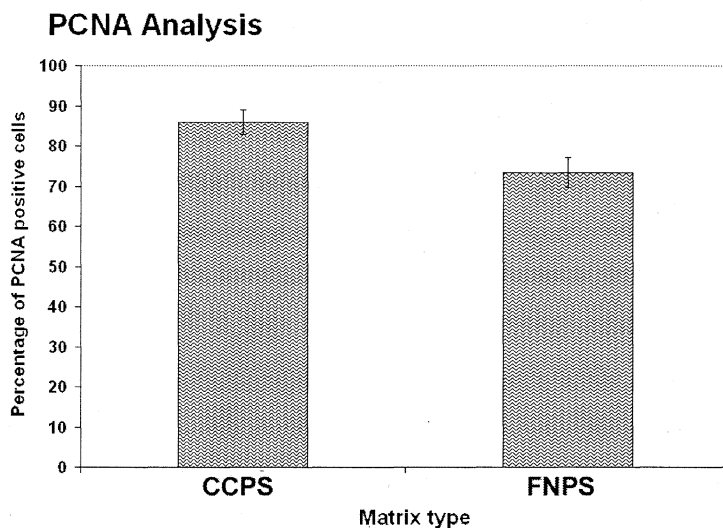


Figure 3.7. Quantitative evaluation of cell proliferation on the matrices by PCNA analysis PCNA-PE stained cells were excited using a blue laser (488 m) and the emitted signal at specific wavelength was captured using the filter BP 576(26). In all cases four replicate experiments were done.

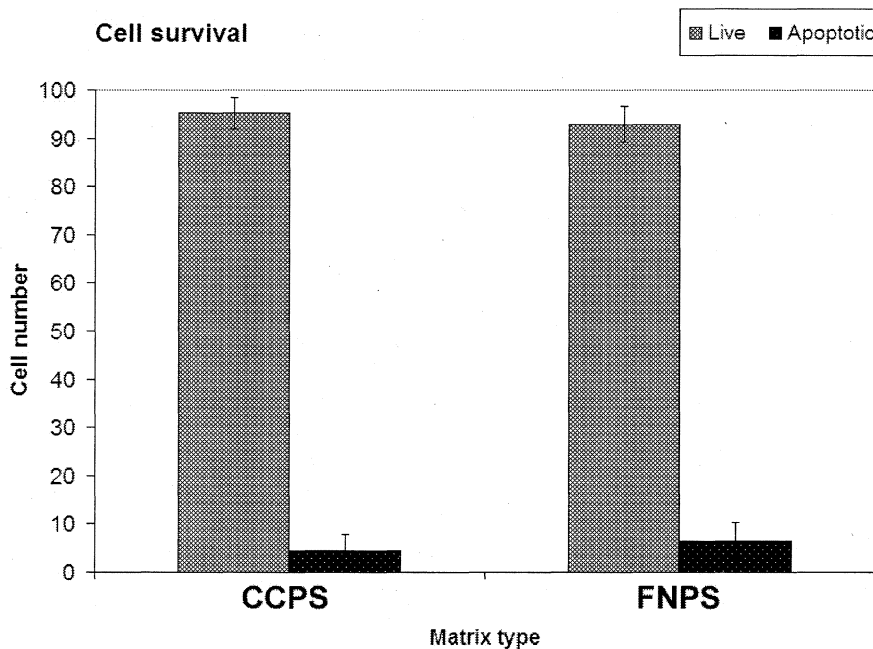


Figure 3.8. Quantification of endothelial cell survival. Quantification of live and apoptotic cells on the defined matrices CCPS and FNPS at 72h after cell seeding were estimated using flow cytometry. Annexin V and Propidium iodide were excited using the blue laser and the emission wavelengths were captured using BP 530(20) and BP 610(20) filters respectively.

Knowing that fibrin composite is favorable for good cell proliferation and survival, it was taken as the basal matrix which was further modified attempting to improve the ECM deposition. During wound repair, adhesive glycoproteins from plasma become incorporated into the fibrin clot by covalent cross-linking, thus in addition to the hemostatic plug, a scaffold is generated for cell migration and proliferation; a reservoir for growth factors, proteases, and protease inhibitors; and a substrate for induction and modulation of cell function (Clark, 1996). The provisional ECM that is formed is different in composition from the ECM in normal tissue and includes fibronectin, collagen, glycosaminoglycans, and proteoglycans. Later this provisional matrix is replaced by fibroblasts which deposit ECM molecules like glycoproteins, glycosaminoglycans (GAGs), proteoglycans, elastin, and fibronectin, which create a matrix that more closely resembles that found in non-injured tissue and facilitate cell migration.

During angiogenesis, the macrophages secrete various growth factors (principally vascular endothelial growth factor—VEGF and basic fibroblast growth factor—bFGF), and "work with" platelets, which secrete platelet derived growth factor—PDGF—to form new tissue. Based on this concept we modified the fibrin matrix with growth factors, Angiogenic growth factors, AGF, that consisted of VEGF and FGF; and Platelet growth factors, from platelet releasate that consisted of a mixture of platelet growth factors (PGF) that include platelet derived growth factor (PDGF), heparin binding platelet factor 4 (PF4), transforming growth factor- β (TGF- β) and β -thromboglobulin (β -TG). The GAGs, Hyaluronic acid (HA) and heparan sulphate (HS) were used. HA has been suggested to play a key role in several biological processes including embryonic development (Toole, 1997), extracellular matrix organization and turnover (Nishida et al, 1999), wound healing (Oksala et al, 1995), and angiogenesis (West, 1985)). Many signaling molecules, such as FGFs, VEGF, TGF- β_1 and - β_2 , as well as several chemokines and cytokines, bind to HS present on cell surface proteoglycans (Forsberg and Kjellén, 2001). The ability of heparan sulfate proteoglycans (HSPG) to interact with major ECM constituents such as fibronectin, collagen type IV, and laminin suggests a key role for HSPG in the self-assembly, insolubility, and integrity of the ECM.

The basal matrix was taken as the control in all the experiments against which various modified matrices were compared. Three formats were tested for EC adhesion, proliferation and ECM synthesis; the first one with different combinations of growth factors, second one with different combinations of GAGs and the 3rd one with GF and GAG together to understand the additive effect. Experiments were designed to compare cell adhesion, proliferation and extra cellular matrix synthesis on different matrix compositions and with each matrix type four replicates were included for each test and/or period. For qualitative analysis the data presented represent four replicate tests and for quantitative analysis, average of four tests is presented with standard deviation.

3.4. Effect of GFs and GAGs on cell adhesion and proliferation

The effect of growth factors and glycosaminoglycans individually and in combination on cell adhesion and proliferation when added to the fibrin matrix were analyzed by Tritiated Thymidine uptake.

3.4.1. Cell adhesion and proliferation – GF/s incorporated matrices

When growth factors were incorporated to CCPS the cell adhesion at 2h was comparable in all the matrices. The cells showed an increased proliferation rate by 72h in all the matrices irrespective of the type of growth factor, when compared to the control. (Fig. 3.9) The proliferation rate was maximum on CCPS + AGF + PGF ($p < 0.01$). CCPS+AGF also showed an increased proliferation rate when compared to CCPS+PGF and CCPS alone.

3.4.2. Cell adhesion and proliferation – GAG/s incorporated matrices

The cell adhesion at 2h was comparable in all the GAG incorporated matrices. Cell proliferation at 72h was maximum on CCPS+HA+HS when compared to the other matrices. Cell proliferation was higher on CCPS+HA when compared to CCPS+HS or CCPS alone (Fig. 3.10).

3.4.3. Cell adhesion and proliferation- GF and GAG incorporated matrices

When GAGs and GFs were incorporated individually and in combination to the basic CCPS matrix, the cell adhesion at 2h was comparable on all the matrices. Though all the matrices showed a higher proliferation rate at 72h when

compared to the control CCPS, cell proliferation rate was maximum on CCPS+GAG+GF ($p < 0.01$) when compared to the other matrices. The CCPS+GF matrix also showed a higher proliferation rate when compared to the CCPS+GAG and CCPS alone (Fig. 3.11).

The cell proliferation on the matrices were also quantitated by PCNA analysis, it was interesting to note that the ^3H thymidine uptake was similar on CCPS+GAG+GF and CCPS+GF, but the percentage of PCNA positive cells were higher on CCPS +GAG+GF (Fig. 3.12) as compared to CCPS+GF. The cell survival rates were good on all the final composite matrices (Fig. 3.13).

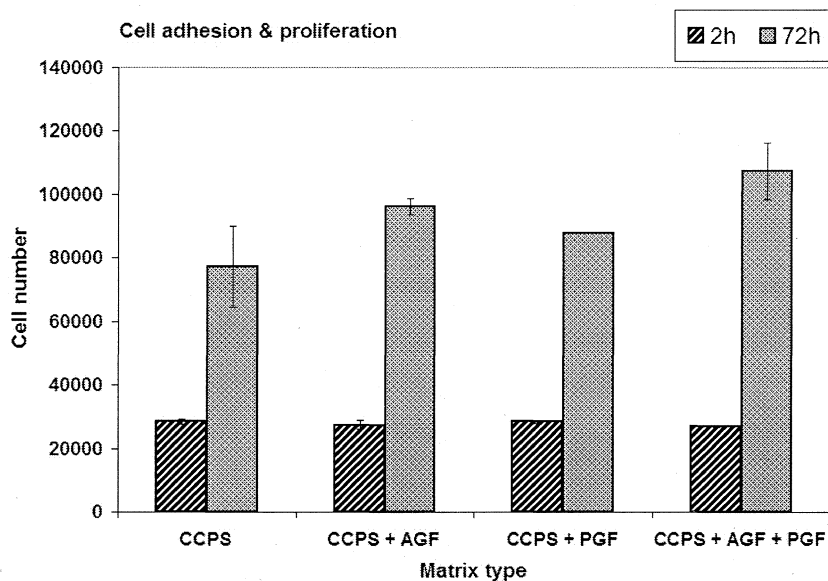


Figure 3.9. Quantification of EC adhesion and proliferation on GF incorporated matrices using ^3H -thymidine uptake. The initial attachment of HUVECs detected at 2h after seeding, and the proliferated cells after 72h on each of matrices are given side by side. The assay was done in 4 replicates experiments and standard deviation ($n = 4$) is given as error bar.

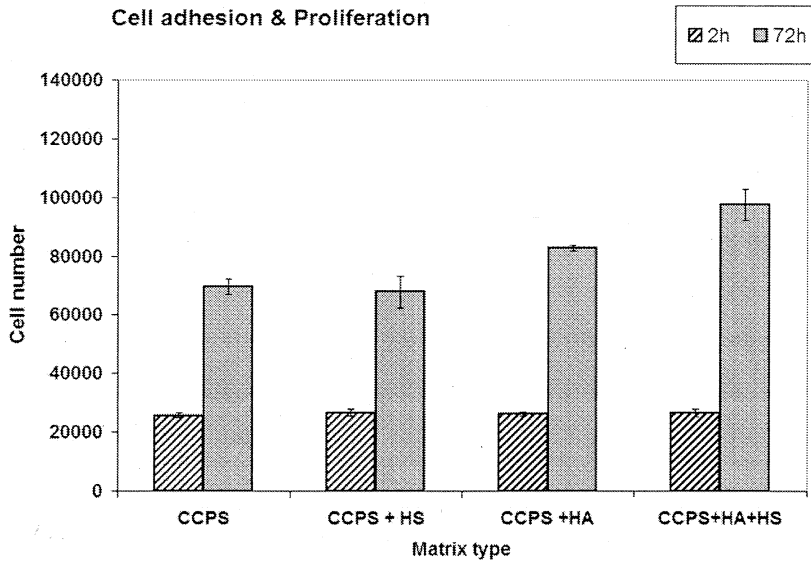


Figure 3.10. Quantification of EC adhesion and proliferation on GAG incorporated matrices using ^3H -thymidine uptake. The initial attachment of HUVECs detected at 2h after seeding, and the proliferated cells after 72h on each of matrices are given side by side. The assay was done in 4 replicates experiments and standard deviation (n =4) is given as error bar.

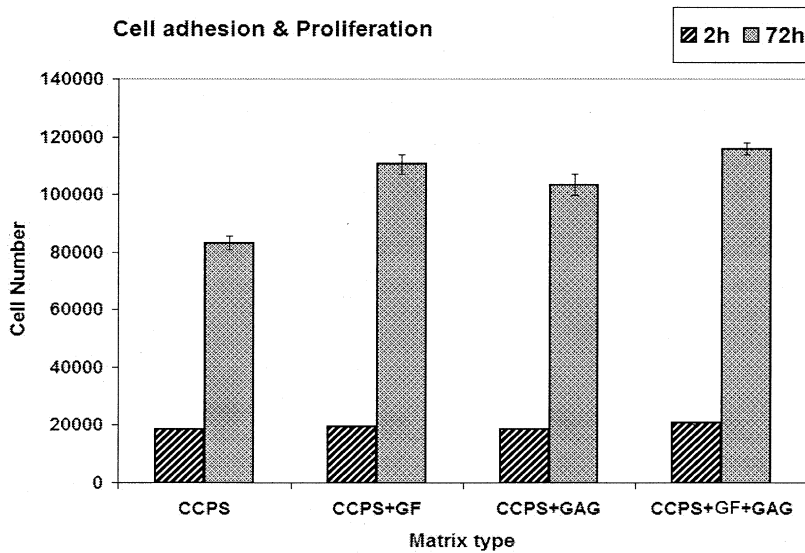


Figure 3.11. Quantification of EC adhesion and proliferation on GF and GAG incorporated matrices using ^3H -thymidine uptake. The initial attachment of HUVECs detected at 2h after seeding, and the proliferated cells after 72h on each of matrices are given adjacently. The assay was done in 4 replicates experiments and standard deviation (n =4) is given as error bar.

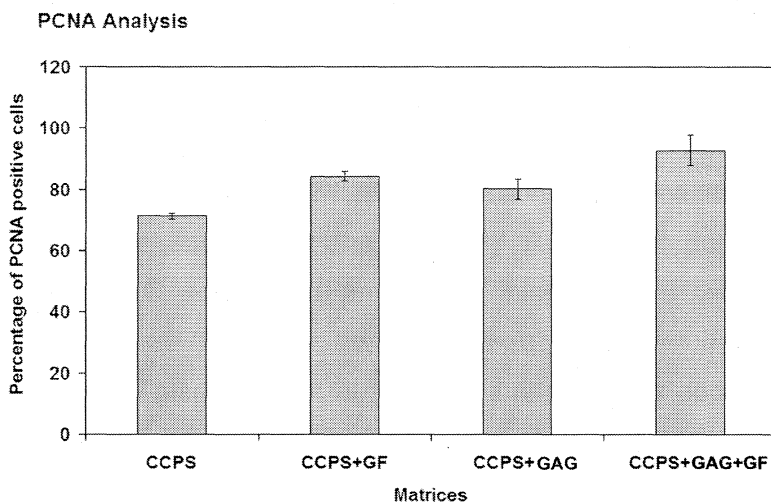


Figure 3.12. Quantification of EC proliferation on GF and GAG incorporated matrices by PCNA analysis. PCNA-PE stained cells were excited using a blue laser (488 m) and the emitted signal at specific wavelength was captured using the filter BP 576(26). In all cases four replicate experiments were done.

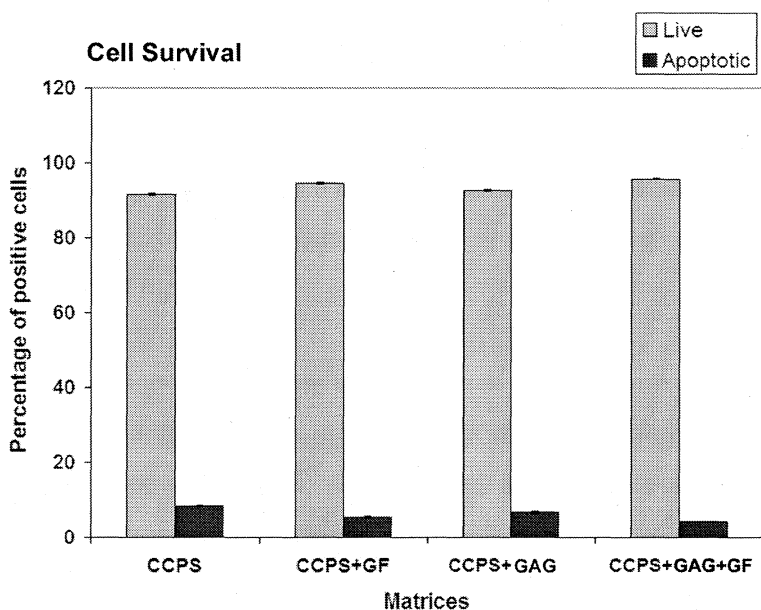


Figure 3.13. Cell viability on the GF and GAG incorporated matrices at 72 h of EC culture. Annexin V and propidium iodide staining of cells were done after harvesting them from the scaffold using trypsin, and stained cells were analysed using flow cytometry. Annexin V and propidium iodide were excited using the blue laser and the emission wavelength was captured using BP 530(20) and BP 610(20) filters, respectively. The percentage of each cell population was calculated using BD FACS Diva software.

Cell adhesion to the matrix is mediated by transmembrane receptors known as integrins. In wound healing and angiogenesis, they play an important role by facilitating the binding of EC to ECM proteins, such as fibrin (ogen)(Ruoslahti, 1996). The α -chain of fibrinogen contains RGD sequences at positions A α 95–97 and A α 572–574 (Ruoslahti and Pierschbacher, 1987), but several studies have shown that the A α 95–97 RGD motif does not play a significant role in EC adhesion (Farrell and Thiagarajan, 1994). The RGD-sequence at position 572–574 of the A α -chain of fibrinogen binds the $\alpha_v\beta_3$ -integrin in humans (Thiagarajan et al, 1996). Fibrinogen has additional binding sites for $\alpha_v\beta_3$ -integrin in the c-chain (Yokoyama et al, 1999) and recombinant fibrinogen missing the RGD-sequences still preserves its interactions with cells (Thiagarajan et al, 1996).

The adhesive potential of EC to fibrin(ogen) is also influenced by the cross-linking (by transglutaminase) and the coagulation (by thrombin) of fibrinogen (Dallabrida *et al.*, 2000). Transglutaminase-mediated oligomerization of the α C-domains of fibrinogen promotes integrin clustering and thereby increases cell adhesion and spreading, which stimulates fibrinogen to bind $\alpha_v\beta_3$ -, $\alpha_v\beta_5$ - and $\alpha_5\beta_1$ -integrins on EC. The oligomerization also promoted integrin-dependent cell signaling via focal adhesion kinase (FAK) and extracellular signal-regulated kinase (ERK), which results in an increased cell adhesion and cell migration (Belkin et al, 2005).

Fibrin can also stabilize the expression of $\alpha_v\beta_3$ -integrin on cultured human micro vascular EC and therefore promote migration of these cells on provisional matrix proteins (Feng et al, 1999). Of the many integrin receptors that recognize one or more specific ECM molecules (Ruoslahti, 1991), only the $\alpha_v\beta_3$ receptor is capable of recognizing all the provisional matrix proteins including fibrin, fibronectin, and vitronectin (Charo *et al.* 1990). The $\alpha_v\beta_3$ receptor is heavily expressed on cultured human endothelial cells and can mediate their attachment to fibrinogen, fibronectin, vitronectin, and von Willebrand factor (Cheresh *et al.* 1989). This receptor has also been shown to mediate endothelial cell migration *in vitro* (Leavesley *et al.* 1993). In addition, FGF induces increased levels of $\alpha_v\beta_3$ on cultured human dermal micro vascular endothelial cells (Swerlick *et al.* 1992).

ECs interact with fibrin via a number of receptors, such as ICAM-1, VE-Cadherin, CD-44, and integrins. It has been observed that ICAM-1 binds the 117–133 sequence on the c-chain of fibrinogen (Altieri et al, 1995). The b15–42 sequence on fibrin plays an important role during the process of neovascularization (Chalupowicz et al, 1995). It has been demonstrated that the first extracellular domain of VE-cadherin (cadherin 5) binds to this sequence (Bach et al, 1998). The 572– 574 RGD sequence on the α -chain of fibrin binds integrin $\alpha_v\beta_3$ and $\alpha_5\beta_1$, and plays a significant role during angiogenesis (Thiagarajan, 1996; Collen, 2001).

Interactions between integrins and growth factor receptors play a critical role in the development and healing of the vasculature. In support of this idea, the mitogenic response of HUVECs evoked by fibrin bound VEGF was unexpectedly stronger (139% over control) compared to the response evoked by soluble VEGF (47% over control) (Zisch et al. 2001). Binding of a complex of fibrinogen and FGF-2 could result in the co-localization of integrin and FGF-2 receptors at the focal adhesion complex, contributing to signal integration (Plopper et al. 1995). PDGF plays a major role in vessel wall maturation. Battegay et al (1994) proved that PDGF has a direct role for PDGF in angiogenesis in vitro through endothelial cell proliferation and cord/tube formation by phenotypically distinct angiogenic endothelial cells.

The fibrin b15–42 sequence binds heparin, thereby participating in cell–matrix interactions (Odrlijin et al, 1996; Yakovlev et al, 2003). The binding of VEGF to heparan sulfate proteoglycan in ECM protects VEGF from proteolytic degradation (Wijelath et al, 2002). FGF is sequestered and protected by binding with heparan sulphate which gives stability to bFGF rather than free bFGF. This binding also gives the necessary conformation for optimal interaction with the cell-surface receptors. Degradation products of HA of specific size (3–10 disaccharide units; o-HA) stimulate EC proliferation (Deed et al, 1997) and migration (Sattar et al, 1994). In vascular EC, both CD44 (Nandi et al, 2000) and RHAMM (receptor for HA mediated motility) (Lokeshwar and Selzer, 2000) have been identified as potential targets for transduction of o-HA-induced mitogenesis.

In this study the cell adhesion was similar at 2h when all the matrices with fibrin backbone are compared. But after 72h, the incorporated biomacromolecules affected the cell proliferation rates. The proliferation and survival rates were highest on the matrix that contained both GAG and GFs, which may be an additive effect of the immobilized components in the matrix.

3.5. ECM Remodeling

3.5.1. Fibrin matrix degradation

Fibrin degradation product D-dimer was estimated in cell culture medium collected at different intervals of EC culture. Estimations were done in serially double diluted medium to detect the titre of antigen. The last dilution at which immuno precipitates are seen is taken as the titre of the antigen for each culture period for any specific matrix.

On the GF incorporated matrices, degradation of fibrin was undetectable at 24 h, however, after 72 h of endothelial cell culture D-Dimer level increased to a factor of 16 in all four types of matrices. At 120 h, the level decreased to 4 and at 168 and 216 h the D-Dimer was again undetectable suggesting complete degradation of the fibrin matrix by 120h.

On GAG incorporated matrices, D dimer was undetectable at 24h showing minimal fibrin degradation, but by 72h and 120h the level increased. The degradation rate of fibrin on HA or HS incorporated fibrin matrices were slow and the D-Dimer was detectable at 168h, whereas it was undetectable by 168h in CCPS and CCPS+HA+HS; and by 210h in CCPS+HA and CCPS + HS.

The fibrin degradation could be detected at 24h in CCPS+GAG+GF matrix but in all the other matrices the levels were undetectable. The rate of degradation was highest at 72h in all the matrices, and by 168h the levels were undetectable showing the entire degradation of the fibrin matrix.

The assay was done in four replicate cultures on each type of matrices with good repeatability of results; however, being semi quantitative data statistical analysis was not done. From the results it could be seen that, in most of the case degradation was highest at 72h culture period and lasted till 120h whereas in the absence of GF but presence of HA/HS it lasted till 168h.

Growth factor incorporated matrices					
Matrices\Time in h	24h	72h	120h	168h	210h
CCPS	0	16	4	0	0
CCPS + AGF	0	16	4	0	0
CCPS + PGF	0	16	4	0	0
CCPS + AGF + PGF	0	16	4	0	0
Glycosaminoglycan incorporated matrices					
Matrices\Time in h	24h	72h	120h	168h	210h
CCPS	0	16	4	0	0
CCPS + HS	0	8	8	4	0
CCPS + HA	0	8	8	4	0
CCPS + HA + HS	0	16	4	0	0
Growth factor/ Glycosaminoglycan incorporated matrices					
Matrices\Time in h	24h	72h	120h	168h	210h
CCPS	0	16	4	0	0
CCPS + GF	0	16	4	0	0
CCPS + GAG	0	16	4	0	0
CCPS + GF + GAG	2	16	2	0	0

Table 3.1. Data representing the D-Dimer levels in the medium at different periods of endothelial cell culture in defined fibrin matrix combinations. Data shown represents the semi quantitative estimation of D-Dimer levels from four independent experiments.

Matrix degradation is an essential part of wound repair and angiogenesis. In wound healing, once the ECs have infiltrated the provisional matrix, they realign to become new vascular structures (angiogenesis). During this process, they, together with different cell types, degrade fibrin by the induction of plasmin activities, matrix metalloproteinases, and the generation of free radicals [Collen, 2003; Marx, 1991]. In post embryonic angiogenesis, the sequence of events for endothelial cells begins with destruction of the basement membrane and local

degradation of the extracellular matrix (ECM). This allows endothelial cells to migrate by extending cytoplasmic buds in the direction of chemotactic factors. In this study, since the basal matrix is fibrin, all the matrices showed an almost similar degradation pattern showing complete degradation by 168h. The degradation rate was slightly accelerated in the matrices that showed an increased EC proliferation rate. From the data, it is clear that once the EC starts populating the surface; fibrin matrix gets degraded and makes space for cell migration and ECM deposition as seen in the case of *in vivo* wound healing and angiogenesis.

3.5.2. ECM deposition

The ECM deposition in the matrices was identified by histochemical/immunostaining of the recovered matrices after defined periods of cell culture. Histochemical and Immuno-staining were done in the case of growth factor incorporated matrices; and in GAG/ GAG & GF incorporated matrices only immuno-staining was done.

3.5.2.1. Growth factor incorporated matrices

3.5.2.1.1. Histochemical staining

Fibrin matrix coating was stained with Masson trichrome which showed well-formed interconnected network of fibrin (Fig. 3.14.A) without any specific color and it served as negative reference for matrices recovered and stained after cell culture. In most of the wells, recovered matrix was found to be retracted and bundled up in several areas probably resulting from digestion and washing during decellularization. While the control CCPS seem to have less ECM deposition after all periods of EC culture, deposition was seen in all the GF containing culture matrices recovered after different periods of EC culture. Specific staining of the matrix recovered after 3 days of EC culture on CCPS, CCPS + AGF, CCPS + PGF and CCPS + AGF + PGF showed a matrix network with indication of additional protein deposition by the cells grown on them (Fig. 3.14.A–D). The observed matrix seems to be none other than the original fibrin network in CCPS (Fig. 3.14.A), but in the other three wells greenish blue color is evident which indicates presence of collagen (Fig. 3.14.B–D). After 10 days of culture, staining of recovered matrices with Masson trichrome has not

demonstrated presence of elastin in CCPS and CCPS + PGF (Fig. 3.15. A and C), but a tinge of pink color along with bluish green collagen indicated deposition of traces of elastin in CCPS + AGF and CCPS + AGF + PGF (Fig. 3.15.B and D). Interestingly by day 20, the matrix recovered after EC culture clearly showed presence of elastin strands as pink irregular retractile aggregates which is more prominent in CCPS + AGF and CCPS + AGF + PGF (Fig. 3.16.B and D) as compared to CCPS and CCPS + PGF (Fig. 3.16. A and C). Staining of the recovered matrices after 30 days of EC culture with PTAH showed nicely remodeled collagen deposition which is seen as pink inter-connected network (Fig. 3.17.A–D). While the matrices recovered after 3 and 10 days of EC culture appeared as loose strands of proteins (Figs. 3.14 and 15), the matrices recovered after 20 and 30 days looked stable and remodeled with sheet like coating on the surface of the culture plate (Figs. 3.16 and 17). The digestion of cells and recovery of matrix was relatively easier at days 3 and 10, complete removal of cell remnants was tougher at days 20 and 30 which may be due to strong adhesion of cells to the remodeled matrix in long-term cultures.

3.5.2.1.2. Immuno-specific staining

The matrices recovered after 10days of EC culture showed only trace amounts of collagen I on all the matrices (Figs. 3.18. A-D), but collagen IV and elastin bundles were seen more intensely when the matrix contained AGF and PGF. Presence of immuno-specific Collagen IV after 10 days seemed to be more prominent and organized in the matrix that contained PGF (Figs. 3.19.C and D), as compared to that without any growth factor or with AGF alone (Figs. 3.19.A and B). Elastin was identified by immunostaining after 10 days culture in all matrices with dense bundles in presence of AGF (Figs. 3.20.B and D), where as in presence of PGF thin elastin fibers were identified (Fig. 3.20.C). Elastin has been found occasionally in only CCPS well by day 10 (Fig. 3.20.A) whereas intensity was maximum in the culture matrix with both AGF and PGF (Fig. 3.20.D). Both immunological and histological staining of the recovered matrices after EC culture show that collagen deposition is prominent when PGF is added to the culture matrix whereas elastin deposition is significant if AGF is present. The deposition was of collagen IV and elastin was maximum in the CCPS+AGF+PGF matrix.

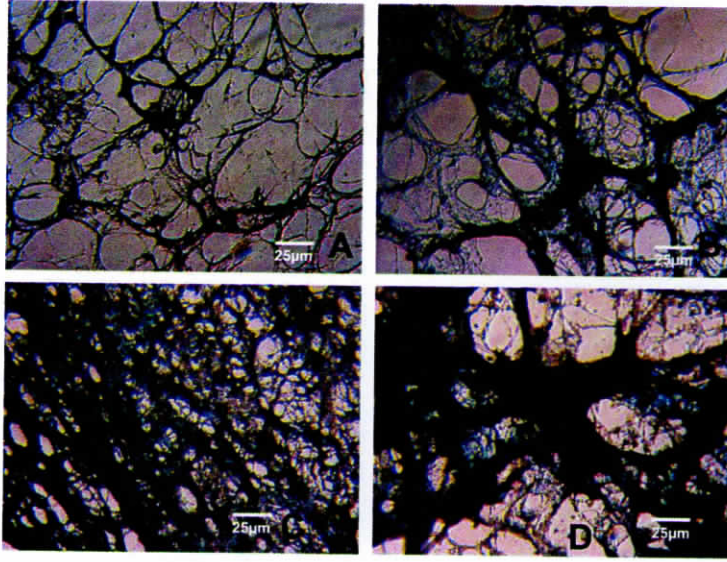


Figure 3.14. Histochemical staining- Photomicrographs of recovered matrices after 3 days of in vitro endothelial cell culture. Masson's Trichrome stain was used to identify the presence of collagen or elastin. Frames A–D represents culture wells: (A) CCPS; (B) CCPS + AGF; (C) CCPS + PGF; (D) CCPS + AGF + PGF

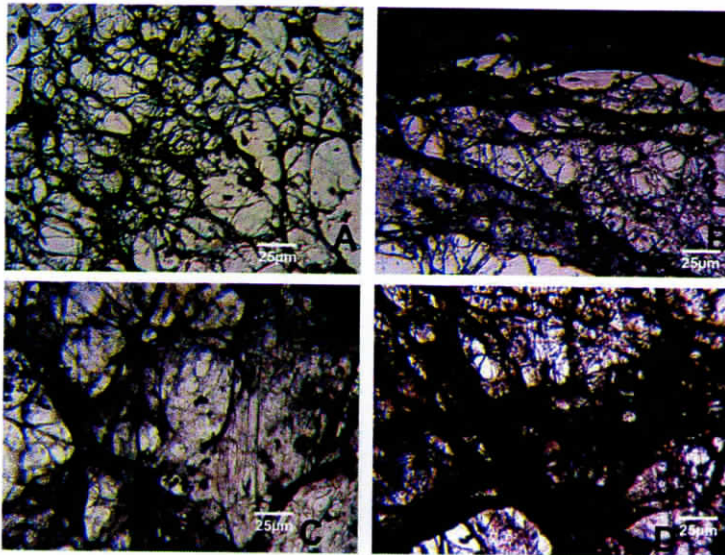


Figure 3.15. Histochemical staining - Photomicrographs of recovered matrices after 10 days of in vitro endothelial cell culture. Masson's Trichrome stain was used to identify the presence of collagen or elastin. Frames A–D represents culture wells: (A) CCPS; (B) CCPS + AGF; (C) CCPS + PGF; (D) CCPS + AGF + PGF

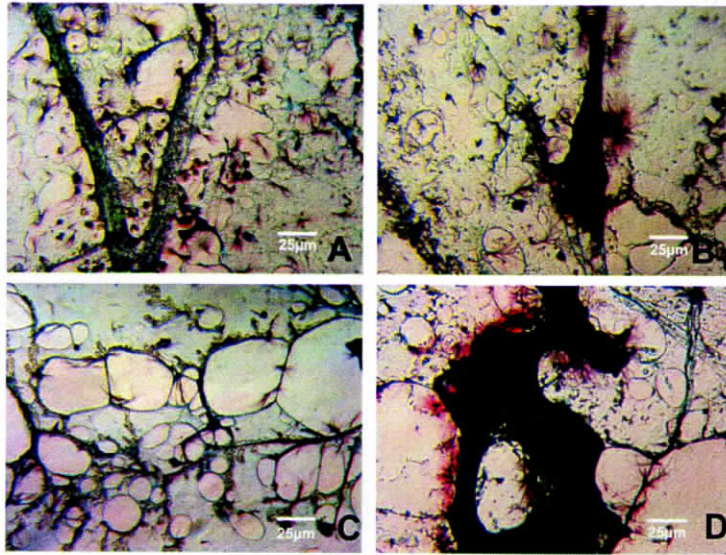


Figure 3.16. Histochemical staining - Photomicrographs of recovered matrices after 20 days of in vitro endothelial cell culture. Masson's Trichrome stain was used to identify the presence of collagen or elastin. Frames A–D represents culture wells: (A) CCPS; (B) CCPS + AGF; (C) CCPS + PGF; (D) CCPS + AGF + PGF

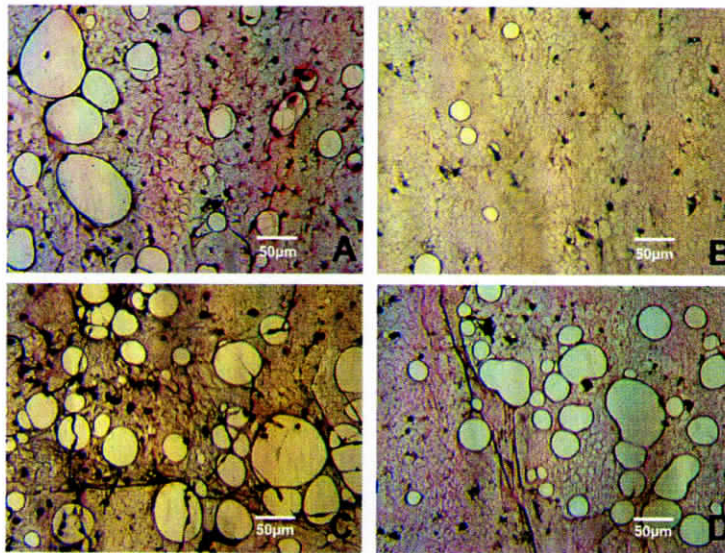


Figure 3.17. Histochemical staining - Photomicrographs of recovered matrices after 30 days of in vitro endothelial cell culture. PTAH stain was used to identify the presence of collagen or fibrin. Frames A–D represents culture wells: (A) CCPS; (B) CCPS + AGF; (C) CCPS + PGF; (D) CCPS + AGF + PGF

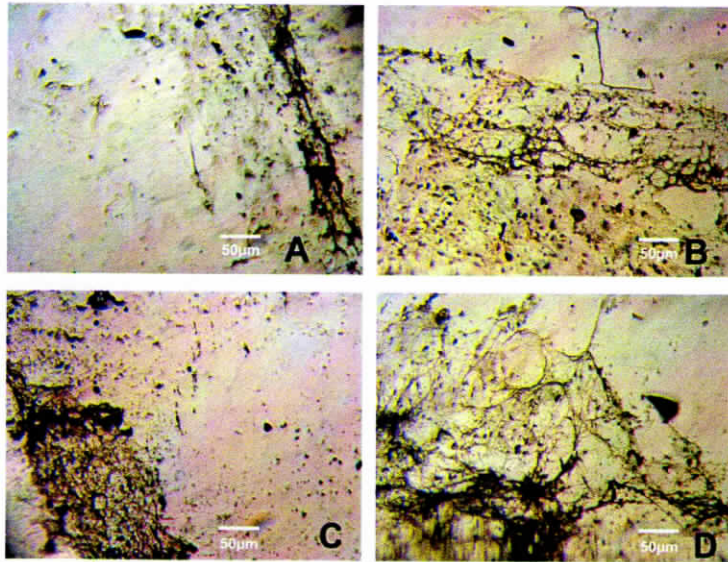


Figure 3.18. Immunostaining - Photomicrographs of recovered matrices after 10 days of in vitro endothelial cell culture. Immunostaining was done to identify the presence of collagen I. Frames A–D represents culture wells: (A) CCPS; (B) CCPS + AGF; (C) CCPS + PGF; (D) CCPS + AGF + PGF

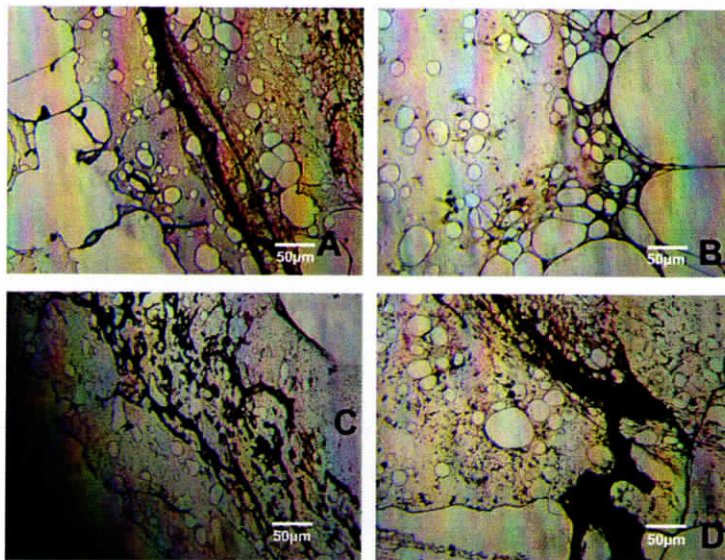


Figure 3.19. Immunostaining - Photomicrographs of recovered matrices after 10 days of in vitro endothelial cell culture. Immunostaining was done to identify the presence of collagen IV. Frames A–D represents culture wells: (A) CCPS; (B) CCPS + AGF; (C) CCPS + PGF; (D) CCPS + AGF + PGF.

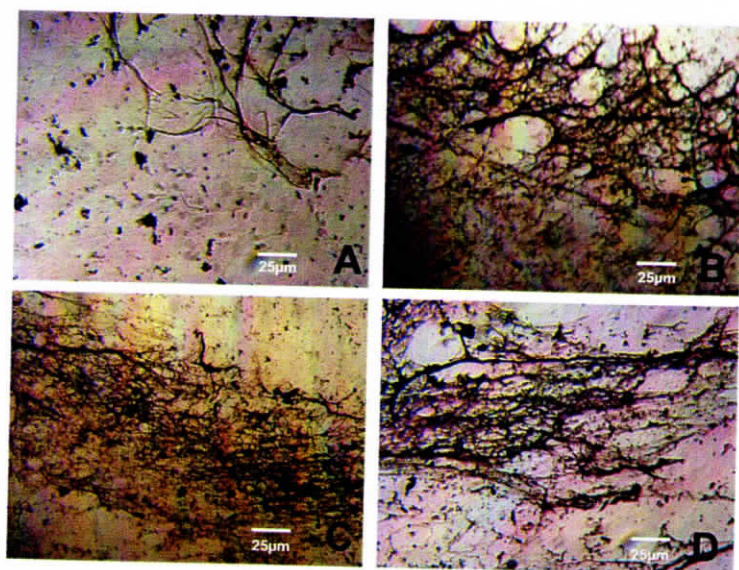


Figure 3.20. Immunostaining - Photomicrographs of recovered matrices after 10 days of in vitro endothelial cell culture. Immunostaining was done to identify the presence of elastin. Frames A–D represents culture wells: (A) CCPS; (B) CCPS + AGF; (C) CCPS + PGF; (D) CCPS + AGF + PGF.

3.5.2.1.3. Immunofluorescence staining.

The fibrin composite coated matrix without growth factors (control) was compared against matrices modified using AGF (0.05µg), PGF (0.02µg) and combination of AGF+PGF (0.05µg+0.02µg). The cells formed a monolayer within 5 days of culture, in all the matrices including the control.

Representative photomicrographs from 10 day and 20 day culture matrices are shown in Figs. 3.22.A-G for elastin, and for collagen IV in Figs. 3.23. A-G. In the control, since the ECM deposition was less, the matrix retracted to the periphery of the well during cell digestion and the border of the stained matrix was evident in Fig 3.22.A and Figs. 3.23.A&B. In the modified wells with growth factors, no such retraction was observed and stained matrix was seen through out the well, though in some areas matrix was retracted and bundled up. Compared to controls, other wells showed presence of more elastin and collagen IV after 10d and 20d culture matrices. Again quantity was more when both AGF and PGF were incorporated within the culture matrix. Culture medium used was same in all four types of coated wells, and monolayer was present in all wells after 120h. Therefore, the effect seen is primarily due to the difference in immobilized growth factors.

3.5.2.1.4. Quantitative analysis of ECM deposition

The amount of collagen and elastin deposited in each matrix was quantified by fluorimetry. A calibration curve was made using doubling dilutions of the FITC conjugated secondary antibodies and their respective Lowry's protein concentrations. From the calibration curve and the mean fluorescent intensity of the entire area of each well the concentration of elastin and collagen in each well was estimated and is shown in the graph (Fig. 3.21). Separate wells were used for collagen and elastin staining for each period, and since FITC-conjugated secondary antibody was used all analysis were done using the same filter settings. It was observed that in CCPS and CCPS+PGF, the elastin and collagen deposition was dependent on time and thus increase in deposition was seen by 20 day, as compared to 10 day. There was no much increase in elastin or collagen deposition between 10day and 20 day when AGF+PGF is added with the matrix, which indicates that probably ECM deposition is a regulated process (Fig. 3.24). Thus it also suggests that if AGF is added ECM deposition is attained at an early period of culture.

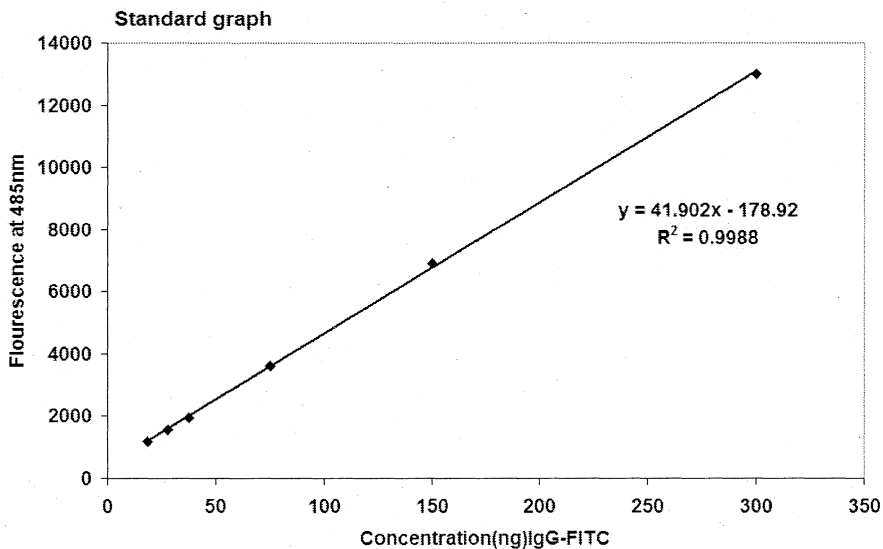


Figure 3.21. Standard graph for quantification. Graph was constructed using MFI of FITC-IgG (secondary Ab) at 485nm against the respective protein concentration to quantify collagen and elastin deposition using mean fluorescence intensity (MFI) of FITC-IgG immuno stained recovered matrices. The protein content of FITC-IgG was estimated using Lowry's method. The secondary antibody was double diluted at respective concentrations and the fluorescence intensity was obtained

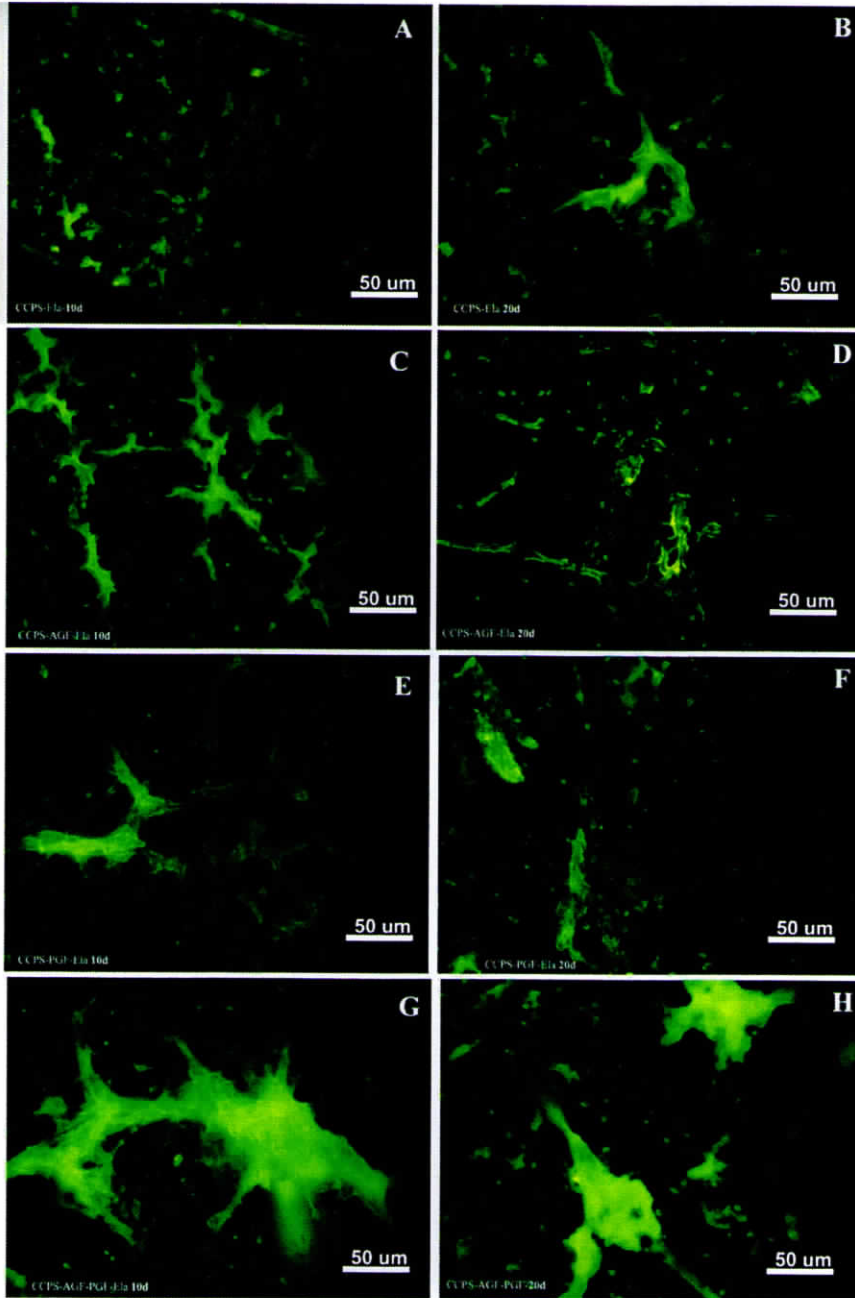


Figure 3.22. Immunostained elastin in matrices recovered after EC culture. Presence of elastin in matrices after 10days and 20days of EC culture on CCPS: A, 10days; B, 20days; on CCPS+AGF: C, 10days; D, 20days; on CCPS+PGF: F, 10days; E, 20days; on CCPS+AGF+PGF: G, 10days; H, 20days. FITC was excited using blue filter.

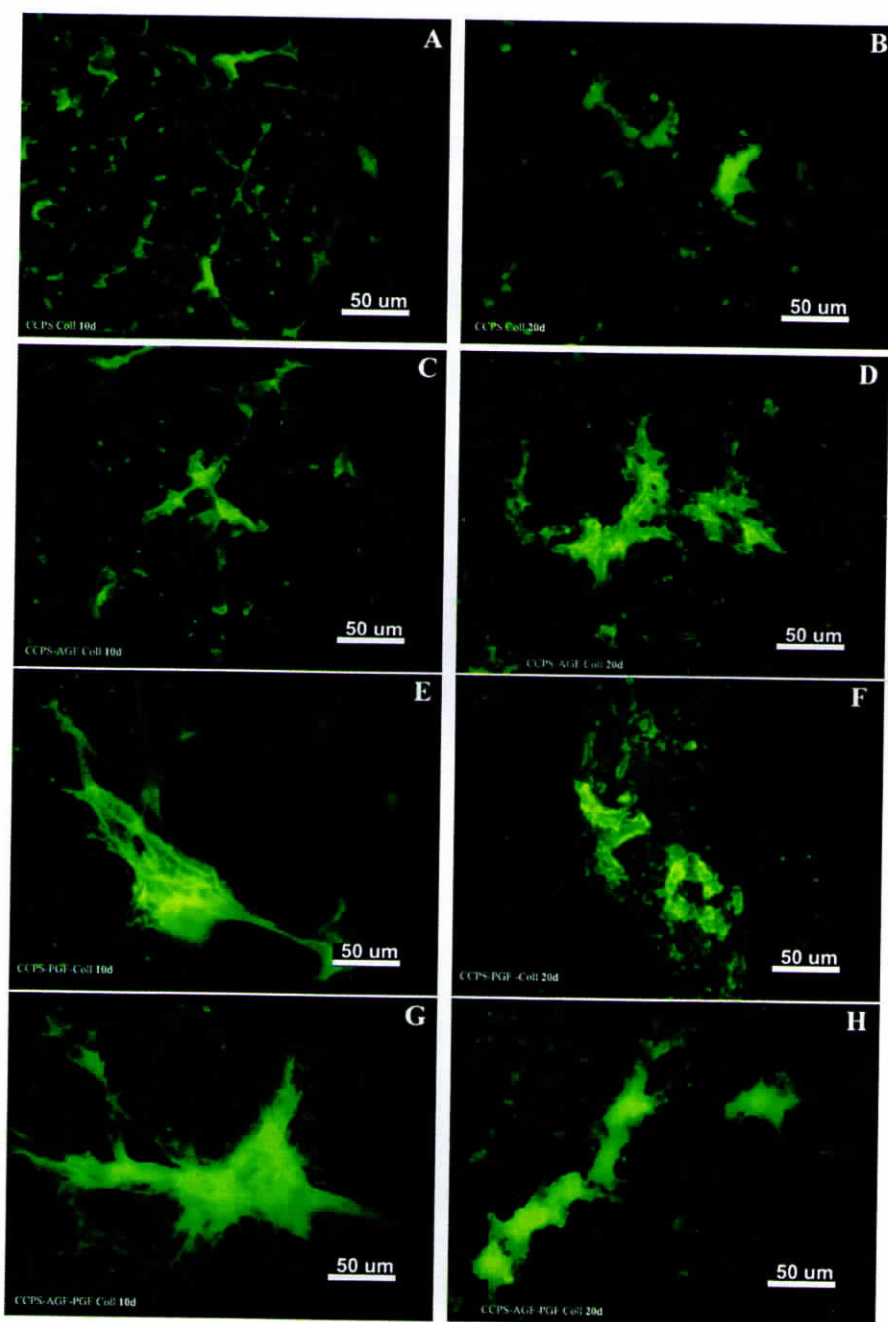
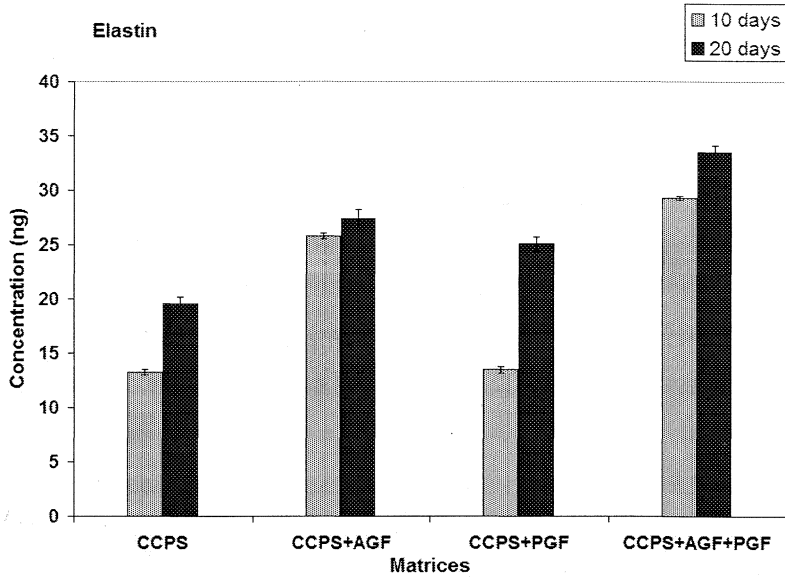
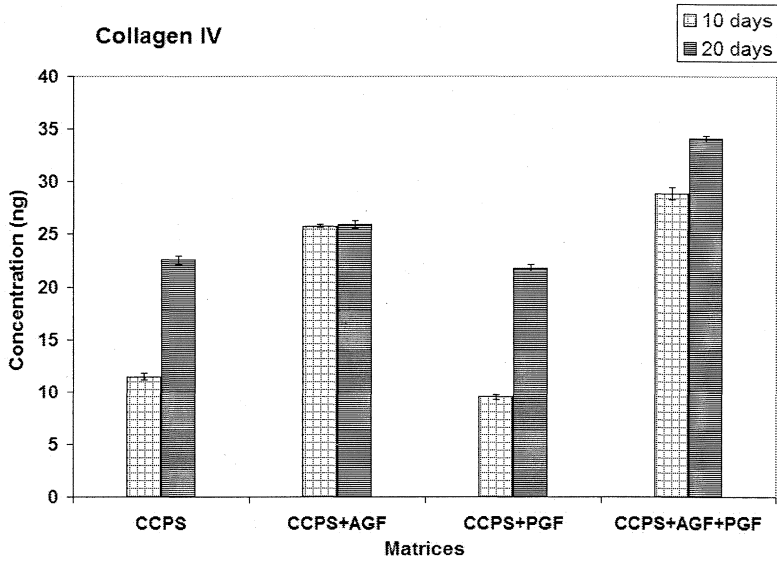


Figure 3.23. Immunostained Collagen IV in matrices recovered after EC culture. Presence of Collagen IV in matrices after 10days and 20days of EC culture on CCPS: A, 10days; B, 20days; on CCPS+AGF: C, 10days; D, 20days; on CCPS+PGF: F, 10days; E, 20days; on CCPS+AGF+PGF: G, 10days; H, 20days. FITC was excited using blue filter.



A



B

Figure 3.24. Fluorimetry data showing the concentration of elastin (A) and collagen IV (B) on CCPS, CCPS+AGF, CCPS+PGF and CPS+AGF+PGF at 10 days and 20 days. Fluorescence in each well was detected using band pass filter [excitation wavelength 485(20) nm, emission wavelength 535(20) nm].

3.5.2.2. Glycosaminoglycan incorporated matrices

3.5.2.2.1. Immunofluorescence staining

Effect of GAGs on ECM deposition was not as prominent as compared to the effect of GFs. The CCPS+HA, CCPS+HS and CCPS+HA+HS matrix showed an improved presence of elastin when compared to CCPS alone in 10days (Fig. 25). But after 20 days, the increased presence of elastin in CCPS+HA+HS was clearly distinguishable from the other matrices (Figs. 3.25.G&H).

Collagen IV deposition appeared more in the CCPS+HA, CCPS+HS and CCPS+HA+HS when compared to the control CCPS in 10 days. But by 20 days increased deposition could be seen in CCPS+HA and CCPS+HA+HS matrix (Fig. 3.26). Collagen I deposition was similar and less stained in all the matrices (Fig. 3.27).

3.5.2.2.2. Quantitative analysis

There was not much quantitative difference in elastin deposition between CCPS, and CCPS+HA matrices recovered after 10d and 20d but with HS deposition was higher. An additive effect was seen when both HS and HA were added together (Fig. 3.28). There was an increase in the quantity of elastin between 10 days and 20 days in the matrix having HS+HA. The quantity of collagen IV was similar in all the matrices after 10days of culture. Collagen IV deposition as an effect of GAGs was time dependent. In the case of all matrix compositions, collagen IV deposition was increased by 20 days as compared to 10 days.

3.5.2.3. Growth factor and glycosaminoglycan incorporated matrices

3.5.2.3.1. Immunofluorescence staining

The GF and GAG incorporated matrix (CCPS+GAG+GF) showed an increase in deposition of collagen IV and elastin after 20days of EC growth when compared to the matrices CCPS, CCPS+AGF+PGF and CCPS+HA+HS (Fig. 3.29). Collagen I appeared to be less and was comparable to CCPS.

3.5.2.3.2. Quantitative analysis

The quantitative data showed that there was increased deposition of elastin and collagen IV in CCPS+GAG+GF matrix when compared to the other matrices. The deposition on CCPS+GF was higher when compared to the CCPS+GAG and CCPS matrices (Fig. 3.30). The data has proven that growth

factors are more effective as compared to GAGs, but combining GFs with GAGs give an additive effect on both elastin and collagen deposition.

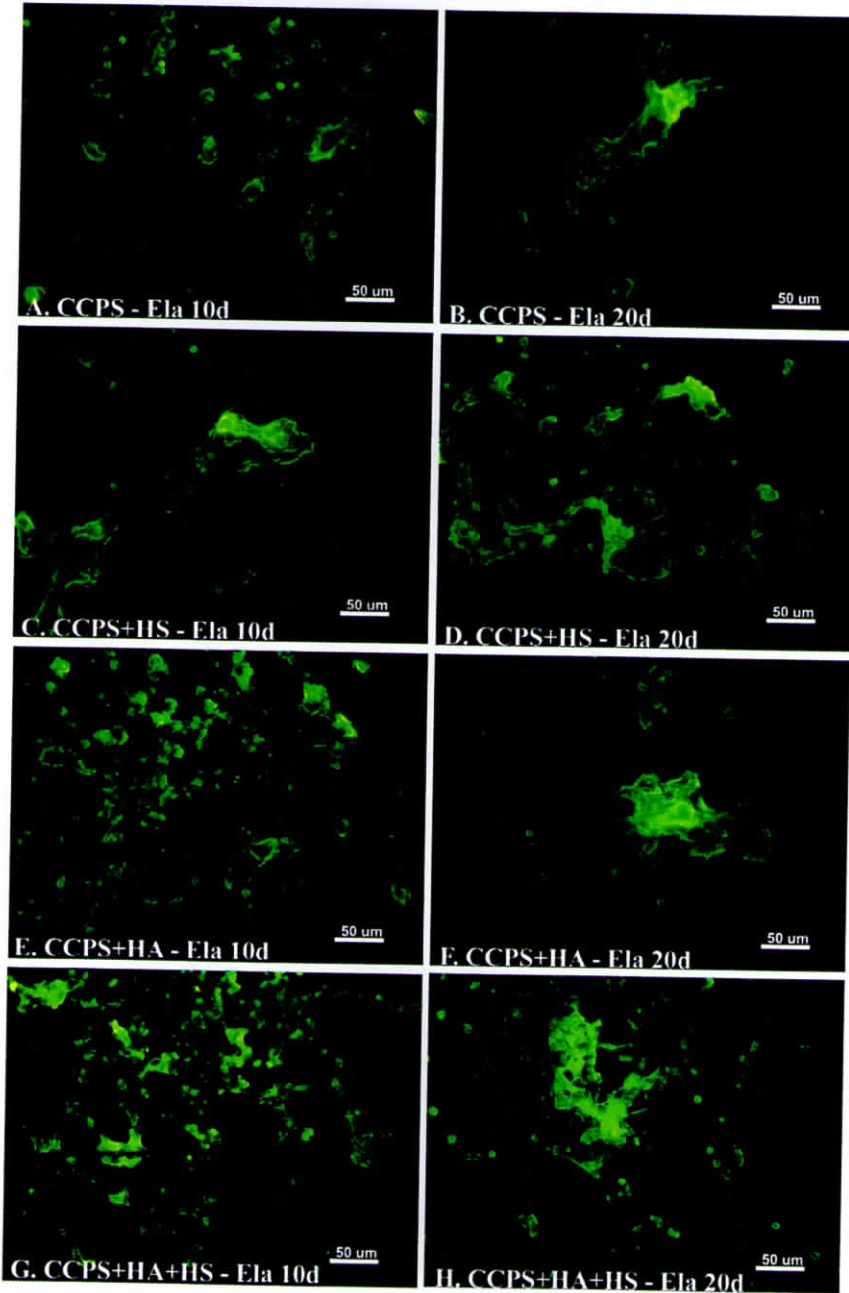


Figure 3.25. Immunostained elastin in matrices recovered after EC culture. Presence of elastin in matrices after 10days and 20days of EC culture on CCPS: A, 10days; B, 20days; on CCPS+HS: C, 10days; D, 20days; on CCPS+HA: F, 10days; E, 20days; on CCPS+HA+HS: G, 10days; H, 20days. FITC was excited using blue filter.

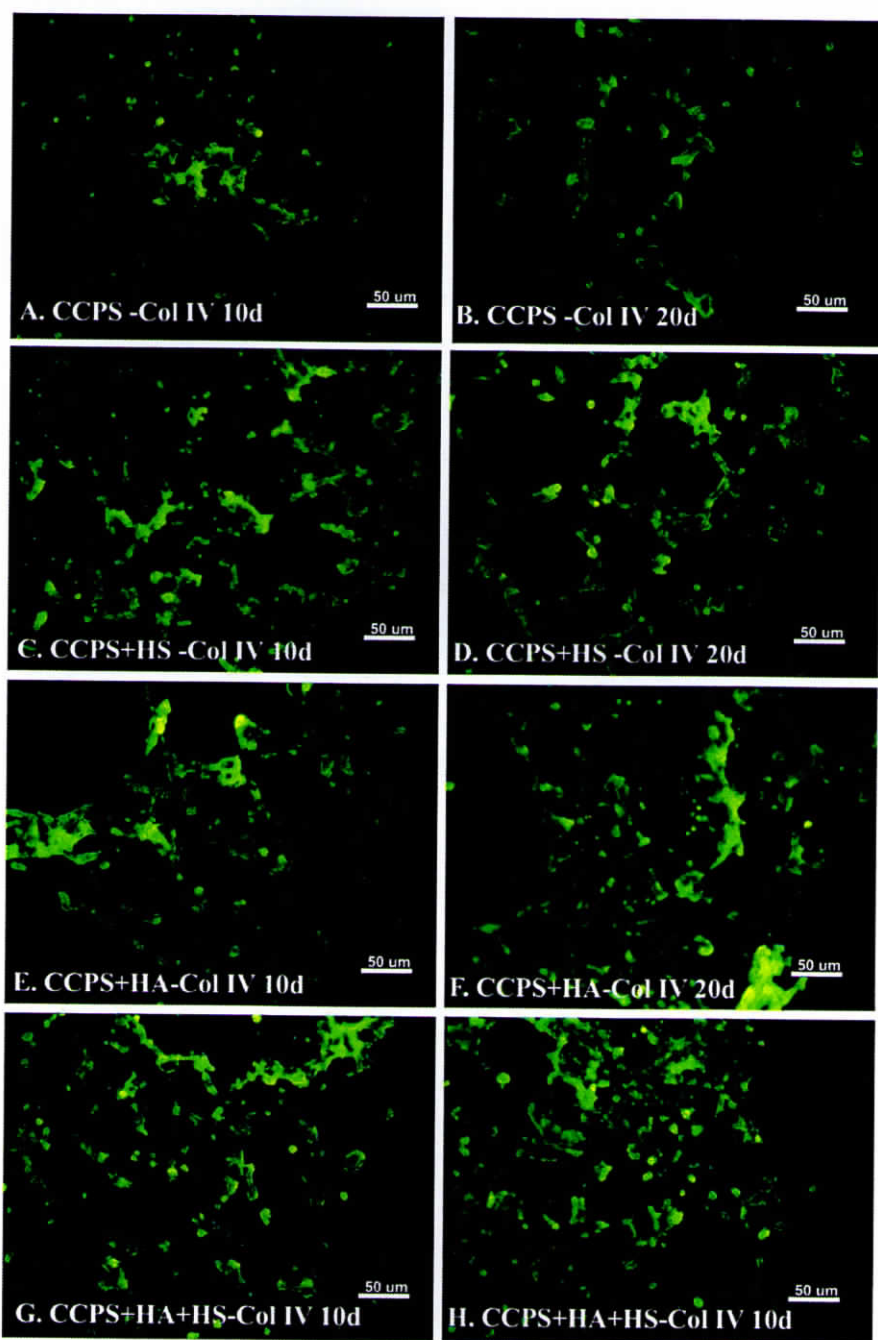


Figure 3.26. Immunostained Collagen IV in matrices recovered after EC culture. Presence of Collagen IV in matrices after 10days and 20days of EC culture on CCPS: A, 10days; B, 20days; on CCPS+HS: C, 10days; D, 20days; on CCPS+HA: F, 10days; E, 20days; on CCPS+HA+HS: G, 10days; H, 20days. FITC was excited using blue filter.

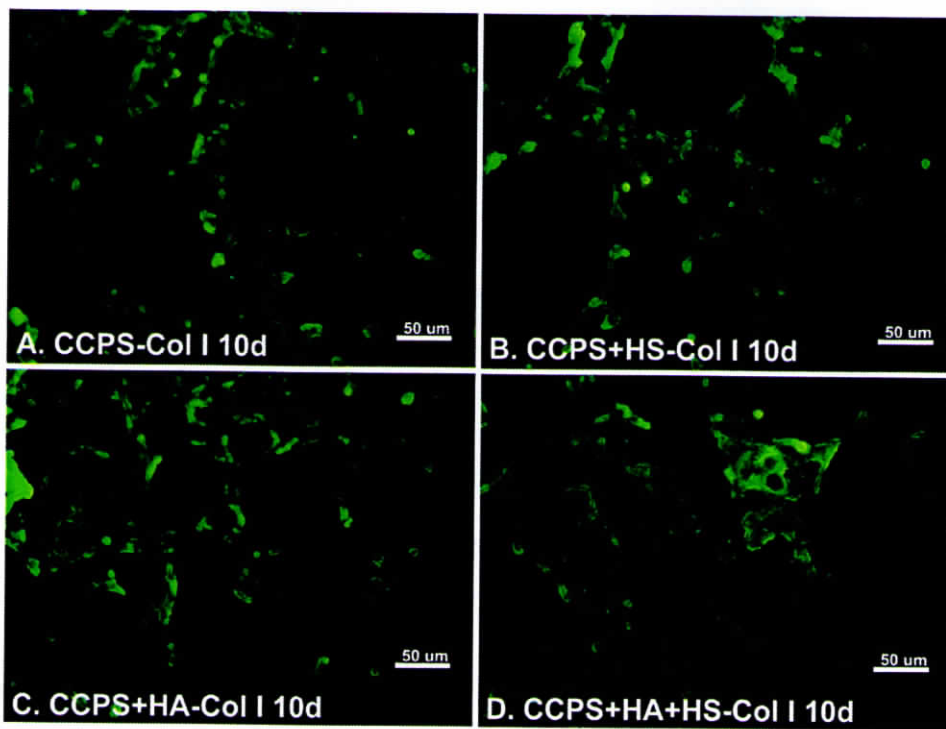


Figure 3.27. Immunostained Collagen I in matrices recovered after 10d of EC culture. (A) CCPS, (B) CCPS+HS, (C) CCPS+HA, (D)CCPS+HA+HS. FITC was excited using blue filter.

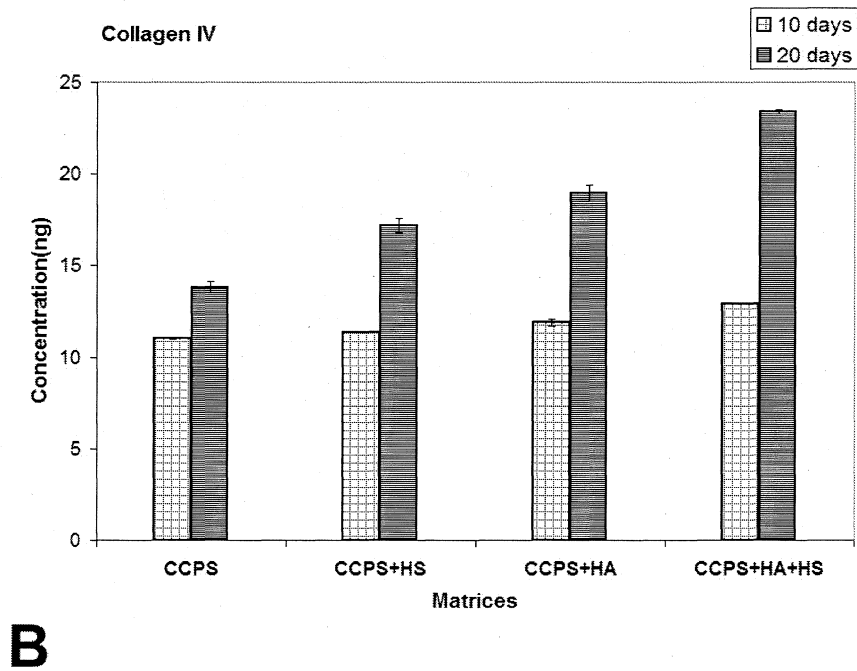
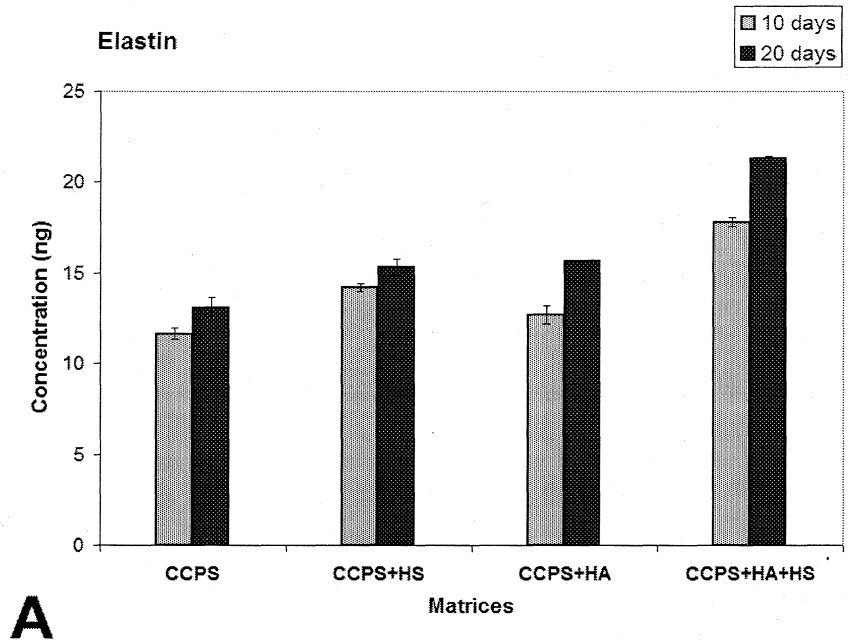


Figure 3. 28. Fluorimetry data showing the concentration of elastin and collagen IV on the CCPS, CCPS+HS, CCPS+HA and CCPS+HA+HS at 10 days and 20 days. Fluorescence in each well was detected using band pass filter [excitation wavelength 485(20) nm, emission wavelength 535(20) nm.

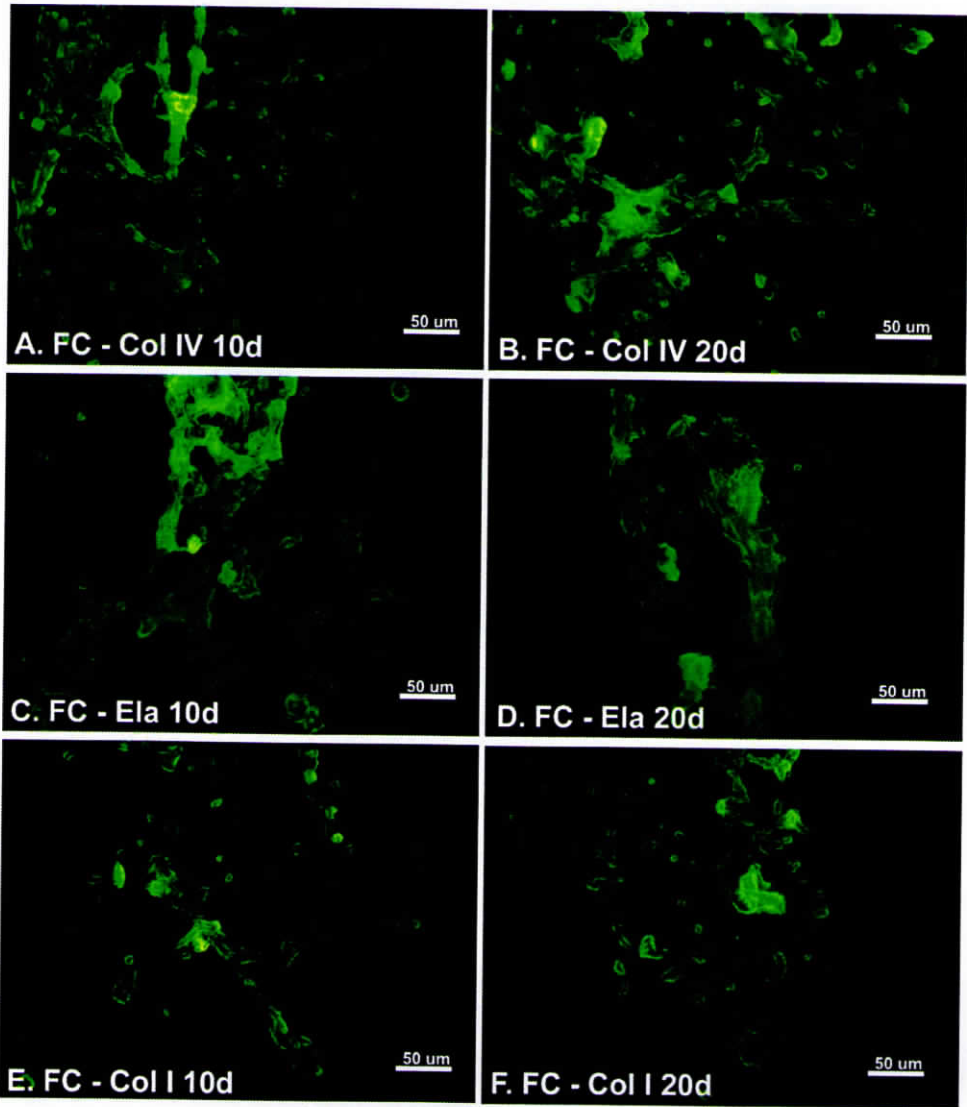
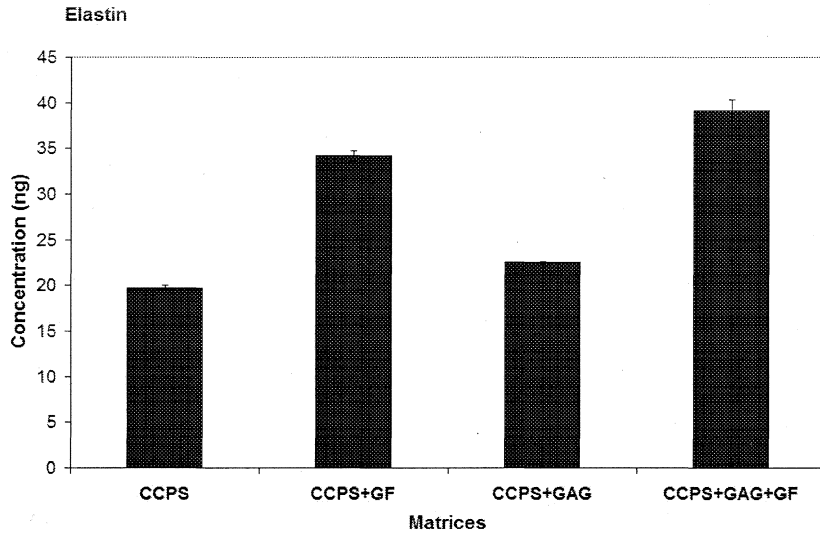
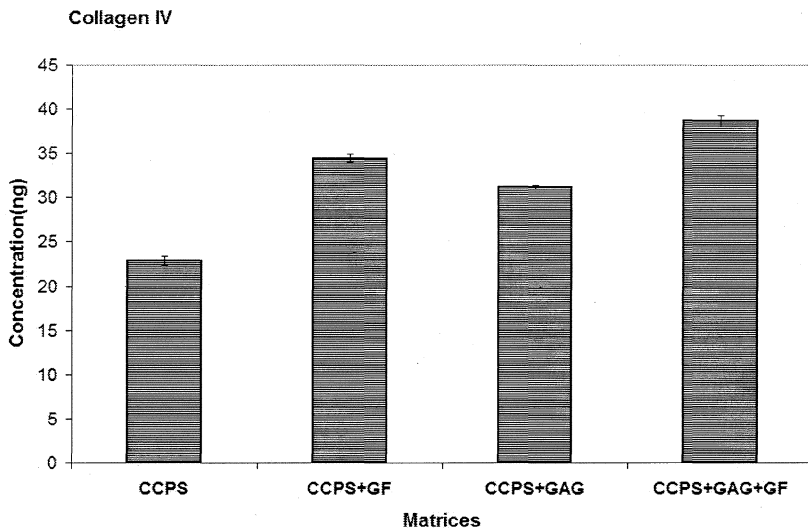


Figure 3. 29. Immunostained Elastin, Collagen IV and Collagen I in CCPS+GAG+GF matrix after 10 and 20days of EC culture. Presence of elastin A, 10days; B, 20days; Presence of Collagen IV C, 10days; D, 20days; Presence of Collagen I E, 10days; F, 20days. FITC was excited using blue filter.



A



B

Figure 3.30. Fluorimetry data showing the concentration of elastin and collagen on the CCPS, CCPS+GF, CCPS+GAG and CCPS+GAG+GF at 10 days. Fluorescence in each well was detected using band pass filter [excitation wavelength 485(20) nm, emission wavelength 535(20) nm].

3.5.2.4. mRNA expression for collagen I, collagen IV and elastin

3.5.2.4.1. Growth factor incorporated matrices

Expression studies were done at periods 72 and 144 h, because histochemical studies indicated new matrix deposition at 72 h (Figs. 2A–D). The results of RT PCR for mRNA expression of elastin and collagen, is represented as fold change with respect to culture period, i.e. 72 and 144 h compared against 24 h. Since in the GF incorporated matrices a change in the expression was noted when compared with the control CCPS even at 24h, the relative fold change in the matrices CCPS+AGF, CCPS+PGF and CCPS+ AGF+ PGF against CCPS was analyzed at 24h, 72h and 144h.

EC grown on CCPS seem to have increased expression for elastin with increase in culture length i.e. 24 h versus 144 h by two-fold (Fig. 3.31). The fold increase was also noted in the CCPS+AGF and CCPS+PGF matrix where the increase was five and four folds respectively. The increase in elastin expression in the CCPS+AGF+PGF matrix was 3 fold. Although this value appears low when compared to the other matrices, the highest expression of elastin was in this matrix which seems less striking because in this at 24h itself the expression was higher (Fig. 3.32). There was nearly 2 fold increased in the collagen IV expression by 144h in all the matrices, but collagen I expression was too low and detected only after 26 cycles of PCR.

Among the GF incorporated matrices, the matrix CCPS+AGF+PGF showed a increased expression of elastin (2-fold) compared to CCPS even at 24h, whereas there was an increase (1.6 fold) in the collagen IV (Fig. 3.32). At 72h and 144h, at all the time periods the expression of elastin was significantly higher in the CCPS+AGF+PGF matrix.

Thus, it is evident that by increasing the culture length on various matrix compositions, it is possible that collagen synthesis and elastin synthesis can be increased. The effect of growth factors on the expression of ECM components could be seen by the change in the mRNA expression of elastin and collagen IV at time periods 24h, 72h and 144h of EC culture. For all transcripts expression

level was highest in wells that contained both AGF and PGF as compared to the basic coating-CCPS.

While collagen IV synthesis was initiated in 24h and seemed to be increased by 144h, it was also observed after immunostaining and fluorimetry analysis after 20 days. The collagen I deposition was not increased after 20 days and the data correlated well with the mRNA expression analysis. More striking observation was the deposition of elastin fibers which is clearly seen by immunostaining in 10-day-old matrix, whereas by 20 days, bundles of elastin fibers are seen prominently in the matrix that contained AGF and PGF with Masson trichrome staining. In parallel, upregulation of elastin mRNA is found to be very prominent by 144 h.

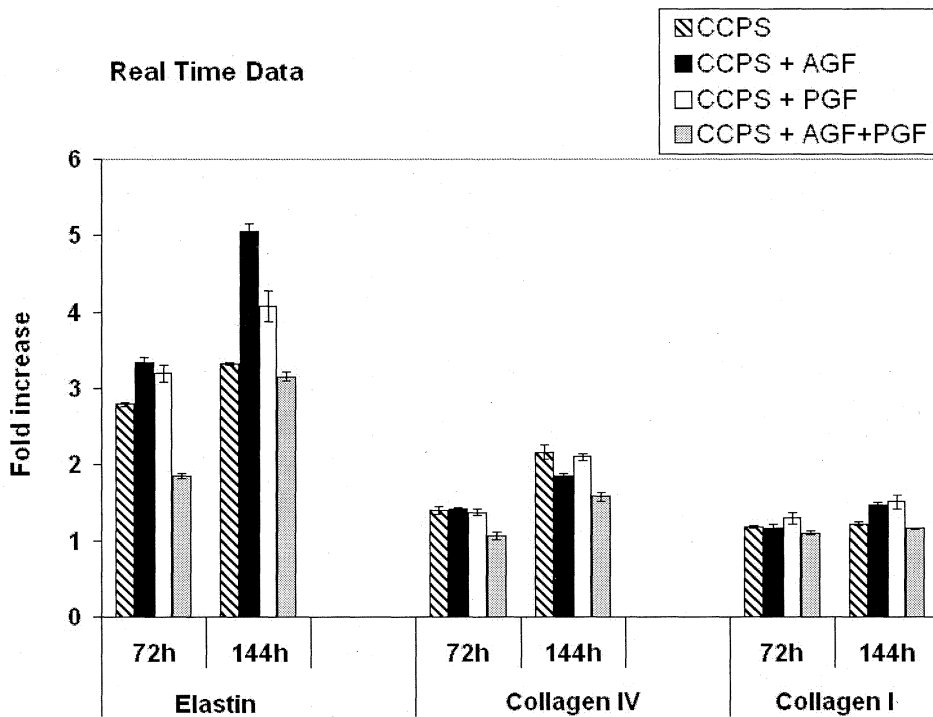


Figure 3.31. Real Time PCR data showing regulation of mRNA expression with culture time Data shows the increase in gene expression levels of Elastin, Collagen IV and Collagen I at 72 and 144 h when compared to 24 h, on the growth factor Incorporated matrices.

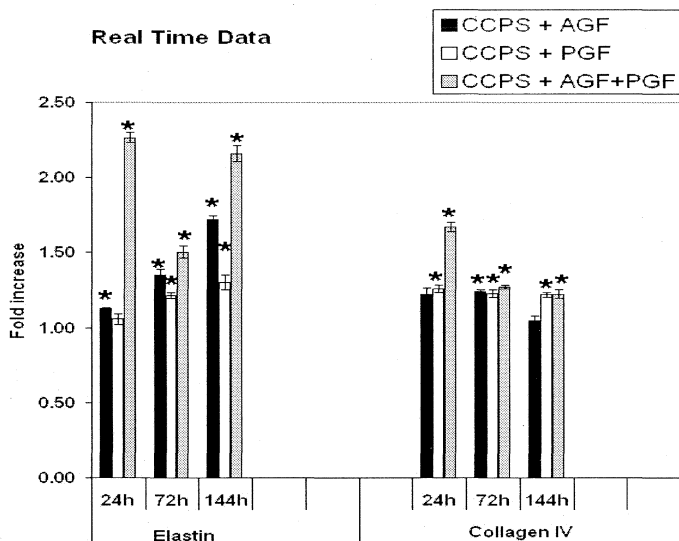


Figure 3.32. Real Time PCR data showing regulation of mRNA expression with added GF. Data shows a comparison of fold change in mRNA expression of the GF incorporated matrices when compared to CCPS, at 24, 72 and 144 h. Asterisk (*) represents significant statistical difference $p < 0.01$ when compared to the mRNA level of CCPS.

3.5.2.4.2. Glycosaminoglycan incorporated matrices

In the GAG incorporated matrices there was an increase in the mRNA expression of elastin and collagen IV with respect to culture period, i.e. 72 and 144 h compared against 24 h (Fig. 3.33). The cells did not show any significant change in the mRNA expression levels at 24h when compared to the control CCPS. At 72h the mRNA levels for elastin upregulated marginally (1.5 fold) in the CCPS, CCPS+HA and CCPS+HS where as it was significant (2.5 fold) in the CCPS+HA+HS matrix. By 144h there was further significant increase (2.7 fold) in the same matrix when compared to other matrices. In the CCPS+HA and CCPS+HS matrix also there was a marginal increase (1.7 fold).

The collagen IV expression was comparable in all the matrices at 72h, but at 144h the expression in CCPS+HA+HS increased significantly (2.6 fold), whereas it was similar in the other matrices. The collagen I expression was hardly seen and the cycling time was very high at the time the PCR product was detectable. The data correlated well with the immunostaining and fluorimetry data which showed an increased deposition of elastin and collagen IV in the CCPS+HA+HS matrix by day 20.

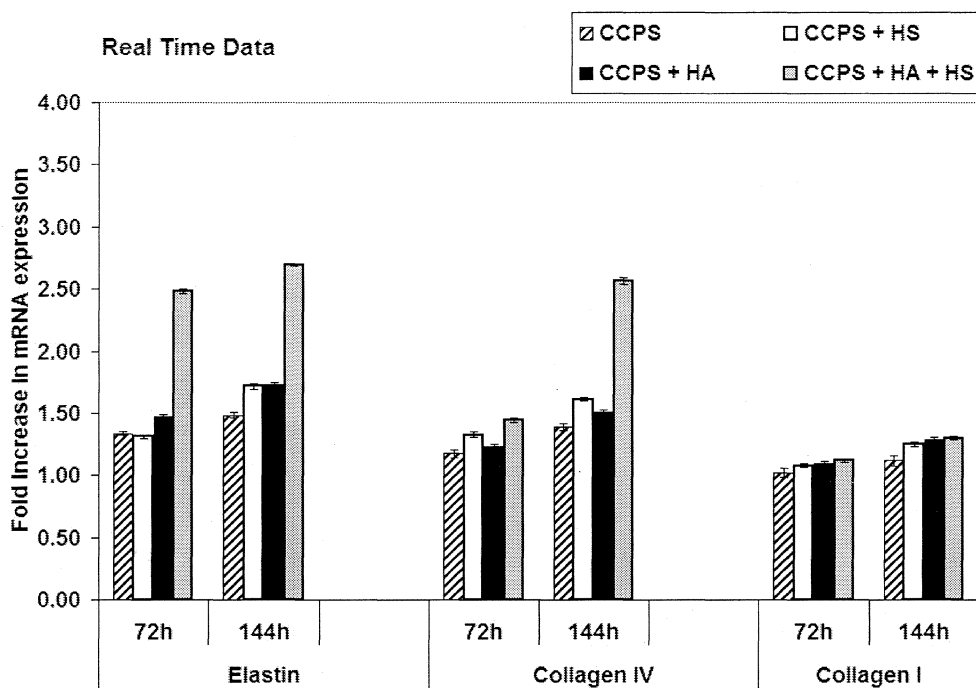


Figure 3.33. Real Time PCR data showing regulation of mRNA expression with added GAG. Data shows the increase in gene expression levels of Elastin, Collagen IV and Collagen I at 72 and 144 h when compared to 24 h, on the glycosaminoglycan incorporated matrices.

3.5.2.4.3. Growth factor and glycosaminoglycan incorporated matrices

Since in the GF incorporated matrices, CCPS+AGF+PGF, and in the GAG incorporated matrices, CCPS+HA+HS showed increased mRNA expression levels of elastin and collagen IV was seen, comparison was made between the two matrices and a combination of the two; CCPS+ GAG + GF matrix with the control to select the best matrix (Fig. 3.34). The Ct values were similar in all the matrices at 24h. The matrix CCPS+ GAG + GF showed about 4-fold increase in the elastin expression, about 3 fold increase in collagen IV expression when compared to the matrices at 24h. The collagen I expression was regulated in all the matrices. The CCPS+GAG and CCPS+GF matrix also showed increased expression of elastin and collagen IV when compared to CCPS, but the best was CCPS+GF+GAG. Collagen I expression was similar in all matrices and was very minimal.

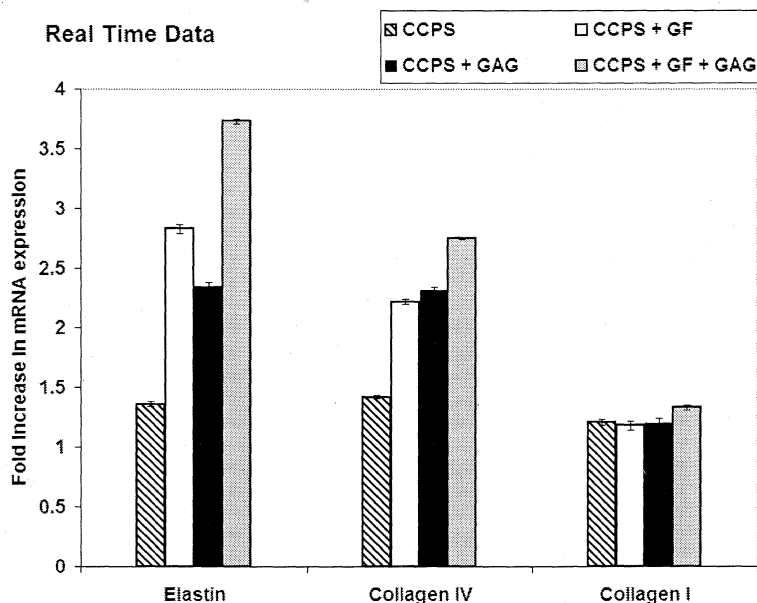


Figure 3.34. Real Time PCR data showing regulation of mRNA expression with added GAG and GF combination. Data shows the increase in gene expression levels of Elastin, Collagen IV and Collagen I at 72 and 144 h when compared to 24 h, on the growth factor and glycosaminoglycan incorporated matrices.

Remodeling implies an alteration in the extracellular matrix (ECM) and in the spatial orientation of cells and intracellular components. ECM remodeling consists of *de novo* deposition of ECM proteins, self-assembly, and network formation. During this process, cell behavior is influenced by altered ECM composition as well as exposed cryptic binding sites. During wound healing the provisional ECM that is formed of fibrin and fibronectin is replaced by the granulation tissue which is characterized by a dynamic reciprocity among fibroblasts, growth factors, and the ECM proteins. After binding to the ECM, macrophages release growth factors that stimulate angiogenesis, collagen synthesis, and fibroblast proliferation. Endothelial cells exhibit integrins, which bind ECM proteins, in order for angiogenesis to proceed. In turn, fibroblasts deposit matrix that further supports migration of cells, including macrophages, endothelial cells, and fibroblasts. During the remodeling phase, as an effect of the dynamic interactions, fibronectin and hyaluronic acid are replaced by collagen bundles that lend strength to the tissue. In this study, we have applied a similar principle, such that multiple growth factors and GAGs were provided

within the matrix to increase the efficiency of the cultured cells for matrix remodeling. Geary et al. (1998) noted that an injured artery wall resembles a healing wound in its sequence of remodeling events. This group proposed that remodeling processes in injured vessels contribute to contraction, as they do in wound healing, and this leads to vessel lumen narrowing.

Elastic fibres are major insoluble extracellular matrix (ECM) assemblies that endow connective tissues with resilience, permitting long-range deformability and passive recoil without energy input. In the medial layer of the aorta and elastic arteries, elastic fibres form concentric fenestrated lamellae separated by smooth muscle cell (SMC) layers and this arrangement imparts elasticity and flexibility to blood vessel walls. These properties are critical to the function of arteries, which undergo repeated cycles of extension and recoil. In most mammalian tissues, the bulk of elastogenesis occurs during late fetal and early neonatal periods (Parks et al, 1993, Davidson and Giro, 1986). As tissue development and growth are completed, elastin production is turned off, and except in response to injury or disease, no new elastin is made over the lifetime of the organism (Davidson, 1990; Rucker and Dubick, 1984; Shapiro, 1991).

Genesis of elastic fibres in early development involves deposition of tropoelastin (the soluble precursor of mature elastin) on a preformed template of fibrillin-rich microfibrils (Mecham and Davis, 1994). Mature elastic fibres are thus a composite biomaterial comprising an outer microfibrillar mantle and an inner core of amorphous crosslinked elastin. Elastic fibers formed during early development must be of accurate size and orientation to function for a lifetime. However, various enzymes (matrix metalloproteinases and serine proteases) are able to cleave elastic fibre molecules (Kielty et al., 1994; Ashworth et al., 1999c).

During the development of the aorta, synthesis of elastin occurs very early, and its expression is regulated, in part, at the transcriptional level (Perrin and Foster, 1997). Elastic fiber assembly has often been studied with the use of primary cells isolated from fetal or neonatal auricular cartilage, aorta, or lung because of the ability of chondroblasts, smooth muscle cells, and pulmonary fibroblasts to produce and assemble insoluble elastin *in vitro* (Campagnone et al., 1987; Mecham, 1987; Faris et al., 1992). Mecham et al (1981) reported that

cells in viable ligament tissue rapidly incorporate soluble elastin into an insoluble polymer, whereas, elastin precursors synthesized by cultured cells remained soluble. Cells in tissue minces synthesized more elastin per cell (per microgram of DNA) than do ligament cells in culture. In culture, ligament cells failed to covalently link soluble elastin precursor molecules. This might be because elastic fiber formation is dependent upon still undefined matrix components that were missing in culture. Further studies, (Mecham, 1981) reported bovine fetal ligamentum nuchae fibroblasts grown on tissue culture plastic synthesized elastin precursors but were unable to form insoluble elastin whereas cells grown on dead ligament not only formed insoluble elastin, but showed an increase in levels of immunoreactive soluble elastin in culture medium. The results provide evidence that insoluble elastin formation can be reinitiated in cultured cells by providing the proper extracellular matrix, e.g., growing cultured cells on dead ligament tissue.

Confluent primary chick vascular SMCs displayed a dramatic increase in elastin mRNA levels upon serum deprivation, and when serum was added back to the cultures, cell proliferation was induced, and elastin mRNA levels dropped (Wachi *et al.*, 1995). Smith and Carnes (1973) reported the biosynthesis of soluble elastin by normal pig aortic tissue in vitro by the isolation of the radioactively labeled protein, using purified soluble elastin from copper-deficient aorta as carrier protein. The aortic smooth muscle cells form elastic fibers more typical of tissues when maintained in culture for long periods of time without subcultivation (Faris *et al.*, 1992). During this time, the cells form a three-dimensional, multilayered structure that resembles the aortic medium from which they were derived (Stone *et al.*, 1988; Faris *et al.*, 1992). In addition to the spatial orientation of the cells, the organization of the microfibril bundle itself may also be different. Primary cultures of neonatal rat aortic smooth muscle cells (SMC) were found to be differentiated in culture with unique capacity to synthesize and deposit large amounts (μg) of insoluble elastin which aggregate and form elastic fibers in vitro (Oakes *et al.*, 1982). It has also been shown that SMC from rats produce elastin and collagen when they are grown on fibrin gels (Long and Tranquillo, 2003). The amount of elastin secreted was also strongly a function of the cell source since aortic smooth muscle cells from adult rats secreted less

elastin than cells from neonatal rats. Several *in vitro* studies have previously demonstrated that addition of transforming growth factor- β (TGF- β) to aortic smooth muscle cells or skin fibroblasts stimulates elastin synthesis (Sauvage *et al.*, 1998). All the reports presented confer the idea that deposition of elastin could be manipulated by using defined culture conditions and a suitable niche.

Bellingham *et al.* (2001) and Toonkool *et al.* (2001) demonstrated that under appropriate *in vitro* conditions of temperature and ionic strength, elastin undergoes a process of ordered self-aggregation called coascervation caused by multiple and specific interactions of individual hydrophobic domains, which are usually induced by an increase in temperature. The elastin aggregates formed through coascervation appear as ordered fibrillar structures resembling the elastic fibre core, indicating that the protein has an intrinsic ability to organise into polymeric structures. *In vivo*, tropoelastin probably binds microfibrils, and then coascervates and becomes crosslinked by lysyl oxidase enzyme.

Ramamurthi and Vesely (2005) studied hyaluronan gel crosslinked with divinyl sulfone as scaffolds for culturing neonatal rat aortic smooth muscle cells and for their ability to promote elastogenesis. Under similar sets of experimental conditions, cells cultured on hyaluronan gel showed an increased amount of elastin (both soluble and insoluble) when compared to cells grown over standard tissue culture plates. Microscopical analysis of the elastin structure isolated by alkali digestion revealed that elastin was organized into smooth, highly fenestrated sheets composed of fibers, visible at the sheet edges. Interestingly such sheets and fibers were not observed on the elastin obtained from cells grown on tissue culture plates. Davidson *et al.* (1993) has investigated the effects of combinations of the mitogenic cytokines, basic fibroblast growth factor (bFGF), transforming growth factor alpha (TGF- α), and combination of insulin-like growth factor-1 (IGF-1) and transforming growth factor-beta 1 (TGF- β 1) with respect to the production of two matrix components, elastin and type I collagen.

The deposition of elastin appears to be controlled on both the transcriptional level (tropoelastin mRNA message expression (Ritz-Timme *et al.*, 2003, Degterev & Foster, 1999) and-post-transcriptional level (tropoelastin message stability (Kahari *et al.*, 1992; Hew *et al.*, 2000; Kucich *et al.*, 2002).

There are also several other post-transcriptional events, which control secretion of tropoelastin monomers and their proper extracellular assembly (20, 21) and regulate the cross-linking of tropoelastin into the polymeric "insoluble" elastin, the most durable element of the extracellular matrix (Ritz-Timme et al, 2003).

However, production of the precise ECM especially elastin was not achieved during *in vitro* conditions used for endothelial cell (EC) culture and on seeding them on biomaterials for making vascular conduits. When calf pulmonary artery EC was incubated in medium conditioned with arterial SMC, synthesis and secretion of soluble elastin has been observed (Mecham et al., 1983). However, EC synthesized only one-third as much elastin compared to SMC and approximately 80% of the elastin synthesized by EC in confluent culture was released into the culture medium. The remaining 20% remained associated with the cell layer and was readily extractable with dilute acetic acid as uncross-linked, 70,000-Da tropoelastin. In this study, elastin was deposited in all the defined matrices, but they were regulated in the GF and, GF and GAG incorporated matrices. The expression was maximum on matrices incorporated with GF and GAG together.

Howard et al (1976) reported a partial characterization of the collagen synthesized by primary cultures of aortic endothelial cells. The endothelial cells after 7 days in culture synthesize collagen that was similar to basement membrane (Type IV) collagen synthesized by other cell culture systems *in vitro*. The amount of collagen synthesized by these cells was very low as compared to fibroblast cultures. Jaffe et al (1976) also reported that cultured human endothelial cells synthesize material which is morphologically and immunologically similar to amorphous basement membrane and biochemically similar to basement membrane collagen. Kramer et al. (1985) also identified type IV procollagen on that basement membrane of cultured microvascular endothelial cells isolated from human dermis with structure that was biochemically similar to that formed *in vivo*. But all these studies were limited to the characterization the nature of the collagen type that was synthesized by the cells.

Type IV collagen is a nonfibrillar collagen that makes up about 50% of all BM. Nonfibrillar collagens differ from connective tissue fibrillar collagens by the

presence of globular or rod like, non-collagenous domains (NC domains). The collagenous domain consists of a repetitive Gly-X-Y amino acid sequence in which X and Y are often proline and hydroxyproline, or lysine and hydroxylysine. This stretch of amino acids provides for the structural integrity of the type IV collagen protomer and suprastructure. Type IV collagen is secreted from cells in the form of a protomer. Protomers are heterotrimers composed of three α -chains, and the currently known *in vivo* combinations include $\alpha 1\alpha 1\alpha 2$ and $\alpha 3\alpha 4\alpha 5$ protomers, and possibly $\alpha 1\alpha 1\alpha 5$, $\alpha 1\alpha 2\alpha 5$, and $\alpha 5\alpha 5\alpha 6$ protomers. Protomers are the building units of type IV collagen network.

There is evidence of collagen fibril accumulating in fibrin network by fibroblasts (Tuan *et al.*, 1996). Grassl *et al.* (2002) demonstrated the smooth muscle cells synthesize more collagen when entrapped in fibrin as opposed to collagen type-I gel. It is likely that for deposition of these ECM proteins, a specifically designed scaffold is required. Fibrin and fibronectin attached to the fibrin networks seem to play a role in promoting collagen and elastin deposition.

In a recent study to demonstrate production of ECM in tissue engineered blood vessels (TEBV), SMC was cultured for 6 weeks under pulsatile/non-pulsatile conditions after which significantly lower gene expression of ECM components, such as collagen I and elastin were detected in both conditions compared to that of native arteries (Heydarkhan-Hagval *et al.*, 2006). They have analyzed ECM production by SMC, whereas in this study we show that endothelial cells can be induced to synthesize collagen and elastin for which the fibrin– fibronectin matrix could serve as a reservoir of growth factors. In the present study all the defined matrices showed an upregulation in the expression of collagen IV and a regulated expression of collagen 1. On the other hand expression and deposition of collagen I was not appreciable on any of the matrix composition that was tested in this study. This observation indicates that the protein expressions are specific to endothelial cells and none of the matrices have induced any trans-differentiation of EC in *in vitro* culture.

The results of this study suggest that a combination of growth factors and glycosaminoglycans can be immobilized with the fibrin matrix which can form part of a degradable scaffold for cardiovascular tissue engineering.

CHAPTER 4

FABRICATION AND PHYSICO-CHEMICAL CHARACTERIZATION OF A POROUS POLY (ϵ -CAPROLACTONE) – FIBRIN SCAFFOLD FOR VASCULAR TISSUE ENGINEERING APPLICATIONS.

4.1. ABSTRACT

Despite the excellent biodegradability, cell growth and ECM remodeling on the fibrin composite, it lacks adequate mechanical strength to be used as a stand alone matrix. Therefore, in order to fabricate a scaffold with optimum properties, it may be necessary to have a synergy between polymer backbone and a biomimetic coating. Hence, in this study, an effort has been made to develop a mechanically and biologically superior hybrid scaffold of Poly (ϵ -caprolactone) (PCL) and fibrin composite, which may be analogous to an arterial conduit.

The specific objective of this part of study was a) To standardize fabrication of a porous PCL scaffold b) To establish the degradation rate of the scaffold and to prove the degradation products do not affect the endothelial cell (EC) growth c) To prove the scaffold has a tensile strength comparable to that of a blood vessel d) To standardize fabrication of polymer-ECM hybrid scaffold selected from the Phase I experimental results (Chapter III) to get a hybrid scaffold. e) To establish cytocompatibility of hybrid scaffold and demonstrate EC attachment, proliferation, and survival. The methods are described in Chapter II and the results are illustrated and discussed here.

4.2. Polymer scaffold

4.2.1. Morphology

By solvent casting method, PCL films of uniformly distributed porosity were prepared as evidenced by phase contrast microscopy (Fig. 4. 1A) and micro-CT analysis (Fig. 4. 1B). Polyethylene glycol (PEG) proved to be an excellent porogen for the preparation of PCL films. When fabricated through melting techniques, PCL as well as other dense polymers, generally lacks any voids and pores. This lack of pores limits gas and nutrient exchange (Ng *et al.*, 2000). Adequate nutrient diffusion through the scaffold is essential for proper vessel functionality and viability. Hence the scaffold must incorporate an interconnected porous network. The scaffold prepared display pores throughout the thickness of the scaffold that may aid in nutrient diffusion and gaseous exchange.

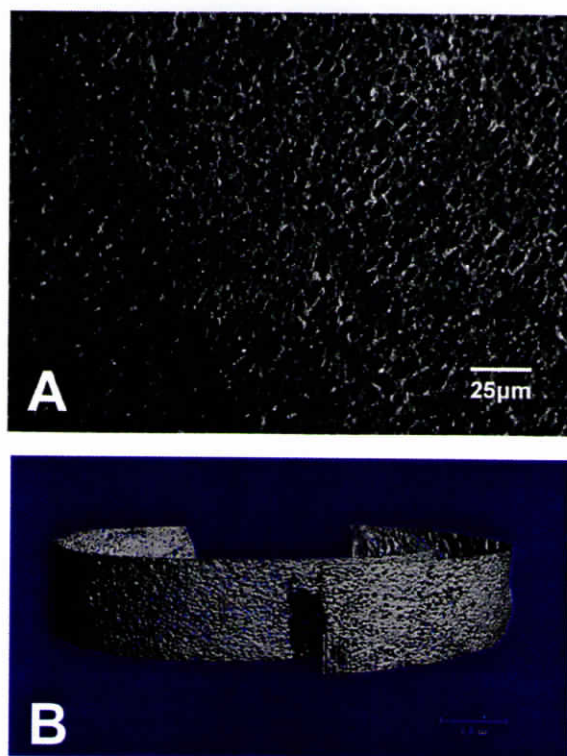


Figure 4.1. Morphology of PCL Films. A. Phase contrast micrograph of PCL scaffold. Porous nature of the scaffold and its uniform distribution is seen as black spots. Shining white particles may be the porogen retained after 3d leaching. B. Micro CT image of PCL scaffold. The uniform porosity of the scaffold can be visualized.

4.2.2. Chemical characterization

4.2.2.1. FTIR studies

ATR-IR spectrum of a PCL film prepared without porogen was compared with porous film after leaching the porogen for 15 days (Fig. 4.2). The characteristic absorption bands at $2800\text{-}3000\text{ cm}^{-1}$ (-CH stretching) and 1720 cm^{-1} (-C=O group of the ester linkage) seem to be similar with porous and nonporous samples. Figure 4.3 shows the spectrum of PCL scaffold leached for a period of 15 days superimposed with the spectrum of PEG alone and that of non leached PCL-PEG film. It is evident that the spectra of PCL scaffold leached for 15 days lacked all the characteristic peaks of PEG indicating the complete removal of PEG during the period.

Complete removal of solvent, dichloromethane, used for casting the film has been ensured by drying for 24h at room temperature, and also by the subsequent lyophilization cycles during the scaffold preparation. Since the selected porogen, PEG, is known to be biocompatible (Cohen *et al.*, 2001) even if traces remain on the scaffold it does not elicit toxicity to the cells. The porogen leaching of the scaffold was initially done for 3 days and the experiments were conducted using this scaffold. To nullify the effect of porogen on the mechanical properties of the porous scaffold and also to study the effect on porosity upon entire removal of the porogen, the leaching time was extended to 15 days and additional experiments were done.

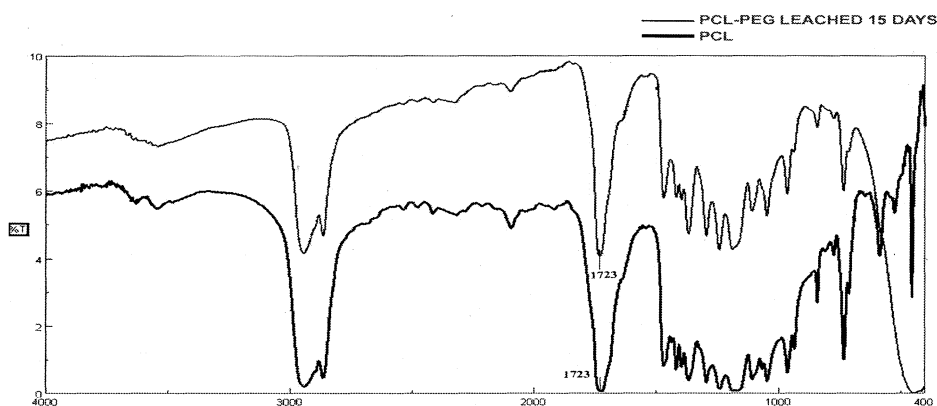


Figure 4.2. FTIR spectrum of PCL . The spectrum marked PCL-leached 15 days is of the film cast with porogen and leached in D/W for 15 days; the spectrum marked PCL is of PCL film prepared without porogen

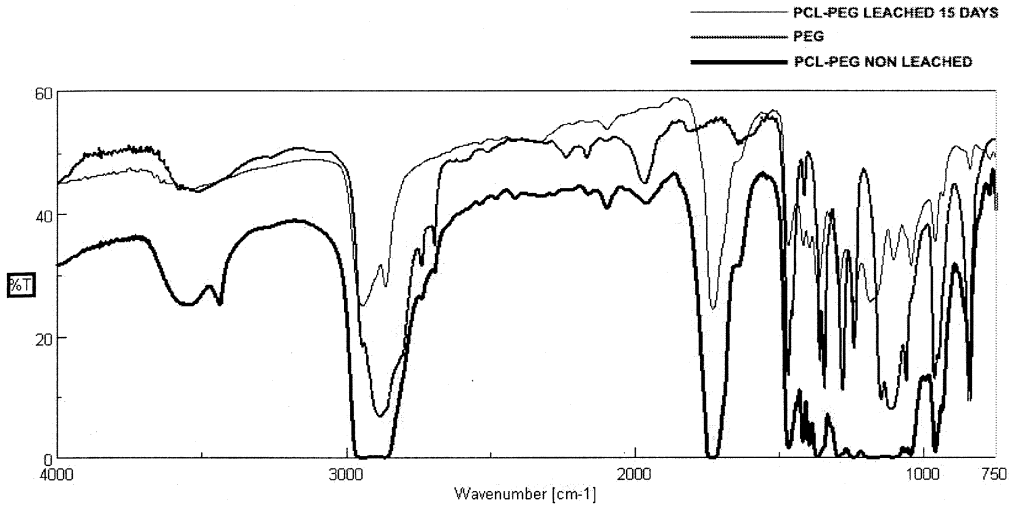


Figure 4.3. FTIR spectrum PCL scaffolds. The spectrum marked PCL-PEG leached 15 days is of the film cast with porogen and leached in D/W for 15 days; the spectrum marked PEG is of PEG film formed on ZnSe cell; the spectrum marked PCL-PEG is of non leached porous PCL.

4.2.3. Physical properties

4.2.3.1. Mechanical properties

The mechanical properties of a blood vessel determine its strength and reaction to hemodynamic forces. Blood vessels and in particular arteries bear three distinct mechanical characteristics, being elastic, determined by the elastin content, tensile stiffness, determined by the collagen content; and compressibility which is taken care of by the glycosaminoglycans (GAGs). Since the reconstructed neovessel has to bear a load immediately after implantation, it should have a certain tensile strength and compliance prior to implantation (Greenwald and Berry, 2000). When the tensile strength and compliance property cannot be achieved during engineering a TEBV, the patency rate reduces greatly with increasing compliance mismatch.

Variation in tensile strength and elongation of the PCL scaffold stored in PBS at 37°C at different intervals is shown in Figs. 4.4. & 4.5. Compared to the initial films, PBS stored films exhibited improved strength and elongation (5.39 MPa to 9.46 MPa and 74.5% to 163%). But tensile strength and elongation at 60 days were reduced to 7.62 MPa and 58% respectively,

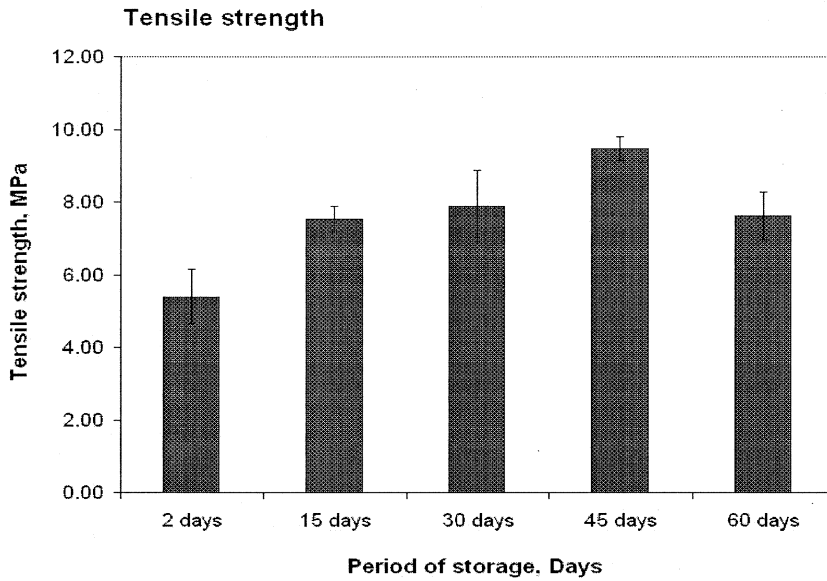


Figure 4.4. Tensile strength of bare PCL scaffolds. Bar graph shows variation in tensile strength values of the bare PCL scaffold after 2, 15, 30, 45 and 60 days of storage in PBS. Average and standard deviation was calculated using measurements of 8 films for each period.

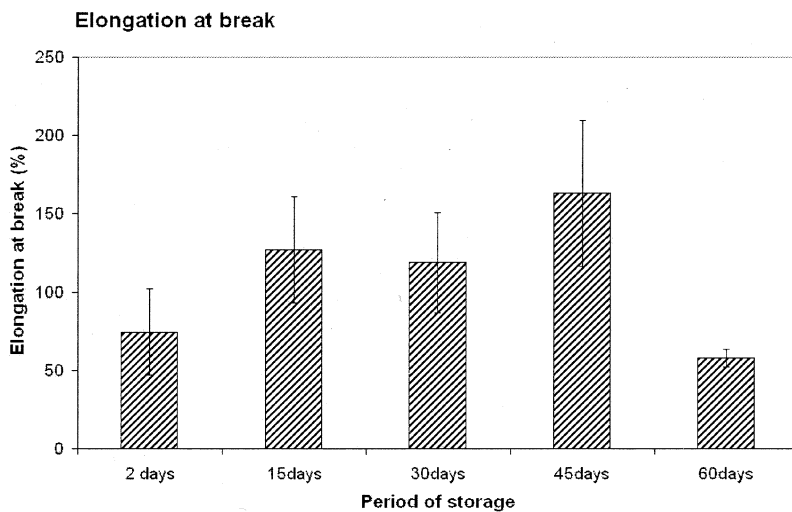


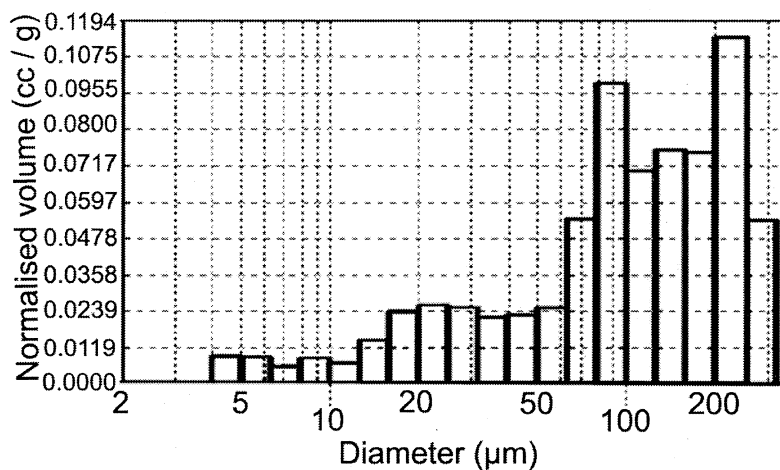
Figure 4.5. Elongation at break of bare PCL scaffolds. Bar graph shows variation in elongation values of the bare PCL scaffold after 2, 15, 30, 45 and 60 days of storage in PBS. Average and standard deviation was calculated using measurements of 8 films for each period.

and compared to the properties at 45 days; the change was significant ($P < 0.05$). Films were lyophilized before they were immersed in PBS and being hydrophobic in nature it is likely that more than 2 days was required to equilibrate PCL in the aqueous medium and to gain the true mechanical strength after complete hydration of the films. It is likely that the mild reduction observed in molecular weight after 60 d has affected the mechanical strength of the film as well. Even with variable results, at all time periods the films showed tensile strength above 5MPa which is adequate for a tissue engineered vascular graft

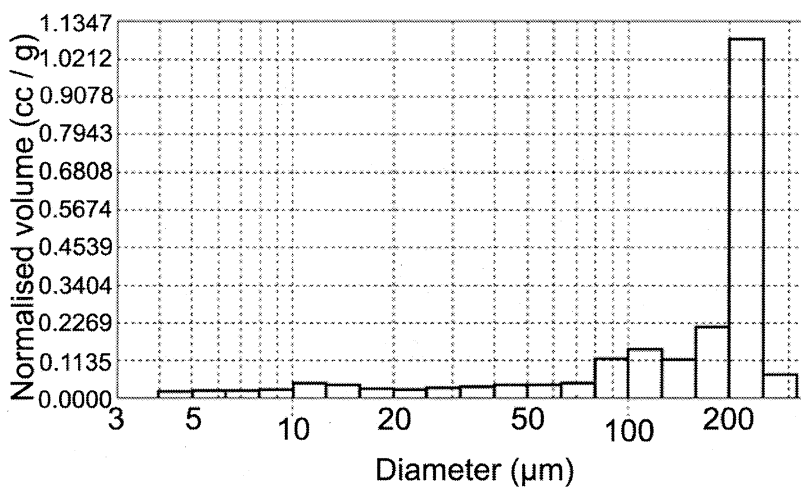
4.2.3.2. Porosity/ Pore size

In vascular tissue engineering, scaffold should have adequate porosity for cellular invasion into the scaffold and for deposition of ECM by the cells that grow on them. It has been reported that porous vascular graft enhances endothelialization of the graft and tissue in-growth whereas in non porous e-PTFE implants limited tissue in-growth and incomplete coverage of endothelial-like cells are evidenced (Zhang *et al.*, 2007). Additionally, pore sizes larger than 10 μ m will allow invasion of fibro-vascular tissue and therefore enhance capillary network development and subsequent vascularization (Mooney and Langer, 1995).

Experiments with mercury porosimeter indicated that the pore size of the scaffolds ranged between 5-200 microns (Fig 4.6.A & B). The histograms generated by the equipment have pore diameter on the x-axis and normalized intrusion volume on the y-axis. It is evident that the pore volume has increased in 15 d leached sample as compared to 3 d leached sample. Clearly, porogen removal continued to take place even after 3 days and the porosity increased. When the Y-axis scale of Fig. 4.6 A and B are compared it is obvious that porosity increased significantly by day 15.



A. PCL-3d



B. PCL-15d

Figure 4.6. Histogram of pore size distribution. Intrusion volume is represented on the y-axis and pore size on the x-axis. Histogram for a representative sample of (A) bare PCL scaffold leached for 3 d; (B) bare PCL leached for 15 d. Scales on the y-axis of each histogram is different and is given as generated by the measurement program.

4.2.4. Scaffold Stability/ Degradation:

4.2.4.1. Gravimetric analysis: Gravimetric analysis of bare polymer scaffold stored in PBS showed a decrease in weight after 30 days (0.59%) as compared to 2 days, and a difference is seen between 30d and 45d (1.35%) whereas there is no difference in weight observed after 60 days compared to 45 days (Fig.4.7). It is seen in this study that there is a marginal loss of weight after immersion for 15 days in PBS, which is primarily due to the removal of the residual progen retained within the polymer film and not due to the degradation of the polymer since there is no weight loss between 45 d and 60 d period. Marginal/absence of weight loss of polymer films during this period indicates that there is considerable no PCL degradation that would affect the scaffold stability during the period of *in vitro* tissue engineering.

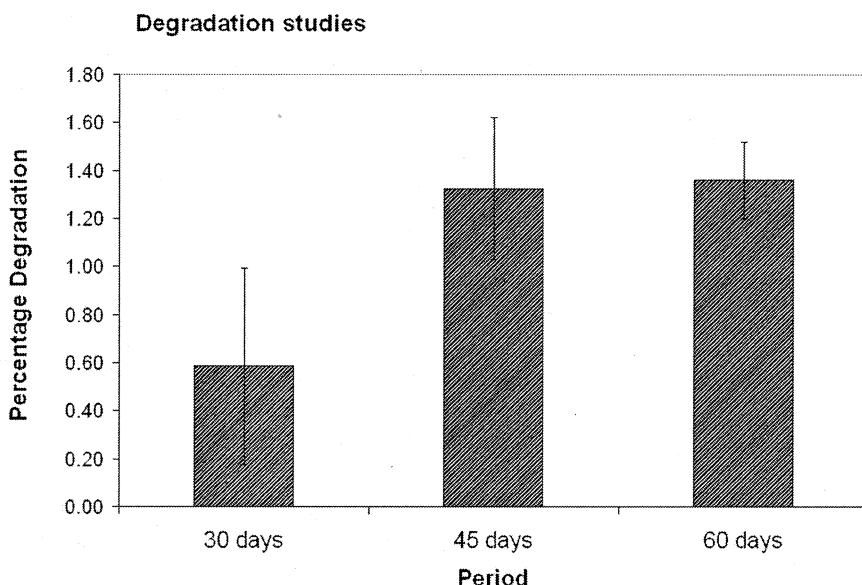


Figure 4.7. Percentage weight loss of the scaffolds. Initial weight W_0 is obtained by gravimetric analysis of films ($n=8$) after treating with PBS for 2 days, and W_r is obtained from films ($n=8$ for each period) incubated with PBS for 30, 45 and 60 days. The percentage degradation was calculated using the equation, $\text{Degradation (\%)} = 100 \times (W_0 - W_1) / W_0$. Significant reduction ($P < 0.05$, $n=8$) in weight is seen after 45 days as compared to 30 days.

4.2.4.2. Viscosity average molecular weight: Viscosity average molecular weight studies showed negligible decrease in molecular weight ($\sim 1.38\%$) after 60 days of storage in PBS at 37°C for bare PCL scaffold. While M_v value of

74443 was calculated initially at the start of the experiment, this value reduced only to 73414 after 60 days (Fig 4.8). This data substantiate the gravimetric observation that PCL degradation is a slow process even though they are highly porous and thin films. Hence, early periods of cell culture and tissue generation is not likely to be affected as a result of degradation products.

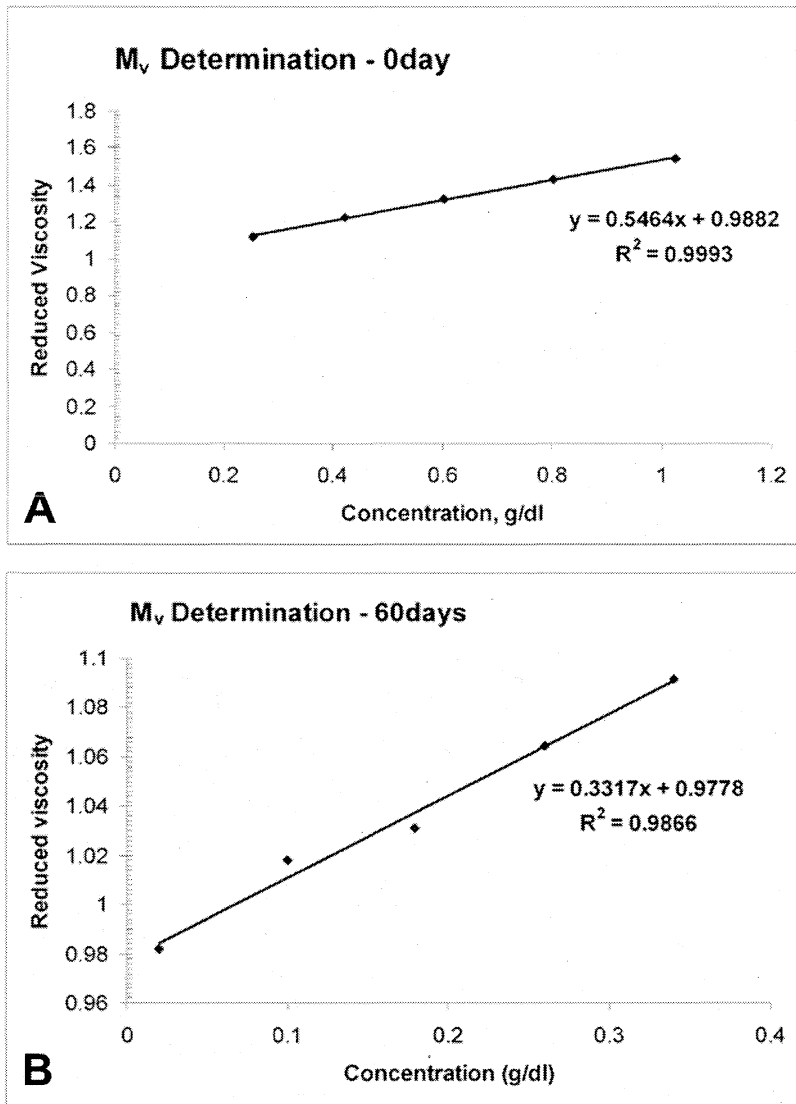


Figure 4.8. Graph showing viscosity vs PCL concentration. Serial dilutions of PCL solution was used to measure reduced viscosity against concentration. A. Graph constructed using polymer before incubation with PBS B. Graph of PCL after 60 days of storage in PBS. Three measurements were made for each concentration and the average was taken for plotting the graph.

It is well known that PCL exhibits slow degradation rate unlike PGA or PLA which degrades within short storage times (Ferrin DE & English JP, 2004).

The degradation of PCL and its co-polymers is known to proceed in at least two stages; the first stage of degradation involves non enzymatic hydrolytic ester cleavage, auto catalyzed by the carboxyl ends of the polymer chains. When the molecular weight has decreased to about 5000, the second stage starts with the slowing down of the rate of chain scission and the beginning of weight loss because of the diffusion of oligomeric species from the bulk. The polymer becomes prone to fragmentation and, at this point either enzymatic surface erosion or phagocytosis can contribute to the adsorption process. It is reported that PCL system with an initial Mn of 50,000 required three years for total removal from the body showing a remarkably slower degradation (Li and Vert, 1995). Sun *et al.* (2006) reported the PCL degradation products did not cumulate in body tissue and was completely excreted in 135 days after subcutaneous implantation of tritium labeled PCL, Mw 3000 in rats.

The polymer is expected to provide a backbone support until tissue remodeling takes place during the fabrication of a vascular construct, and the polymer scaffold developed in this study is found to remain stable during the initial period of tissue regeneration.

4.2.5. Endothelial cell growth on porous PCL

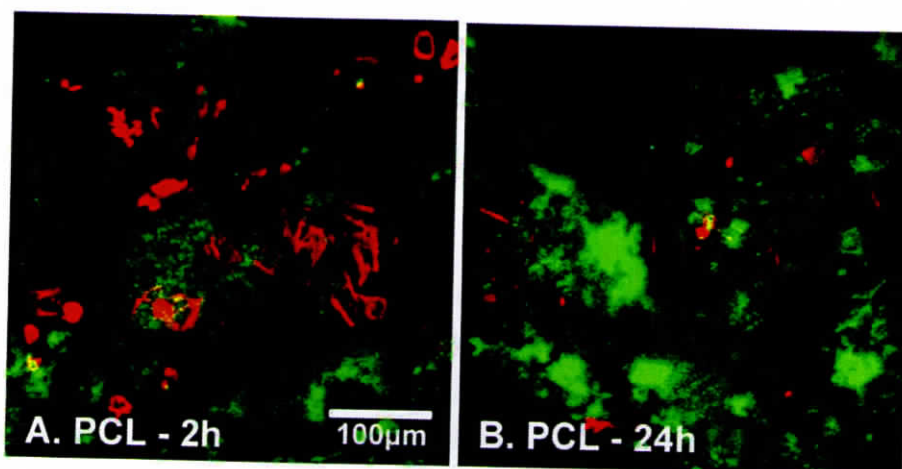


Figure 4.9. Confocal micrographs of actin-stained ECs on PCL scaffold. EC adhesion at 2 h (A) and 24 h (B) after seeding on bare PCL scaffold. In all micrographs the images were from a single plane of the x - y - z axis. Texas red was excited using a He/Ne laser at 594 nm and the emission wavelength was obtained using an LP filter at 610 nm. The polymer was excited using an argon laser and the signal at specific wavelength was captured using a BP 505–530 nm filter. The cells are coloured red and the polymer is false-coloured green.

Analysis of actin-stained EC seeded bare PCL scaffold revealed less cell adhesion. Although few cells tend to attach to bare PCL polymer, the actin filaments were not well spread (Fig 4.9 A). After 24h of EC seeding, the PCL scaffold (shown as green in Figure) could be clearly visualized but the actin stained filaments were scarcely seen (Fig 4.9B).

From the above results it is understood that though PCL scaffolds showed excellent mechanical properties, slow degradation rate and sufficient porosity, they failed to support EC growth. In spite of providing suitable mechanical support and elasticity, it was expected that PCL may not support adequate EC adhesion to its surface and cell growth that is required to produce tissue constructs. It has been shown earlier that the ECs adhere and spread on moderately wettable polymers and that the hydrophobic surfaces lead to poor cell attachment (van Wachem *et al.*, 1985). Cells need adhesive proteins to recognize integrin receptors that would give focal adhesions and stimulus response coupling for cell growth and differentiation (Mercedes and Elaser, 2002). Adhesion, proliferation and differentiation of cells on polymer substrates can be modified by providing signals to the cells through specific biological agents incorporated on polymer surfaces. PCL has been modified or coated with biomimetic molecules to create a functional endothelium over the polymer surface. The PCL surface was grafted with RGD peptide to enhance the growth rate of human ECs (HUVEC) on the surface by Chung *et al.* (2005). Gelatin grafting has enhanced EC spreading and proliferation on electrospun poly (caprolactone) (PCL) nanofibers (Ma *et al.*, 2005). Prasad *et al.* (2007) demonstrated earlier that some of the biomaterials used for cardiovascular implants do not promote sufficient EC adhesion, proliferation and survival whereas coating of a biomimetic matrix improves cell adhesion and spreading on such materials. Hence, the scaffold was coated with the biomimetic ECM coating standardized in the Phase I studies to facilitate EC culture.

4.3. Hybrid Scaffold Characterization

4.3.1. Morphology

Light microscopic analysis of the PCL scaffold showed uniform distribution of pores (Fig. 4.10A), and after coating with fibrin composite, a fibrin

network is deposited with uniform bundle thickness (Fig. 4.10B). Both bare and hybrid scaffolds were analyzed after lyophilization. Immersion of the hybrid scaffold in the culture medium or cell seeding and culture did not affect the fibrin structure for 48 h.

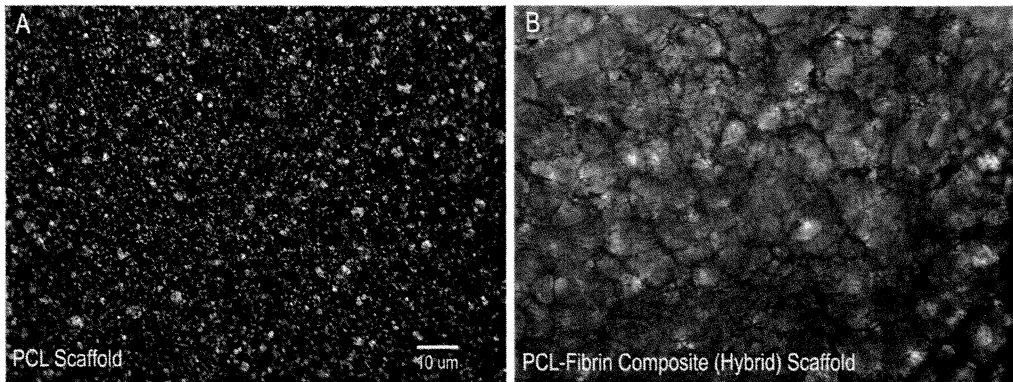


Figure 4.10. Light micrographs of scaffolds. Bare PCL scaffold morphology is shown in (A) and surface morphology of the fibrin coated PCL (hybrid scaffold) in (B). Scaffolds, dried by lyophilization, were viewed under an inverted light microscope (Lieca DMIRB, Germany). Original magnification, 64X

4.3.2. Chemical characterization

4.3.2.1. FTIR studies

Gravimetric analysis revealed a fibrin density of nearly $170\mu\text{g}/\text{cm}^2$ after fibrin composite coating on the bare polymer. The spectrum of hybrid scaffold which is superimposed with the bare PCL scaffold in Fig 4.11 confirms deposition of fibrin composite over the scaffold. The coating is indicated by the shift of earlier OH stretching band at 3394 cm^{-1} to 3285 cm^{-1} due to the predominance of the N-H stretching absorption band over the hydroxyl group. The amide I and amide II bands observed on the hybrid scaffold at 1641 cm^{-1} and 1541 cm^{-1} further confirmed the presence of fibrin composite on the PCL scaffold. The 1723 cm^{-1} peak is rather weak in the hybrid scaffold probably due to the fibrin composite coating on the surface suppressing the characteristic peaks of PCL in the ATR spectrum.

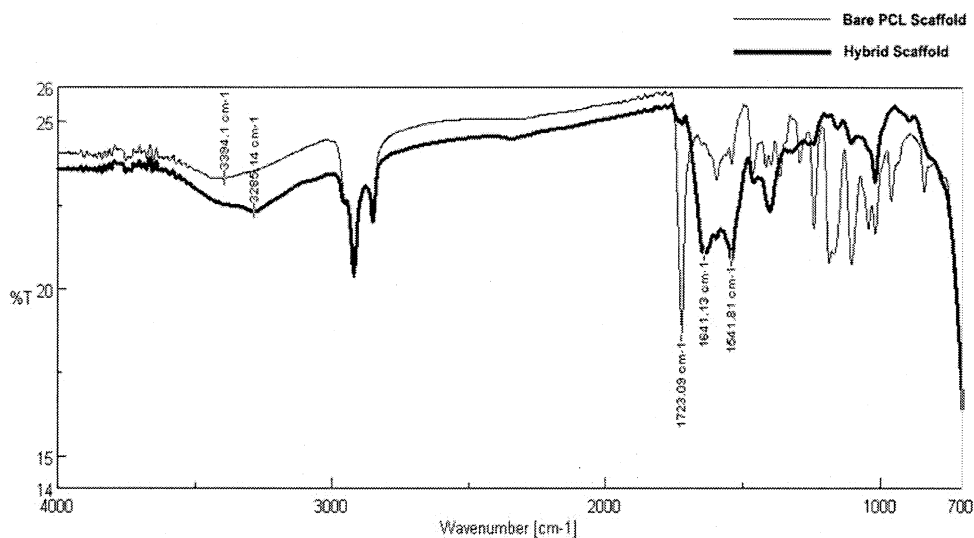


Figure 4.11. FTIR spectra of bare PCL and hybrid scaffolds. Spectrum of hybrid scaffold was overlaid with the spectrum of bare PCL in the region of wave numbers 700 to 4000cm⁻¹ to distinguish the characteristic NH-band of proteins due to fibrin composite coating.

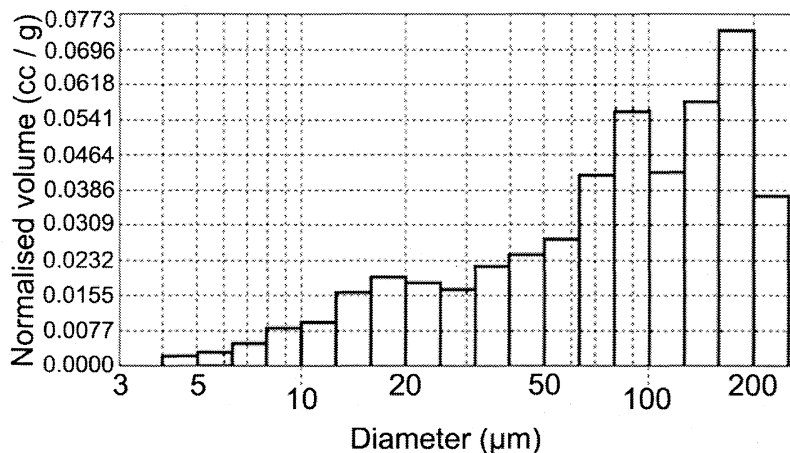
4.3.3. Physical characterization

4.3.3.1. Porosity and pore size

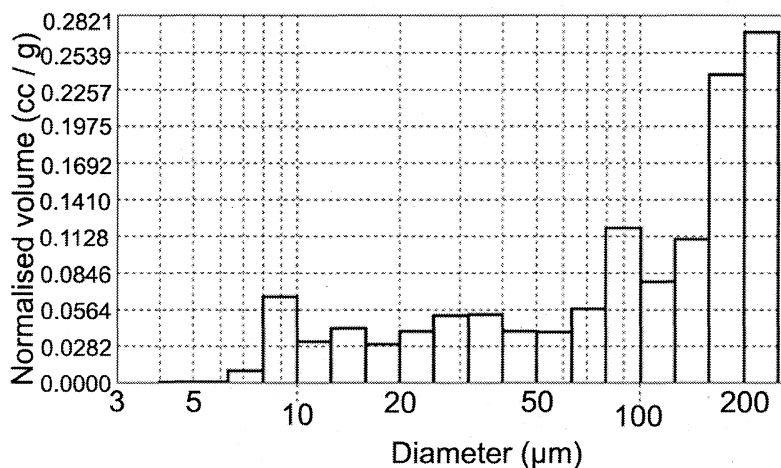
The mercury porosimetry data showed a pore distribution similar to that of bare PCL scaffold ranging from 5-200 μ m, but upon fibrin composite coating volume of the pores in PCL reduced significantly after 15 day leaching (Fig 4.12 A & B) as seen in the case of hybrid scaffold after 3 day leaching (Fig.4.6 A & B). The results indicate that an effective coating of the fibrin composite was formed inside the pores in the scaffold and thus cell migration and growth may be facilitated.

Fibrin coating on the PCL scaffold has reduced the pore volume but the coating is thin and do not close the pores as may be seen in the porosity histograms. After lyophilization, the fibrin composite coating is stable and coated surfaces can be stored at 4°C until they are used for cell seeding (Kumar and Krishnan, 2002). It has been demonstrated that fibrin degrades within 24 h of EC culture, and degradation is complete in 120h of culture. Hence, fibrin coating is unlikely to prevent invasion of cells through the pores that is required to populate the hybrid scaffold with cells and new tissue. Therefore, the fibrin composite

coated PCL produce a hybrid scaffold that has stable functional proteins and can be stored at 4°C until they are used for tissue engineering applications.



A. PCL 3d L- FC coated



B. PCL 15d L- FC coated

Figure 4.12. Histogram of pore size distribution. Intrusion volume is on the y-axis and pore size on the x-axis. Histogram for a representative sample of (A) PCL scaffold leached for 3 d and FC coated (B) PCL scaffold leached for 3 d and FC coated. Scales on the y-axis of each histogram is different and is given as generated by the measurement program.

4.3.4. Biological properties

4.3.4.1. Analysis of cell growth on hybrid scaffold

Analysis of actin-stained EC seeded hybrid scaffolds revealed significant cell attachment and spreading on the hybrid scaffold (Fig 4.13. A&B) when compared to the bare PCL (Fig. 4.9. A&B). After 24h there was a remarkable difference between bare PCL and hybrid scaffold in terms of EC spreading and actin filament organization. In the hybrid scaffold actin-stained (red) cells covered the entire surface (Fig 4.13. A&B) and the green colour of scaffold were less prominent.

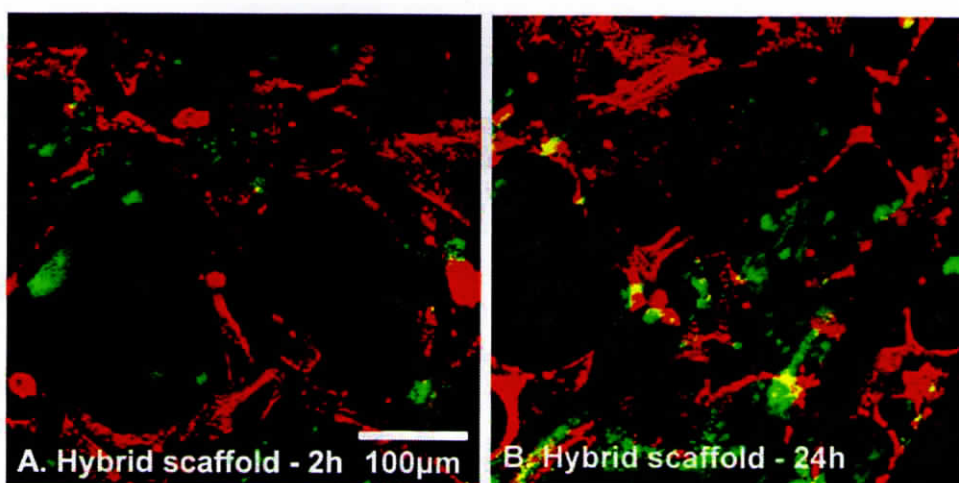


Figure 4.13. Confocal micrographs of actin-stained ECs. EC adhesion at 2 h (A) and 24 h (B) after seeding on hybrid scaffold were analyzed. In all micrographs the images were from a single plane of the x - y - z axis. Texas red was excited using a He/Ne laser at 594 nm and the emission wavelength was obtained using an LP filter at 610 nm. The polymer was excited using an argon laser and the signal at specific wavelength was captured using a BP 505–530 nm filter. The cells are coloured red and the polymer is false-coloured green.

From the above observations, it is understood that the spreading of ECs on the hybrid scaffold is more favorable because of the improved focal adhesions and signaling from the composite matrix to which they are attached, whereas the surface chemistry of the bare PCL scaffold does not seem to favor EC attachment. It is well known that fibrin is a natural provisional matrix on which ECs attach and grow in wound healing. In addition to fibrin, fibronectin and

gelatin are also present to promote cell attachment and spreading (Prasad *et al.*, 2007) in the composite matrix coated-PCL. As we observed minimal cell adhesion on the PCL scaffolds, it is apparent that modification of the scaffold through ECM mimetic coating is beneficial to obtain enhanced cell adhesion. Hence the hybrid scaffold was further evaluated for long-term *in vitro* EC culture.

Environmental scanning electron micrographs of PCL film, hybrid scaffold and cell seeded hybrid scaffold at 15 and 30 days are shown in Fig. 4.14. All PCL films in this experiment were leached for 3 days. On the bare PCL scaffold, porogen micro particles are seen (Fig. 4.14A) and fibrin network is found to have occupied most of the pore volume in the hybrid scaffold, though some macro pores are still seen (Fig. 4.14B). After 15 days, the scaffold surface revealed a continuous EC monolayer (Fig. 4.14C&D). The EC junctions could be clearly seen. The continuous EC layer covered even the surface of macro pores even at 30 days (Figs. 4.14E&F). No qualitative difference in cell population could be visualized between the 15d and 30d EC grown surfaces. The porogen particles seen in Fig 4.14A may be entrapped in the fibrin composite coating or it may have leached out during the culture period.

A major drawback in the use of polymers as scaffolds has been the release of acidic by-products upon degradation, both in *in vitro* and *in vivo* conditions which raise concerns that the scaffold microenvironment may not be ideal for tissue growth (Sachlos and Czernuszka, 2003). Significant observation in this study was that no adverse effects on the cell growth occurred due to porogen/PCL degradation products during this period. The ingrowth of the cells even to the interior of the pores is seen in Fig 4.14D after 15 days of EC culture. The normal morphology of the cells at 15 days and 30 days of cell culture could be clearly visualized by the ultra high magnification images in Fig. 4.14 D&F. The typical cobble stone morphology of EC and cell junctions was clearly visible (Fig. 4.14F).

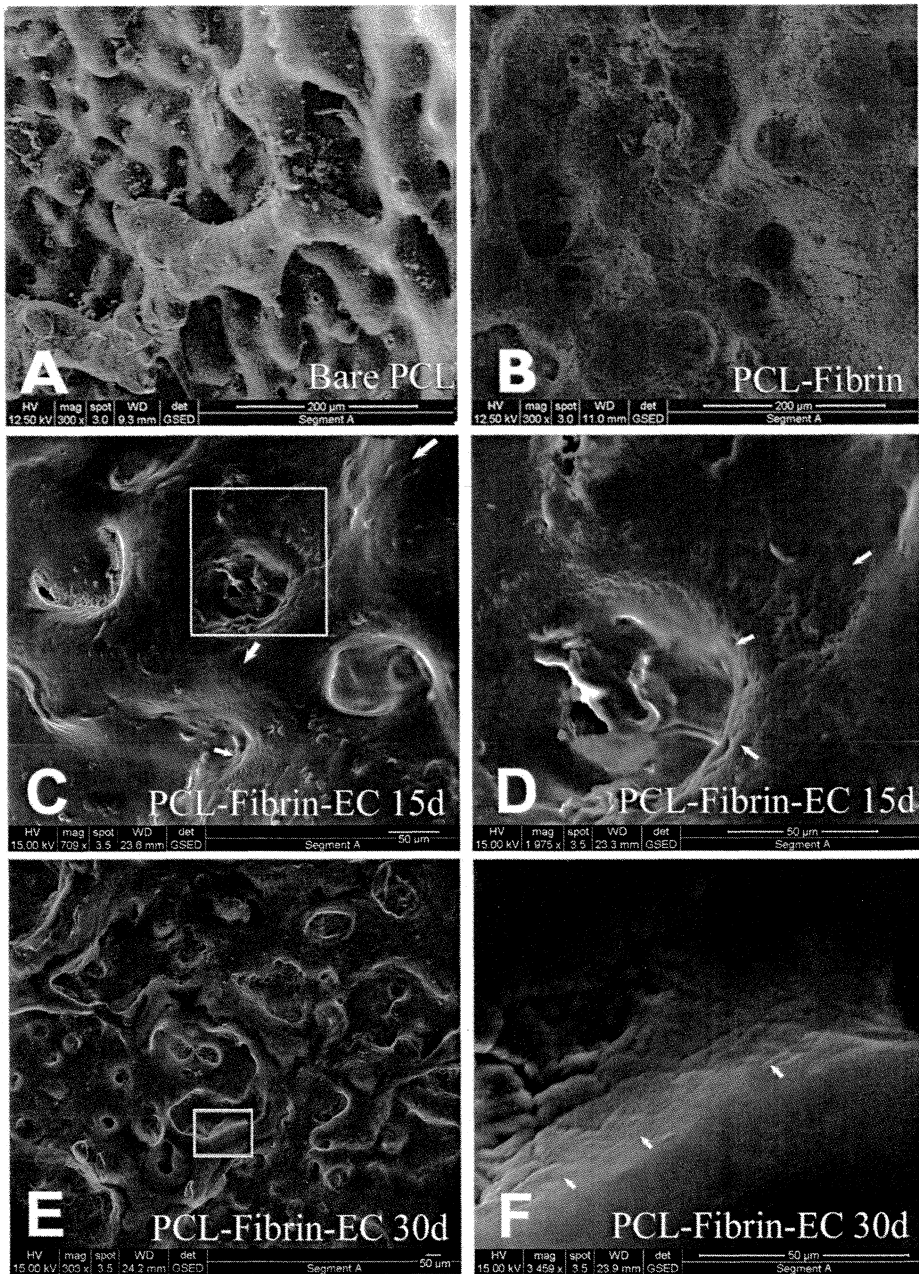


Figure 4.14. Electron micrographs of scaffolds. Environmental scanning electron micrographs depicting PCL scaffold [A], PCL-fibrin scaffold. [C] EC seeded hybrid scaffold at 15 days [D] Higher magnification image of the area marked in the Fig C ECs could be clearly visualized as a uniform monolayer [E] EC seeded scaffold at 30 days [F] Higher magnification image of the area marked in the Fig E. Magnifications are printed at the bottom of each micrograph.

4.3.5. Mechanical properties

Fibrin composite coating seems to have significantly affected ($P < 0.05$) the strength of the porous PCL scaffold (3days leached) reducing from nearly 5.09 MPa to 4.2 MPa (Fig. 4.15A). The reduction in strength after fibrin composite coating on PCL may be an effect of lyophilization of the scaffold after coating. However, there is no significant reduction in % elongation after fibrin composite coating (Fig. 4.15B).

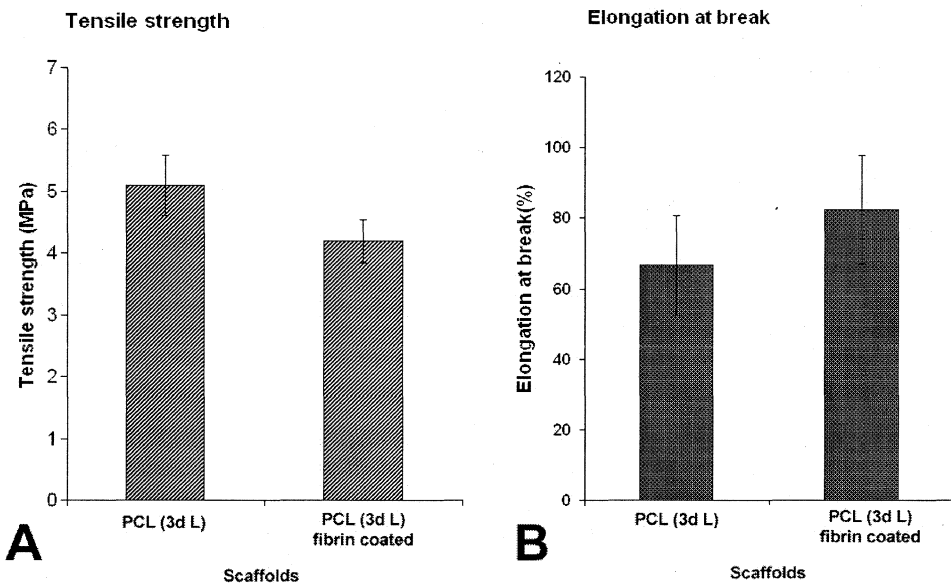


Figure 4.15. Mechanical properties of porous PCL scaffold and (3d leached) and hybrid fibrin- PCL scaffold. A. Bar graph compares tensile strength of 3d leached PCL scaffold and 3d leached fibrin coated PCL scaffold. **B.** Bar graph compares percentage elongation of 3d L PCL scaffold and 3d leached fibrin coated PCL scaffold. Average and standard deviation was calculated using measurements of 8 films for each period.

There is a significant difference ($P < 0.05$) between 3 d and 15 d leached samples in terms of tensile strength (Fig. 4.16) and elongation at break (Fig. 4.17). After fibrin coating, tensile strength of the hybrid scaffolds seem to decrease marginally but the elongation is not affected (Fig. 4.16). The films that were lyophilized after fibrin composite coating was suspended in medium for 24 h before measuring the mechanical properties to ensure proper hydration of scaffold before the mechanical properties were measured. The hybrid scaffolds, after being immersed for 15 d in culture media for cell growth seem to have

improved strength compared to that of the films after 15 d leaching alone. However, elongation at break has reduced marginally (Fig. 4.17) after 15d EC culture.

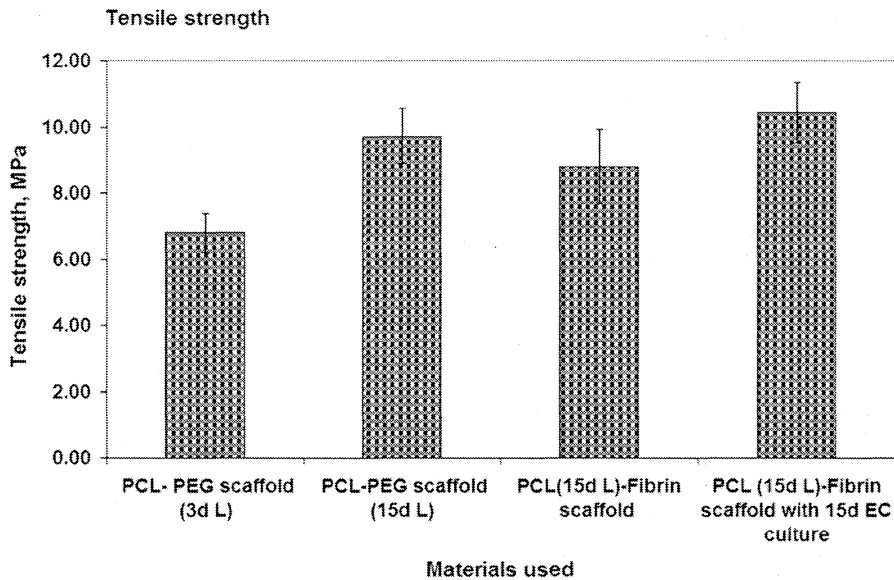


Figure 4.16. Tensile strength of bare, hybrid and EC- seeded hybrid scaffolds. Bar graph compares tensile strength of 3d leached PCL, 15d leached PCL, 15 d leached PCL coated with fibrin, and 15 d leached PCL-fibrin hybrid scaffold after 15 days of EC culture. Average and standard deviation was calculated using measurements of 8 films for each period.

The mechanical properties critical to blood vessel function include tensile stiffness and elasticity. Though nonporous PCL film has been reported to have strength values of nearly 16 MPa (Agrawal *et al.*, 2001), here it was observed that incorporation of 50% porogen and resultant porosity after 3 d or 15 d of porogen leaching produced polymer films with tensile strength varying from 6-10 MPa. Tensile strength is likely to be dependent on various processing parameters, the final properties of the product such as percentage porosity and film thickness as well.

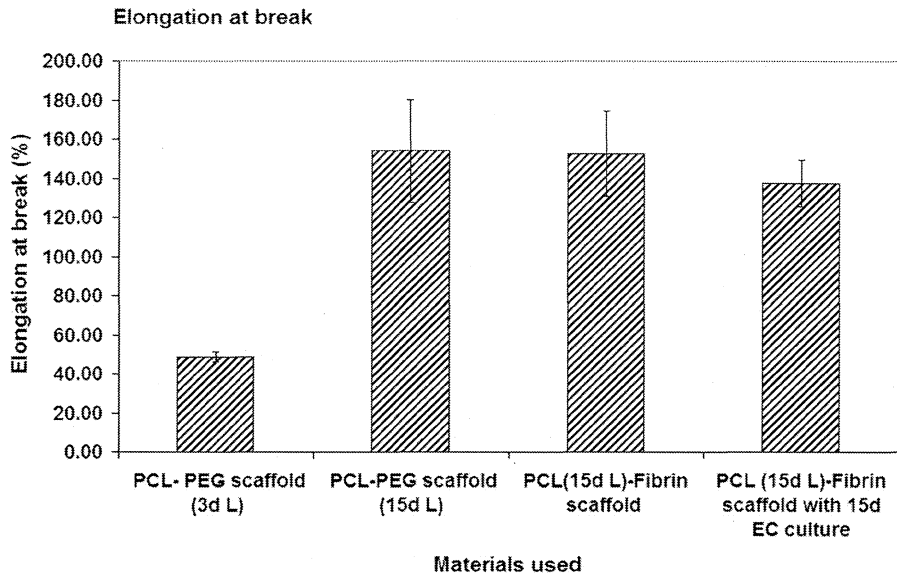


Figure 4.17. Elongation at break of tissue engineered hybrid scaffolds. Bar graph compares tensile strength of 3 d leached, 15d leached, 15 d leached PCL & coated with fibrin, and 15 day leached PCL-fibrin hybrid scaffold after 15 days of EC culture. Average and standard deviation was calculated using measurements of 8 films for each period.

The best option to select suitable scaffold for vascular tissue engineering is to have a film that has mechanical properties which is similar or better than the native blood vessel. The reduction in strength after fibrin composite coating on PCL may be an effect of lyophilization of the scaffold after coating and when the coated scaffolds were immersed in the culture medium for 15d the strength was regained. It is seen in this study that when EC grow on the surface, the provisional composite matrix is degraded and new ECM is deposited by the growing cell. The increase in strength seen with the EC cultured scaffold (15 d) as compared to hybrid scaffold is probably due to deposition of elastin and collagen by proliferating cells. It is promising that there was no significant reduction in elongation of the tissue engineered samples after 15 d culture as compared to bare scaffold.

It has been reported (Gildner *et al.*, 2004) that natural small diameter vascular conduits have strength of nearly 1-2 MPa. The hybrid scaffold produced in this study provided enough strength, elongation and facilitated EC growth with an encouraging outlook for their use as potential conduits in vascular tissue engineering applications.

ENDOTHELIAL CELL GROWTH AND FUNCTIONAL TISSUE GENERATION

5.1. ABSTRACT

Development of a functional, adherent endothelium over the polymeric scaffolds is one of the major factors limiting the successful development of tissue-engineered grafts. Tissue-engineered vascular grafts should encourage endothelial cell functions besides facilitating spreading morphology, cell viability, and cell attachment, with the deposition of ECM molecules that will provide mechanical strength to the construct. The construct should also be blood compatible.

The specific objectives of this part of the study were; 1) To prove the hybrid scaffold promote EC adhesion, proliferation, survival and ECM remodeling 2) To establish the EC maintain quiescent phenotype and expression of ECM molecules on the hybrid scaffold. 3) To prove that the EC grown on the hybrid scaffold is non-thrombogenic. The methods are described in Chapter II, the results are illustrated and discussed here.

5.2. Cell adhesion and proliferation

5.2.1. Visualization of EC on scaffold

Confocal microscopic analysis of actin-stained scaffolds after 15 days of EC culture revealed a scaffold surface completely covered by EC and the PCL

scaffold was rarely seen (Figure 5.1). No significant difference in actin distribution was observed between 15 days and 30 days on the scaffold surfaces, as it was completely covered with ECs. Sectioning along the z axis to analyze the cell population within the pores of the scaffold revealed cell survival at different planes; as evidenced by confocal images of the empty area in a 27 μm slice when compared with the 48/51/54 or 57 μm slices of the same x–y plane (Figure 5.1). The results indicate that ECs cultured on the hybrid scaffold for 15 days cover the interior surface of the pores as well.

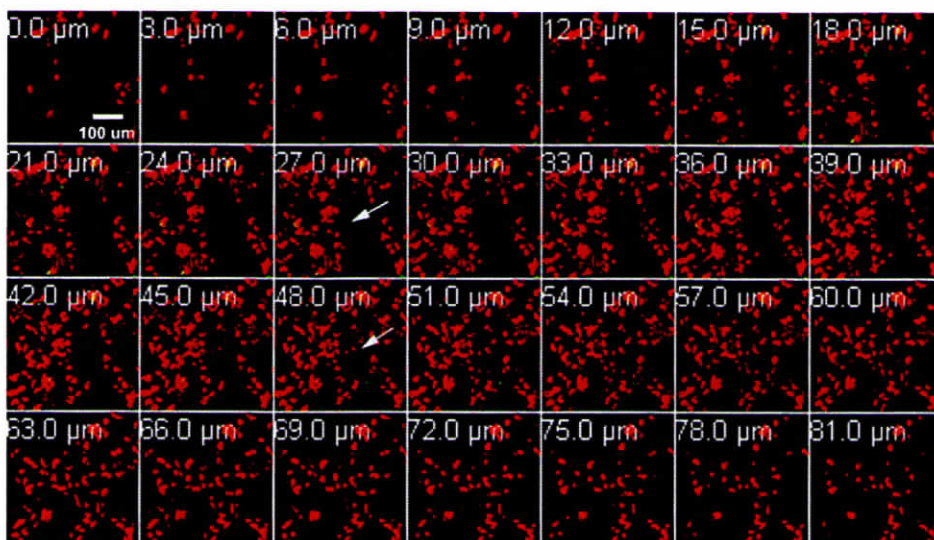


Figure 5.1. Actin-stained ECs on a hybrid scaffold. Confocal views of actin-stained ECs are shown in the same x–y plane with varying z axis planes after 30 days of cell culture. Slicing was done at 3 μm intervals to view cells lying in different z planes. Texas red was excited using a He/Ne laser at 594 nm and the emission wavelength was obtained using an LP 610 nm filter. The polymer was excited using an argon laser at 488 nm and the emitted signal at specific wavelength was captured using a BP 505–530 nm filter. The cells are colored red and the polymer is false-colored green

5.2.2. Quantification of Adhesion & Proliferation

Although confocal microscopy of actin-stained scaffolds revealed a difference in cell adhesion on the two scaffolds (Figs. 4.9 & 4.13), quantification of cell adhesion by tritiated thymidine assay showed attachment of similar number of cells on both scaffolds at 2 h (Fig. 5.2). The actin staining method is likely to be more reliable, because cells could be visualized throughout the hybrid scaffold but the cell number was relatively low on PCL scaffold. In the case of ^3H -

thymidine assay, a possibility exists that, due to its porous nature, ECs may be non-specifically held onto the scaffold which were not included during the counting of unattached ECs, whereas in the case of actin staining, the non-specifically bound cells are removed during the washing steps in the staining procedure. Thus, it may prove more appropriate to rely on the actin-staining method and conclude that EC adhesion is likely to be less on PCL compared to the hybrid scaffold.

Analysis of cell proliferation indicated that EC proliferation was significant ($p < 0.001$) on the hybrid scaffold at 72 h compared to bare PCL (Figure 5.2). The population doubling times were 136.6 h and 41.82 h for bare and hybrid scaffolds, respectively. The rate of increase was approximately 4-fold when compared to PCL where the cells failed to proliferate even one fold. The scaffolds were washed thoroughly before DNA extraction was done and it is unlikely that dead cells and non-specifically bound cells were included in the assay.

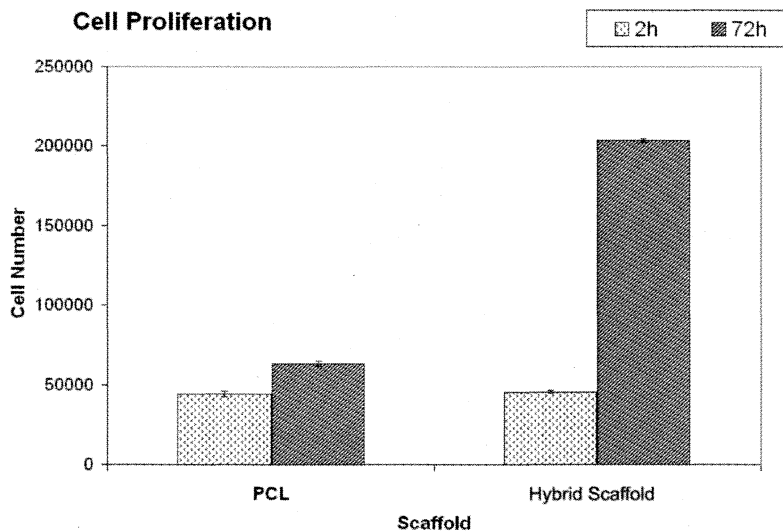


Figure 5.2. Data on ^3H -thymidine uptake assay. Graph shows indirect estimation of cell adhesion at 2 h and direct estimation of cell number after 72 h of EC culture on each scaffold type. Four replicates were included for both bare and hybrid scaffolds. Average and SD are shown in the graph

5.2.3. Proliferation using PCNA as marker

Quantitative data shown in Fig. 5.4. compare the percentages of PCNA-positive cells on the two scaffold types. While $84.4 \pm 1.57\%$ ($n = 4$) of the EC population on the hybrid scaffold were PCNA-positive, only $17.85 \pm 2.19\%$ were positive in the case of bare PCL at 72h. Using a flow-cytometric technique, reliable analysis of PCNA-positive cells could be carried out in spite of the cell number harvested from the PCL scaffold being less. The percentage of proliferating cells on the bare polymer seems to be minimal compared to that on the hybrid scaffold.

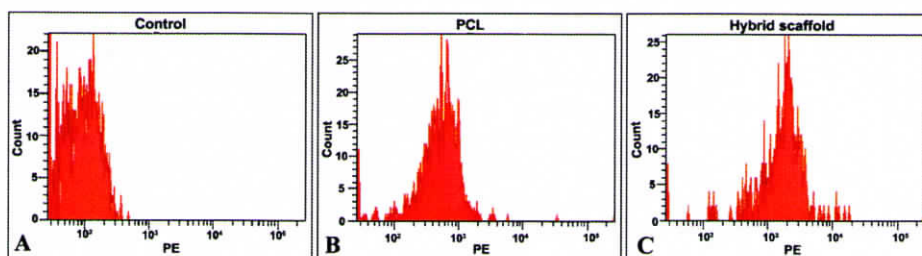


Figure 5.3. PCNA analysis. Data showing the shift in the fluorescence in PCL(B) and Hybrid scaffold (C) compared to the control.

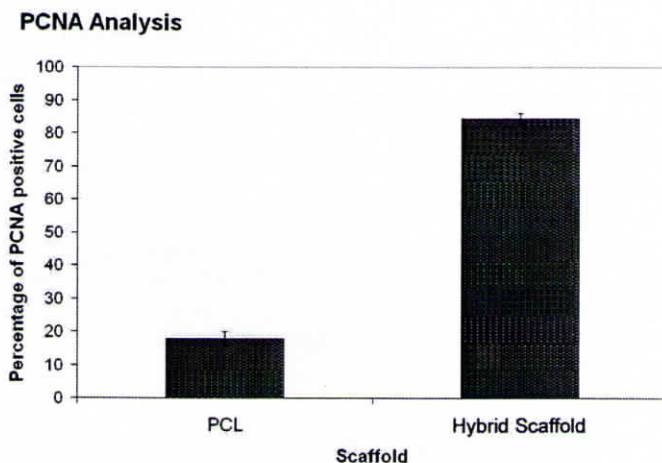


Figure 5.4. Data on quantification of PCNA. PCNA-PE was excited using a blue laser (488 m) and the emitted signal at specific wavelength was captured using the filter BP 576(26). In both cases four replicate scaffolds were used.

Data from both PCNA analysis and ^3H -thymidine uptake assay are analogous to each other. These experiments tend to show that the proliferation

rate is unacceptably poor on bare polymer. EC proliferation on hybrid scaffolds does not seem to be affected adversely by leachants or polymer degradation products. The composite matrix coated onto the scaffold and its components, especially growth factors and glycosaminoglycans seems to have supported steady proliferation of cells on the hybrid scaffold.

5.3. Cell viability

The quantitative data on cell viability demonstrate that nearly 85% of ECs on the hybrid scaffold were viable and that <30% on bare PCL was viable (Table 5.1). A high percentage of apoptotic and necrotic cells was indicated on the PCL scaffold, whereas only 13% on the hybrid scaffolds were apoptotic and no necrotic cells were found. This observation is also promising for the use of the hybrid scaffold for long-term culture of ECs to fabricate tissue-engineered cardiovascular constructs.

Scaffold type	Viability status		
	(% of EC at 72 h)		
	Living	Apoptotic	Dead
Bare PCL	30.7 ± 2.1	68.75 ± 2.1	0.53 ± 0.1
Hybrid	86.6 ± 2.9	13.4 ± 2.9	0.0 ± 0.0

Table 5.1. Viability of ECs: The table demonstrates the viability of cells on the PCL and hybrid scaffolds at 72 h of EC culture. Annexin V and propidium iodide staining of cells were done after harvesting them from the scaffold using trypsin, and stained cells were analysed using flow cytometry. Annexin V and propidium iodide were excited using the blue laser and the emission wavelength was captured using BP 530(20) and BP 610(20) filters, respectively. The percentage of each cell population was calculated using BDFACS Diva software.

From the results presented above, it may be concluded that EC proliferation was minimal on the PCL scaffold. For synthetic surfaces the major disadvantage is the lack of cell recognition sites (Kim and Mooney, 1998). The increase in cell adhesion, proliferation and survival are thus attributed to the presence of cell adhesion molecules and signaling molecules on the hybrid scaffold. The dynamic interactions between cells and the matrix, by means of

integrins allow the cells to perceive, respond and influence signals from the ECM and the flowing blood. Through signaling, integrins can control gene expression, cell shape, proliferation, differentiation and survival. The fibrin composite coating forms a very thin layer and as the fibrin network is a highly porous network, the degradation of polymer is not likely to be affected by the coating.

ECs express at least nine integrins (Dejana et al, 1993). For matrix adherence the β_1 integrins ($\alpha_1\beta_1$, $\alpha_2\beta_1$, $\alpha_3\beta_1$, $\alpha_5\beta_1$, $\alpha_6\beta_1$, $\alpha_v\beta_1$) and $\alpha_v\beta_3$ integrins (Hynes, 1987) appear to be most important. EC also express $\alpha_6\beta_4$ and $\alpha_v\beta_5$ integrins. The EC response to a fibrin surface is dependent on specific structural features of the fibrin molecule. Cell adhesion to fibrinogen is mediated through binding of the integrin receptor α & to RGD(S) sites near the carboxyl termini of the α chain that are also available in fibrin (Sporn et al, 1995). The fibrin matrix contains numerous integrin binding domains that can enhance the cell binding ability to the scaffold. ECs adhere, spread and proliferate on both fibrinogen and fibrin *in vitro* through binding to integrins $\alpha_v\beta_3$ and $\alpha_5\beta_1$ (Cheresh et al, 1989; Suehiro et al, 1997). The fibrin composite coating contains growth factors and glycosaminoglycans that activate EC proliferation. Fibroblast growth factor-2 (FGF-2) and vascular endothelial cell growth factor (VEGF) bind specifically and saturably to fibrinogen and fibrin with high affinity (Sahni et al, 2000; Sahni & Francis, 2000). It has been shown that VEGF165 stimulates $\alpha_1\beta_1$, $\alpha_2\beta_1$, and $\alpha_v\beta_3$ integrins, that bFGF increases expression of $\alpha_v\beta_3$ integrins in microvascular ECs, and that VEGF enhances migration through $\alpha_v\beta_3$ as well as activating $\alpha_v\beta_5$, $\alpha_5\beta_2$, and $\alpha_2\beta_1$ integrins. (Rupp & Little, 2001). For adherent cells, anchorage to the matrix is a necessary condition for survival. When ECs are completely denied adhesion to the substrate they lose viability within 10 hours (Re et al, 1994).

As cell adhesion, spreading, proliferation and viability in short term EC culture were insignificant on the PCL scaffold and optimal cell growth was observed on hybrid scaffold, long-term culture of ECs was carried out only on the hybrid scaffold. The objective of long-term culture on hybrid scaffold was to establish that tissue generation takes place with deposition of elastin and collagen IV to form remodeled basal laminae-like structure below the EC monolayer, and to prove that the EC maintain a non-thrombogenic phenotype on the hybrid scaffold.

5.4. Analysis of ECM remodeling

In this study, one of the major objectives was to demonstrate the ability of EC to synthesize and deposit insoluble ECM components such as collagen and elastin. Since fibrin is bioresorbable and might result in the non-availability of the other matrix components upon degradation, it is important to prove that the ECs are able to deposit the ECM at an early stage of *in vitro* cell culture. In addition, the rate of polymer degradation must be subsequently balanced by the rate of ECM production for a vascular graft to be successful.

5.4.1. Elastin Deposition

Immunostaining and confocal microscopy analysis of recovered matrix on the scaffold after 15 days of cell culture demonstrated the deposition of elastin by ECs. The z-sectioning revealed that elastin filaments are deposited throughout the scaffold; they lie in different planes (Fig. 5.5) and more prominently inside the pores. It was observed that, while the z-section at 75 μm was devoid of elastin, 105 μm sections of the same x-y plane showed the presence of elastin. No drastic difference in the elastin intensity or distribution was observed when matrices recovered after 15 days (not shown) and 30 days of culture (Fig. 5. 5) are compared.

The extra cellular matrix (ECM) protein elastin plays an essential role in the cardiovascular system by imparting elasticity to blood vessel walls. The formation of elastic fibers requires the assembly and crosslinking of tropoelastin monomers, and organization of the resulting insoluble elastin matrix into functional fibers. The assembly of elastic fibers is critical for both the structural development and the ultimate function of a number of vital tissues, including the aorta. Unlike many components of the extra cellular matrix, elastic fibers are formed only in developing tissues, with little or no synthesis in adults (Davis EC, 1993). It is reported that ECs synthesize only one-third as much elastin as fibroblasts and smooth muscle cells in cultures on polystyrene (Mecham *et al.*, 2005). These authors demonstrated that 80% of the elastin synthesized by ECs in confluent culture is released into the culture medium and ECM recovered after solubilization of cellular material with Triton X-100 stained positive for fibronectin,

but not for elastin. Their data suggest that elastin deposition is not often achieved in *in vitro* EC cultures.

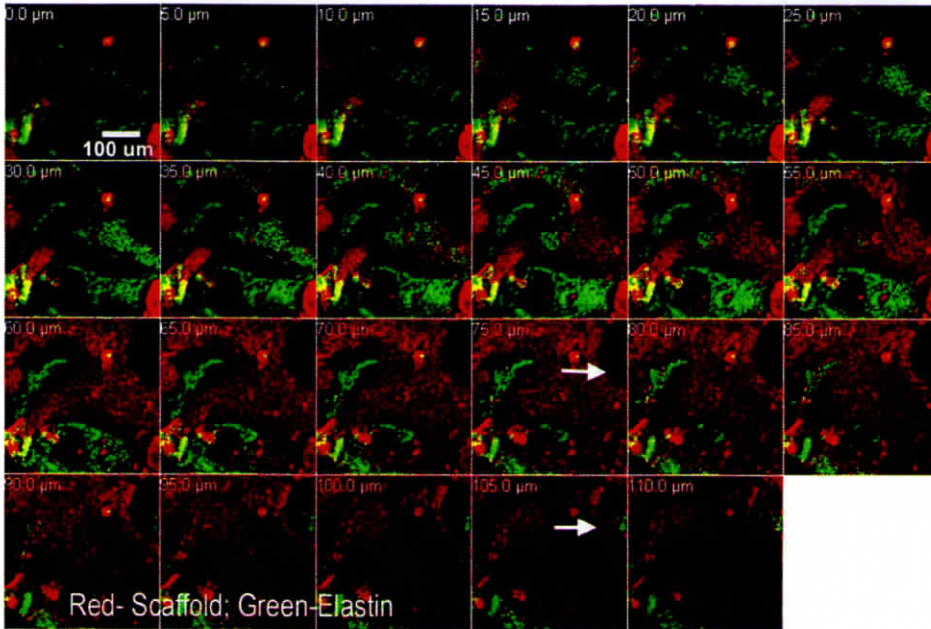


Figure 5.5. Elastin-stained scaffold recovered after EC culture. Confocal images show elastin deposition on the scaffold in the same x - y plane with varying z axis planes. The scaffold shown with ECM deposition was recovered after 30 days of EC culture. The FITC conjugated to elastin was excited using an argom laser at 488 nm and the emitted signal at specific wavelength was captured using a BP 505–530 nm filter. The polymer was excited using a He/Ne Laser at 594 nm and the emission wavelength was captured using a LP 610 nm filter and was false-coloured red, whereas elastin is green

To ensure appropriate mechanical function of the vessel and to prevent vessel stenosis, successful tissue-engineered vascular replacements must incorporate an elastic component and as such, represents a critical design goal. During the primary phase of implantation the lack of mature elastic components will be compensated by the elasticity of the scaffold. However, after degradation of the scaffold material, the elastic fibres must be newly formed to withstand the aortic blood pressures. Therefore, the hybrid scaffold should provide the right chemistry for the cells to secrete elastin.

The major challenge in promoting *in vitro* elastogenesis utilizing three-dimensional scaffolds is that the signals controlling the expression of elastin mRNA are not mimicked during *in vitro* vascular tissue engineering. Stock et al.

(2001) attempted to promote elastogenesis on polyglycolic acid and polyhydroxyalkanoate composite scaffolds coated with laminin to enhance initial cell attachment and were cultured over a period of 4 days. No elastin was detected in the tissue engineered blood vessel matured exclusively *in vitro* while 4% elastin was found in the engineered vascular tissue implanted in lambs.

Opitz et al. (2004) demonstrated that poly 4-hydroxybutyrate scaffolds seeded with smooth muscle cells and lined with ECs and externally wrapped with ovine small intestinal submucosa, after culture in a pulsatile flow bioreactor for 24 days and implantation in descending aortas sheep for 24 weeks, indicated the presence of elastin after retrieval but the level of elastin cross-linking was low. Biosynthesis and subsequent cross-linking of elastin appears to be one of the most complex and tightly regulated processes during the maturation of blood vessels (Bunda et al, 2005).

Despite high burst strength and excellent vasoactivity of tissue engineered blood vessels created by cell-self assembly approach (L'Heureux et al., 1998) where the vessels were exclusively made of cultured human vascular cells, the lack of viscoelastic response under physiological condition due to the compliance mismatch occluded the vessel in just 7days of implantation. Inadequate elastin biosynthesis into the medial layer is likely the main reason for compliance mismatch.

In the *in vitro* tissue-engineering process that was adopted here, the hybrid scaffold facilitates the production of elastin fibres by the ECs within 15d of *in vitro* culture by providing specific signals to the cells that might enhance the mechanical strength of the scaffold and may provide viscoelastic response that prevents the graft from failure upon implantation. This effect may be attributed to the presence of various biomimetic signalling molecules within the composite matrix.

5.4.2. Collagen IV Deposition

Analysis of immuno-stained (collagen IV) scaffold recovered after 15 days (not shown) and 30 days (Fig. 5.6) of cell culture demonstrated a network of

collagen IV distributed throughout the scaffold surface. The collagen network was visualized at different planes by z-sectioning, using confocal microscopy. Collagen was found in the pores of the scaffold and the distribution was similar in the 15- and 30-day samples.

The collagens constitute the largest percentage of the matrix structure in all ECMs. To resist the high blood pressures and flows in vivo, a blood vessel must have the ability to resist dilatation and rupture. The required mechanical integrity is provided in large part by the collagen content within the blood vessel wall (Cox, 1978). Collagen fibres possess a high tensile strength and are responsible for the ultimate tensile strength of the blood vessel (Barra et al, 1993). Hence, the increase in collagen content is beneficial to the development of completely functional artery. Collagen fibres that are sufficiently cross-linked are less susceptible to digestion by proteases. Collagen fibres in the healthy artery are cross-linked to each other via lysine groups on the pro-collagen chains and the cross-linking is catalyzed by the enzyme lysyl oxidase. The collagen content of the engineered vessels is a result of ECM deposition as well as remodeling (Solan et al, 2003).

Type IV collagen is a network-forming collagen type (Prockop and Kivirikko, 1995), and is the most abundant building blocks of the basement membrane. Type IV collagen is composed of three α chains, which in turn form a triple helical structure. This triple helical molecule forms the building block (monomer) of the collagen network. EC basement membranes are thought to contain predominantly the collagen type IV isoform $[\alpha_1]_2\beta_1$ (Kalluri R., 2003) and its deletion results in embryonic lethality when defects arise in cells in contact with basement membranes that are placed under mechanical stress such as in the heart and in blood vessels (Poschl E et al, 2004). Madri et al (1986) compared growth of human microvascular ECs on the two basement membrane components, laminin and type IV collagen and indicated that growth of these cells on laminin can be modulated by the presence of collagen IV. Although fibrin is not an ECM protein that is normally found in the blood vessel wall, it has the potential to augment the biochemical and mechanical properties of scaffolds for vascular tissue engineering by facilitating ECM deposition.

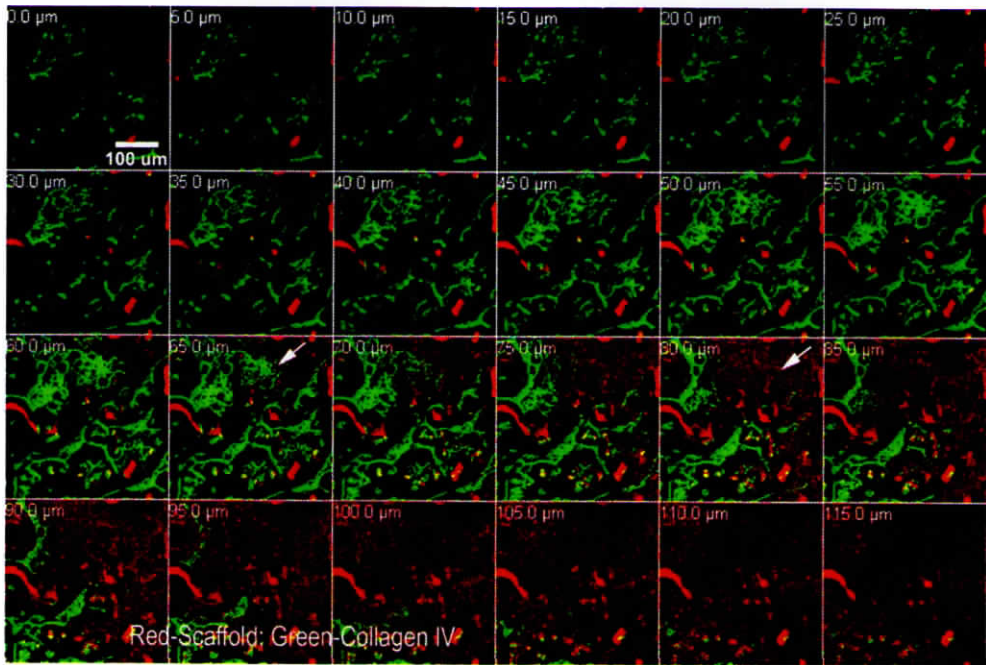


Figure 5.6. Collagen IV-stained scaffold recovered after EC culture. Confocal images show collagen deposition on the scaffold in the same x - y plane with varying z axis planes. The scaffold shown with ECM deposition was recovered after 30 days of EC culture. The FITC conjugated to collagen was excited using an argon laser at 488 nm and the emission wavelength was captured using a BP 505–530 nm filter. The polymer was excited using a He/Ne Laser at 594 nm and the emitted signal at specific wavelength was captured using a LP 610 nm filter and was false-coloured red, whereas collagen is green

The presence of elastin and collagen may be crucial for the stability of remodeled vascular tissue and therefore the deposition of both these molecules was studied. It has largely been assumed that ECs are primarily responsible for the synthesis and deposition of these ECM components, however, little is known about basement membrane assembly regulation by ECs. (Davis et al, 1996) reported that ECM synthesis was not seen when EC was cultured *in vitro* in collagen gels but in this study we have seen effective cell proliferation and synthesis of both elastin and collagen by EC when they are grown on the matrix composition that was coated on the PCL scaffold. Collagen is seen as network which is typical of collagen IV.

The process of *in vitro* tissue engineering is somewhat similar to *in vivo* angiogenesis. For all aspects of vascular biology, the ECM is critical and during angiogenesis it serves essential functions in supporting key signaling events

involved in regulating EC migration, invasion, proliferation and survival (Davis *et al.*, 2005). Provisional ECM provides mechanical guidance forces for distal ECs for organization in the absence of cell–cell contact. In this study, the provisional ECM plays a significant role in organizing the cell alignment. Although the scaffold is irregular, with pores of various sizes, complete coverage by ECs is attained due to the presence of biomimetic provisional matrix coated onto the PCL scaffold. Specific integrin-dependent signal transduction pathways are elicited from the ECM for vascular morphogenesis and in the organization of functional luminal EC layer. Although the composition of ECM plays a major role in neovessel stability and maturation, a variety of ECM components provide sufficient support for EC migration, although without equal potency (Senger and Perruzzi, 1996). ECM components exhibit maximal activity in combination with each other (Perruzzi *et al.*, 2003). A combination of biomimetic ECM molecules which include adhesive proteins such as fibrin, fibronectin and gelatin, angiogenic growth factors from bovine hypothalamus, pituitary and human platelets, and proteoglycans such as hyaluronic acid and heparan sulphate was used in this study. The composite thus formed seems to have enhanced EC adhesion, proliferation, viability and long-term survival and ECM remodeling compared to bare PCL.

5.5. ECM remodeling

The results from quantitative RT-PCR indicated up-regulation of mRNA for both elastin, and collagen IV in 144h after cell seeding as compared to that of 24h culture. The fold increase in mRNA expression is significantly high in FC TCPS and FC PCL when compared to that of FN TCPS (Fig 5.7). There is a marked increase in expression of elastin on FC PCL and FC TCPS as compared to FN TCPS (~ 4 fold). Collagen IV expression also showed a marked increase (~ 3 fold) on FC TCPS and FC PCL as compared to FN TCPS. Expression of mRNA for Collagen I was similar in all the matrices with no significant up/down regulation, but the cycling time was high when the product was in detectable range.

The ability of ECs and their supporting cellular elements to directly modify (ie, remodel) their immediate ECM environment by the deposition of elastin and

collagen on fibrin composite coated TCPS is described in chapter III of this report. Here it is demonstrated that the mRNA of elastin and collagen IV is up regulated when EC is grown on the hybrid scaffold.

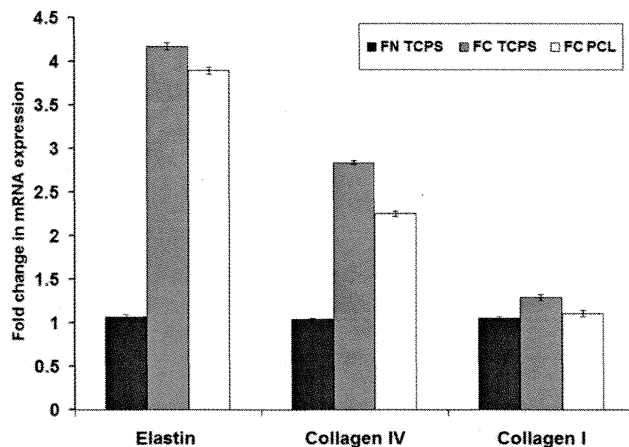


Figure 5.7. ECM Remodeling: Data shows the increase in mRNA expression levels of Elastin, Collagen IV and Collagen I at 144 h when compared to 24 h, on the different matrices.

Abnormal extra cellular matrix accumulation is an important component in the pathophysiology of lesions involving intimal hyperplasia. The increased amount of type I collagen-producing cells has been established in all types of human atherosclerotic lesions (Andreeva *et al.* 1997). In animal models, the collagen content in atherosclerotic lesions has been shown to increase consistently over time (Kratky *et al.* 1999). The collagen plaque is mainly produced by smooth muscle cells (SMCs), but ECs are also able to synthesize collagen (Canfield *et al.* 1992). Furthermore, cells different from typical SMCs are known to produce type I collagen in human atherosclerotic lesions (Rekhter *et al.* 1996). Collagen I expression is not affected by the hybrid scaffold during *in vitro* culture. Since collagen I is expressed more prominently by the smooth muscle cells, the results also shows that the ECs are maintaining the normal phenotypic characteristics and is not trans- differentiated to other cell types and thus the matrix resists excessive production of undesirable collagen.

5.6. Characterization of EC phenotype

The EC mRNA expression of prothrombotic factors vWF and PAI-1 were down regulated at 144h when compared to that of 24h, whereas there was significant upregulation of antithrombotic factors, eNOS and tPA expression at 144h, in all the matrices. The upregulation of eNOS and tPA mRNA expression in FC TCPS and FC PCL was significant when compared to fibronectin coated plates. There was no significant difference between FC TCPS and FC PCL in the up/down regulation of the genes (Fig 5.8).

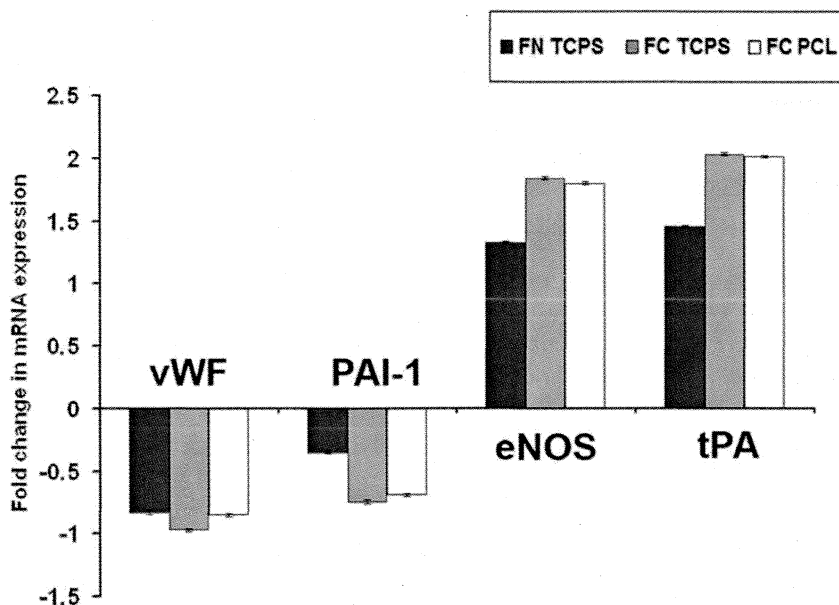


Figure 5.8. EC phenotype: Data shows a comparison of fold change in gene expression on the defined matrices at 144h when compared to 24h. The fold change when compared to the cells grown on 24h matrix is denoted, the relative fold change was calculated using the equation, $A_0/B_0 = (1+E)^{(Ct,B-Ct,A)}$. A_0 = initial copy number of sample A; B_0 : initial copy number of sample B; E = efficiency of amplification; Ct, A = threshold cycle of sample A (24h sample); Ct, B = threshold cycle of sample B. (144h sample)

The EC maintain antithrombotic phenotype on FC PCL, FC TCPS and FN TCPS with mild down regulation of vWF and PAI-1. The down regulation was considerably higher on FC TCPS and FC PCL.

Maintenance of normal cell function in tissue-engineered constructs is a key element in successful tissue substitution. In this study, there was an ultimate need to create a scaffold surface lining with functional endothelium that will

provide an anticoagulant and antithrombogenic surface to the circulating blood constituents. It is the relative amounts of many different molecules that determine the thrombogenic state of ECs in a scaffold. Therefore we evaluated two prothrombotic molecules vWF and PAI-1, and two antithrombotic molecules, eNOS and tPA to assess the thrombogenic potential of the ECs cultured over the various matrices.

The prothrombotic molecule, von Willebrand factor (vWF), is an adhesive glycoprotein synthesized exclusively in ECs and megakaryocytes. The molecule is present in both circulating blood plasma and platelets, as well as in ECs and the subendothelial matrix of the vessel wall (Ruggeri, 2007). Endothelial vWF is stored in rod-shaped organelles called Weibel–Palade bodies and affects platelet adhesion and aggregation, blood coagulation, and fibrinolysis. It serves as the carrier for procoagulant factor VIII in circulating blood, where the two molecules are present as the factor VIII/vWF complex (Ruggeri and Ware, 1993). Through multiple functional domains, von Willebrand factor mediates the attachment of platelets to exposed tissues, where discontinuity of the vascular endothelium occurs, and the subsequent platelet aggregation leading to the formation of platelet thrombi.

Jansson et al (1991) demonstrated that a high concentration of von Willebrand factor was an indicator of increased risk for re-infarction and mortality in survivors of myocardial infarction. Increased concentrations of von Willebrand factor have also been associated with clinical severity of angina (Heper & Bayraktaroğlu, 2003), deep venous thrombosis, (Wahlberg et al, 1980) and ischemic cerebro-vascular disease (Mettinger, 1982). Moreover, high concentrations of vWF seem to be correlated with high concentrations of atherogenic growth factors (Nilsson et al, 1989).

Plasminogen activator inhibitor-1 (PAI-1), another prothrombotic molecule is the major physiologic inhibitor of tissue plasminogen activator (tPA) and urokinase plasminogen activator and hence is an inhibitor of fibrinolysis, the physiological process that degrades blood clots. PAI-1 is a serine protease inhibitor (serpin) protein (SERPINE1). Schneiderman et al., (1992) revealed significantly increased levels of PAI-1 mRNA in severely atherosclerotic vessels

compared with normal or mildly affected arteries. Tipping et al. (1993) demonstrated the upregulation of PAI-1 production by macrophages in atheromatous plaques and the capacity of soluble products from plaque macrophages to upregulate PAI-1 production by ECs and vascular smooth muscle cells *in vitro*.

Since the cell phenotype is controlled by the ECM molecules, use of an inappropriate scaffold or matrix can result in upregulation of prothrombotic factors by EC. Storck et al (1996) reported that more plasminogen activator inhibitor 1 (PAI-1) was released from cells grown on PVC than from those on the plates coated with gelatin and collagen. Furthermore, Zhang et al (1995) showed that human umbilical vein ECs grown on polytetrafluoroethylene or polyurethane released more PAI-1 into the conditioned media than did human umbilical vein ECs grown on tissue culture polystyrene. Hence, type of plastic and matrix used to culture HUVEC play a definite role in their growth and function.

Tissue plasminogen activator (t-PA) is a serine protease, which converts plasminogen to plasmin to degrade fibrin clot. ECs in culture synthesize and constitutively secrete t-PA. The rate of synthesis is increased by a number of substances, including thrombin and histamine (Hans and Collen, 1987) and is reduced by plasmin (Shi et al, 1992). However, although protein kinase C appears to play a role, (Levin and Santell, 1988) the mechanisms regulating t-PA synthesis have not been characterized in detail. Gillis et al., (1996) reported that tPA secretion was lower by cells seeded on both collagen type-I and serum precoated ePTFE was lower as compared to collagen type-1 gel. Hence the cellular function on scaffolds can differ depending upon the polymer scaffold and matrix chosen.

Nitric oxide, widely expressed in virtually all vascular cell types, is mostly produced by the endothelial isoform (eNOS) from the precursor L-arginine in ECs where it plays a crucial role in vascular tone and structure regulation. It also exerts an anti-inflammatory influence, inhibits platelet adhesion and aggregation, and prevents smooth muscle cell proliferation and migration (Desjardins and Balligand, 2006). Transfection of eNOS to vessel wall after balloon injury has been reported to cause a 70% reduction of intimal hyperplasia 14 days after

injury (von der Leyen et al, 1995). Bellamkonda et al (1997) reported that seeding of eNOS-transfected ECs onto vascular grafts, increase NO production by the surviving cells.

EC behaviour *in vivo* is controlled by chemical and mechanical cues generated by ECM, peripheral cells, growth factors and other signaling molecules. In the present study it is found that the expression of vWF and PAI-1 is downregulated and that of tPA and eNOS was upregulated indicating the quiescent EC function when cultured over the hybrid scaffold as well as the fibronectin and fibrin composite coated TCPS dishes. Scaffold precoating with extracellular matrix proteins can allow more precise "engineering" of cellular behavior during tissue engineering to alter extra cellular matrix production and cell phenotype (Sales et al, 2007). On a biomaterial or scaffold surface, the number and type of cell binding sites on the material surface created using ECM coatings initially mediate the chemical and mechanical cues which determine EC thrombogenicity. The fibrin composite mimicking the provisional ECM matrix is able to provide appropriate signals to regulating the EC thrombogenicity.

5.7. Nitric oxide (NO) release

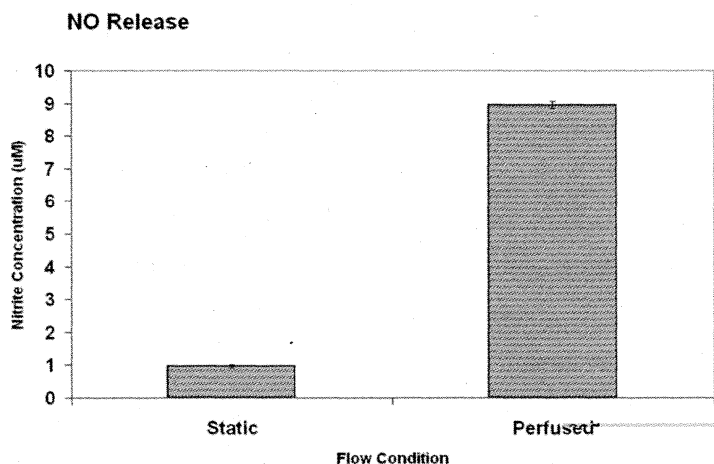


Figure 5.9. Analysis of nitric oxide by nitrite assay: For static conditions, cell seeded hybrid scaffold was incubated with 1ml serum-free medium and total nitrite in 1ml medium was estimated. For dynamic exposure, the scaffolds were perfused with 8ml and total nitrite in 8ml was calculated. Data of two groups were compared using ANOVA.

The release of NO by EC monolayer grown over the hybrid scaffold in static and perfused flow conditions is given in Fig.5.9. The nitrite level is significantly higher (~9 times) in perfused sample (8.95 μ M) when compared to that of static samples (0.97 μ M). The NO synthesized is expressed per cm² area of the scaffold.

Nitric oxide contributes to the resting vascular tone, impairs platelet activation, and prevents leukocyte adhesion to the endothelium (Shapira et al, 1999). These effects of nitric oxide on the vessel wall are important to protect the implanted graft against thrombosis and later atherosclerosis. The production of NO by an EC monolayer under varying physical conditions has been well documented in the literature. Uematsu et al (1995) reported that shear stress with an appropriate magnitude enhances the synthesis and secretion of various bioactive substances such as endothelial cell nitric oxide. Kuchan et al (1994) have established that an initial burst in production is followed by sustained steady-state NO production when ECs are exposed to sustained shear. In this study, ECs on the hybrid scaffold respond to shear stress in a predictable fashion and remain functional. The enhanced release of nitric oxide stimulated by shear stress explains the normal phenotype of ECs cultured over the scaffold.

5.8. Response to shear stress

Micrographs of the cell seeded scaffold in static condition and after subjecting to a shear stress of ~19.6 dynes/cm² for 1h are shown in Fig 5.10. In static condition during culture, the entire surface of the scaffold was covered with HUVEC with a cobble stone morphology. After exposure to flow, majority of the cells remain attached to the hybrid scaffold. Cells could be visualized all over the scaffold showing minimum cellular detachment or dislodging. There is a marked difference in the morphology of the EC before and after subjecting to shear. ECs showed tendency to align parallel to the direction of flow after shear as compared to that of EC before exposure. These results indicate that the scaffold supports improved cell adhesion and remodeling that prevents loss of cells from the scaffold fabricated on exposure to shear stress. ECs grown on the hybrid scaffold can adjust according to the direction of the mechanical force provided the cell attachment is optimum and the period of exposure to shear force is long enough.

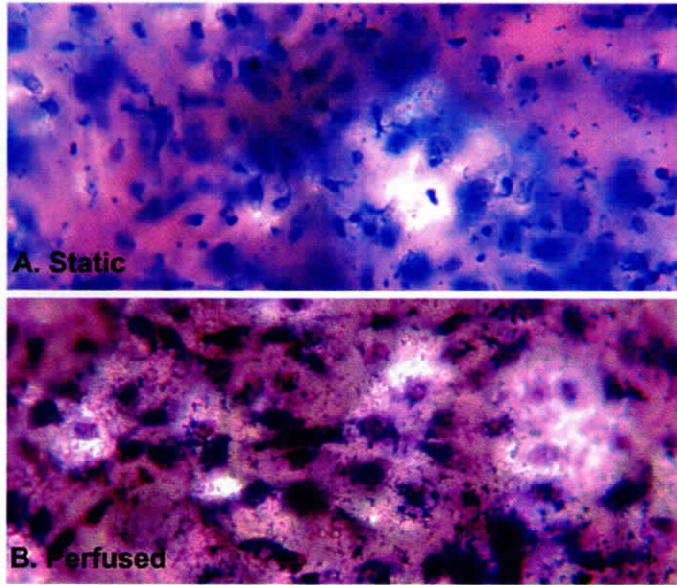


Figure 5.10. Effect of shear stress on EC seeded FC PCL

Light micrographs of EC seeded on hybrid scaffold (A) Static (B) after perfusion. The cell seeded on to the scaffold were allowed to grow for 120h and then placed in flow chamber. After 1h perfusion the scaffolds were fixed in 0.1% gluteraldehyde and were stained with May Grundwald-Geimsa.

ECs covering the inner surface of blood vessels are continuously exposed to hemodynamically imposed mechanostress *in vivo*, and they are able to sense and respond to mechanical forces such as shear stress generated by blood flow, which regulates EC structure and functions (Ali et al, 2002; Lehoux et al, 2003). The shear stress in arteries has been reported to be approximately 10 - 25 dynes cm^{-2} : 10-16 dynes cm^{-2} for large diameter arteries (diameter; 0.3cm) and 18 - 26 dynes cm^{-2} for small diameter arteries (0.1-0.06cm) where as those in veins are approximately 1.5 - 3 dynes cm^{-2} (Kamiya *et al.*, 1984). Shear stress caused by blood flow *in vivo* orient EC growth along the direction of the blood flow, which may increase the ability of ECs to resist the forces of flow and decrease desquamation of these cells from vascular grafts. Dewey et al (1981) demonstrated that when exposed to a laminar shear stress of 5-10 dynes/ cm^2 , confluent monolayer undergo a time-dependent change in cell shape from polygonal to ellipsoidal and become uniformly oriented with flow. Remodeling of actin is an important mechanism for the cell to distribute the stress it experiences by minimizing the load and/or by optimizing its structure to resist the surface mechanical load. Thus, it is important to mimic the orientation of ECs *in vitro* on

vascular grafts. In this study, the cells adhered nicely to the fibrin coated PCL scaffold, and the confluent layer resisted the shear stress with minimal cell detachment and the scaffold did not alter the endothelium's ability to realign according to flow.

5.9. Platelet Adhesion

5.9.1. Qualitative analysis

Scanning electron micrographs revealed that there is considerable amount of platelet adhesion on PCL and FC PCL (Fig. 5.11). It is interesting to note that on PCL the adhesion was confined to the crevices and sharp edges of the scaffold that were artifacts of scaffold preparation (Fig 5.11A). There was limited adhesion of platelets to the surface regions of the PCL scaffold (Fig 5.11B). But in FC PCL the platelets adhered throughout the surface of the scaffold (Fig 5.11C). The presence of fibrin has lead to the activation and adhesion of platelets over the FC PCL surface (Fig 5.11D). On EC FC PCL, there is limited platelet adhesion suggesting the presence of a non-thrombogenic endothelium over the scaffold surface (Fig 5.11E). Few platelets appeared to be present on the edges of the scaffold rather than over the surface of the endothelium (Fig 5.11F). The results of SEM analysis were further confirmed by the quantitative difference in platelet adhesion, estimated by radiosciintigraphy.

5.9.2. Quantitative analysis by Radiosciintigraphy

Quantification of platelet adhesion was done by exposing the scaffolds to radiolabeled platelets. Calibration graph plotted using known number of platelets is shown in Fig 5. 12. The significant difference in platelet adhesion between the bare versus modified scaffolds could be visualized from the intensity of radioimages of the samples. All six replicates of FC PCL showed a higher degree of radiointensity when compared to the PCL and EC FC PCL. In PCL the intensity was lesser when compared to FC PCL. In EC FC PCL the platelet adhesion was minimal and the images were difficult to visualize. Quantitative data of platelet adhesion on the different scaffolds are given in Fig 5.13. The number of platelets adhered is significantly high ($p < 0.01$) on FC PCL when compared to that of PCL and EC FC PCL (Fig 5.13). The platelet adhesion on EC FC PCL was significantly low when compared to other scaffolds

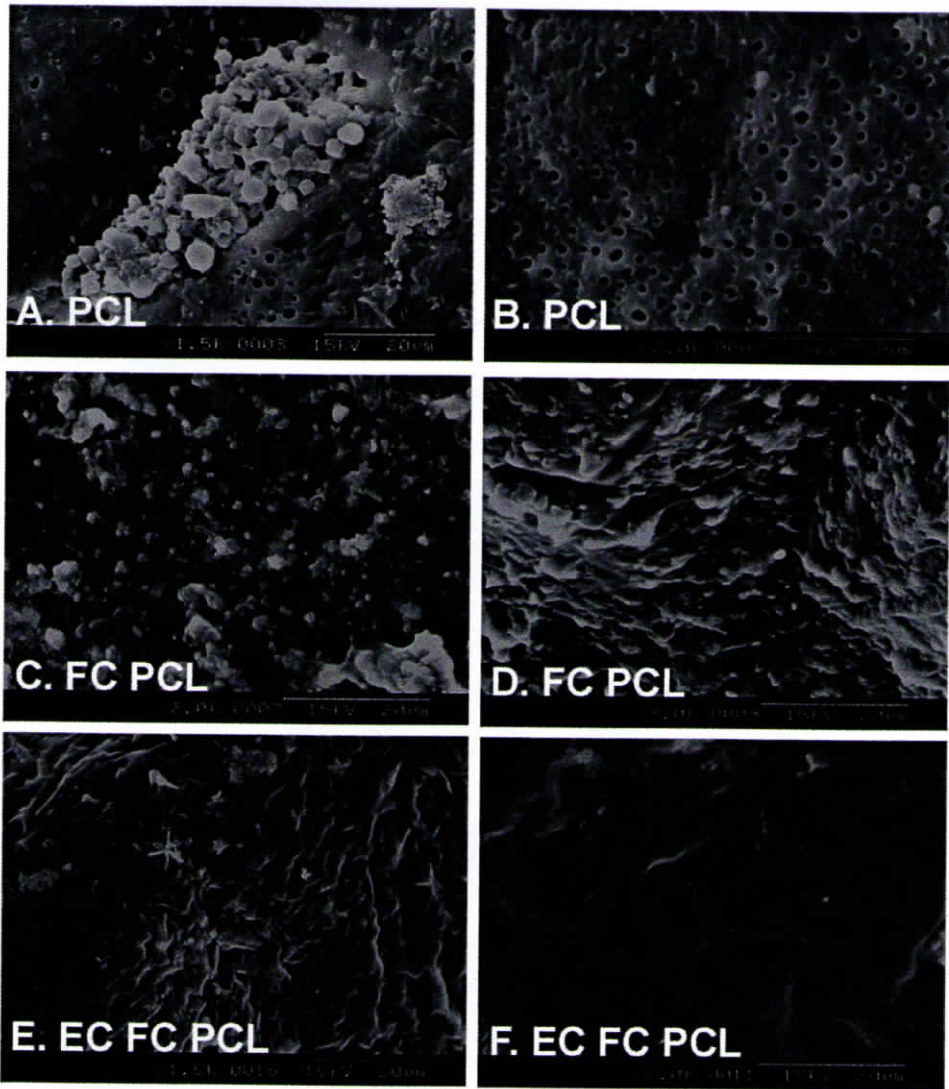


Figure 5.11. Scanning electron micrographs depicting PCL scaffold [A &B], FC-PCL scaffold [C&D], EC seeded FC PCL scaffold [E&F] after 30 min PRP exposure. Magnifications are printed at the bottom of each micrograph

Platelet adhesion and activation is an index of the antithrombotic status of the EC layer on the scaffold surface. A healthy endothelium inhibits platelet adhesion to the vascular surface and maintains a balance of prothrombotic, antithrombotic and fibrinolytic activity. Usually, platelets respond to minimal stimulation and become activated when they contact any thrombogenic surface

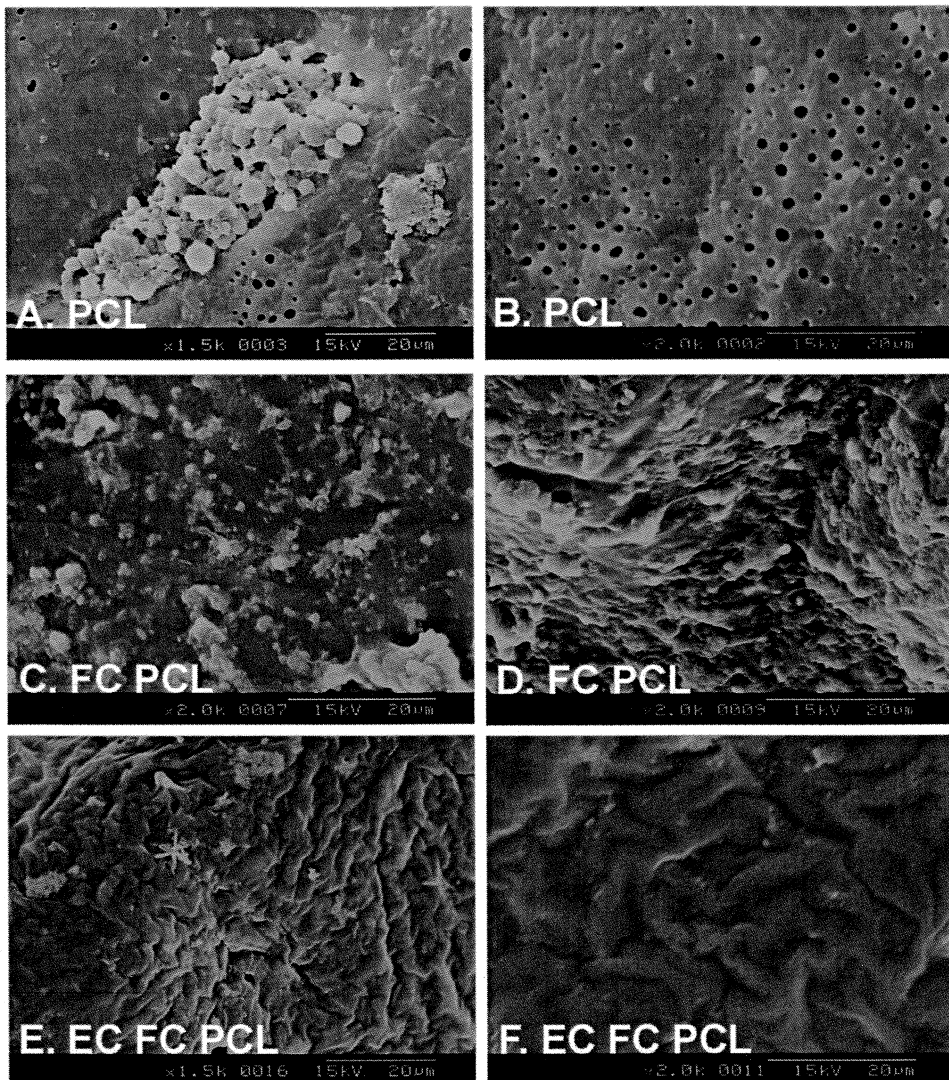


Figure 5.11. Scanning electron micrographs depicting PCL scaffold [A &B], FC-PCL scaffold [C&D], EC seeded FC PCL scaffold [E&F] after 30 min PRP exposure. Magnifications are printed at the bottom of each micrograph

Platelet adhesion and activation is an index of the antithrombotic status of the EC layer on the scaffold surface. A healthy endothelium inhibits platelet adhesion to the vascular surface and maintains a balance of prothrombotic, antithrombotic and fibrinolytic activity. Usually, platelets respond to minimal stimulation and become activated when they contact any thrombogenic surface

such as dysfunctional or injured endothelium, subendothelium and artificial surfaces.

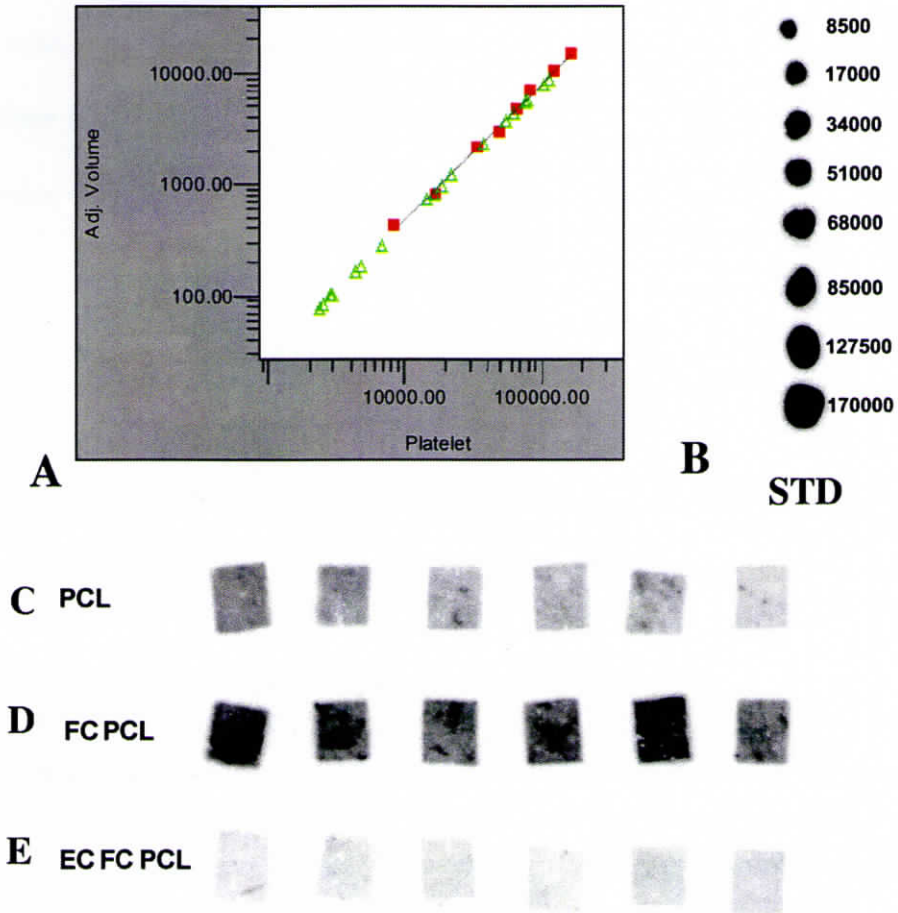


Figure 5.12. Radioscintigraphy data showing platelet adhesion on various PCL surfaces: (A) Calibration graph plotted using a serial dilution of known number of radiolabeled platelets. The graph showed a correlation coefficient of 0.995; (B) Images of serially diluted platelets used as standard for plotting the calibration graph; (C) Radioimages of six replicates of PCL,(D) fibrin coated PCL (FCPCL) and (E)endothelial cell seeded fibrin coated PCL (ECFCPCL) after radiolabeled platelet exposure.

Following contact with a layer of adsorbed proteins on the artificial surface, platelets will either adhere or bounce off (Godo & Sefton, 1999), most likely depending upon their state of activation and the ligands present at the interface (Sheppard et al,1994). Platelet adhesion to the surface is mediated by

such as dysfunctional or injured endothelium, subendothelium and artificial surfaces.

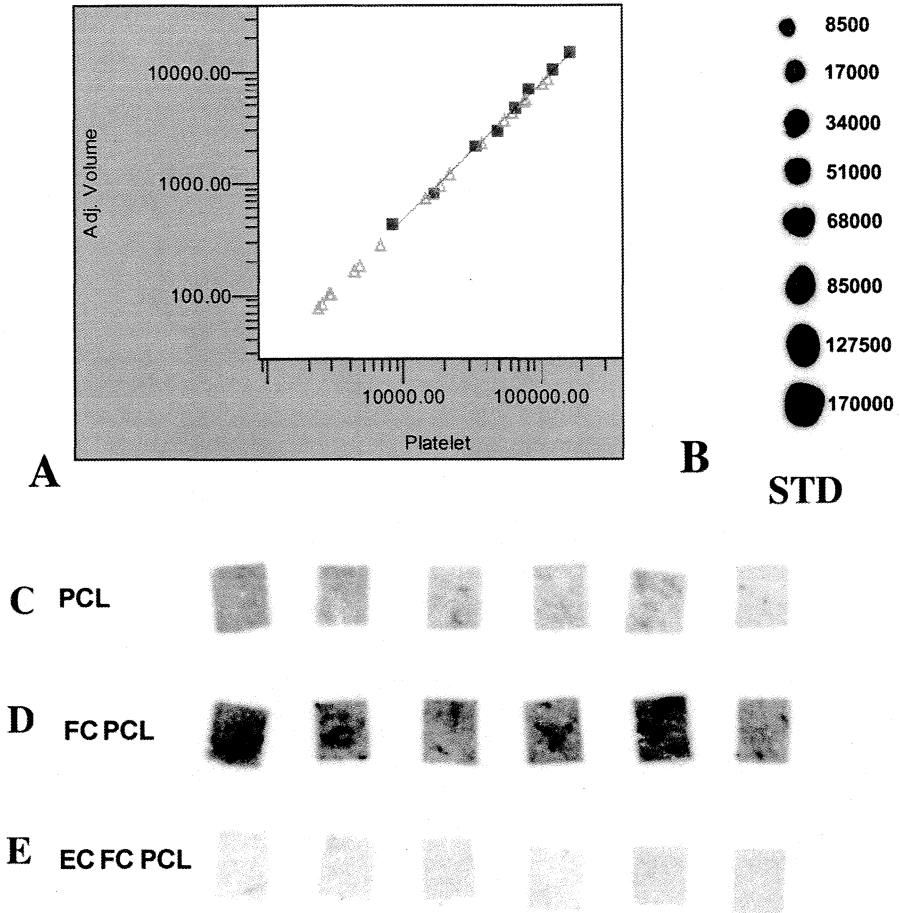


Figure 5.12. Radioscintigraphy data showing platelet adhesion on various PCL surfaces: (A) Calibration graph plotted using a serial dilution of known number of radiolabeled platelets. The graph showed a correlation coefficient of 0.995; (B) Images of serially diluted platelets used as standard for plotting the calibration graph; (C) Radioimages of six replicates of PCL, (D) fibrin coated PCL (FCPCL) and (E) endothelial cell seeded fibrin coated PCL (ECFCPCL) after radiolabeled platelet exposure.

Following contact with a layer of adsorbed proteins on the artificial surface, platelets will either adhere or bounce off (Godo & Sefton, 1999), most likely depending upon their state of activation and the ligands present at the interface (Sheppard et al, 1994). Platelet adhesion to the surface is mediated by

glycoprotein IIb/IIIa and fibrinogen and interaction between GPIb/IIa can also occur (Tsai et al, 1999; Bailly et al, 1996).

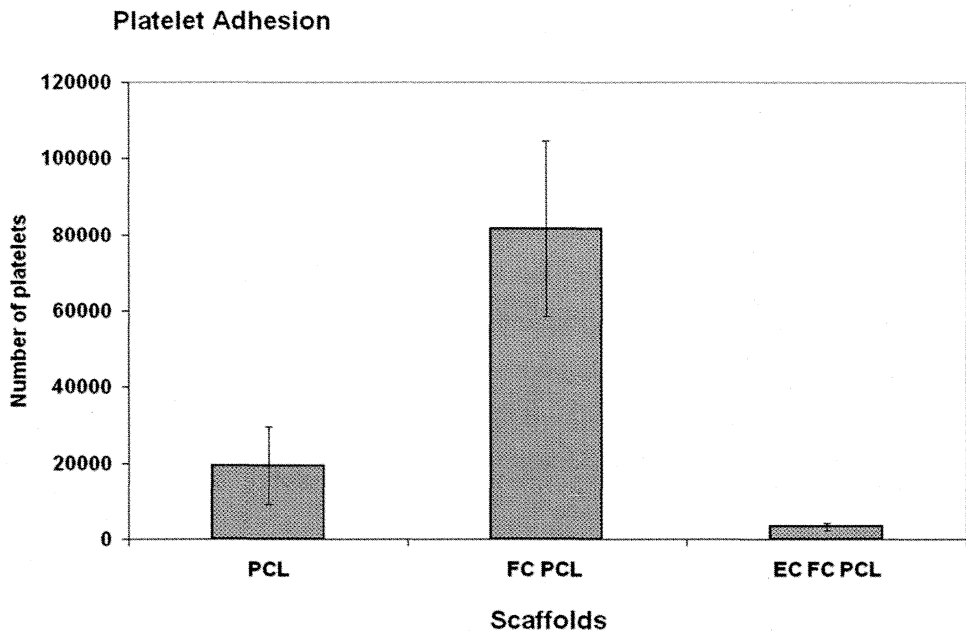


Figure 5.13. Quantitative estimation of platelet adhesion by Radioscintigraphy.

In normal conditions, synthesis of NO by EC can inhibit platelet activation. The endothelium can also counter-act platelet mediated thrombosis initiated by the release of ADP, Ecto ADPase, an enzyme on the EC surface catalyses the degradation of ADP and thereby suppresses additional platelet activation. In addition the ECs also generate prostacyclin which can directly inhibit the activity of platelets. On the prothrombotic state, endothelial vWF can directly stimulate platelet activation. Indirectly, endothelial mediated stimulation of the coagulation cascade leads to generation of thrombin, which stimulates platelets through cleavage of surface protease receptors.

Since fibrin activates platelet aggregation, the enhanced platelet adhesion on the FCPCL surface was expected. Maintenance of a functional endothelium over the hybrid scaffold seems mandatory for graft patency upon implantation. The negligible platelet adhesion observed on the EC seeded scaffold reflects the non thrombogenic nature of the EC layer. The number of platelets adhered on

ECFCPCL surface was lesser when compared to PCL alone, indicating the improved biocompatibility of endothelialized surface. Bombeli et al (1999) demonstrated that apoptotic HUVEC appear to bind nonactivated platelets as effectively as the subendothelium. However, after binding of a single layer, the recruitment of additional platelets into the evolving thrombus would likely be less effective, as compared with subendothelial matrix proteins. Hence the result also confirms the non apoptotic nature of the endothelium on the scaffold.

During this study it is demonstrated that EC monolayer grown on the hybrid scaffold does not promote platelet adhesion. In the clinical perspective it is an encouraging result because thrombotic occlusion of implanted materials and devices are known to be caused by the initial platelet adhesion and subsequent thrombotic and inflammatory responses elicited by the initial layer of adhered platelets and the chemokines released from the adhered platelets. Thus, one of the major outcomes of this study is generation of a nonthrombotic layer of EC on the hybrid scaffold.

CHAPTER 6

SUMMARY AND CONCLUSION

6.1. RESTATEMENT OF THE PROBLEM

Although routinely applied and ubiquitously used, vascular grafting is not without significant constraints and complications. Arterial conduits are in limited supply and restricted dimensions. Venous conduits are more abundant but lack vasomotor tone and are prone to thrombotic and hyperplastic occlusion and, less frequently, infection. Synthetic materials do not fare well in small-bore vascular beds and are excessively thrombotic. Graft passivation has been attempted to minimize material blood interaction by surface modification with coatings of proteins, polymer materials, or cells. Although somewhat successful in limiting thrombosis and hyperplasia, such linings do not provide vascular responsiveness or other biochemical secretory function seen with the normal blood vessel. Furthermore, passivated grafts are still subject to bacterial colonization and graft infection. As a result of these problems with native, synthetic, and modified grafts, there have been multiple attempts for creating tissue-engineered vessels composed of biological materials and autologous cells (Edelman ER, 1999).

The classic tissue engineering strategy is to isolate specific cells through a biopsy from a patient, to grow them on a three-dimensional (3D) biomimetic scaffold under precisely controlled culture conditions, to deliver the construct to

the desired site in the patient's body, and to direct new tissue formation on the scaffold that can be degraded over time (Vacanti & Langer, 1999). The scaffold simulates the extracellular matrix (ECM). The ECM is custom designed and manufactured by the resident cells of each tissue and organ and is in a state of dynamic equilibrium with its surrounding microenvironment. The structural and functional molecules of ECM provide the means by which adjacent cells communicate with each other and the external environment. ECM proteins interact directly with cell surface receptors to initiate signal transduction pathways and modulate those triggered by growth factors.

The development of a small-diameter blood vessel substitute for use in bypass surgery has been a long-time 'holy grail' for vascular tissue engineering. The TEVGs should fulfill several well defined requisites: mechanical strength to withstand arterial pressure, elasticity to provide compliance and recoil, maintenance of normal phenotype, ability to be repopulated and remodeled by host cells, devoid of thrombogenicity and should possess a confluent, shear resistant endothelium to resist forces of blood flow. More importantly, it is evident that this is 'all or nothing', i.e. unless each and every one of these requisites is fulfilled; imperfect grafts may never be suitable for clinical use.

In vascular tissue engineering, the ECM proteins deposited by the cells play a major role in determining the construct stability as well as regulation of the cell-matrix interactions. To provide stability for a vascular construct the cells should deposit ECM proteins, elastin and collagen, these proteins provide mechanical strength and vaso responsiveness to the construct (Heydarkhan-Hagvall *et al.*, 2006). It is also important to get ECM deposition at an early period of tissue construction so that construct can be developed with short culture time. Once ECM remodeling takes place cells would receive appropriate signals to support normal phenotype. Hence, an ideal matrix/scaffold for VTE should facilitate cell adhesion and proliferation as well as assist in the production of appropriate matrix proteins leading to tissue remodeling.

To achieve the aims of tissue engineering, formation of well defined biomimetic microenvironments that surround cells and promote controlled cell interactions is important. A successful TEVG cannot be achieved without the

inclusion of an inner cellular layer resembling a native endothelium. Within a blood vessel, the endothelial cell (EC) layer functions to prevent the adhesion of platelets and other blood components (e.g., macrophages) by acting not only as a physical barrier, but also through the continued release of inhibitory factors such as NO, thrombomodulin, tPA, and PGI₂. Therefore, this study was undertaken to standardize a suitable matrix that facilitated EC proliferation, survival and most importantly, remodeling of culture matrix with the deposition of elastin and collagen to form new tissue. This matrix was then coated on biodegradable polymeric scaffold film and was assessed for its potential to create an engineered vascular tissue with optimum ECM remodeling and maintenance of functional EC phenotype.

6.2. DESCRIPTION OF PROCEDURES

The initial objective of this study was to standardize a suitable matrix composition that facilitates required endothelial cell growth and survival, with subsequent deposition of ECM components for vascular tissue engineering applications. The structural and biochemical properties of the polymerized fibrin make it a promising candidate as a scaffold in tissue engineering and regenerative medicine. Fibrin plays a major role in promoting tissue remodeling during wound healing (Neidert et al, 2001). The fibrin clot contains sites for cell binding, and therefore provides a structural scaffold for the adhesion, proliferation and migration of cells important in wound healing. Fibrin degrades and gets remodeled by cell associated enzymatic activity during cell migration and wound healing (Lee and Mooney, 2001). Because of its established effects on vascular cells, fibrin is of particular interest as a scaffold in vascular tissue engineering (Grassl et al., 2002; Cummings et al., 2004; Swartz et al., 2005).

HUVECs were isolated and characterized by positive staining for vWF and Dil labeled acetylated LDL uptake. A basic fibrin matrix, that was already standardized in our laboratory, composed of fibrinogen, fibronectin, gelatin and angiogenic growth factors, was used as the biological skeleton for all the studies. The role of individual component of the basal matrix was studied by actin and vinculin staining, tritiated thymidine uptake, PCNA analysis and Annexin V staining. The basal matrix was compared to the commercially available

fibronectin coated tissue culture polystyrene in terms of cell adhesion, proliferation and survival. In order to study the effect of growth factors [angiogenic growth factors (AGF) /and Platelet growth factors (PGF)] and GAGs [heparan sulphate (HS) and hyaluronic acid (HA)], on cell adhesion, proliferation and survival each component was incorporated to the basic fibrin matrix individually and in combination and the effects were studied by tritiated thymidine uptake, PCNA analysis and Annexin V staining. For assessing the ECM remodeling, the fibrin matrix degradation on each matrix during EC culture was estimated by D Dimer assay. The deposition of ECM proteins, elastin, collagen IV and collagen I in various matrices was assessed qualitatively by immunostaining and quantitated by flourometry. The mRNA expression of ECM molecules at 24h and 144h after EC seeding on the defined matrices were analyzed by Real Time PCR. Finally, the matrix with best cell growth, survival and matrix remodeling was selected for coating on a biodegradable scaffold.

The porous PCL scaffold was prepared by solvent casting and leaching method. The morphology of the scaffold was visualized by light microscopy and micro-CT. The degradation rate of the PCL scaffold after 60 days of storage in PBS was assessed by gravimetric analysis and viscosity average molecular weight determination. The mechanical properties of the porous scaffold were evaluated by Universal testing machine. The porous PCL scaffold and the scaffold after fibrin composite coating was characterized by ATR-FTIR; porosity and pore size of the scaffolds were determined by mercury porosimetry. The EC were seeded on PCL and grown for 24h to evaluate the EC growth on bare PCL. On detecting the EC adhesion and growth on PCL is poor, biomimetic matrix composite standardized during the initial part of the study was coated on the porous PCL to obtain the hybrid scaffold. ECs were grown for a period of 15 days and the scaffolds were characterized by ESEM. The mechanical properties of the hybrid scaffolds and after 15d of EC culture was also evaluated

Extensive studies were carried out to assess the potential of the fibrin-PCL hybrid scaffold in vascular tissue engineering. The cell adhesion, proliferation and survival on bare PCL and hybrid scaffold was compared by actin staining, PCNA analysis, tritiated thymidine uptake and apoptosis assay. The

actin staining (confocal microscopy analysis) and ESEM was applied to study the long term survival of the cells on the scaffolds. After immunostaining for collagen IV and elastin, confocal microscopy was done to evaluate the requisite remodeling of the fibrin composite matrix. The normal phenotype of the cells grown on the hybrid scaffold as well as final fibrin composite and fibronectin coated plates were evaluated by checking mRNA expression of von Willebrand factor (vWF) – a prothrombotic molecule, nitric oxide (NO)- an antithrombotic and vasodilator molecule, tissue plasminogen activator (t-PA) – a fibrinolytic factor, and plasminogen activator inhibitor (PAI)- an antifibrinolytic factor. The real time PCR analysis of mRNA for ECM Collagen I, Collagen IV and Elastin was compared at different periods of EC culture to evaluate suitable ECM remodeling on the scaffold. The Nitric oxide release of EC grown hybrid scaffold was done under static and dynamic conditions to confirm the physiological status of EC. The ability of the cells on the scaffold to resist shear was studied by perfusion experiment and studied by light microscopy. The blood compatibility evaluation of the bare PCL scaffold, hybrid scaffold (FC PCL) and EC grown fibrin - PCL scaffolds (EC FC PCL) were analyzed using tests selected according to ISO 10993, Part 4. The platelet adhesion on the scaffold was studied qualitatively using scanning electron microscopy and quantitatively using radiolabeled platelets (radioscintigraphy).

6.3. MAJOR FINDINGS

The study was carried out in three phases: 1. Standardization of suitable matrix with optimal cell proliferation survival and matrix deposition in tissue culture polystyrene by culturing HUVEC. 2. Fabrication and physicochemical characterization of a porous fibrin-poly (ϵ -caprolactone) scaffold for vascular tissue engineering. 3. Evaluation of the EC behavior on the hybrid scaffold for vascular tissue engineering.

The objective of the first phase of the study was to select a fibrin matrix composition that is best suited for EC proliferation, survival and most importantly, matrix deposition on tissue culture polystyrene. The importance of each component of the basic fibrin composite (CCPS) was proved by the reduced cell adhesion, proliferation and survival in the factor deprived matrices compared to

CCPS. The CCPS also showed better EC proliferation and survival compared to commercially available fibronectin coated tissue culture polystyrene (FNPS). Hence CCPS, was chosen as the biological skeleton on which growth factors (AGFs and PGFs) and glycosaminoglycans (HA and HS) were immobilized individually and in combination to choose the best matrix. The cell adhesion, proliferation and survival was optimal on the matrix that contained both the growth factors and GAGs (CCPS+GF+GAG) compared to the other matrices. In all the matrices, the fibrin matrix degraded by 168h after EC seeding. Immunological and flourometric analysis of the matrices showed enhanced matrix remodeling, deposition of collagen IV and elastin, on the matrix CCPS+GF+GAG when compared to all the other formulations. Among the GF matrices, the matrix that contained both angiogenic and platelet growth factors showed improved cell growth and matrix remodeling whereas in GAG matrices, the matrix which contained both heparan sulphate and hyaluronic acid demonstrated the same. Real time PCR analysis showed maximum up regulation of mRNA expression of ECM proteins, elastin (4 fold) and collagen IV (3 fold), on the CCPS+GF+GAG whereas that of collagen I was negligible in all the matrices. Hence the matrix CCPS+GF+GAG was proved to be effective in optimal EC growth and survival, and deposition of ECM proteins elastin and collagen IV. Therefore, for coating on the biodegradable scaffold the above combination was selected.

The objective of phase II was to fabricate a biodegradable scaffold for vascular tissue engineering. By solvent casting technique, porous PCL scaffolds with uniform distribution of pores of 5-200 microns size were prepared using polyethylene glycol as porogen. Mechanical properties evaluated with bare porous PCL did not show significant deterioration in physico-chemical characteristics up to 60 days when stored in PBS. Slow degradation rate was evidenced by gravimetric analysis and viscosity average molecular weight determination of PCL scaffolds stored in PBS and this property is expected to be an advantage for maintenance of compliance and tensile strength of the films during the initial days of in vitro tissue engineering of implants. The porous polymer was coated with fibrin composite, because EC adhesion and proliferation was unacceptably poor on bare PCL, which acted as a suitable substrate for EC growth. The presence of the fibrin over the PCL scaffold was

confirmed by the decrease in the porosity of the scaffold after coating and also by the amide I and amide II bands on the FTIR spectra of the hybrid scaffold. Cells formed a continuous layer on the hybrid scaffold within 15 days as evidenced by ESEM and no adverse effect on cell growth was observed. In case of modified scaffolds, the mechanical properties were improved with EC growth as compared to hybrid scaffolds showing the deposition of ECM proteins, elastin and collagen. The mechanical properties and good cytocompatibility of the cell-grown scaffold proved its suitability for tissue engineering applications.

The objective of the third phase was to demonstrate the prolonged survival of EC on the hybrid scaffold, with maintenance of normal antithrombotic phenotype and ECM remodeling through deposition of elastin and collagen IV. The long term survival of cells on the matrix could be visualized by the confocal microscopy. EC culture for 15 days remodeled the fibrin matrix with deposition of elastin and collagen showing that the presence of biomimetic components in the hybrid scaffold was effective to translate signals necessary for ECM deposition by the growing ECs. The remodeling of provisional fibrin matrix is likely to give sufficient strength and elasticity to the vascular tissue construct, even after degradation of the polymer backbone.

Analysis of mRNA expression at different periods of cell culture by real time PCR demonstrated that the fibrin composite play a crucial role in inducing the ECM synthesis because FN TCPS has not induced up regulation of mRNA for elastin and collagen. On the other hand when the EC were cultured over the hybrid scaffold significant up regulation of elastin and collagen IV mRNA was achieved within 144 h of EC culture and the process is expected to confer tensile strength and flexibility to the construct. The maintenance of normal EC phenotype was demonstrated by the quiescent expression of vWF and PAI-1 and upregulation of tPA and eNOS mRNA expression. The EC function was also confirmed by enhanced release of nitric oxide in response to shear stress. The confluent EC layer on the scaffold resisted shear stress with minimal or no cell detachment. Finally, it is also shown that the tissue engineered patch generated on hybrid scaffold maintains non-thrombogenic EC phenotype with negligible platelet adhesion to the EC surface.

6.4. CONCLUSIONS

- ❖ Fibronectin, gelatin and growth factors was found to be crucial adhesion molecules in fibrin composite matrix for *in vitro* cell adhesion, proliferation and survival.
- ❖ Commercially available fibronectin- coated tissue culture polystyrene (FNPS) was found to have properties inferior to fibrin composite coated tissue culture polystyrene (CCPS) for supporting EC growth and differentiation.
- ❖ Modified fibrin composite matrix with added growth factor (GF) and glycosaminoglycan (GAG) combinations was proven to support adequate EC adhesion, proliferation, and survival with ECM deposition.
- ❖ Elastin and Collagen IV deposition by ECs cultured on the modified fibrin composite was found to be dependent on culture period and is a regulated process.
- ❖ Elastin and collagen IV mRNA expression was upregulated in EC grown on modified matrix but that of collagen I was minimal.
- ❖ From the experiments conducted with various combinations of GFs & GAGs it was proven that using a biomimetic approach with immobilized components, ECM remodeling by EC is induced with simultaneous degradation of the fibrin matrix and hence this combination was found suitable for cardiovascular tissue generation.
- ❖ Porous PCL films and fibrin-PCL hybrid scaffold showed mechanical properties comparable to that of native blood vessel and the mechanical properties marginally improved upon EC growth.
- ❖ Biodegradable bare PCL was found to be a poor substrate for EC adhesion and growth, whereas when the standardized fibrin matrix was coated to make a hybrid scaffold, it supported long term EC culture and matrix remodeling with deposition of ECM proteins, elastin and collagen.
- ❖ The EC grown over the hybrid scaffold maintained normal phenotype with the regulated expressions of vWF, tPA, PAI-1 and eNOS.

- ❖ The cell seeded hybrid scaffold exhibited antithrombogenic properties and the cells were resistant to shear upon exposure to flow
- ❖ From the results obtained in this study it is concluded that the developed scaffold is suitable for *in vitro* tissue generation that has normal physiological function.

6.5. RECOMMENDATIONS FOR FURTHER INVESTIGATION

In the past few years, it has emerged that the extra cellular matrix is a dynamic action zone that functions to instruct cellular phenotype. Specialized cells are surrounded by different combinations of ECM proteins and express an array of tissue-specific integrin receptors. This diversity represents a way to generate unique intracellular signals that give rise to tissue-specific phenotypes. Since the composite matrix which contains multiple adhesion sites favors the maintenance of normal phenotypic expression and ECM deposition, modified fibrin matrix formulations with the incorporation of different cell specific growth factors could be used to regenerate tissues that maintain cell function and ECM remodeling. Hence, the study throws light to the development of designer matrices that regulate the local cellular microenvironment precisely. Advances in the design of matrix materials that regulate cell function will have important implications for improving engineered tissue functionality and also for our basic understanding how signals from environment regulate cell function in natural and pathological tissue environment. In this context, the findings of this study are of great significance in the area of tissue engineering and cell-matrix interactions.

Some of the important cues for future investigations upcoming from this study are highlighted below:

- ◆ The fibrin matrix may be modified using cell specific growth factors, and cell behavior and deposition of specific ECM proteins could be evaluated, and might be exploited for various other tissue engineering applications.
- ◆ Little is known about the signaling pathways that cause the up regulation of mRNA of ECM proteins in response to specific growth factors. The pathways need to be elucidated.

- ◆ Since the standardized composite matrix have a composition similar to the matrix of wound site the potential of the fibrin composite as bandages for skin surfaces could be evaluated.
- ◆ Stem cells isolated from patients peripheral blood, bone marrow/ embryonic stem cells can be differentiated to ECs and cultured on hybrid scaffold, so that the cells show low immunogenicity and remain immuno privileged on transplantation, but the regulation of EC phenotype and ECM remodeling needs to be addressed.
- ◆ There is significant evidence that mechanical stimulation *in vitro* within bioreactors improves or accelerates tissue regeneration or cellular differentiation prior to implantation. Hence, the developed construct could be exposed to mechanical conditioning in a bioreactor, primarily through cyclical flow and pressure changes that mimic physiological conditions, and be further evaluated *in vitro*.
- ◆ *In vivo* evaluation of EC seeded hybrid scaffolds on animal models should be done to identify the effect of long term degradation of polymer and tissue stability.
- ◆ Endothelial inflammation plays a key role in the development of cardiovascular pathology. The influence of the hybrid scaffold on the expression of inflammatory markers by EC needs to be further investigated.
- ◆ The hybrid scaffold created could be used for cardiac tissue regeneration using cardiac myocytes and ECs. The polymer ECM 'patches' containing beating cardiomyocytes could be evaluated to sustain the cyclic loading of the heart muscle under physiological conditions.
- ◆ Specialized ECM of aortic valve, consisting of collagen, elastin, and GAGs enables dynamic aortic valve function. By culturing ECs surface and interstitial cells over the fibrin-PCL scaffold the feasibility of scaffold for valvular tissue engineering could be assessed.

- ◆ Biodegradable fibrin-PCL tubular scaffolds containing neurotrophic factors may have the potential to be used as nerve guidance conduits for autologous nerve regeneration.

- ◆ Since the data presented in this study suggest that the modified fibrin matrix composition maintains EC phenotype, the effect of EC interactions with smooth muscle cells (SMC) by cultivation of ECs and smooth muscle cells on the scaffold to incorporate the functions of SMCs could be evaluated to produce TEVGs.

BIBLIOGRAPHY

Agrawal CM, Ray RB. Biodegradable polymeric scaffolds for musculoskeletal tissue engineering. *J Biomed Mater Res.* 2001;55(2):141-150.

Aldenhoff YB, van Der Veen FH, ter Woorst J, Habets J, Poole-Warren LA, Koole LH. Performance of a polyurethane vascular prosthesis carrying a dipyridamole (Persantin) coating on its luminal surface. *J Biomed Mater Res.* 2001;54(2):224-233.

Ali MH, Schumacker PT. Endothelial responses to mechanical stress: where is the mechanosensor? *Crit Care Med.* 2002;30(5):S198-S206.

Altieri DC, Duperray A, Plescia J, Thornton GB, Languino LR. Structural recognition of a novel fibrinogen gamma chain sequence (117-133) by intercellular adhesion molecule-1 mediates leukocyte-endothelium interaction. *J Biol Chem.* 1995;270(2):696-699.

Amiel GE, Komura M, Shapira O, Yoo JJ, Yazdani S, Berry J, Kaushal S, Bischoff J, Atala A, Soker S. Engineering of blood vessels from acellular collagen matrices coated with human endothelial cells. *Tissue Eng.* 2006;12(8):2355-2365.

Anderson JS, Price TM, Hanson SR, Harker LA. In vitro endothelialization of small-caliber vascular grafts. *Surgery.* 1987;101(5):577-586.

Andreeva ER, Pugach IM, Orekhov AN. Collagen-synthesizing cells in initial and advanced atherosclerotic lesions of human aorta. *Atherosclerosis.* 1997;130(1-2):133-142.

Andreeva ER, Pugach IM, Orekhov AN. Subendothelial smooth muscle cells of human aorta express macrophage antigen in situ and in vitro. *Atherosclerosis.* 1997;135(1):19-27.

Arrigoni C, Camozzi D, Remuzzi A. Vascular tissue engineering. *Cell Transplant.* 2006;15(1):S119-125.

Ashworth JL, Sherratt MJ, Rock MJ, Murphy G, Shapiro SD, Shuttleworth CA, Kielty CM. Fibrillin turnover by metalloproteinases: implications for connective tissue remodelling. *Biochem J.* 1999;340 (1):171-181.

Bach AD, Bannasch H, Galla TJ, Bittner KM, Stark GB. Fibrin glue as matrix for cultured autologous urothelial cells in urethral reconstruction. *Tissue Eng.* 2001;7(1):45-53.

Bach TL, Barsigian C, Chalupowicz DG, Busler D, Yaen CH, Grant DS, Martinez J. VE-Cadherin mediates endothelial cell capillary tube formation in fibrin and collagen gels. *Exp Cell Res.* 1998;238(2):324-334.

Badylak S, Liang A, Record R, Tullius R, Hodde J. Endothelial cell adherence to small intestinal submucosa: an acellular bioscaffold. *Biomaterials.* 1999; 20(23-24):2257-2263.

Badylak SF, Lantz GC, Coffey A. Small intestine submucosa as a large-diameter vascular graft in the dog. *J Surg Res.* 1989;47(1):74-80.

Bailly AL, Laurent A, Lu H, Elalami I, Jacob P, Mundler O, Merland JJ, Lautier A, Soria J, Soria C. Fibrinogen binding and platelet retention: relationship with the thrombogenicity of catheters. *J Biomed Mater Res.* 1996;30(1):101-108.

Bancroft JD, Stevens A. *Theory and Practice of Histological Techniques* 2nd edition. Edinburgh: Churchill Livingstone; 1990.

Barra JG, Armentano RL, Levenson J, Fischer EC, Pichel RH, and Simon A. Assessment of smooth muscle contribution to descending thoracic aorta elastic mechanics in conscious dogs. *Circ Res.* 1993;73(6):1040-1050.

Battegay EJ, Rupp J, Iruela-Arispe L, Sage EH, Pech M. PDGF-BB modulates endothelial proliferation and angiogenesis in vitro via PDGF beta-receptors. *J Cell Biol.* 1994;125(4):917-928.

Begovac PC, Thomson RC, Fisher JL, Hughson A, Gallhagen A. Improvements in GORE-TEX vascular graft performance by Carmeda BioActive surface heparin immobilization. *Eur J Vasc Endovasc Surg.* 2003;25(5):432-437.

Bell SE, Mavila A, Salazar R, Bayless KJ, Kanagala S, Maxwell SA, Davis GE. Differential gene expression during capillary morphogenesis in 3D collagen matrices: regulated expression of genes involved in basement membrane matrix assembly, cell cycle progression, cellular differentiation and G-protein signaling. *J Cell Sci.* 2001;114(15):2755-2773.

Bellamkonda RV, Kader K, Akella R, Ranieri JP. Gene therapy approaches in the cardiovascular system. *J Cell Eng.* 1997; 2: 66-74.

Bellingham CM, Woodhouse KA, Robson P, Rothstein SJ, Keeley FW. Self-aggregation of recombinantly expressed human elastin polypeptides. *Biochim Biophys Acta.* 2001;1550(1):6-19.

Berglund JD, Mohseni MM, Nerem RM, Sambanis A. A biological hybrid model for collagen-based tissue engineered vascular constructs. *Biomaterials*. 2003;24(7):1241-1254.

Berglund JD, Nerem RM, Sambanis A. Incorporation of intact elastin scaffolds in tissue-engineered collagen-based vascular grafts. *Tissue Eng*. 2004;10(9-10): 1526-1535.

Bombeli T, Schwartz BR, Harlan JM. Endothelial cells undergoing apoptosis become proadhesive for nonactivated platelets. *Blood*. 1999;93(11):3831-3838.

Bottaro DP, Liebmann-Vinson A, Heidarman MA. Molecular signaling in bioengineered tissue microenvironments. *Ann N Y Acad Sci*. 2002;961:143-153.

Bouck N, Stellmach V, Hsu SC. How tumors become angiogenic. *Adv Cancer Res*. 1996;69:135-174.

Brizzi MF, Defilippi P, Rosso A, Venturino M, Garbarino G, Miyajima A, Silengo L, Tarone G, Pegoraro L. Integrin-mediated adhesion of endothelial cells induces JAK2 and STAT5A activation: Role in the control of c-fos gene expression. *Mol Biol Cell*. 1999;10(10):3463-3471.

Brooks PC, Clark RA, Cheresh DA. Requirement of vascular integrin alpha v beta3 for angiogenesis. *Science*. Requirement of vascular integrin alpha v beta 3 for angiogenesis. *Science*. 1994;264(5158):569-571.

Bunda S, Kaviani N, Hinek A. Fluctuations of intracellular iron modulate elastin production. *J Biol Chem*. 2005; 280(3):2341 -2351.

Campagnone R, Regan J, Rich CB, Miller M, Keene DR, Sakai L, Foster JA. Pulmonary fibroblasts: a model system for studying elastin synthesis. *Lab Invest*. 1987;56(2): 224-230.

Campbell JH, Efendy JL, Campbell GR. Novel vascular graft grown within recipient's own peritoneal cavity. *Circ Res*. 1999;85(12):1173-1178.

Campbell PG, Durham SK, Hayes JD, Suwanichkul A, Powell DR. Insulin-like growth factor-binding protein-3 binds fibrinogen and fibrin. *J Biol Chem*. 1999;274(42):30215-30221.

Canfield AE, Wren FE, Schor SL, Grant ME, Schor AM. Aortic endothelial cell heterogeneity in vitro. Lack of association between morphological phenotype and collagen biosynthesis. *J Cell Sci*. 1992;102(4):807-814.

Carampin P, Conconi MT, Lora S, Menti AM, Baiguera S, Bellini S, Grandi C, Parnigotto PP. Electrospun polyphosphazene nanofibers for in vitro rat endothelial cells proliferation. *J Biomed Mater Res A*. 2007;80(3):661-668.

Chalupowicz DG, Chowdhury ZA, Bach TL, Barsigian C, Martinez J. Fibrin II induces endothelial cell capillary tube formation. *J Cell Biol*. 1995;130(1):207-215.

Charo IF, Nannizzi L, Smith JW, Cheresh DA. The vitronectin receptor $\alpha_v\beta_3$ binds fibronectin and acts in concert with $\alpha_5\beta_1$ in promoting cellular attachment and spreading on fibronectin. *J Cell Biol.* 1990;111(6):2795–2800.

Cheresh DA, Berliner SA, Vicente V, Ruggeri ZM. Recognition of distinct adhesive sites on fibrinogen by related integrins on platelets and endothelial cells. *Cell.* 1989;58(5):945-953.

Chung CY, Zardi L, Erickson HP. Binding of tenascin-C to soluble fibronectin and matrix fibrils *J Biol Chem.* 1995;270(48):29012-29017.

Chung TW, Yang MG, Liu DZ, Chen WP, Pan CI, Wang SS. Enhancing growth human endothelial cells on Arg-Gly-Asp (RGD) embedded poly (epsilon-caprolactone) (PCL) surface with nanometer scale of surface disturbance. *J Biomed Mater Res A.* 2005;72(2):213-219.

Clark RA, Lanigan JM, DellaPelle P, Manseau E, Dvorak HF, Colvin RB. Fibronectin and fibrin provide a provisional matrix for epidermal cell migration during wound reepithelialization. *J Invest Dermatol.* 1982;79(5):264-269.

Clark RAF. *The Molecular and Cellular Biology of Wound Repair.* 2nd ed. New York: Plenum Press; 1996.

Cohen O, Kronman C, Chitlaru T, Ordentlich A, Velan B, Shafferman A. Effect of chemical modification of recombinant human acetylcholinesterase by polyethylene glycol on its circulatory longevity. *Biochem J.* 2001;357(3):795-802.

Collen A, Hanemaaijer R, Lupu F, Quax PH, van Lent N, Grimbergen J, Peters E, Koolwijk P, van Hinsberg VW. Membrane-type matrix metalloproteinase-mediated angiogenesis in a fibrin-collagen matrix. *Blood.* 2003;101(5):1810–1817.

Collen A, Maas A, Kooistra T, Lupu F, Grimbergen J, Haas FJ, Biesma DH, Koolwijk P, Koopman J, van Hinsbergh VW. Aberrant fibrin formation and cross-linking of fibrinogen Nieuwegein, a variant with a shortened A alpha-chain, alters endothelial capillary tube formation. *Blood.* 2001;97(4):973–980.

Corbett SA, Lee L, Wilson CL, Schwarzbauer JE. Covalent crosslinking of fibronectin to fibrin is required for maximal cell adhesion to a fibronectin-fibrin matrix. *J Biol Chem* 1997;272(40):24999–5005.

Corbett SA, Wilson CL, Schwarzbauer JE. Changes in cell spreading and cytoskeletal organization are induced by adhesion to a fibronectin-fibrin matrix. *Blood.* 1996;88(1):158-166.

Cox RH. Passive mechanics and connective tissue composition of canine arteries. *Am J Physiol.* 1978;234(5):H533-41.

Cummings CL, Gawlitta D, Nerem RM, Stegemann JP. Properties of engineered vascular constructs made from collagen, fibrin and collagen-fibrin mixtures. *Biomaterials.* 2004;25(17):3699–3706.

Dallabrida SM, Falls LA, Farrell DH. Factor XIIIa supports microvascular endothelial cell adhesion and inhibits capillary tube formation in fibrin. *Blood*. 2000;95(8):2586-2592.

Daniel J, Abe K, McFetridge PS. Development of the human umbilical vein scaffold for cardiovascular tissue engineering applications. *ASAIO J*. 2005;51(3):252-261.

Darland DC, D'Amore PA. Blood vessel maturation: vascular development comes of age. *J Clin Invest*. 1999;103(2):157-158.

Davidson JM, Giro MG. Control of elastin synthesis: Molecular and cellular aspect. In: Mecham RP, ed. *Regulation of Matrix Accumulation*. New York: Academic Press; 1986:177-216.

Davidson JM, Zoia O, Liu JM. Modulation of transforming growth factor-beta 1 stimulated elastin and collagen production and proliferation in porcine vascular smooth muscle cells and skin fibroblasts by basic fibroblast growth factor, transforming growth factor-alpha, and insulin-like growth factor-I. *J Cell Physiol*. 1993;155(1):149-156.

Davidson JM. Biochemistry and turnover of lung interstitium. *Eur Respir J*. 1990;3(9):1048-1063.

Davis EC. Stability of elastin in the developing mouse aorta: a quantitative radioautographic study. *Histochemistry*. 1993;100(1):17-26.

Davis GE, Camarillo CW. An alpha 2 beta1 integrin-dependent pinocytotic mechanism involving intracellular vacuole formation and coalescence regulates capillary lumen and tube formation in three-dimensional collagen matrix. *Exp Cell Res*. 1996;224(1):39-51.

Davis GE, Senger DR. Endothelial extra cellular matrix biosynthesis, remodelling, and functions during vascular morphogenesis and neovessel stabilization. *Circ Res*. 2005;97(11):1093-1107.

Deed R, Rooney P, Kumar P, Norton JD, Smith J, Freemont AJ, Kumar S. Early-response gene signalling is induced by angiogenic oligosaccharides of hyaluronan in endothelial cells Inhibition by non-angiogenic, high-molecular-weight hyaluronan. *Int J Cancer*. 1997;71(2):251-256.

Degterev A, Foster JA. The role of NF-1 factors in regulation of elastin gene transcription. *Matrix Biol*. 1999;18(3):295-307.

Dejana E, Raiteri M, Resnati M, Lampugnani MG. Endothelial integrins and their role in maintaining the integrity of the vessel wall. *Kidney Int*. 1993;43(1):61-65.

Desjardins F, Balligand JL. Nitric oxide-dependent endothelial function and cardiovascular disease. *Acta Clin Belg*. 2006;61(6):326-334.

Deutsch M, Meinhart J, Vesely M, Fischlein T, Groscurth P, von Oppell U, Zilla P. In vitro endothelialization of expanded polytetrafluoroethylene grafts: a clinical case report after 41 months of implantation, *J Vasc Surg.* 1997;25(4):757-763.

Dewey CF, Bussolari SR, Gimbrone MA, Davies PF. The dynamic response of vascular endothelial cells to fluid shear stress. *J Biomech Eng.* 1981;103(3):177-185.

Doi K, Satoh S, Oka T, Matsuda T. Impregnation of basic fibroblast growth factor on a microporous small caliber graft enhances vascularization. *ASAIO J.* 1996; 42(5):M394-398.

Dvorak HF, Brown LF, Detmar M, Dvorak AM. Vascular permeability factor/vascular endothelial growth factor, microvascular hyperpermeability, and angiogenesis. *Am J Pathol.* 1995;146(5):1029-1039.

Dvorak HF. Tumors: Wounds that do not heal. Similarities between tumor stroma generation and wound healing. *N Engl J Med.* 1986;315(26):1650-1659.

Edelman ER. Vascular Tissue Engineering, Designer Arteries. *Circ Res.* 1999;85(12):1115-1117.

Eliceiri BP, Klemke R, Stromblad S, Cheresh DA. Integrin α v β 3 requirement for sustained mitogen-activated protein kinase activity during angiogenesis. *J Cell Biol.* 1998;140(5):1255-1263.

Fang F, Orend G, Watanabe N, Hunter T, Ruoslahti E. Dependence of cyclin E-CDK2 kinase activity on cell anchorage. *Science.* 1996;271(5248):499-502.

Faries PL, LoGerfo FW, Arora S, Hook S, Pulling MC, Akbari CM, Campbell DM, Pomposelli FG. A comparative study of alternative conduits for lower extremity revascularization: All-autogenous conduit versus prosthetic grafts. *J Vasc Surg.* 2000;32(6):1080-1090.

Faris B, Tan OT, Toselli P, Franzblau C. Long-term neonatal rat aortic smooth muscle cell cultures: a model for the tunica media of a blood vessel. *Matrix.* 1992;12(3):185-188.

Farrell DH, Thiagarajan P. Binding of recombinant fibrinogen mutants to platelets. *J Biol Chem.* 1994;269(1):226-231.

Feng X, Clark RA, Galanakis D, Tonnesen MG. Fibrin and collagen differentially regulate human dermal microvascular endothelial cell integrins: stabilization of α v β 3 mRNA by fibrin1. *J Invest Dermatol.* 1999;113(6):913-919.

Ferrin DE, English JP. Polycaprolactone. In: Shalaby SW, Burg KJL, eds. *Absorbable and Biodegradable Polymers.* New York: CRC Press; 2004:63-75.

Folkman J, D'Amore PA. Blood vessel formation: what is its molecular basis? *Cell.* 1996;87(7):1153-1155.

- Forsberg E, Kjellén L. Heparan sulfate: lessons from knockout mice. *J Clin Invest.* 2001;108(2):175-80.
- Fujisawa N, Poole-Warren LA, Woodard JC, Bertram CD, Schindhelm K. A novel textured surface for blood-contact. *Biomaterials.* 1999;20(10): 955-962.
- Gao J, Ensley AE, Nerem RM, Wang Y. Poly(glycerol sebacate) supports the proliferation and phenotypic protein expression of primary baboon vascular cells. *J Biomed Mater Res A.* 2007;83(4):1070-1075.
- Geary RL, Nikkari ST, Wagner WD, Williams JK, Adams MR, Dean RH. Wound healing: a paradigm for lumen narrowing after arterial reconstruction. *J Vasc Surg.* 1998;27(1):96-106.
- Giancotti FG, Ruoslahti E. Integrin signaling. *Science.* 1999;285(5430):1028-1032.
- Gildner CD, Lerner AL, Hocking DC. Fibronectin matrix polymerization increases tensile strength of model tissue. *Am J Physiol Heart Circ Physiol.* 2004; 287:H46-53.
- Gillis C, Bengtsson L, Wilman B, Haegerstrand A. Secretion of prostacyclin, tissue plasminogen activator and its inhibitor by cultured adult human endothelial cells grown on different matrices. *Eur J Vasc Endovasc Surg.* 1996;11(2):127-133.
- Gimbrone MA, Cotran SR, Folkman J. Human vascular endothelial cells in culture : Growth and DNA synthesis. *J Cell Biol.* 1974; 60(3):673-684.
- Giraud E, Primo L, Audero E, Gerber HP, Koolwijk P, Soker S, Klagsbrun M, Ferrara N, Bussolino F. Tumor necrosis factor-alpha regulates expression of vascular endothelial growth factor receptor-2 and of its co-receptor neuropilin-1 in human vascular endothelial cells. *J Biol Chem.* 1998;273(34):22128-22135.
- Girton TS, Oegema TR, Grassl ED, Isenberg BC, Tranquillo RT. Mechanisms of stiffening and strengthening in media-equivalents fabricated using glycation. *J Biomech Eng.* 2000;122(3):216-223.
- Godo MN, Sefton MV. Characterization of transient platelet contacts on a polyvinyl alcohol hydrogel by video microscopy. *Biomaterials.* 1999;20(12):1117-1126.
- Goissis G, Suzigan S, Parreira DR, Maniglia JV, Braile DM, Raymundo S. Preparation and characterization of collagen-elastin matrices from blood vessels intended as small diameter vascular grafts. *Artif Organs.* 2000;24(3):217-23.
- Gomez DE, Alonso DF, Yoshiji H, Thorgeirsson UP. Tissue inhibitors of metalloproteinases: Structure, regulation and biological functions. *Eur J Cell Biol.* 1997;74(2):111-122.
- Gosselin C, Vorp DA, Warty V, Severyn DA, Dick EK, Borovetz HS, Greisler HP. ePTFE coating with fibrin glue, FGF-1, and heparin: effect on retention of seeded endothelial cells. *J Surg Res.* 1996;60(2):327-332.

Grassl ED, Oegema TR, Tranquillo RT. Fibrin as a alternative biopolymer to type-I-collagen for the fabrication of a media equivalent. *J Biomed Mater Res.* 2002;60(4):607-612.

Greenwald SE, Berry CL. Improving vascular grafts: the importance of mechanical and haemodynamic properties. *J Pathol.* 2000;190(3):292-299.

Greisler H, Gosselin C, Ren D, Kang S, Kim D. Biointeractive polymers and tissue engineered blood vessels. *Biomaterials* 1996;17(3):329-336.

Greisler HP, Cziperle DJ, Kim DU, Garfield JD, Petsikas D, Murchan PM, Applegren EO, Drohan W, Burgess WH. Enhanced endothelialization of expanded polytetrafluoroethylene grafts by fibroblast growth factor type 1 pretreatment. *Surgery.* 1992;112(2):244-254.

Greisler HP, Klosak JJ, Dennis JW, Karesh SM, Ellinger J, Kim DU. Biomaterial pretreatment with ECGF to augment endothelial cell proliferation. *J Vasc Surg.* 1987;5(2):393-399.

Gupta K, Kshirsagar S, Li W, Gui L, Ramakrishnan S, Gupta P, Law PY, Hebbel RP. VEGF prevents apoptosis of human microvascular endothelial cells via opposing effects on MAPK/ERK and SAPK/JNK signaling. *Exp Cell Res.* 1999;247(2):495-504.

Haegerstrand A, Bengtsson L, Gillis C. Serum proteins provide a matrix for cultured endothelial cells on expanded polytetrafluoroethylene vascular grafts. *Scand J Thorac Cardiovasc Surg.* 1993;27(1):21-26.

Hanahan D. Signalling vascular morphogenesis and maintenance. *Science.* 1997;277(5322):48-50.

Hanss M, Collen D. Secretion of tissue-type plasminogen activator and plasminogen activator inhibitor by cultured human endothelial cells: modulation by thrombin, endotoxin, and histamine. *J Lab Clin Med.* 1987;109(1):97-104.

Hay ED. Role of cell-matrix contacts in cell migration and epithelial-mesenchymal transformation. *Cell Differ Dev.* 1990;32(3):367-75.

He CM, Roach MR. The composition and mechanical properties of abdominal aortic aneurysms. *J Vasc Surg.* 1994;20(1):6-13.

He W, Yong T, Ma ZW, Inai R, Teo WE, Ramakrishna S. Biodegradable polymer nanofiber mesh to maintain functions of endothelial cells. *Tissue Eng.* 2006;12(9):2457-2466.

Heper G, Bayraktaroglu M. The importance of von Willebrand factor level and heart rate changes in acute coronary syndromes: a comparison with chronic ischemic conditions. *Angiology.* 2003;54(3):287-299.

Herring M, Gardner A, Glover J. A single staged technique for seeding vascular grafts with autologous endothelium. *Surgery.* 1978;84(4):498-504.

Hew Y, Lau C, Grzelczak Z, Keeley FW. Identification of a GA-rich sequence as a protein-binding site in the 3'-untranslated region of chicken elastin mRNA with a potential role in the developmental regulation of elastin mRNA stability. *J Biol Chem.* 2000;275(32):24857-24864.

Heydarkhan-Hagvall S, Esguerra M, Helenius G, Soderberg R, Johansson BR, Risberg B. Production of extracellular matrix components in tissue-engineered blood vessels. *Tissue Eng.* 2006;12(4):831-842.

Heyligers JM, Arts CH, Verhagen HJ, de Groot PG, Moll FL. Improving small-diameter vascular grafts: from the application of an endothelial cell lining to the construction of a tissue-engineered blood vessel. *Ann Vasc Surg.* 2005;19(3):448-456.

Higgins SP, Solan AK, Niklason LE. Effects of polyglycolic acid on porcine smooth muscle cell growth and differentiation. *J Biomed Mater Res A.* 2003;67(1):295-302.

Hirai J, Kanda K, Oka T, Matsuda T. Highly oriented, tubular hybrid vascular tissue for a low pressure circulatory system. *ASAIO J.* 1994;40(3):M383-388.

Hirai J, Matsuda T. Venous reconstruction using hybrid vascular tissue composed of vascular cells and collagen: tissue regeneration process. *Cell Transplant.* 1996;5(1):93-105.

Hirschi KK, D'Amore PA. Control of angiogenesis by the pericyte: molecular mechanisms and significance. *EXS.* 1997;79:419-428.

Hoening MR, Campbell GR, Rolfe BE, Campbell JH. Tissue-engineered blood vessels: alternative to autologous grafts? *Arterioscler Thromb Vasc Biol.* 2005;25(6):1128-1134.

Howard B V, Macarak E J, Gunson D, Kefalides N A. Characterization of the collagen synthesized by endothelial cells in culture. *Proc Natl Acad Sci U S A.* 1976;73(7):2361-2364.

Huynh T, Abraham G, Murray J, Brockbank K, Hagen PO, Sullivan S. Remodeling of an acellular collagen graft into a physiologically responsive neovessel. *Nat Biotechnol.* 1999;17(11):1083-1086.

Hynes RO. Integrins a family of cell surface receptors. *Cell.* 1987;48(4):549-554.

Inoue Y, Anthony JP, Leon P, Young DM. Acellular human dermal matrix as a small vessel substitute. *J Reconstr Microsurg.* 1996;12(5):307-311.

Isenberg BC, Tranquillo RT. Long-term cyclic distention enhances the mechanical properties of collagen based media-equivalents. *Ann Biomed Eng.* 2003;31(8):937-949.

Ishibashi K, Matsuda T. Reconstruction of a hybrid vascular graft hierarchically layered with three cell types. *ASAIO J.* 1994;40(3):M284-290.

ISO 10993-4:2002(E). Biological Evaluation of Medical Devices - Part 4: Selection of tests for interaction with blood. Table 4, Page 10; Section B.3, 18-20.

Itoh H, Aso Y, Furuse M, Noishiki Y, Miyata T. A honeycomb collagen carrier for cell culture as a tissue engineering scaffold. *Artif Organs*. 2001;25(3):213-217.

Jaffe EA, Minick CR, Adelman B, Becker CG, Nachman R. Synthesis of basement membrane collagen by cultured human endothelial cells. *J Exp Med*. 1976;144(1):209-225.

Jaffe EA, Nachman RL, Becker CG, Minick CR. Culture of human endothelial cells derived from umbilical veins: Identification by morphological and immunologic criteria. *J Clin Invest*. 1973;52(11):2745-2756.

Jansson JH, Nilsson TK, Johnson O. von Willebrand factor in plasma: a novel risk factor for recurrent myocardial infarction and death. *British Heart Journal*. 1991;66(5):351-355.

Kähäri VM, Olsen DR, Rhudy RW, Carrillo P, Chen YQ, Uitto J. Transforming growth factor-beta up-regulates elastin gene expression in human skin fibroblasts. Evidence for post-transcriptional modulation. *Lab Invest*. 1992;66(5):580-588.

Kainulainen V, Wang H, Schick C, Bernfield M. Syndecans, heparan sulfate proteoglycans, maintain the proteolytic balance of acute wound fluids. *J Biol Chem*. 1998;273(19):11563-11569.

Kalluri R. Basement membranes: structure, assembly and role in tumour angiogenesis. *Nat Rev Cancer*. 2003;3(6):422-433.

Kamiya A, Bukhari R, Togawa T. Adaptive regulation of wall shear stress optimizing vascular tree function. *Bull Math Biol*. 1984;46(1):127-137.

Kanda S, Landgren E, Ljungström M, Claesson-Welsh L. Fibroblast growth factor receptor 1-induced differentiation of endothelial cell line established from tsA58 large T transgenic mice. *Cell Growth Differ*. 1996;7(3):383-395.

Katagiri Y, Brew SA, Ingham KC. All six modules of the gelatin-binding domain of fibronectin are required for full affinity. *J Biol Chem*. 2003;278(14):11897-11902.

Kato M, Wang H, Kainulainen V, Fitzgerald ML, Ledbetter S, Ornitz DM, Bernfield M. Physiological degradation converts the soluble syndecan-1 ectodomain from an inhibitor to a potent activator of FGF-2. *Nat Med*. 1998;4(6):691-697.

Kaushal S, Amiel GE, Guleserian KJ, Shapira OM, Perry T, Sutherland FW, Rabkin E, Moran AM, Schoen FJ, Atala A, Soker S, Bischoff J, Mayer JE. Functional small-diameter neovessels created using endothelial progenitor cells expanded ex vivo. *Nat Med*. 2001;7(9):1035-1040.

Kiely CM, Woolley DE, Whittaker SP, Shuttleworth CA. Catabolism of intact fibrillin microfibrils by neutrophil elastase, chymotrypsin and trypsin. *FEBS Lett.* 1994;351(1):85-89.

Kim BS, Mooney DJ. Development of biocompatible synthetic extracellular matrices for tissue engineering. *Trends Biotechnol.* 1998;16(5): 224-230.

Kim SH, Kwon JH, Chung MS, Chung E, Jung Y, Kim SH, Kim YH. Fabrication of a new tubular fibrous PLCL scaffold for vascular tissue engineering. *J Biomater Sci Polym Ed.* 2006;17(12):1359-1374.

King SR, Hickerson WL, Proctor KG. Beneficial actions of exogeneous hyaluronic acid on wound healing. *Surgery.* 1991;109(1):76-84.

Klein S, Roghani M, Rifkin DB. Fibroblast growth factors as angiogenesis factors: new insights into their mechanism of action. *EXS.* 1997;79:159-192.

Kramer RH, Fuh GM, Karasek MA. Type IV collagen synthesis by cultured human microvascular endothelial cells and its deposition into the subendothelial basement membrane. *Biochemistry.* 1985;24(25):7423-7430.

Kratky RG, Ivey J, Roach MR. Local changes in collagen content in rabbit aortic atherosclerotic lesions with time. *Atherosclerosis.* 1999;143(1):7-14.

Kuchan MJ, Jo H, Frangos JA. Role of G proteins in shear stress mediated nitric oxide production by endothelial cells. *Am J Physiol.* 1994;267(3):C753-758.

Kucich U, Rosenbloom JC, Abrams WR, Rosenbloom J. Transforming growth factor-beta stabilizes elastin mRNA by a pathway requiring active Smads, protein kinase C-delta, and p38. *Am J Respir Cell Mol Biol.* 2002;26(2):183-188.

Kumar TR, Krishnan LK. A stable matrix for generation of tissue-engineered nonthrombogenic vascular grafts. *Tissue Eng* 2002;8(5):763-770.

L'Heureux N, Germain L, Labbe R, Auger FA. In vitro construction of a human blood vessel from cultured vascular cells: a morphologic study. *J Vas Surg.* 1993;17(3):499-509.

L'Heureux N, Paquet S, Labbe R, Germain L, Auger FA. A completely biological tissue-engineered human blood vessel. *FASEB J.* 1998;12(1):47-56.

Langer R, Vacanti JP. Tissue engineering. *Science.* 1993;260(5110):920-926.

Lantz GC, Badylak SF, Coffey AC. Small intestine submucosa as a small-diameter vascular graft in dogs. *J Invest Surg.* 1990;3(3):217-227.

Lantz GC, Badylak SF, Hiles MC, Coffey AC, Geddes LA, Kokini K, Sandusky GE, Morff RJ. Small intestine submucosa as a vascular graft: a review. *J Invest Surg.* 1993;6(3):297-310.

- Lareu RR, Arsianti I, Subramhanya HK, Yanxian P, Raghunath M. In vitro enhancement of collagen matrix formation and crosslinking for applications in tissue engineering: a preliminary study. *Tissue Eng.* 2007;13(2):385-391.
- Leavesley DI, Schwartz MA, Rosenfeld M, Cheresch DA. Integrin beta 1- and beta 3-mediated endothelial cell migration is triggered through distinct signaling mechanisms. *J Cell Biol.* 1993;121(1):163-170.
- Lee KY, Mooney DJ. Hydrogels for tissue engineering. *Chem Rev.* 2001;101(7):1869-1879.
- Lehoux S, Tedgui A. Cellular mechanics and gene expression in blood vessels. *J Biomech.* 2003;36(5):631-643.
- Leon L, Greisler HP. Vascular grafts. *Expert Rev Cardiovasc Ther.* 2003;1(4):581-594.
- Levin EG, Santell L. Stimulation and desensitization of tissue plasminogen activator release from human endothelial cells. *J Biol Chem.* 1988;263(19): 9360-9365.
- Lewis AK, Bridgman PC. Nerve growth cone lamellipodia contain two populations of actin filaments that differ in organization and polarity. *J Cell Biol.* 1992;119(5):1219-1243.
- L'Heureux N, McAllister TN, de la Fuente LM. Tissue-engineered blood vessel for adult arterial revascularization. *N Engl J Med.* 2007;357(14):1451-1453.
- Li M, Mondrinos MJ, Chen X, Gandhi MR, Ko FK, Lelkes PI. Co-electrospun poly(lactide-co-glycolide), gelatin, and elastin blends for tissue engineering scaffolds. *J Biomed Mater Res A.* 2006;79(4):963-973.
- Li S, Vert M. Biodegradation of aliphatic polyesters. In: Gerald Scott, Dan Gilead, eds. *Degradable Polymers: Principles and Applications.* London: Chapman and hall publishers; 1995: 66-68.
- Libby P. The active roles of cells of the blood vessel wall in health and disease. *Mol Aspects Med.* 1987;9(6):499-567.
- Lim SH, Cho SW, Park JC, Jeon O, Lim JM, Kim SS, Kim BS. Tissue-engineered blood vessels with endothelial nitric oxide synthase activity. *J Biomed Mater Res B Appl Biomater.* 2007;85B(2):537-546.
- Lokeshwar VB, Selzer MG. Differences in hyaluronic acid-mediated functions and signaling in arterial, microvessel, and vein-derived human endothelial cells. *J Biol Chem.* 2000;275(36):27641-27649.
- Long JL, Tranquillo RT. Elastic fiber production in cardiovascular tissue-equivalents. *Matrix Biol.* 2003;22(4):339-350.
- Lowry OH, Rosebrough NJ, Farr AL, Randall RJ. Protein measurement with the Folin phenol reagent. *J Biol Chem.* 1951;193(1):265-275

- Ma Z, He W, Yong T, Ramakrishna S. Grafting of gelatin on electrospun poly(caprolactone) nanofibers to improve endothelial cell spreading and proliferation and to control cell Orientation. *Tissue Eng.* 2005;11(7-8):1149-1158.
- Maciang T, Cerundolo J, Ilsley S, Kelly PR and Forand R. An endothelial cell growth factor from bovine hypothalamus: Identification and partial characterization. *Proc Natl Acad Sci.* 1979;76(11):5674-5678.
- Madri JA, Pratt BM. Endothelial cell-matrix interactions: in vitro models of angiogenesis. *J Histochem Cytochem.* 1986 ;34(1):85-91.
- Mann BK, Tsai AT, Scott-Burden T, West JL. Modification of surfaces with cell adhesion peptides alters extracellular matrix deposition. *Biomaterials.* 1999;20(23-24):2281-2286.
- Marois Y, Sigot-Luizard MF, Guidoin R. Endothelial cell behavior on vascular prosthetic grafts: effect of polymer chemistry, surface structure, and surface treatment. *ASAIO J.* 1999;45(4):272-280.
- Marx G. Immunological monitoring of Fenton fragmentation of fibrinogen. *Free Radic Res Commun.* 1991;12-13(2):517-520.
- Massia SP, Hubbell JA. Vascular endothelial cell adhesion and spreading promoted by the peptide REDV of the IIIICS region of plasma fibronectin is mediated by integrin alpha 4 beta 1. *J Biol Chem.* 1992;267(20):14019-14026.
- Matsuda T, Miwa H. A hybrid vascular model biomimicking the hierarchic structure of arterial wall: neointimal stability and neoarterial regeneration process under arterial circulation. *J Thorac Cardiovasc Surg.* 1995;110(4):988-997.
- Matsumura G, Miyagawa-Tomita S, Shin'oka T, Ikada Y, Kurosawa H. First evidence that bone marrow cells contribute to the construction of tissue-engineered vascular autografts in vivo. *Circulation.* 2003;108(14):1729-1734.
- McFetridge PS, Daniel JW, Bodamyali T, Horrocks M, Chaudhuri JB. Preparation of porcine carotid arteries for vascular tissue engineering applications. *J Biomed Mater Res A.* 2004;70(2):224-234.
- Mecham RP, Davis EC. Elastic fiber structure and assembly. In: Yurchenco PD, Birk DE, Mecham RP eds. *Extracellular Matrix Assembly and Structure.* New York: Academic Press; 1994: 281 -314.
- Mecham RP, Lange G, Madaras J, Starcher B. Elastin synthesis by ligamentum nuchae fibroblasts: effects of culture conditions and extracellular matrix on elastin production. *J Cell Biol.* 1981;90(2):332-338.
- Mecham RP, Madaras J, McDonald JA, Ryan U. Elastin production by cultured calf pulmonary artery endothelial cells. *J Cell Physiol.* 1983;116(3):282-288.

- Mecham RP. Effects of extracellular matrix upon elastogenesis. *Connect Tissue Res.* 1981;8(3-4):241-244.
- Mecham RP. Modulation of elastin synthesis: in vitro models. *Methods Enzymol.* 1987;144:232-246.
- Meinhart J, Fussenegger M, Hobling W. Stabilization of fibrin - chondrocyte constructs for cartilage reconstruction. *Ann Plast Surg.* 1999;42(6):673-678.
- Menashi S, Campa JS, Greenhalgh RM, Powell JT. Collagen in abdominal aortic aneurysm: typing, content, and degradation. *J Vasc Surg.* 1987;6(6):578-582.
- Mercedes B, Elaser RE. Effect of pre-adsorbed proteins on attachment, proliferation, and function of endothelial cells. *J Cell Physiol.* 2002;191(2):155-161.
- Merzkirch C, Davies N, Zilla P. Engineering of vascular ingrowth matrices: are protein domains an alternative to peptides? *Anat Rec.* 2001;263(4):379-387.
- Mettinger KL. A study of hemostasis in ischemic cerebrovascular disease I. Abnormalities in factor VIII and antithrombin. *Thromb Res.* 1982;27(2):155-160.
- Meyer SR, Chiu B, Churchill TA, Zhu L, Lakey JR, Ross DB. Comparison of aortic valve allograft decellularization techniques in the rat. *J Biomed Mater Res A.* 2006;79(2):254-262.
- Miller DC, Thapa A, Haberstroh KM, Webster TJ. Endothelial and vascular smooth muscle cell function on poly(lactic-co-glycolic acid) with nano-structured surface features. *Biomaterials.* 2004;25(1):53-61.
- Mooney DJ, Langer R. Engineering biomaterials for tissue engineering; The 10-100 micron size scale. In: Bronzino JD, ed. *Biomedical engineering handbook.* Boca Raton, FL: CRC Press, 1995:1609-1618.
- Naito M, Funaki C, Hayashi T, Yamada K, Asai K, Yoshimine N, Kuzuya F. Substrate-bound fibrinogen, fibrin and other cell attachment-promoting proteins as a scaffold for cultured vascular smooth muscle cells. *Atherosclerosis* 1992;96(2-3):227-234.
- Nandi A, Estess P, Siegelman MH (2000) Hyaluronan anchoring and regulation on the surface of vascular endothelial cells is mediated through the functionally active form of CD44. *J Biol Chem.* 2000;275(20):14939-14948.
- Nathan A, Nugent MA, Edelman ER. Tissue engineered perivascular endothelial cell implants regulate vascular injury. *Proc Natl Acad Sci U S A.* 1995;92(18):8130-8134.
- Neidert MR, Lee ES, Oegema TR, Tranquillo RT. Enhanced fibrin remodeling in vitro with TGF-beta1, insulin and plasmin for improved tissue-equivalents. *Biomaterials.* 2002;23(17):3717-3731.
- Nerem RM, Ensley AE. The tissue engineering of blood vessels and the heart. *Am J Transplant.* 2004;4(6):36-42.

- Nerem RM, Seliktar D. Vascular tissue engineering. *Annual Review of Biomedical Engineering*. 2001;3:225-243.
- Nerem RM. Tissue engineering of the vascular system. *Vox Sang*. 2004;87(2):158-160.
- Ng CS, Teoh SH, Chung TS, Hutmacher DW. Simultaneous biaxial drawing of poly(e-caprolactone) films. *Polymer*. 2000;41:5855-5864.
- Nieponice A, Soletti L, Guan J, Deasy BM, Huard J, Wagner WR, Vorp DA. Development of a tissue-engineered vascular graft combining a biodegradable scaffold, muscle-derived stem cells and a rotational vacuum seeding technique. *Biomaterials*. 2008;29(7):825-833.
- Nikkari ST, O'Brien KD, Ferguson M, Hatsukami T, Welgus HG, Alpers CE, Clowes AW. Interstitial collagenase (MMP-1) expression in human carotid atherosclerosis. *Circulation*. 1995;92(6):1393-1398.
- Niklason LE, Gao J, Abbott WM, Hirschi KK, Houser S, Marini R, Langer R. Functional arteries grown *in vitro*. *Science*. 1999;284(5413):489-493.
- Nilsson J, Elgue G, Wallin M, Hamsten A, Blomback M. Correlation between plasma levels of growth factors and von Willebrand factor. *Thromb Res*. 1989;54(2):125-132.
- Nishida Y, Knudson CB, Nietfeld JJ, Margulis A, Knudson W. Antisense inhibition of hyaluronan synthase-2 in human articular chondrocytes inhibits proteoglycan retention and matrix assembly. *J Biol Chem*. 1999;274(31):21893-21899.
- Nugent HM, Groothuis A, Seifert P, Guerraro L, Nedelman M, Mohanakumar T, Edelman ER. Perivascular endothelial implants inhibit intimal hyperplasia in a model of arteriovenous fistulae: a safety and efficacy study in the pig. *J Vasc Res*. 2002;39(6):524-533.
- Nugent HM, Rogers C, Edelman ER. Endothelial implants inhibit intimal hyperplasia after porcine angioplasty. *Circ Res*. 1999;84(4):384-391.
- Oakes BW, Batty AC, Handley CJ, Sandberg LB. The synthesis of elastin, collagen, and glycosaminoglycans by high density primary cultures of neonatal rat aortic smooth muscle. An ultrastructural and biochemical study. *Eur J Cell Biol*. 1982;27(1):34-46.
- Odrlijin TM, Francis CW, Sporn LA, Bunce LA, Marder VJ, Simpson-Haidaris PJ. Heparin-binding domain of fibrin mediates its binding to endothelial cells. *Arterioscler Thromb Vasc Biol*. 1996;16(12):1544-1551.
- Oksala O, Salo T, Tammi R, Häkkinen L, Jalkanen M, Inki P, Larjava H. Expression of proteoglycans and hyaluronan during wound healing. *J Histochem Cytochem*. 1995;43(2):125-135.

Opitz F, Schenke-Layland K, Cohnert TU, Starcher B, Halbhuber KJ, Martin DP, Stock UA. tissue engineering of aortic tissue: dire consequence of suboptimal elastic fiber synthesis in vivo. *Cardiovasc Res.* 2004;63(4):719-730.

Parks WC, Pierce RA, Lee KA, Mecham RP. Elastin. In: Kleinman HK. ed. *Advances in Molecular and Cell Biology.* Greenwich: JAI Press;1993:133-182.

Patel A, Fine B, Sandig M, Mequanint K. Elastin biosynthesis: The missing link in tissue-engineered blood vessels. *Cardiovasc Res.* 2006;71(1):40-49.

Pereira M, Rybarczyk BJ, Odrliin TM, Hocking DC, Sottile J, Simpson-Haidaris PJ. The incorporation of fibrinogen into extracellular matrix is dependent on active assembly of a fibronectin matrix. *J Cell Sci.* 2002;115(Pt 3):609-617.

Perruzzi CA, de Fougérolles AR, Koteliensky VE, Whelan MC, Westlin WF, Senger DR. Functional overlap and cooperativity among alpha and beta1 integrin subfamilies during skin angiogenesis. *J Invest Dermatol.* 2003;120(6):1100-1109.

Phaneuf MD, Szycher M, Berceci SA, Dempsey DJ, Quist WC, LoGerfo FW. Covalent linkage of recombinant hirudin to a novel ionic poly(carbonate) urethane polymer with protein binding sites: determination of surface antithrombin activity. *Artif Organs.* 1998;22(8):657-665.

Pitt CG, Schindler A. Biodegradation of polymers. In: Bruck SD, ed. *Controlled Drug Delivery (Vol. 1).* Boca Raton: CRC Press; 1983:53-80.

Plopper GE, McNamee HP, Dike LE, Bojanowski K, Ingber DE. Convergence of integrin and growth factor receptor signaling pathways within the focal adhesion complex. *Mol Biol Cell.* 1995;6(10):1349-1365.

Pöschl E, Schlötzer-Schrehardt U, Brachvogel B, Saito K, Ninomiya Y, Mayer U. Collagen IV is essential for basement membrane stability but dispensable for initiation of its assembly during early development. *Development.* 2004;131(7):1619-1628.

Prasad Chennazhy K, Krishnan LK. Effect of passage number and matrix characteristics on differentiation of endothelial cells cultured for tissue engineering. *Biomaterials.* 2005;26(28):5658-5667.

Prasad CK, Muraleedharan CV, Krishnan LK. Bio-mimetic Composite Matrix that Promotes Endothelial Cell Growth for Modification of Biomaterial Surface *J Biomed Mater Res A.* 2007;80(3):644-654.

Prevel CD, Eppley BL, McCarty M, Jackson JR, Voytik SL, Hiles MC, Badylak SF. Experimental evaluation of small intestinal submucosa as a microvascular graft material. *Microsurgery.* 1994;15(8):586-591.

Prockop DJ, Kivirikko KI. Collagens: molecular biology, diseases, and potentials for therapy. *Annu Rev Biochem.* 1995;64:403-434.

Ramamurthi A, Vesely I. Evaluation of the matrix-synthesis potential of crosslinked hyaluronan gels for tissue engineering of aortic heart valves. *Biomaterials*. 2005;26(9):999-1010.

Re F, Zanetti A, Sironi M, Polentarutti N, Lanfrancone L, Dejana E, Colotta F. Inhibition of anchorage-dependent cell spreading triggers apoptosis in cultured human endothelial cells. *J Cell Biol*. 1994;127(2):537-46.

Rekhter MD, O'Brien E, Shah N, Schwartz SM, Simpson JB, Gordon D. The importance of thrombus organization and stellate cell phenotype in collagen I gene expression in human, coronary atherosclerotic and restenotic lesions. *Cardiovasc Res*. 1996; 32(3):496-502.

Remuzzi A, Mantero S, Colombo M, Morigi M, Binda E, Camozzi D, Imberti B. Vascular smooth muscle cells on hyaluronic acid: culture and mechanical characterization of an engineered vascular construct. *Tissue Eng*. 2004;10(5-6):699-710.

Resmi KR, Krishnan LK. Protease action and generation of beta- thromboglobulin-like protein followed by platelet activation. *Thromb Res*. 2002;107(1-2):23-29.

Resmi KR, Varghese N, Krishnan LK. Procedure for quantification of platelet adhesion to biomaterials by radiosciintigraphy. *Thromb Res*. 2004;114(2):121-128.

Ritz-Timme S, Laumeier I, Collins MJ. Aspartic acid racemization: evidence for marked longevity of elastin in human skin. *Br J Dermatol*. 2003;149(5):951-959.

Roberts R, Gallagher J, Spooncer E, Allen TD, Bloomfield F, Dexter TM. Heparan sulphate bound growth factors: a mechanism for stromal cell mediated haemopoiesis. *Nature*. 1988;332(6162):376-378.

Roh JD, Nelson GN, Brennan MP, Mirensky TL, Yi T, Hazlett TF, Tellides G, Sinusas AJ, Pober JS, Saltzman WM, Kyriakides TR, Breuer CK. Small-diameter biodegradable scaffolds for functional vascular tissue engineering in the mouse model. *Biomaterials*. 2008;29(10):1454-1463.

Rucker RB, Dubick MA. Elastin metabolism and chemistry: potential roles in lung development and structure. *Environ Health Perspect*. 1984;55:179-191.

Ruggeri ZM, Ware J. von Willebrand factor. *FASEB J*. 1993;7(2):308-316.

Ruggeri ZM. The role of von Willebrand factor in thrombus formation. *Thromb Res*. 2007;120(1):S5-9.

Ruoslahti E, Engvall E. Integrins and vascular extracellular matrix assembly. *J Clin Invest*. 1997;99(6):1149-1152.

Ruoslahti E, Pierschbacher MD. New perspectives in cell adhesion: RGD and integrins. *Science*. 1987;238(4826):491-497.

Ruoslahti E, Yamaguchi Y. Proteoglycans as modulators of growth factor activities. *Cell*. 1991;64(5):867-869.

Ruoslahti E. Integrins. *J Clin Invest*. 1991;87(1):1-5.

Ruoslahti E. RGD and other recognition sequences for integrins. *Annu Rev Cell Dev Biol*. 1996;12:697-715.

Rupp PA, Little CD. Integrins in vascular development. *Circ Res*. 2001;89(7):566-572.

Sachlos E, Czernuszka JT. Making tissue engineering scaffolds work. Review: the application of solid freeform fabrication technology to the production of tissue engineering scaffolds. *Eur Cell Mater* 2003;5:29-39.

Sahni A, Baker CA, Sporn LA, Francis CW. Fibrinogen and fibrin protect fibroblast growth factor-2 from proteolytic degradation. *Thromb Haemost*. 2000; 83(5):736-741.

Sahni A, Francis CW. Vascular endothelial growth factor binds to fibrinogen and fibrin and stimulates endothelial cell proliferation. *Blood*. 2000;96(12):3772-3778.

Sahni A, Odrijin T, Francis CW. Binding of basic fibroblast growth factor to fibrinogen and fibrin. *J Biol Chem*. 1998;273(13):7554-7559.

Sahni A, Sporn LA, Francis CW. Potentiation of endothelial cell proliferation by fibrinogen bound fibroblast growth factor-2. *J Biol Chem*. 1999;274(21):14936-14941.

Salacinski HJ, Goldner S, Giudiceandrea A, Hamilton G, Seifalian AM, Edwards A, Carson RJ. The mechanical behavior of vascular grafts: a review. *J Biomater Appl*. 2001;15(3):241-278.

Sales VL, Engelmayer GC Jr, Johnson JA Jr, Gao J, Wang Y, Sacks MS, Mayer JE Jr. Protein precoating of elastomeric tissue-engineering scaffolds increased cellularity, enhanced extracellular matrix protein production, and differentially regulated the phenotypes of circulating endothelial progenitor cells. *Circulation*. 2007;116(11):155-163.

Sandusky GE Jr, Badylak SF, Morff RJ, Johnson WD, Lantz G. Histologic findings after in vivo placement of small intestine submucosal vascular grafts and saphenous vein grafts in the carotid artery in dogs. *Am J Pathol*. 1992;140(2):317-324.

Santhosh Kumar TR, Krishnan LK. Endothelial cell growth factor (ECGF) enmeshed with fibrin matrix enhances proliferation of EC in vitro. *Biomaterials*. 2001;22(20):2769-2776.

Sattar A, Rooney P, Kumar S, Pye D, West DC, Scott I, Ledger P. Application of angiogenic oligosaccharides of hyaluronan increases blood vessel numbers in rat skin. *J Invest Dermatol*. 1994;103(4):576-579.

- Sauvage M, Hinglais N, Mandet C, Badier C, Deslandes F, Michel JB, Jacob MP. Localization of elastin mRNA and TGF-beta1 in rat aorta and caudal artery as a function of age. *Cell Tissue Res.* 1998;291(2):305-314.
- Schaner PJ, Martin ND, Tulenko TN, Shapiro IM, Tarola NA, Leichter RF, Carabasi RA, Dimuzio PJ. Decellularized vein as a potential scaffold for vascular tissue engineering. *J Vasc Surg.* 2004;40(1):146-153.
- Schmidt CE, Baier JM. Acellular vascular tissues: natural biomaterials for tissue repair and tissue engineering. *Biomaterials.* 2000;21(22):2215-2231.
- Schmoekel HG, Weber FE, Schense JC, Gratz KW, Schawalder P, Hubbell JA. Bone repair with a form of BMP-2 engineered for incorporation into fibrin cell ingrowth matrices. *Biotechnol Bioeng* 2005;89(3):253-262.
- Schneider A, Melmed RN, Schwalb H, Karck M, Vlodavsky I, Uretzky G. An improved method for endothelial cell seeding on polytetrafluoroethylene small caliber vascular grafts. *J Vasc Surg.* 1992;15(4):649-656.
- Schneiderman J, Sawdey MS, Keeton MR, Bordin GM, Bernstein EF, Dilley RB, Loskutoff DJ. Increased type 1 plasminogen activator inhibitor gene expression in atherosclerotic human arteries. *Proc Natl Acad Sci U S A.* 1992;89(15):6998-7002.
- Schwartz MA, Ginsberg MH. Networks and crosstalk: integrin signalling spreads. *Nat Cell Biol.* 2002;4(4):E65-68.
- Sechler JL, Corbett S, Wenk MB, Schwarzbauer JE. Modulation of Cell-Extracellular Matrix Interactions. *Ann N Y Acad Sci.* 1998;857:143-154.
- Seifalian AM, Tiwari A, Hamilton G, Salacinski HJ. Improving the clinical patency of prosthetic vascular and coronary bypass grafts: the role of seeding and tissue engineering. *Artif Organs.* 2002;26(4):307-320.
- Seliktar D, Black RA, Vito RP, Nerem RM. Dynamic mechanical conditioning of collagen-gel blood vessel constructs induces remodeling in vitro. *Ann Biomed Eng.* 2000;28(4):351-362.
- Seliktar D, Nerem RM, Galis ZS. Mechanical strain-stimulated remodeling of tissue-engineered blood vessel constructs. *Tissue Eng.* 2003;9(4):657-666.
- Senger DR, Perruzzi CA. Cell migration promoted by a potent GRGDS-containing thrombin-cleavage fragment of osteopontin. *Biochim Biophys Acta.* 1996 ;1314(1-2):13-24.
- Serrano MC, Pagani R, Ameer GA, Vallet-Regí M, Portolés MT. Endothelial cells derived from circulating progenitors as an effective source to functional endothelialization of NaOH-treated poly(epsilon-caprolactone) films. *J Biomed Mater Res A.* 2008. [Epub ahead of print]

Serrano MC, Pagani R, Manzano M, Comas JV, Portolés MT. Mitochondrial membrane potential and reactive oxygen species content of endothelial and smooth muscle cells cultured on poly(epsilon-caprolactone) films. *Biomaterials*. 2006;27(27):4706-4714.

Shapira OM, Xu A, Aldea GS, Vita JA, Shemin RJ, Keaney JF. Enhanced nitric oxide-mediated vascular relaxation in radial artery compared with internal mammary artery or saphenous vein. *Circulation*. 1999;100(19):11322-327.

Shapiro SD, Endicott SK, Province MA, Pierce JA, Campbell EJ. Marked longevity of human lung parenchymal elastic fibers deduced from prevalence of D-aspartate and nuclear weapons-related radiocarbon. *J Clin Invest*. 1991;87(5):1828-1834.

Sheppard JI, McClung WG, Feuerstein IA. Adherent platelet morphology on adsorbed fibrinogen: effects of protein incubation time and albumin addition. *J Biomed Mater Res*. 1994;28(10):1175-1186.

Shi GY, Hau JS, Wang SJ, Wu IS, Chang BI, Lin MT, Chow YH, Chang WC, Wing LY, Jen CJ, Wu HL. Plasmin and the regulation of tissue-type plasminogen activator biosynthesis in human endothelial cells. *J Biol Chem*. 1992;267(27):19363-19368.

Shi Q, Bhattacharya V, Hong-De Wu M, Sauvage LR. Utilizing granulocyte colony-stimulating factor to enhance vascular graft endothelialization from circulating blood cells. *Ann Vasc Surg*. 2002;16(3):314-320.

Shimada T, Nishibe T, Miura H, Hazama K, Kato H, Kudo F, Murashita T, Okuda Y. Improved healing of small-caliber, long-fibril expanded polytetrafluoroethylene vascular grafts by covalent bonding of fibronectin. *Surg Today*. 2004;34(12):1025-1030.

Shin'oka T, Imai Y, Ikada Y. Transplantation of a tissue-engineered pulmonary artery. *N Engl J Med*. 2001;344:532-533.

Shin'oka T, Matsumura G, Hibino N, Naito Y, Watanabe M, Konuma T, Sakamoto T, Nagatsu M, Kurosawa H. Midterm clinical result of tissue-engineered vascular autografts seeded with autologous bone marrow cells. *J Thorac Cardiovasc Surg*. 2005;129(6):1330-1338.

Shinoka T, Shum-Tim D, Ma P, Tanel R, Isogai N, Langer R, Vacanti J, Mayer J. Creation of viable pulmonary autografts through tissue engineering. *J Thorac Cardiovasc Surg*. 1998;115(3):536-545.

Shireman PK, Greisler HP. Fibrin sealant in vascular surgery: a review. *J Long Term Eff Med Implants*. 1998;8(2):117-132.

Shivakumar K, Nair RR, Valiathan MS. Paradoxical effect of cerium on collagen synthesis in cardiac fibroblasts. *J Mol Cell Cardiol*. 1992;24(7):775-780.

Shum-Tim D, Stock U, Hrkach J, Shinoka T, Lien J, Moses MA, Stamp A, Taylor G, Moran AM, Landis W, Langer R, Vacanti JP, Mayer JE. Tissue engineering of autologous aorta using a new biodegradable polymer. *Ann Thorac Surg.* 1999;68(6):2298-2304.

Simionescu DT, Lu Q, Song Y, Lee JS, Rosenbalm TN, Kelley C, Vyavahare NR. Biocompatibility and remodeling potential of pure arterial elastin and collagen scaffolds. *Biomaterials.* 2006;27(5):702-713.

Skarja GA, Brash JL, Bishop P, Woodhouse KA. Protein and platelet interactions with thermally denatured fibrinogen and cross-linked fibrin coated surfaces. *Biomaterials.* 1998;19(23):2129-2138.

Smith DW, Carnes WH. Biosynthesis of soluble elastin by pig aortic tissue in vitro. *J Biol Chem.* 1973;248(23):8157-8161.

Solan A, Mitchell S, Moses M, Niklason L. Effect of pulse rate on collagen deposition in the tissue-engineered blood vessel. *Tissue Eng.* 2003;9(4):579-586.

Sporn LA, Bunce LA, Francis CW. Cell Proliferation on Fibrin: modulation by Fibrinopeptide Cleavage Blood. 1995;86(5):1802-1810.

Stetler-Stevenson WG. Matrix metalloproteinases in angiogenesis: a moving target for therapeutic intervention. *J Clin Invest.* 1999;103(9):1237-1241.

Stitzel J, Liu J, Lee SJ, Komura M, Berry J, Soker S, Lim G, Van Dyke M, Czerw R, Yoo JJ, Atala A. Controlled fabrication of a biological vascular substitute. *Biomaterials.* 2006;27(7):1088-1094.

Stock UA, Wiederschain D, Kilroy SM, Shum-Tim D, Khalil PN, Vacanti JP, Mayer JE Jr, Moses MA. Dynamics of extra cellular matrix production and turnover in tissue engineered cardiovascular structures. *J Cell Biochem.* 2001;81(2):220-228.

Stone PJ, Morris SM, Martin BM, McMahon MP, Faris B, Franzblau C. Repair of protease-damaged elastin in neonatal rat aortic smooth muscle cell cultures. *J Clin Invest.* 1988;82(5):1644-1654.

Storck J, Del Razek A, Zimmermann ER. Effect of polyvinyl chloride plastic on the growth and physiology of human umbilical vein endothelial cells. *Biomaterials.* 1996;17(18):1791-1794.

Streuli C. Extracellular matrix remodelling and cellular differentiation. *Curr Opin Cell Biol.* 1999;11(5):634-640.

Suehiro K, Gailit J, Plow EF. Fibrinogen is a ligand for integrin alpha5beta1 on endothelial cells. *J Biol Chem.* 1997;272(8):5360-5366.

Sun H, Mei L, Song C, Cui X, Wang P. The in vivo degradation, absorption and excretion of PCL-based implant. *Biomaterials.* 2006;27(9):1735-40.

Sun LB, Utoh J, Moriyama S, Tagami H, Okamoto K, Kitamura N. Pretreatment of a Dacron graft with tissue factor pathway inhibitor decreases thrombogenicity and neointimal thickness: a preliminary animal study. *ASAIO J.* 2001;47(4):325-328.

Swartz DD, Russell JA, Andreadis ST. Engineering of fibrin-based functional and implantable small-diameter blood vessels. *Am J Physiol Heart Circ Physiol.* 2005;288(3):H1451-1460.

Swerlick RA, Brown EJ, Xu Y, Lee KH, Manos S, Lawley TJ. Expression and modulation of the vitronectin receptor on human dermal microvascular endothelial cells. *J Invest Dermatol.* 1992;99(6):715-722.

Taylor L, Edwards J, Porter J. Present status of reversed vein. bypass grafting: five-year results of a modern series. *J Vasc Surg.* 1990;11(2):193-205.

Teebken OE, Bader A, Steinhoff G, Haverich A. Tissue engineering of vascular grafts: human cell seeding of decellularised porcine matrix. *Eur J Vasc Endovasc Surg.* 2000;19(4):381-386.

Thiagarajan P, Rippon AJ, Farrell DH. Alternative adhesion sites in human fibrinogen for vascular endothelial cells. *Biochemistry* 1996;35(13):4169-4175.

Tipping PG, Davenport P, Gallicchio M, Filonzi EL, Apostolopoulos J, Wojta J. Atheromatous plaque macrophages produce plasminogen activator inhibitor type-1 and stimulate its production by endothelial cells and vascular smooth muscle cells. *Am J Pathol.* 1993;143(3):875-885.

Toole BP. Glycosaminoglycans in morphogenesis. In: Hay EB, ed. *Cell Biology of Extracellular Matrix.* New York: Plenum Press; 1981: 259-294.

Toole BP. Hyaluronan in morphogenesis. *J Intern Med.* 1997;242(1):35-40.

Tranquillo RT, Girton TS, Bromberek BA, Tribes TG, Mooradian DL. Magnetically orientated tissue-equivalent tubes: application to a circumferentially orientated media-equivalent. *Biomaterials.* 1996;17(3):349-357.

Trentin D, Hall H, Wechsler S, Hubbell JA. Peptide-matrix-mediated gene transfer of an oxygen-insensitive hypoxia-inducible factor-1 α variant for local induction of angiogenesis. *Proc Natl Acad Sci USA.* 2006;103(8):2506-2511.

Tsai WB, Grunkemeier JM, Horbett TA. Human plasma fibrinogen adsorption and platelet adhesion to polystyrene. *J Biomed Mater Res.* 1999;44(2):130-139.

Tuan TL, Song A, Chang S, Younai S, Nimni ME. In vitro fibroplasia: matrix contraction, cell growth and collagen production of fibroblasts cultured in fibrin gels. *Exp Cell Res* 1996;223(1):127-134.

Turner NJ, Kielty CM, Walker MG, Canfield AE. A novel hyaluronan-based biomaterial (Hyaff-11) as a scaffold for endothelial cells in tissue engineered vascular grafts. *Biomaterials*. 2004;25(28):5955-5964.

Uchida T, Ikeda S, Oura H, Tada M, Nakano T, Fukuda T, Matsuda T, Negoro M, Arai F. Development of biodegradable scaffolds based on patient-specific arterial configuration. *J Biotechnol*. 2008;133(2):213-218.

Uematsu M, Ohara Y, Navas JP, Nishida K, Murphy TJ, Alexander RW, Nerem RM, Harrison DG. Regulation of endothelial cell nitric oxide synthase mRNA expression by shear stress. *Am J Physiol*. 1995 ;269(6):C1371-1378.

Vacanti JP, Langer R. Tissue engineering: the design and fabrication of living replacement devices for surgical reconstruction and transplantation. *Lancet*. 1999 ;354(1):S132-134.

Vailhe B, Ronot X, Tracqui P, Usson Y, Tranqui L. In vitro angiogenesis is modulated by the mechanical properties of fibrin gels and is related to alpha(v)beta3 integrin localization. *In Vitro Cell Dev Biol Anim*. 1997;33(10):763-73.

van Wachem PB, Beugeling T, Feijen J, Bantjes A, Detmers JP, van Aken WG. Interaction of cultured human endothelial cells with polymeric surfaces of different wettabilities. *Biomaterials*. 1985;6(6):403-408.

Vara DS, Salacinski HJ, Kannan RY, Bordenave L, Hamilton G, Seifalian AM. Cardiovascular tissue engineering: state of the art. *Pathol Biol (Paris)*. 2005;53(10):599-612.

Vinals F, Pouyssegur J. Confluence of vascular endothelial cells induces cell cycle exit by inhibiting p42/p44 mitogen-activated protein kinase activity. *Mol Cell Biol*. 1999;19(4):2763-2772.

Vlodavsky I, Bar-Shavit R, Ishai-Michaeli R, Bashkin P, Fuks Z. Extracellular sequestration and release of fibroblast growth factor: a regulatory mechanism? *Trends Biochem Sci*. 1991;16(7):268-271.

von der Leyen HE, Gibbons GH, Morishita R, Lewis NP, Zhang L, Nakajima M, Kaneda Y, Cooke JP, Dzau VJ. Gene therapy inhibiting neointimal vascular lesion: in vivo transfer of endothelial cell nitric oxide synthase gene. *Proc Natl Acad Sci U S A*. 1995;92(4):1137-1141.

Voyta JC, Via DP, Butterfield CE, Zetter BR. Identification and isolation of endothelial cells based on their increased uptake of acetylated-low density lipoprotein. *J Cell Biol*. 1984;99(6):2034-40.

Wachi H, Seyama Y, Yamashita S, Tajima S. Cell cycle-dependent regulation of elastin gene in cultured chick vascular smooth-muscle cells. *Biochem J*. 1995;309 (2):575-9.

Wahlberg T, Blomback M, Overmark I. Blood coagulation studies in 45 patients with ischemic cerebrovascular disease and 44 patients with venous thromboembolic disease. *Acta Med Scand.* 1980;207(5):385-390.

Walluscheck KP, Steinhoff G, Kelm S, Haverich A. Improved endothelial cell attachment on ePTFE vascular grafts pretreated with synthetic RGD-containing peptides. *Eur J Vasc Endovasc Surg.* 1996;12(3):321-330.

Weigel PH, Fuller GM, LeBoeuf RD. A model for the role of hyaluronic acid and fibrin in the early events during the inflammatory response and wound healing. *J Theor Biol.* 1986;119(2):219-34.

Weinberg CB, Bell E. A blood vessel model constructed from collagen and cultured vascular cells. *Science.* 1986;231(4736):397-400.

West DC, Hampson IN, Arnold F, Kumar S. Angiogenesis induced by degradation products of hyaluronic acid. *Science.* 1985;228(4705):1324-1326.

Wijelath ES, Murray J, Rahman S, Patel Y, Ishida A, Strand K, Aziz S, Cardona C, Hammond WP, Savidge GF, Rafii S, Sobel M. Novel vascular endothelial growth factor binding domains of fibronectin enhance vascular endothelial growth factor biological activity. *Circ Res.* 2002;91(1):25-31.

Wijelath ES, Rahman S, Murray J, Patel Y, Savidge G, Sobel M. Fibronectin promotes VEGF induced CD34 cell differentiation into endothelial cells. *J Vasc Surg.* 2004;39(3):655-660.

Williamson MR, Black R, Kieley C. PCL-PU composite vascular scaffold production for vascular tissue engineering: attachment, proliferation and bioactivity of human vascular endothelial cells. *Biomaterials.* 2006;27(19):3608-3616.

Yakovlev S, Gorlatov S, Ingham K, Medved L. Interaction of fibrin(ogen) with heparin: further characterization and localization of the heparin-binding site. *Biochemistry.* 2003;42(25):7709-7716.

Ye Q, Zund G, Jockenhoevel S, Schoeberlein A, Hoerstrup SP, Grunenfelder J, Benedikt P, Turina M. Scaffold precoating with human autologous extracellular matrix for improved cell attachment in cardiovascular tissue engineering. *ASAIO J.* 2000;46(6):730-733.

Yokoyama K, Zhang XP, Medved L, Takada Y. Specific binding of integrin alpha v beta 3 to the fibrinogen gamma and alpha E chain C-terminal domains. *Biochemistry.* 1999;38(18):5872-5877.

Yoneyama T, Ito M, Sugihara K, Ishihara K, Nakabayashi N. Small diameter vascular prosthesis with a nonthrombogenic phospholipid polymer surface: preliminary study of a new concept for functioning in the absence of pseudo- or neointima formation. *Artif Organs.* 2000;24(1):23-28.

Yoshida S, Ono M, Shono T, Izumi H, Ishibashi T, Suzuki H, Kuwano M. Involvement of interleukin-8, vascular endothelial growth factor, and basic fibroblast growth factor in tumor necrosis factor alpha-dependent angiogenesis. *Mol Cell Biol.* 1997;17(7):4015-23.

Zhang WJ, Liu W, Cui L, Cao Y. Tissue engineering of blood vessel. *J Cell Mol Med.* 2007;11(5):945-57.

Zhang Z, Wang Z, Liu S, Kodama M. Pore size, tissue ingrowth, and endothelialization of small-diameter microporous polyurethane vascular prostheses. *Biomaterials.* 2004;25(1):177-187.

Ziche M, Morbidelli L, Choudhuri R, Zhang HT, Donnini S, Granger HJ, Bicknell R. Nitric oxide synthase lies downstream from vascular endothelial growth factor-induced but not basic fibroblast growth factor-induced angiogenesis. *J Clin Invest.* 1997;99(11):2625-2634.

Zilla P, Fasol R, Preiss P, Kadletz M, Deutsch M, Schima H, Tsangaris S, Groscurth P. Use of fibrin glue as a substrate for in vitro endothelialization of PTFE vascular grafts. *Surgery.* 1989;105(4):515-522.

Zisch A, Schenk U, Schweitzer B, Sakiyama-Elbert S, Schense JC, Hubbell JA. Fibrin-based matrices for angiogenic stimulation. *J Vasc Surg* 2000;31(6):1303-1305.

Zisch AH, Schenk U, Schense JC, Sakiyama-Elbert SE, Hubbell JA. Covalently conjugated VEGF-fibrin matrices for endothelialization. *J Control Release.* 2001;72(1-3):101-113.

ANNEXURE – I

LIST OF MEDIA AND BUFFERS

1. Water for tissue culture

Tap water distilled three times, deionised by passing through Millipore water purifying system, autoclaved and used fresh.

2. Collagenase enzyme solution for EC isolation

Type I collagenase is dissolved in serum free M199 medium to get 0.2% solution (w/v). Sterile filtered through 0.22 μ filter, aliquoted and stored frozen.

3. M199 medium

The powdered medium is dissolved in one liter of sterile water and after adding 2.2g NaHCO₃ the pH is adjusted to ~7.2. Sterile filtered through 0.22 μ filter, and stored at (2-8)^oC.

4. MCDB131 Medium

The liquid media is supplied with 10mM final concentration of L-Glutamine. Sterile filtered through 0.22 μ filter, and stored at (2-8)^oC.

5. HBSS (Ca²⁺ and Mg²⁺ free)

KCL	5.4 mM
KH ₂ PO ₄	4.4 mM
NaCl	136.9mM
Na ₂ HPO ₄	2.7 mM
Distilled water	upto 1000 ml
pH	7.2

The prepared solution is autoclaved for 30 min at 121°C. Glucose solution autoclaved separately was added to the buffer (0.1% final concentration) and stored at (2-8)°C. Used within one week.

6. PBS

NaCl	150 mM
KH ₂ PO ₄	1.5 mM
Na ₂ HPO ₄	10 mM
Distilled water	upto 1000 ml
pH	7.4

7. Acid Citrate Dextrose (ACD)

Citric acid, monohydrate	4.2 mM
Trisodium Citrate, dihydrate	7.5 mM
Dextrose	13.9mM
Distilled water	upto 100 ml
pH	7.4

8. Tyrodes Buffer

Glucose	5.5 mM
MgCl ₂	2.09 mM
KCl	5.39 mM
NaCl	140 mM
Tris	14.49 mM
Distilled water	upto 1000 ml
pH	7.4

ANNEXURE – II

LIST OF PUBLICATIONS

- ❑ **Divya P**, Lizymol PP, Minshiya P, Krishnan VK, Krishnan LK. Development of a fibrin composite-coated poly(epsilon-caprolactone) scaffold for potential vascular tissue engineering applications. *J Biomed Mater Res B Appl Biomater.* 2008;87B(2):570-579.
- ❑ **Divya P**, Krishnan VK, Krishnan LK. Vascular tissue generation in response to signaling molecules integrated with a novel poly(epsilon-caprolactone)-fibrin hybrid scaffold. *J Tissue Eng Regen Med.* 2007;1(5):389-397.
- ❑ **Divya P**, Sreerekha PR, Krishnan LK. Growth factors upregulate deposition and remodeling of ECM by endothelial cells cultured for tissue-engineering applications. *Biomol Eng.* 2007;24(6):593-602.
- ❑ **Divya P**, Krishnan LK. Design of fibrin matrix composition to enhance endothelial cell growth and extra cellular matrix deposition for *in vitro* tissue engineering. *Artificial Organs* (Article in press).
- ❑ Sreerekha PR, **Divya P**, Krishnan LK. Adult stem cell homing and differentiation *in vitro* on composite fibrin matrix. *Cell Prolif.* 2006;39(4):301-312.
- ❑ **Divya P**, Krishnan VK, Krishnan LK. Functional Stability of Endothelial Cell Phenotype on a Novel Hybrid Scaffold during Vascular Tissue Engineering. (Under communication).
- ❑ **Divya P**, Krishnan LK. Standardization of an optimum fibrin matrix composite with accelerated endothelial cell proliferation and ECM remodeling for vascular tissue engineering applications (Under communication).

Poster presentations (International Conferences)

- ❑ **Divya P**, Krishnan LK. Effect of Growth Factors on Extra Cellular Matrix Remodeling in Vascular Tissue Engineering, Regenerate 2005, Atlanta, Georgia, USA.
- ❑ **Divya P**, Krishnan VK, Krishnan LK. Study of Endothelial Cell Phenotype and ECM Remodeling on Novel PCL-Fibrin Hybrid Scaffold for Cardiovascular Tissue Engineering Applications. TERMIS NA 2007, Toronto, Ontario, Canada.

- **Divya P,** Krishnan VK, Krishnan LK. Endothelial Cell Behavior on a Novel Hybrid Fibrin-PCL Scaffold for Potential Application in Vascular Tissue Engineering. Indo Australian Conference, BITE 2007, SCTIMST, Trivandrum, India.

- Lizymol PP, **Divya P,** Krishnan LK, Krishnan VK. A Novel Fibrin Coated Poly(caprolactone) Scaffold for Vascular Tissue Engineering Applications: Physicochemical Characterization. Indo Australian Conference, BITE 2007, SCTIMST, Trivandrum, India.